

**STUDY OF THE YAW STABILITY
OF A DOWNWIND
HORIZONTAL AXIS WIND TURBINE**

BY

KHANDKAR AFTAB HOSSAIN

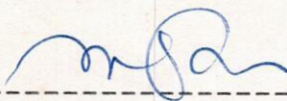
A Thesis
is Submitted to the Department of Mechanical Engineering in
Partial fulfilment of the requirements of the degree of
Master of Science
in
Mechanical Engineering

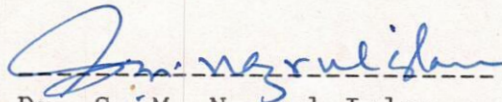
January, 1990


BANGLADESH UNIVERSITY OF ENGINEERING AND TECHNOLOGY, DHAKA-1000, BANGLADESH.

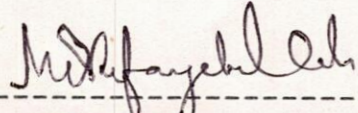
The thesis title " STUDY OF THE YAW STABILITY OF A DOWNWIND HORIZONTAL AXIS WIND TURBINE " submitted by Khandkar Aftab Hossain Roll No. 871402F, Registration No. 85502 of M.Sc. Engineering (Mechanical) has been accepted as satisfactory in partial fulfilment of the Master of Science in (Mechanical Engineering) on 30th. January 1990.

BOARD OF EXAMINERS

1. 

Dr. Md. Quamrul Islam
Professor
Deptt. of Mech. Engg.
BUET, Dhaka. Chairman
(Supervisor)
2. 

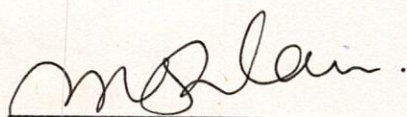
Dr. S. M. Nazrul Islam
Professor & Head
Deptt. of Mech. Engg.
BUET, Dhaka. Member
3. 

Dr. Md. Abdur Razzaq Akhanda
Professor,
Deptt. of Mech. Engg.
BUET, Dhaka. Member
4. 

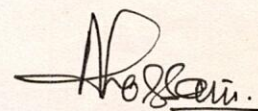
Dr. Md. Refayet Ullah
Associate Professor,
Deptt. of Naval Architecture
and Marine Engineering
BUET, Dhaka. Member
(External)

CERTIFICATE OF RESEARCH

This to certify that the work presented in this thesis is the outcome of the investigation carried out by the candidate under the supervision of Dr. M. Quamrul Islam in the Department of Mechanical Engineering, Bangladesh University of Engineering & Techonology, Dhaka and it has not been submitted anywhere for any award of degree or diploma.



Supervisor



Candidate

ACKNOWLEDGEMENTS

The author is grateful to Professor Dr. Md. QUAMRUL ISLAM for his supervision, guidance, encouragement and necessary suggestions.

The author expresses his thankfulness to the members of the Mechanical Engineering Department of Bangladesh University of Engineering and Technology (BUET) for their helpful discussions.

Special gratitude is due to my wife for her encouragement, help and hard work throughout the years of this research. Otherwise, it is not possible to complete this work smoothly. Special gratitude is also due to my only son for his patience during the period of preparation of this thesis.

Thanks to Mr. Harun-ur-Rashid for his assistance in drafting the figures and graphs.

Finally, the author wishes to thank UNDP(United Nation Development Program.) for their financial support given under the award of a scholarship. The author also expresses his thankfulness to Bangladesh Institute of Technology (BIT), Khulna-9203, for granting leave for the period of study in BUET.

Author.

ABSTRACT

Present thesis discuss a method to calculate the overall design, performance and structural analysis of a horizontal axis wind turbine. For a particular wind velocity, the optimum rotor configuration for twist and chord is determined using the momentum theory and the blade element theory, assuming zero drag, no coning and no tilting angle.

After determining the optimal aerodynamic shape of the blade, the forces and moments on blades and tower top are calculated. At this stage, the equations may be extended to include the effects of coning and tilting angles, and the effect of several wind conditions such as wind gradient, wind shift and tower shadow. In this thesis, effects of coning and tilting angles are not considered. But the analysis of stability by determining the forces and moments acting on a horizontal axis wind turbine when yawed to non-axial flow is presented.

The effect of tower blockage on the stability at various yaw angle is also considered. Three types of blade shape such as, Optimum-chord Optimum-twist, Linear-chord Linear-twist and Linear-chord Zero-twist are considered .

CONTENTS

Acknowledgements		(iv
Abstract		(v
Contents		(vi
List of symbols		(viii
CHAPTER-I	: Introduction.	1
1.0:	General	1
1.1:	Historical Background.	1
1.2:	Motive of this Thesis.	3
CHAPTER-II	: Literature Survey.	7
2.0:	General	7
2.1:	Review of Existing Literature.	7
2.2:	Scope of the Thesis.	10
CHAPTER-III	: Existing Theories	13
3.0:	General	13
3.1:	Axial Momentum Theory.	13
3.2:	Effect of Wake Rotation on Momentum Theory.	16
3.3:	Blade Element Theory.	19
3.4:	Strip Theory.	21
3.5:	Tip and Hub Losses.	22
3.6:	Equations for Total Thrust, Torque and Power Coefficients.	24
3.7:	Expressions for Maximum Power.	25
CHAPTER-IV	: Modification of Existing Theories.	30
4.0:	General	30
4.1:	Velocity Components at the Blade at the Different Frame of Reference.	30
4.2:	Effect of Wind Shear.	32
4.3:	Momentum Theory.	33
4.4:	Blade Element Theory.	34
4.5:	Strip Theory.	37
4.6:	Equations for Thrust, Torque and Power Coefficients.	38
4.7:	Forces and Moments at the Different Frame of Reference.	38
4.7.1 :	Forces.	39
4.7.2 :	Moments.	39
CHAPTER-V	: Design of Wind Turbine.	46
5.0:	General	46
5.1:	Selection of Design Tip Speed Ratio and Number of Blades.	46
5.2:	Selection of Airfoil Data.	48
5.3:	Calculation Scheme for Blade Configuration.	48

		vii
	5.4: Deviation from Ideal Form.	50
	5.5: Calculation Scheme for Performance Analysis.	51
	5.6: Design fo a 350 kW Wind Turbine.	53
CHAPTER-VI	: Yaw Stability Analysis.	58
	6.0: General	58
	6.1: Present Approach.	58
	6.2: Blade Forces under the Influence of Yaw.	58
	6.3: Stability Analysis.	59
CHAPTER-VII	: Results and Discussion	63
	7.0: General	63
	7.1: Results of a 350 kW Wind Turbine.	63
	7.2: Effect of Pitch Angle Variation.	63
	7.3: Effect of Blade shapes.	64
	7.4: Effect of Wind Shift.	65
	7.5: Effect of Tower Shadow.	66
	7.6: Effect of Wind Shear.	68
	7.7: Effect of Number of Blades.	68
	7.8: Effect of Blade Coning Angle.	69
	7.9: Effect of Rotor Tilt.	69
CHAPTER-VIII	: Conclusions and Recommendations.	94
REFERENCES	:	97
APPENDICES	:	102
APPENDIX	A : Local Frame of Reference.	102
APPENDIX	B : Selections of Design parameters.	105
	B.1 : Determination of Minimum C_D/C_L Ratio.	105
	B.2 : Determination of Design C_P .	105
APPENDIX	C :	108
	C.1 : Maximum Power Coefficient.	108
	C.2 : Influence of Wake Axial Induction Factor.	108
	C.3 : Relation between ω and U	109
APPENDIX	D :	111
	D.1 : C_P in Terms of λ .	111
	D.2 : Relation between a and a' .	112
	D.3 : Table for Average Wind Speed	113
COMPUTER PROGRAM	:	114

LIST of SYMBOLS

- a axial interference factor.
 \acute{a} tangential interference factor.
 A turbine disc area, πR^2 .
 A_2 wake cross sectional area.
 B number of blades.
 B_f tower blockage factor.
 C chord of the blade.
- C_D blade drag coefficient, $\frac{dD}{1/2 \rho C W^2 dr}$.
- C_L blade lift coefficient, $\frac{dL}{1/2 \rho C W^2 dr}$.
- C_{Ld} design lift coefficient.
- C_{mp} pitching moment coefficient, $\frac{M_P}{1/2 \rho A V_\infty^2 R}$.
- C_{mz} yawing moment coefficient, $\frac{M_{yaw}}{1/2 \rho A V_\infty^2 R}$.
- C_P power coefficient, $\frac{P}{1/2 \rho A V_\infty^3}$.
- C_Q torque coefficient, $\frac{Q}{1/2 \rho A V_\infty^2 R}$.
- C_T thrust coefficient, $\frac{T}{1/2 \rho A V_\infty^2 R}$.
- D drag force.
 dA blade element area, Cdr .
- dC_P elemental power coefficient, $\frac{dP}{1/2 \rho A V_\infty^3}$.
- dC_Q elemental torque coefficient, $\frac{dQ}{1/2 \rho A V_\infty^2 R}$.
- dC_T elemental thrust coefficient, $\frac{dT}{1/2 \rho A V_\infty^2 R}$.
- dD blade element drag force.
 dF_n blade element normal force.
 dF_t blade element tangential force.
 dP blade element power.
 dL blade element lift force.

dQ	blade element torque.	ix
dT	blade element thrust.	
F	Prandtl's loss factor.	
F _{hub}	hub loss factor.	
F _{tip}	tip loss factor.	
F _{x0}	force acting along X-direction in S ₀ coordinate system.	
F _{x3}	force acting along X-direction in S ₃ coordinate system.	
F _{y0}	force acting along Y-direction in S ₀ coordinate system.	
F _{y3}	force acting along Y-direction in S ₃ coordinate system.	
F _{z0}	force acting along Z-direction in S ₀ coordinate system.	
F _{z3}	force acting along Z-direction in S ₃ coordinate system.	
g	acceleration due to gravity.	
H	hub height from ground level.	
K _T	transformation matrix for tilting.	
K _{β}	transformation matrix for coning.	
K _{θ}	transformation matrix for azimuth.	
L	lift force.	
M _P	pitching moment.	
M _x	flapwise bending moment.	
M _y	edgewise bending moment.	
M _{yaw}	yawing moment.	
P	turbine power.	
P _e	amount of power to be extracted.	
P ⁺	pressure immediately in front of the rotor.	
P ⁻	pressure immediately behind the rotor.	
r	local blade radius.	
r _{hub}	hub radius.	
R	rotor radius.	
R _L	radial distance along the blade.	
Q	torque.	
Q _{st}	starting torque.	
S ₀	fixed reference coordinate system.	
S ₁	coordinate system considering tilt angle.	
S ₂	coordinate system considering blade azimuth .	
S ₃	coordinate system considering blade coning.	
T	thrust force.	
U	wind speed through the turbine.	
V	wake velocity behind the rotor.	
\bar{V}	average wind velocity.	
V _d	design wind velocity.	
V _R	wind velocity at the centre line of the rotor.	
V _{ref}	reference wind velocity.	
V _{s0}	wind velocity corresponding to S ₀ coordinate system.	
V _{s3}	wind velocity corresponding to S ₃ coordinate system.	
V _t	tangential wind velocity.	
V _{∞}	undisturbed wind velocity.	
V _{∞0}	local wind velocity considering wind shear.	
V _{θk}	instantaneous wind velocity corresponding to an azimuthal point.	
W	relative wind velocity.	
X ₀	distance along X-direction in S ₀ coordinate system.	
Y ₀	distance along Y-direction in S ₀ coordinate system.	
Z ₀	distance along Z-direction in S ₀ coordinate system.	
Z	height of a particular point from the ground level.	
Z _{ref}	height of a reference point from the ground level.	

GREEK ALPHABETS

α	angle of attack.
α_d	design angle of attack.
α_T	tilt angle.
β	coning angle.
β_T	blade twist angle.
γ^*	yawing angle.
n	power law exponent.
η_{eff}	efficiency of a windmill.
θ_k	blade azimuth angle.
θ_p	blade pitch angle.
λ	tip speed ratio.
λ_d	design tip speed ratio.
λ_r	local tip speed ratio.
v_a	induced axial velocity.
v_{s3}	induced velocity in S3 coordinate system.
v_t	induced tangential velocity.
v_v	induced vertical velocity.
ρ	air density.
σ	solidity, $\frac{BC}{2\pi r}$
ϕ	angle of relative wind velocity.
ω	wake rotational velocity.
Ω	angular velocity of the rotor.

SUBSCRIPTS

a	axial.
d	design.
D	drag.
eff.	efficiency.
g	gravity.
L	lift.
max.	maximum.
min.	minimum.
n	normal.
P	power.
Q	torque.
r	local.
ref.	reference.
St	starting.
T	tilt, twist and thrust.
t	tangential.
v	vertical.
ω	wake.
β	coning.
θ	azimuth.

LIST OF FIGURES

Sl. No.	Figure No.	Captions	Page No.
1.	1.1.1	: Savonius Rotor	5
2.	1.1.2	: Darries Rotor	5
3.	1.1.3	: Smith- Putnam wind turbine	6
4.	1.1.4	: Enfield-Andreau wind energy conversion system	6
6.	2.1.1	: Various rotor states	12
7.	3.1.1	: Wind turbine stream tube	27
8.	3.2.1	: Stream tube showing wake rotation	27
9.	3.2.2	: Blade element annular ring	28
10.	3.3.1	: Blade element velocity diagram	28
11.	3.5.1	: Tip and hub losses flow diagram	29
12.	4.1.1	: Reference frame S_0 coordinate system	42
13.	4.1.2	: Translation over Y' and rotation about X_0 by angle αr	42
14.	4.1.3	: Rotation about Y_1 by angle θ	42
15.	4.1.4	: Rotation about X_2 by angle β	42
16.	4.2.1	: Effect of wind gradient on rotor	43
17.	4.3.1	: Analytical model for momentum theory	43
18.	4.4.1	: Velocity diagram for rotor blade element	44
19.	4.7.2.1	: Flapwise and Edgewise bending moment	44
20.	4.7.2.2	: Pitching moment due to wind gradient	45
21.	4.7.2.3	: Yawing moment due to wind shift	45
22.	5.1.1	: Maximum power coefficient versus λ for a rotor with a Rankine vortex wake	54
23.	5.1.2	: $C_p - \lambda$, Characteristics curve showing the effect of C_L/C_D ratio ($B=\infty$)	54

			xiii
24.	5.2.1	: C_L — α , Characteristics curve for a given airfoil section[21]	55
25.	5.2.2	: C_L — C_D , Characteristics curve for a given airfoil section[21]	55
26.	5.6.1	: Starting torque coefficient as a function of overall pitching angle	56
27.	5.6.2	: Blade twist distribution for optimum distribution	56
28.	5.6.3	: Blade chord distribution for optimum performance	57
29.	5.6.4	: Wind velocity variation with tip speed ratio	57
30.	6.2.1	: The relative wind velocities at upper and lower position of the blade in yaw	61
31.	6.3.1	: Downwind rotor without coning angle	62
32.	6.3.2	: Downwind rotor with coning angle	62
33.	6.3.3	: Upwind rotor without coning or tilting angle	62
34.	6.3.4	: Upwind rotor with coning or tilting angle	62
35.	7.1.1	: Variation of power coefficient with tip speed ratio	71
36.	7.1.2	: Variation of thrust coefficient with tip speed ratio	71
37.	7.1.3	: Variation of torque coefficient with tip speed ratio	72
38.	7.2.1	: Variation of power coefficient with tip speed ratio at different pitching angles	72
39.	7.2.2	: Variation of thrust coefficient with tip speed ratio at different pitching angles	73
40.	7.2.3	: Variation of torque coefficient with tip speed ratio at different pitching angles	73
41.	7.3.1	: Variation of power coefficient with tip speed ratio for linear-chord linear-twist blade at different pitching angles	74
42.	7.3.2	: Variation of torque coefficient with tip speed ratio for linear-chord linear-twist blade at different pitching angles	74

43.	7.3.3	: Variation of thrust coefficient with tip speed ratio for linear-chord linear-twist blade at different pitching angles	75
44.	7.3.4	: Variation of power coefficient with tip speed ratio for linear-chord zero-twist blade at different pitching angles	75
45.	7.3.5	: Variation of torque coefficient with tip speed ratio for linear-chord zero-twist blade at different pitching angles	76
46.	7.3.6	: Variation of thrust coefficient with tip speed ratio for linear-chord zero-twist blade at different pitching angles	76
47.	7.3.7	: Variation of power coefficient with tip speed ratio for different blade shapes	77
48.	7.3.8	: Variation of torque coefficient with tip speed ratio for different blade shapes	77
49.	7.3.9	: Variation of thrust coefficient with tip speed ratio for different blade shapes	78
50.	7.3.10	: Radial variation of power coefficient	78
51.	7.3.11	: Radial variation of thrust coefficient	79
52.	7.3.12	: Radial variation of torque coefficient	79
53.	7.3.13	: Radial variation of power	80
54.	7.3.14	: Radial variation of thrust	80
55.	7.3.15	: Radial variation of torque	81
56.	7.3.16	: Radial variation of axial force	81
57.	7.3.17	: Radial variation of axial bending moment	82
58.	7.3.18	: Radial variation of tangential bending moment	82
59.	7.3.19	: Optimum & linearized blade twist distribution	83
60.	7.3.20	: Optimum & linearized blade chord distribution	83
61.	7.3.21	: Comparison of starting torque coefficients for different blade shapes wind turbines	84
62.	7.4.1	: Effect of yaw angles on power coefficient	84
63.	7.4.2	: Effect of yaw angles on thrust coefficient	85
64.	7.4.3	: Effect of yaw angles on torque coefficient	85

65.	7.4.4	: Power coefficient as a function of blade angular position at different yawing angles	86
66.	7.4.5	: Thrust coefficient as a function of blade angular position at different yawing angles	86
67.	7.4.6	: Blade flapwise bending moment as a function of blade angular position at different yawing angles	87
68.	7.4.7	: Blade edgewise bending moment as a function of blade angular position at different yawing angles	87
69.	7.4.8	: Effect of yawing angles on yawing moment coefficient during one revolution	88
70.	7.4.9	: Effect of yawing angles on pitching moment coefficient during one revolution	88
71.	7.4.10	: Tower top axial force during one revolution at different yawing angles	89
72.	7.4.11	: Effect of yawing angles on tower top tangential force during one revolution	89
73.	7.5.1	: Effect of tower shadow on power coefficient at different yaw angles during one revolution	90
74.	7.5.2	: Variation of thrust coefficient due to tower shadow & yawing angles during one revolution	90
75.	7.5.3	: Effect of tower shadow on blade flapwise root bending moment at different yaw angles during one revolution	91
76.	7.5.4	: Effect of tower shadow on blade edgewise bending moment at different yaw angles during one revolution	91
77.	7.5.5	: Effect of tower shadow on yawing moment coefficient at different yaw angles during one revolution	92
78.	7.5.6	: Variation of pitching moment coefficient due to tower shadow and yaw angles during one revolution	92
79.	7.5.7	: Effect of tower shadow on tower top axial force at different yaw angles during one revolution	93
80.	7.5.8	: Effect of tower shadow on tower top tangential force at different yaw angles during one revolution	93

CHAPTER I

INTRODUCTION

1.0 General

In the present world, energy crisis is the vital problem. There are many sources of energy such as gas, petroleum oils, minerals, solar, tidal, wind power etc. The wind power is one of the cheapest source of energy. Wind energy can be converted into mechanical energy through wind turbine. The people of twentieth century interested to get energy from wind, so they are looking for different type of wind turbines at different countries of the world. Environmental pollution and public health hazard due to energy conversion may be avoided, if we extract energy from wind power.

Various studies have indicated that wind energy has the potential to make significant contributions to the national needs. Therefore, our nation is interested to new cheapest energy sources and to justify their parcticability.

1.1 Historical Background

From the ancient period different types of windmill have been designed and constructed to extract power from the wind. The earliest type of windmill known as Persian millwright built in 644 A.D. and windmills in Seistan, Persia 915 A.D. [13] were used for moving water, consisted of several sails that rotated on a vertical axis.

By the eleventh century A.D., windmills were in extensive use in the Middle East and were brought to Europe in the thirteenth century by the returning Crusaders. Many horizontal axis windmills had been constructed for grinding grains and lifting water in that period in Europe.

In the fourteenth century, the Dutch had improved the design of windmills and used for draining the marshe and lakes of Rhine river delta. The first oil mill was built in Holland in 1582, and the first paper mill was built in 1586. Sawmills were introduced to process timber, at the end of sixteenth century. About 9000 windmills were used in Netherlands for different purposes in the middle of nineteenth century. The Dutch improved the design of windmills particularly in the design of rotors. In the sixteenth century, the premitive jib sails on wooden booms had been used. The sails were typically constructed from sailcloth stretched over a wooden frame. But in modern designs sheet metal replaced the sailcloth. In the twentieth century, only 2500 windmills were still in operation in the Netherlands. In 1960, fewer than 1000 were still in working condition.

Since the mid-nineteenth century, many small multi-bladed windmills, power output capacity less than 1 hp each in an average wind speed, have been built and used in the United States

to pump water, generate electricity and perform similar functions.

During the early part of the twentieth century, two quite different vertical types windmill were developed. One of the two, known as the Savonius rotor was formed by cutting a cylinder into two semi-cylindrical surfaces, moving these surfaces sideways along the cutting plane to form a rotor with cross-section in the form of the letter "S", placing a shaft in the centre of the rotor, and closing the end surfaces with circular end plates as shown in the Figure 1.1.1. The other vertical windmill design, patented in 1927 by George Darrieus consisted of two thin airfoils with one end mounted in the lower end of a vertical shaft and the other end mounted on the upper end of the same shaft, as shown in the Figure 1.1.2.

Palmer Putnam had constructed a windmill with the help of the S. Morgan Smith company of New York, Pennsylvania using NACA 4418 as shown in the Figure 1.1.3 and operated the plant in the early 1940. The two bladed, 175 ft. diameter, propeller type rotor, weighed 16 tons and operated at a constant rotational speed of 28 rpm to produce up to 1.25 Megawatts (MW) of power during the period from 1941 to 1945.

At the end of nineteenth century, about 2500 windmills were in operation, supplying a total power of about 40,000 hp or 30 MW. During the world war-II, the Danes developed and operated a number of new types of large scale wind machines to produce electricity. The number of these machines were increased from 16 in the summer of 1940, to 88 in the beginning of 1944. After the world war-II the number of operating machines started to decrease, and at the end of 1947, it dropped to 57. The decrease continued up to 1950, as a result production of electricity decreases and windmills again returned for experimental work, with units rated 12 kW, 45 kW and 200 kW in Denmark. The 200 kW Gedser windmill, which was the latest in this series, was operated until 1968. After the energy crisis of 1973, the 200 kW Gedser windmill was refurbished, and in 1977 it was again put back into service. In 1931, the Russians built an advanced 100 kW wind turbine near Yalta on the Black sea. The annual output was found about 280,000 kWhr.

In the 1950, the Enfield cable company built a wind-powered generator as shown in the Figure 1.1.4. This machine was operated at St. Albans, England, and later in Algeria. It was designed for 100 kW output of A.C. power in a 13.41 m/sec wind speed. It was an interesting design rather than conventional design. It used air instead of gears to transmit the propeller power to the generator.

The propeller blades were hollow, and when it rotated, it acted as centrifugal pumps. The air entered into the ports in the lower part of the tower, passed through an air turbine which turned the electric generator, went up through the tower; and went out through the hollow tips of the blades. The efficiency of

this unit was low compared to conventional horizontal axis wind turbine. The main advantage of this system is that the power generating equipment is not supported aloft.

The French built and operated several large wind powered electric generators in the period from 1958 to 1966. These included three horizontal-axis units, each consists of three propeller type blades. The smaller unit had a 70 ft. diameter rotor operated at 56 r.p.m. The largest one was rated at 1,000 kW in wind speed of 18.25 m/sec and weighed 96 tons, excluding the tower.

In Germany the number of windmill was in use about 18,000 in 1895, 17,000 in 1907, 11,400 in 1914 and between 4,000 to 5,000 in 1933. The Germans introduced a number of improvements in the design of wind-powered generator. The largest unit generated 100 kW in 8 m/sec of wind speed. These units operated successfully for more than 4,000 hrs. during the period from 1957 to 1968.

Recently, large wind energy conversion systems have been built and tested in a number of countries around the world. But the problem was the installation cost per kilowatt which was too high when compared with the costs of other methods of producing electric power. Today's increasing cost of fuel, coupled with energy crisis, the nation is forced to reexamine the wind energy as a cheap source of power.

1.2 Motive of this thesis

Due to recent world wide energy crisis our nation is interested to search a new energy source rather than conventional energy source i.e. petroleum oil, mineral fuels, which may be solar and wind energy.

The availability of faster and more economical digital computer has encouraged to do research on computational basis. Aerodynamic and structural analysis are important but in most existing design only aerodynamic design is considered. Most of these programs do not considered important effect of coning, tilting and azimuth. Again, there is no such program which considers the effect of yawing angle and tower shadow for a downwind horizontal axis wind turbine at different wind conditions. It is obvious that this lack of adequate method results in both uneconomical and dangerous situation. It is dangerous because structural safety is not always guaranteed and designs without consideration of all important parameters are not safe.

In this work, only aerodynamic performance of the turbine is analysed. The obtained results are forces, moments, thrusts, torque and power. The present analysis is based on the combination of the momentum theory and blade element theory, which is known as strip theory. Therefore, the design &

performance and stability of a horizontal axis wind turbine is carried out by using a simplified method, which covers all the important parameters that are necessary for a best design.

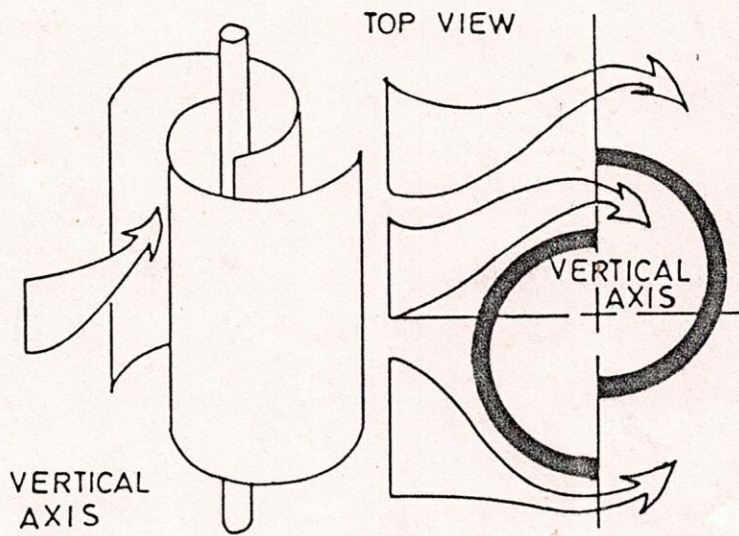


FIGURE 1.1.1: SAVONIUS ROTOR

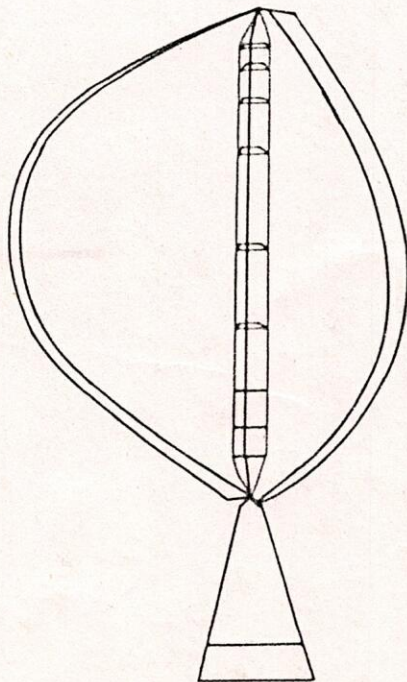


FIGURE 1.1.2: DARRIEUS ROTOR

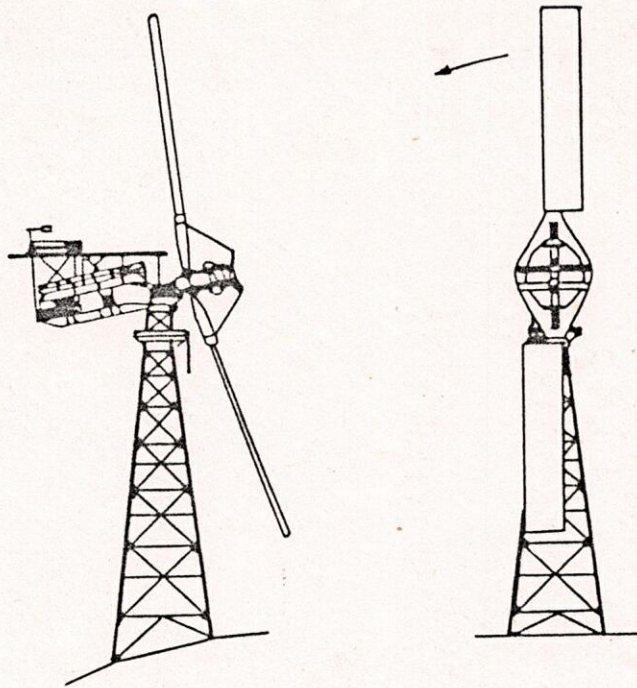


FIGURE 1.1.3 : SMITH - PUTNAM WIND TURBINE

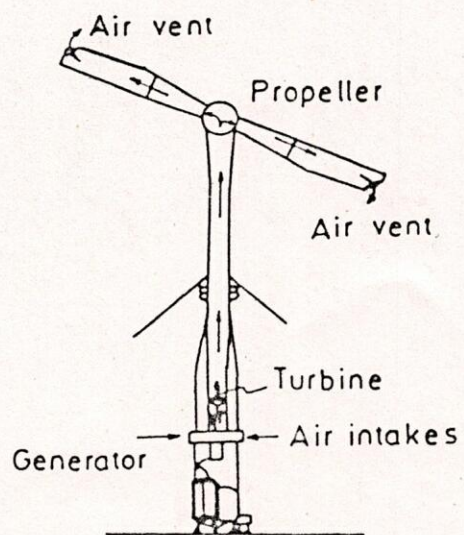


FIGURE 1.1.4 : ENFIELD - ANDREAU WIND ENERGY CONVERSION SYSTEM

CHAPTER II

LITERATURE SURVEY

2.0 General

The research on the wind turbine is very little and a few literature has been published on structural and aerodynamical design for stability problem and for the effect of tower shadow of the horizontal axis wind turbine. In order to visualize actual flow field and much of the general behavior, propeller technology has been used. Because of the restricted interest and financial support, wind power studies is very recent. Prototype experiment is very difficult, owing to the size of the rotors and steadiness of the wind over sufficiently long periods. Model experiments are possible but difficult due to wind tunnel walls blockage. In the following chapter the review of the existing literature which forms the foundation of the present analysis is presented.

2.1 Review of Existing Literature

The horizontal axis wind turbine is to be considered as a airscrew that extracts energy from the driving air and converts it into mechanical energy. But a propeller delivers energy into the air which extracts from the another source of energy. Since there is a similarity between the propeller and the wind turbine, it is possible to use same theoretical development for the performance analysis. The propeller theory was developed based on two different independent methods of approach, one of which is called as momentum theory approach and the other is blade element theory approach.

W.J.M.Rankine [6], developed and described the axial momentum theory in 1865 and it was improved later by R.E.Froude [12]. The basis of the theory is to determine the forces acting on the rotor to produce the motion of the fluid. The theory predicts the ideal efficiency and flow velocity, but it gives no information about the blade shape, which is necessary to generate wake effects later were included by A.Betz [41] in this theory.

The blade element theory was first originated by W.Froude [11] in 1878 and later developed by S.Drzewiecki [8]. The approach of blade element theory is opposite to that of momentum theory. The blade element theory determines, the forces produced by the blades as a result of the fluid motion. It was hampered in its original development by lack of knowledge of sectional aerodynamics and mutual interference blades.

Modern propeller theory has developed from the concept of free vortices being shed from the rotating blades. These vortices define a slipstream and generate induced velocities. The theory can be attributed to the work of Lanchester [42] and Flamm [43] for the original concept. Later, Joukowski [7] introduced the induced velocity analysis and A.Betz [6] introduced optimization concept. L. Prandtl [29] and Goldstein [37] developed seperately

the circulation distribution or tip loss analysis and H.Glauert [15,16,17], E. Pistolesti [35] and S.Kawada [26], for general improvements. Recently, R.E.Wilson, Stel N. Walker and P.B.S. Lissaman [45] have further analysed the aerodynamic performance of wind turbines. They have introduced a new method to apply tip loss which is sometimes referred as the linear method. This method is based on the assumption that the axial and tangential induced velocities are localised at the blade and only a fraction of these occur in the plane of the rotor. The theory has been referred by a number of names; vortex theory, modified blade element theory and strip theory.

The strip theory used extensively for the performance analysis of a horizontal axis wind turbine and helicopter rotors. The technique which assumes local two dimensional flow at each radial rotor station is a design analysis approach in which the airfoil sectional aerodynamics, chord and pitch angle are required in order to calculate the forces and torque.

The application limit of the momentum theory is the state where reverse flow begins to occur downstream of the rotor. The operating states of a wind turbine can be classified theoretically into four categories depends on interference factor [47].

For $a < 0$, the regime is called, the propeller state. In this state the rotor is acting as a propeller accelerating the flow, with thrust opposing flow and power is to be added. The thrust coefficient and the power coefficient are then negative.

For $0 < a < 1$, the regime is called the windmill state. The windmill state is divided into two regime namely, windmill brake state ($0 < a < 0.5$) and turbulent wake state ($0.5 < a < 1$). Both are for decelerating flow with positive thrust coefficient and power coefficient and power is extracted from the flow. At $a = 0.5$, thrust coefficient is maximum and at $a = 1/3$, power coefficient is maximum. At $a > 0.5$, the wake velocity is zero and streamlines cease to exist. In the turbulent wake state, the simple theory would require flow reversal in the far wake, velocity is zero somewhere between disk and infinity and the rotor operates continuously in this anomalous state, characterized by large recirculating flows and high turbulence.

For $a > 1$, the rotor enters the propeller brake state, with power being added to the flow to create downwind thrust, corresponding to reversing propeller thrust on loading. For values of a , slightly greater than unity, the flow regime is called the vortex ring state, experienced by helicopter rotors during part-power descent. Airplane propellers pass through this state to that of the brake state with reversing thrust, as shown in the Figure 2.1.1.

The states mentioned above can occur simultaneously at different positions of the blade. In the helicopter analysis, several experimental studies have been made on the vortex ring

state and on the turbulent wake state. Lock [30,31] conducted wind tunnel tests using two model rotors and Glauert [18], defined a characteristic curve utilizing the data of Lock and its approximate formula is given by Johnson [23]. Wilson [46], has suggested linear algebraic expressions for the local thrust at high tip speed ratios where a wind turbine may operate in the vortex ring state. There is very little published literature on the performance of a wind turbine operating in the turbulent wake state. Yamane [52] has introduced a performance prediction method for windmill in the turbulent wake state utilizing the empirical characteristic curve of Glauert in combination with the blade element theory. Recently, Anderson [1], has published the results of a vortex-wake analysis of a horizontal axis wind turbine and he compared his results with those obtained from strip theory. He suggests unless information is required about the wake, it is satisfactory to use the blade element theory with a suitable model for tip loss. Viterna [19] has suggested an improved method to calculate the aerodynamic performance of a horizontal axis wind turbine at tip speed ratios where aerodynamic stall can occur as the blade experiences high angle of attack.

Walker [50] has developed a method to determine the blade shapes for maximum power. According to his method, the blade chord and twist angle are continuously varied at each radial station until the elemental power coefficient has been maximized. This is obtained when every radial element of the blade is operating at the airfoil's maximum lift to drag ratio. This results in the lift coefficient and angle of attack being identical at each radial element. Anderson [2] has compared near-optimum and optimum blade shapes for turbines operating at both constant tip speed ratio and constant rotational speed. Shepherd [38], has suggested a simplified method for design and performance analysis of a horizontal axis wind turbine which can be carried out on a hand held calculator by elimination of iteration process. It is based on the use of the ideal and optimised analysis to determine the blade geometry. It requires only fixed values of the axial induction factors and corresponding optimised rotational induction factors.

Jansen [24] worked on the theories that form the basis for calculation of the design and the behaviour of a windmill. A modification of the Prandtl tip loss model is derived. Due to this modification, relatively heavy loading of the windmill rotor, takes into account. It is argued that, in contrast with propeller design, a maximum energy extraction may be achieved by enlarging the chords of the blades near the tips. He concluded that with simple materials high power coefficients are possible. Large horizontal axis wind turbines must be designed for optimum performance with minimum maintenance and weight. It should be stable under different wind conditions. Ormiston [33] reported a qualitative discussion of the effects of size, number of blades, hub configuration and type of control system on the turbine dynamic characteristics. Ormiston [34] considers the basic flapping response of a wind turbine blade using elementary analytical techniques. Various other effects such as cross wind,

rotor shaft and yaw precession were also treated in a simple manner.

Powells [36,51] investigated the effects of tower shadow on a downwind two-bladed horizontal axis wind turbine. A rotor aero-elastic simulation is used to predict the blade response to tower shadow, and subsequently to estimate increased blade fatigue damage. He suggested to reduce the effect of tower shadow by making the aerodynamically smooth tower, thereby reducing the flow disturbance. Due to change in wind direction, it is necessary to have an aerodynamic tower fairing which is free to move in yaw with the turbine nacelle. Since an effective fairing has been easily and cheaply built, and since it encounters a far easier regime than the blades of the machine, it follows that this may well be a worthwhile addition for small and medium size downwind machines. By reducing both the strains on the blades can be considerably moderate. The reduction in the noise levels observed would help to make such machines more environmentally acceptable as well.

Islam M.Q. [21] presented a procedure for the aerodynamic design and structural analysis of horizontal axis wind turbines using simplified methods. In the first part of this programme, optimum rotor configuration is determined, using the momentum and blade element theories. The equations are extended to include the effects of wind shift, wind gradient, blade azimuth, and tilting angle. Forces and moments are then calculated and compared with the results of existing wind turbines.

2.2 Scope of the Thesis

This thesis discussed a method for determining aerodynamic design, problems of stability and effect of tower shadow of the horizontal axis wind turbine due to various wind conditions. In chapter one, a general outline concerning wind turbine, a historical background of different types of wind turbine and motive behind the present work is discussed.

In chapter two, a review of the existing literature is discussed.

In chapter three, axial momentum theory and blade element theory including the effect of wake rotation is presented. Modifications of these theories due to various losses are also presented to make these theories adequate for performance analysis of wind turbines. With the help of these theories, expressions for maximum power extraction is also derived.

In the chapter four, the existing theories are modified further for various important effects such as coning angle, tilting angle, yawing angle and blade azimuth angle. Performance calculations are performed for each blade segment taking the relative wind speed and angle of attack axially axisymmetric. Also the expressions for various forces and moments that are responsible for instability are derived.

In the chapter five, the selection criteria and investigation techniques of various design parameters are presented. The procedure of calculation of blade configurations for optimum performance is also presented in this chapter.

Chapter six discussed with the problems of unstablity of horizontal axis wind turbine under the influence of yaw. Equations of tower top forces and moments are derived here.

Chapter seven deals with the results obtained and the general dicussions.

In the chapter eight conclusions and recommendations are presented.

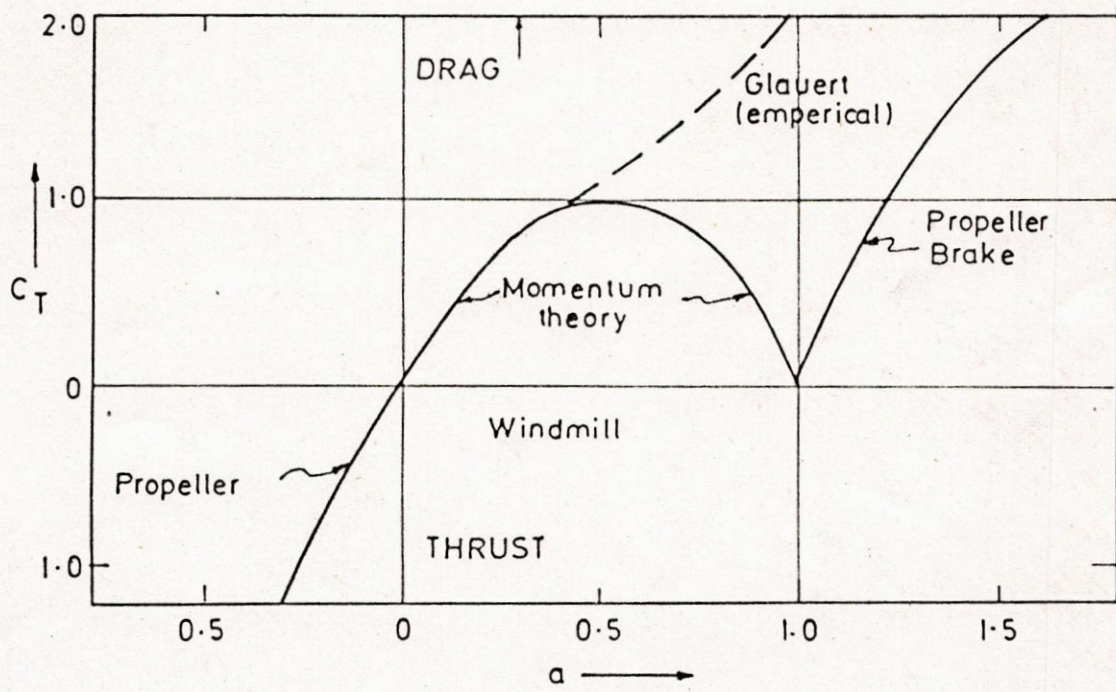


Fig.2.1.1 Various Rotor States

CHAPTER III

EXISTING THEORIES

3.0 General

Wind turbine is a device that extract energy from the flowing air and converts the extract energy into mechanical energy which later transformed into other forms of energy. For performance analysis of the wind turbine the flow of air is considered as steady flow and the influence of turbulence of the atmospheric boundary layer is neglected.

Most existing theoretical models are based on the strip theory. The basic theoretical development of strip theory is discussed in the present chapter. Effects of wake rotation, tip and hub losses and expressions for maximum power are also presented in this chapter.

3.1 Axial Momentum Theory

The axial momentum theory was presented by Rankine in 1865 and later modified by Froude [12]. The theory determines the forces, acting on the rotor to create motion of the fluid. The theory is useful to predict the ideal efficiency of a wind turbine. For the maximum possible output of a wind turbine the assumptions underlying the axial momentum theory are:

1. The fluid is inviscid and incompressible.
2. Infinite number of blades.
3. Flow is entirely axial with no rotational motion.
4. Thrust loading is uniform over the disc.
5. The flow is homogenous.
6. Static pressure far ahead and far behind the rotor are equal to the undisturbed ambient static pressure ($P_2 = P_\infty$).

Considering the control volume in Figure 3.1.1, where the upstream and downstream control volume planes are infinitely far away from the turbine disc plane. The air approach velocity V_∞ , decelerated to velocity U , at the turbine disc and exit velocity become V , at the downstream plane. The conservation of mass can be expressed as

$$\rho A_1 V_\infty = \rho A U = \rho A_2 V \quad (3.1.1)$$

where,

- V_∞ = Undisturbed wind velocity.
- U = Wind velocity through the rotor.
- V = Wind velocity far behind the rotor.
- A = Turbine disc area.
- A_1 = Cross sectional area of incoming wind.
- A_2 = Wake cross sectional area.
- ρ = Mass density of air.

The thrust force T on the rotor is given by the change of momentum of the flow,

$$T = \dot{m}(V_{\infty} - V) = \rho A_1 V_{\infty}^2 - \rho A_2 V^2 \quad (3.1.2)$$

From the equation (3.1.1) and (3.1.2) we have,

$$T = \rho AU(V_{\infty} - V) \quad (3.1.3)$$

The thrust on the rotor can also be expressed from the pressure difference over the rotor area,

$$T = A(P^+ - P^-) \quad (3.1.4)$$

where,

P^+ = Pressure immediately in front of the rotor.

P^- = pressure immediately behind the rotor.

Now applying Bernoulli's equation between the upstream plane and the rotor plane, we have

$$P_{\infty} + \frac{1}{2} \rho V_{\infty}^2 = P^+ + \frac{1}{2} \rho U^2 \quad (3.1.5)$$

Again applying Bernoulli's equation between the rotor plane and downstream plane, we get

$$P_{\infty} + \frac{1}{2} \rho V^2 = P^- + \frac{1}{2} \rho U^2 \quad (3.1.6)$$

Subtracting equation (3.1.6) from equation (3.1.5), we get

$$P^+ - P^- = \frac{1}{2} \rho (V_{\infty}^2 - V^2) \quad (3.1.7)$$

The expression for thrust from equation (3.1.4) becomes,

$$T = \frac{1}{2} \rho A (V_{\infty}^2 - V^2) \quad (3.1.8)$$

Equating the equation (3.1.8) with (3.1.3),

$$\frac{1}{2} \rho A (V_{\infty}^2 - V^2) = \rho AU(V_{\infty} - V)$$

or,
$$U = \frac{V_{\infty} + V}{2} \quad (3.1.9)$$

Above results show that the velocity through the turbine rotor is equal to the average of the wind velocity ahead of the turbine and wake velocity behind the turbine.

The velocity at the rotor U is often defined in terms of an axial interference factor a as,

$$U = V_{\infty} (1-a) \quad (3.1.10)$$

Balancing equations (3.1.9) and (3.1.10), the wake velocity can be expressed as,

$$V = V_{\infty} (1-2a) \quad (3.1.11)$$

The change in kinetic energy of the mass flowing through the rotor area is the power absorbed by the rotor,

$$P = \dot{m} \Delta KE = \frac{1}{2} \rho A U (V_{\infty}^2 - V^2) \quad (3.1.12)$$

With equations (3.1.10) and (3.1.11) the expression for power becomes,

$$P = 2 \rho A V_{\infty}^3 a(1-a)^2 \quad (3.1.13)$$

Power coefficient C_p is given by

$$\begin{aligned} C_p &= \frac{P}{\frac{1}{2} \rho A V_{\infty}^3} \\ &= \frac{2 \rho A V_{\infty}^3 a(1-a)^2}{\frac{1}{2} \rho V_{\infty}^3 A} \\ &= 4a(1-a)^2 \end{aligned} \quad (3.1.14)$$

Differentiating equation (3.1.13) with respect to a , and equating to zero, maximum power is found,

$$\frac{dp}{da} = 2 \rho A V_{\infty}^3 (1-4a+3a^2) = 0$$

Which gives an optimum interference factor,

$$a = 1/3.$$

Putting $a=1/3$, in equation (3.1.13), maximum power becomes,

$$P_{\max.} = \frac{16}{27} \left(\frac{1}{2} \rho A V_{\infty}^3 \right) \quad (3.1.15)$$

Again putting $a=1/3$, in equation (3.1.14) maximum power coefficient can be obtained,

$$(C_p)_{\max.} = \frac{16}{27} = 0.593$$

The factor $16/27$ is known as Betz coefficient [55] and represents maximum fraction of power which an ideal rotor can extract from the flow.

The fraction is related to the power of an undisturbed flow through an area A , whereas in reality the mass flow rate through A is not $AV\omega$, it will be AU . Hence the efficiency for maximum power can be written as,

$$\eta_{\text{eff.}} = \frac{P_{\text{max.}}}{1/2 \rho A U V \omega^2} = \frac{16}{27} \times \frac{3}{2} \times \frac{8}{9} = \frac{16}{27}$$

This modelling does not take into account additional effects of wake rotation. As the initial stream is not rotational, interaction with a rotating windmill will cause to rotate in opposite direction.

The produced torque implies tangential forces and thus momentum changes in tangential direction, the flow is entirely axial is acceptable only for very high speed turbines. As the produced torque will be higher, the tangential momentum in the downstream will also be higher. This is the first reason, than the other losses that occur in reality, why the value of $(C_p)_{\text{max.}} = 0.593$ cannot be achieved in a real construction [22].

3.2 Effect of Wake Rotation on Momentum Theory

To include the effect of wake rotation in the momentum theory, the following assumptions are considered,

1. At the upstream of the rotor, the flow is entirely axial and at the downstream the flow rotates with an angular velocity ω , but the flow remains irrotational.
 2. The angular velocity of the flow at the downstream, is considered to be small compared to the angular velocity Ω of the rotor.
 3. Pressure in the wake is equal to the free stream pressure.
- Writing the energy equation, illustrated in the Figure 3.2.1.

$$\text{K.E.translational } (V_\omega) = \text{Power extracted} + \text{K.E.translational}(U) + \text{K.E.rotational}(\omega) \quad [48]. \quad (3.2.1)$$

The above equation shows that the rotational kinetic energy reduces the power, which is extracted by the turbine. The wake rotation is opposite to the rotation of the rotor. Since the power is equal to the product of the torque Q , acting on the rotor and the angular velocity Ω , maximum power is available with high angular velocity and low torque, since high torque will result large wake rotational energy. The angular velocity of the wake and the angular velocity of the rotor Ω , are related

by an angular interference factor \acute{a} ,

$$\acute{a} = \frac{\text{Angular velocity of the wake}}{\text{Twice the angular velocity of the rotor}} = \frac{\omega}{2\Omega} \quad (3.2.2)$$

The annular ring through which a blade element will pass, is illustrated in the Figure 3.2.2.

Using the relation for momentum flux through the ring the axial thrust force dT can be expressed as,

$$dT = \dot{m}(V_{\infty} - V) = \rho dAU(V_{\infty} - V) \quad (3.2.3)$$

Using the equation (3.1.10) and (3.1.11)

$$U = V_{\infty} (1-a) \quad (3.1.10)$$

$$\text{and } V = V_{\infty} (1-2a) \quad (3.1.11)$$

And expressing the area of the annular ring dA as,

$$dA = 2\pi r dr \quad (3.2.4)$$

The expression for the thrust becomes,

$$dT = 4\pi r \rho V_{\infty}^2 a(1-a) dr \quad (3.2.5)$$

The thrust force may also be calculated from the pressure difference over the blades by applying Bernoulli's equation. Since the relative angular velocity changes from Ω to $(\Omega + \omega)$, while the axial components of the velocity remains unchanged. Bernoulli's equation gives,

$$P^+ - P^- = \frac{1}{2} \rho (\Omega + \omega)^2 r^2 - \frac{1}{2} \rho \Omega^2 r^2$$

$$\text{or, } P^+ - P^- = \rho \left(\Omega + \frac{\omega}{2} \right) \omega r^2$$

The resulting thrust on the annular element is given by,

$$dT = (P^+ - P^-) dA$$

$$\text{or, } dT = \rho \left(\Omega + \frac{\omega}{2} \right) \omega r^2 2\pi r dr$$

Using equation (3.2.2),

$$dT = 4\acute{a} (1+\acute{a}) \frac{1}{2} \rho \Omega^2 r^2 2\pi r dr \quad (3.2.6)$$

Equating equation (3.2.5) and (3.2.6),

$$\frac{a(1-a)}{a(1+a)} \frac{\Omega^2 r^2}{V_\infty^2} = \lambda_r^2 \quad (3.2.7)$$

Where, λ_r is called as the local tip speed ratio which is given by,

$$\lambda_r = \frac{r\Omega}{V_\infty} \quad (3.2.8)$$

An expression for the torque acting on the rotor can be derived by considering the change in angular momentum flux dQ through the annular ring.

$$dQ = \dot{m} V_t r$$

$$\text{or, } dQ = \omega dA \rho r r$$

where, V_t is the tangential wind velocity.

Inserting equations (3.1.10), (3.2.2) and (3.2.4), the expression for the torque acting on the annular ring is given by,

$$dQ = 4\pi r^3 \rho V_\infty a(1-a) \Omega dr \quad (3.2.9)$$

Again, the power generated through the annular ring is equal to $dP = \Omega \cdot dQ$, so the total power becomes,

$$P = \int_0^R \Omega \cdot dQ \quad (3.2.10)$$

The tip speed ratio,

$$\lambda = \frac{R\Omega}{V_\infty} \quad (3.2.11)$$

Now, the equation of total power from the equations (3.2.9) and (3.2.10) is,

$$P = \int_0^R 4\pi r^3 \rho V_\infty a(1-a) \Omega^2 dr$$

The above equation can be expressed in terms of the local tip speed ratio as,

$$P = \frac{1}{2} \rho A V_\infty^3 \frac{8}{\lambda^2} \int_0^\lambda a(1-a) \lambda r^3 d\lambda_r \quad (3.2.12)$$

Where, A is the turbine swept area, $A = \pi R^2$.

The power coefficient is,

$$C_p = \frac{P}{\frac{1}{2} \rho A V_\infty^3}$$

Using the equation (3.2.12) power coefficient becomes,

$$C_p = \frac{8}{\lambda^2} \int_0^{\lambda} a(1-a) \lambda_r^3 d\lambda_r \quad (3.2.13)$$

From the equation (3.2.7) angular interference factor,

$$\dot{a} = -\frac{1}{2} + \frac{1}{2} \left[1 + \frac{4}{(\lambda_r)^2} a(1-a) \right]^{1/2} \quad (3.2.14)$$

Substituting the value of \dot{a} in (3.2.13) and taking the derivative equal to zero, the relation between λ_r and a for maximum power becomes,

$$\lambda_r = \frac{(1-a)(4a-1)^2}{(1-3a)} \quad (3.2.15)$$

Taking the derivative equal to zero of the equation (3.2.13) and from the derivative of (3.2.7), the relation between a and \dot{a} is found (Appendix-D),

$$\dot{a} = \frac{(1-3a)}{(4a-1)} \quad (3.2.16)$$

The above relation will be used later for design purposes.

3.3: Blade Element Theory

The blade element theory determines the forces acting on a differential element of a blade due to the motion of the fluid. By integrating over the length of the blade the performance of the entire rotor is calculated. The following assumptions are considered for the blade element theory:

1. There is no interference between adjacent blade elements along each blade.
2. The forces acting on a blade element are solely due to the lift and drag characteristics of the sectional profile of the element.
3. The pressure in the far wake is equal to the free stream pressure.

The aerodynamic force components acting on the blade element are the lift force dL perpendicular to the resulting velocity vector and the drag force dD acting in the direction of the resulting velocity vector. The following expressions for the sectional lift and drag forces may be introduced:

$$dL = C_L \frac{1}{2} \rho W^2 C dr \quad (3.3.1)$$

$$dD = C_D \frac{1}{2} \rho W^2 C dr \quad (3.3.2)$$

The thrust and torque found by the blade element are,

$$dT = (dL \cos\phi + dD \sin\phi) \quad (3.3.3)$$

$$dQ = (dL \sin\phi - dD \cos\phi)r \quad (3.3.4)$$

Assuming that the rotor has B blades, the expressions for the thrust and torque becomes,

$$dT = BC \frac{1}{2} \rho W^2 (C_L \cos\phi + C_D \sin\phi) dr$$

$$\text{or, } dT = BC \frac{1}{2} \rho W^2 C_L \cos\phi \left(1 + \frac{C_D}{C_L} \tan\phi\right) dr \quad (3.3.5)$$

$$\text{and, } dQ = BC \frac{1}{2} \rho W^2 (C_L \sin\phi - C_D \cos\phi) r \cdot dr$$

$$\text{or, } dQ = BC \frac{1}{2} \rho W^2 C_L \sin\phi \left(1 - \frac{C_D}{C_L} \frac{1}{\tan\phi}\right) r \cdot dr \quad (3.3.6)$$

From the Figure 3.3.1, the expressions for relative velocity W ,

$$W = \frac{V_\infty(1-a)}{\sin\phi} = \frac{r\Omega(1+a)}{\cos\phi} \quad (3.3.7)$$

From the equation (3.3.7) and trigonometric relation,

$$\tan\phi = \frac{(1-a)V_\infty}{r\Omega(1+a)} = \frac{(1-a)}{(1+a)} \times \frac{1}{\lambda_r} \quad (3.3.8)$$

$$\text{and, } \beta_T = \phi - \alpha \quad (3.3.9)$$

The local solidity ratio σ is

$$\sigma = \frac{B C}{2\pi r} \quad (3.3.10)$$

The equations of the blade element theory become,

$$dT = (1-a)^2 \frac{\sigma C_L \cos\phi}{\sin^2\phi} \left(1 + \frac{C_D}{C_L} \tan\phi\right) - \frac{1}{2} \rho V_\infty^2 2\pi r \cdot dr \quad (3.3.11)$$

$$dQ = (1+\acute{a})^2 \frac{\sigma C_L \sin\phi}{\cos^2\phi} \left(1 - \frac{C_D}{C_L} \frac{1}{\tan\phi}\right) - \frac{1}{2} \rho \Omega^2 r^3 2\pi r \cdot dr \quad (3.3.12)$$

3.4 Strip Theory

From the axial momentum theory and the blade element theory a series of relationships can be developed to calculate the performance of a wind turbine. By equating the thrust obtained from the momentum theory equation (3.2.5) to equation (3.3.11) of blade element theory for an annular element at a radius r , we have,

$$dT_{\text{Momentum}} = dT_{\text{Blade Element}}$$

$$\text{or, } \frac{a}{(1-a)} = \frac{\sigma C_L \cos\phi}{4 \sin^2\phi} \left(1 + \frac{C_D}{C_L} \tan\phi\right) \quad (3.4.1)$$

Again, equating the angular momentum, determined from the axial momentum theory equation (3.2.9) and equation (3.3.12) of blade element theory, we get,

$$dQ_{\text{Momentum}} = dQ_{\text{Blade Element}}$$

$$\frac{\acute{a}}{(1+\acute{a})} = \frac{\sigma C_L}{4 \cos\phi} \left(1 - \frac{C_D}{C_L} \frac{1}{\tan\phi}\right) \quad (3.4.2)$$

Equations (3.4.1) and (3.4.2) which determines axial and angular interference factor contain drag terms. It has been suggested in [46, 47] that the drag terms may be neglected in determining a and \acute{a} . Because of the retarded air due to drag is confined to thin helical sheets in the wake and have little effects on the induced flow. Omitting the drag terms the induction factors a and \acute{a} may be calculated with the following equations.

$$\frac{a}{1-a} = \frac{\sigma C_L \cos\phi}{4 \sin^2\phi} \quad (3.4.3)$$

$$\text{and, } \frac{\acute{a}}{1+\acute{a}} = \frac{\sigma C_L}{4 \cos\phi} \quad (3.4.4)$$

Considering the equations (3.4.3) and (3.3.11), elemental thrust

may be written as,

$$dT = 4a(1-a) \left(1 + \frac{C_D}{C_L} \tan\theta\right) \frac{1}{2} \rho V_\infty^2 2\pi r dr \quad (3.4.5)$$

From equations(3.4.4) and(3.3.12) we have elemental torque,

$$dQ = 4a(1-a) \left(1 - \frac{C_D}{C_L} \frac{1}{\tan\theta}\right) \frac{1}{2} \rho V_\infty \Omega 2\pi r^3 dr \quad (3.4.6)$$

Elemental power is given by,

$$dP = \Omega \cdot dQ$$

$$\text{or, } dP = 4a(1-a) \left(1 - \frac{C_D}{C_L} \frac{1}{\tan\theta}\right) \frac{1}{2} \rho V_\infty \Omega^2 2\pi r^3 dr \quad (3.4.7)$$

Introducing the local tip speed ratio λ_r with,

$$\lambda_r = \frac{\Omega r}{V_\infty} \quad (3.2.8)$$

Equation of total thrust, torque and power become,

$$T = \frac{1}{2} \rho A V_\infty^2 \frac{8}{\lambda^2} \int_0^\lambda a(1-a) \left(1 + \frac{C_D}{C_L} \tan\theta\right) \lambda_r d\lambda_r \quad (3.4.8)$$

$$Q = \frac{1}{2} \rho A V_\infty^2 R \frac{8}{\lambda^3} \int_0^\lambda a(1-a) \left(1 - \frac{C_D}{C_L} \frac{1}{\tan\theta}\right) (\lambda_r)^3 d\lambda_r \quad (3.4.9)$$

and,

$$P = \frac{1}{2} \rho A V_\infty^3 \frac{8}{\lambda^2} \int_0^\lambda a(1-a) \left(1 - \frac{C_D}{C_L} \frac{1}{\tan\theta}\right) (\lambda_r)^3 d\lambda_r \quad (3.4.10)$$

These equations are valid only for a wind turbine having infinite number of blades.

3.5 Tip and Hub Losses

In the preceding sections the rotor was assumed to be possessing an infinite number of blades with infinitely small chord. Practically, the number of blades is finite. In the theory discussed early, the wind imparts a rotation to the rotor, therefore, dissipating some of its kinetic energy or velocity and creating a pressure difference between one side on the blade to the other side. At tip and hub, this pressure difference leads to secondary flow effects. The flow becomes three-dimensional and

tries to equalize the pressure difference as shown in the Figure 3.5.1. This effect is more pronounced as one approaches the tip. As a result, the torque on the rotor is reduced and output power also reduced.

Several different existing models take into account this loss, discussed in reference[48]. The method suggested by Prandtl will be used here. The idea in Prandtl's method is to replace the system of vortices at the tip with a series of parallel planes for which the flow is more easily calculated. The correction factor suggested by Prandtl is,

$$F_{tip} = \frac{2}{\pi} \arccos e^{-f}$$

Where, $f = \frac{B}{2} \frac{R-r}{R \sin \phi}$

For hub region f is defined as,

$$f = \frac{B}{2} \frac{r-r_{hub}}{r_{hub} \sin \phi}$$

Hence, the correction factor F for total losses will be,

$$F = F_{tip} \times F_{hub} \quad (3.5.1)$$

The loss factor F may be introduced in several ways for the rotor performance calculations. In the method adopted by Wilson and Lissaman [47], the induction factors a and a' are multiplied with F , and thus the axial and tangential velocities in the rotor plane are modified. Further assumption is that these corrections only involve in the momentum formulas. Therefore, the thrust and torque from momentum theory become,

$$dT = 4\pi \rho r V_{\infty}^2 a F (1-aF) dr \quad (3.5.2)$$

$$dQ = 4\pi \rho r^3 V_{\infty} a F (1-aF) \Omega dr \quad (3.5.3)$$

The expressions of the blade element theory remain unchanged.

$$dT = (1-a)^2 \frac{\sigma C_L \cos \phi}{\sin^2 \phi} \left(1 + \frac{C_D}{C_L} \tan \phi\right) \frac{1}{2} \rho V_{\infty}^2 2\pi r dr \quad (3.3.11)$$

$$\text{and, } dQ = (1+a)^2 \frac{\sigma C_L \sin \phi}{\cos^2 \phi} \left(1 - \frac{C_D}{C_L} \frac{1}{\tan \phi}\right) \frac{1}{2} \rho \Omega^2 r^3 2\pi r dr \quad (3.3.12)$$

Equation (3.3.12) can also be written as,

$$dQ = (1-a)^2 \frac{\sigma C_L}{\sin \phi} \left(1 - \frac{C_D}{C_L} \frac{1}{\tan \phi}\right) \frac{1}{2} \rho V_{\infty}^2 2\pi r^2 dr \quad (3.5.4)$$

Balancing the equation (3.5.2) with (3.3.11) one can obtain,

$$aF(1-aF) = \frac{\sigma C_L \cos \phi (1-a)^2}{4 \sin^2 \phi} \left(1 + \frac{C_D}{C_L} \tan \phi\right) \quad (3.5.5)$$

and considering the equations (3.5.3) and (3.5.4),

$$aF(1-aF) = (1-a)^2 \frac{\sigma C_L}{4 \sin \phi} \left(1 - \frac{C_D}{C_L} \frac{1}{\tan \phi}\right) \quad (3.5.6)$$

Neglecting the drag terms in equations (3.5.5) and (3.5.6),

$$aF(1-aF) = \frac{\sigma C_L \cos \phi (1-a)^2}{4 \sin^2 \phi} \quad (3.5.7)$$

$$aF(1-aF) = (1-a)^2 \frac{\sigma C_L}{4 \sin \phi} \quad (3.5.8)$$

From the equations (3.5.7) and (3.5.8), the final expressions for elemental torque and thrust become,

$$dT = 4aF(1-aF) \left(1 + \frac{C_D}{C_L} \tan \phi\right) \rho V_\infty^2 \pi r dr \quad (3.5.9)$$

and,

$$dQ = 4aF(1-aF) \left(1 - \frac{C_D}{C_L} \frac{1}{\tan \phi}\right) \rho V_\infty^2 \pi r^2 dr \quad (3.5.10)$$

3.6 Equations for Total Thrust, Torque and Power Coefficient

Elemental thrust, torque and power coefficients are defined as,

$$dC_T = \frac{dT}{\frac{1}{2} \rho A V_\infty^2} \quad (3.6.1)$$

$$dC_Q = \frac{dQ}{\frac{1}{2} \rho A V_\infty^2 R} \quad (3.6.2)$$

$$\text{and, } dC_P = \frac{dP}{\frac{1}{2} \rho A V_\infty^3} = \frac{\Omega \cdot dQ}{\frac{1}{2} \rho A V_\infty^3}$$

$$\text{or, } dC_P = \frac{dQR \cdot \Omega}{\frac{1}{2} \rho A V_\infty^2 R V_\infty} = \lambda \cdot dC_Q \quad (3.6.3)$$

Considering the equations (3.5.9) and (3.6.1), elemental thrust coefficient can be written as,

$$dC_T = \frac{8}{R^2} aF(1-aF) \left(1 + \frac{C_D}{C_L} \tan\theta\right) r dr \quad (3.6.4)$$

Again from equations (3.5.10) and (3.6.2), elemental torque coefficient can be written as,

$$dC_Q = \frac{8}{R^3} aF(1-aF) \left(1 - \frac{C_D}{C_L} \frac{1}{\tan\theta}\right) r^2 dr \quad (3.6.5)$$

Elemental power coefficient can be found from the equations (3.6.3) and (3.6.5),

$$dC_P = \frac{8\Omega}{R^2 V_\infty} aF(1-aF) \left(1 - \frac{C_D}{C_L} \frac{1}{\tan\theta}\right) r^2 dr \quad (3.6.6)$$

Finally, the total thrust, torque and power coefficients can be found by integrating along the radius R.

$$C_T = \frac{8}{R^2} \int_0^R aF(1-aF) \left(1 + \frac{C_D}{C_L} \tan\theta\right) r dr \quad (3.6.7)$$

$$C_Q = \frac{8}{R^3} \int_0^R aF(1-aF) \left(1 - \frac{C_D}{C_L} \frac{1}{\tan\theta}\right) r^2 dr \quad (3.6.8)$$

and,

$$C_P = \frac{8\Omega}{R^2 V_\infty} \int_0^R aF(1-aF) \left(1 - \frac{C_D}{C_L} \frac{1}{\tan\theta}\right) r^2 dr \quad (3.6.9)$$

3.7 Expressions for Maximum Power

For maximum power output the relation between a and a may be expressed by the equation (3.2.16),

$$\dot{a} = \frac{(1-3a)}{(4a-1)} \quad (3.2.16)$$

Introducing the equations of induction factors as follows,

$$\frac{a}{1-a} = \frac{\sigma C_L \cos\theta}{4 \sin^2\theta} \quad (3.4.3)$$

$$\text{and, } \frac{\dot{a}}{1+\dot{a}} = \frac{\sigma C_L}{4 \cos\theta} \quad (3.4.4)$$

From the above equations (3.2.16), (3.4.3) and (3.4.4), the

following expression is found,

$$\sigma C_L = 4(1 - \cos\phi) \quad (3.7.1)$$

Considering the local solidity σ as,

$$\sigma = \frac{B C}{2\pi r} \quad (3.3.10)$$

From equations (3.7.1) and (3.3.10), we have

$$C = \frac{8\pi r}{B C_L} (1 - \cos\phi) \quad (3.7.2)$$

Local tip speed ratio r is given by,

$$\lambda_r = \frac{r\Omega}{V_\infty} \quad (3.2.8)$$

From the equation (3.3.8),

$$\tan\phi = \frac{(1-a)V_\infty}{r\Omega(1+a)} = \frac{(1-a)}{(1+a)} \times \frac{1}{\lambda_r} \quad (3.3.8)$$

Now, replacing the values of $(1-a)$ and $(1+a)$ from equations (3.4.3) and (3.4.4), and putting the value of σC_L from equation (3.7.1), the following relation can be deduced,

$$\lambda_r = \frac{\sin\phi(2\cos\phi - 1)}{(1 - \cos\phi)(2\cos\phi + 1)} \quad (3.7.3)$$

and this can be reduced to,

$$\phi = \frac{2}{3} \arctan \frac{1}{\lambda_r} \quad (3.7.4)$$

Equation of the blade twist angle can be written as,

$$\beta_r = \phi - \alpha \quad (3.3.9)$$

equations (3.7.2), (3.2.8), (3.7.4) and (3.3.9) will be required to calculate the blade configuration later.

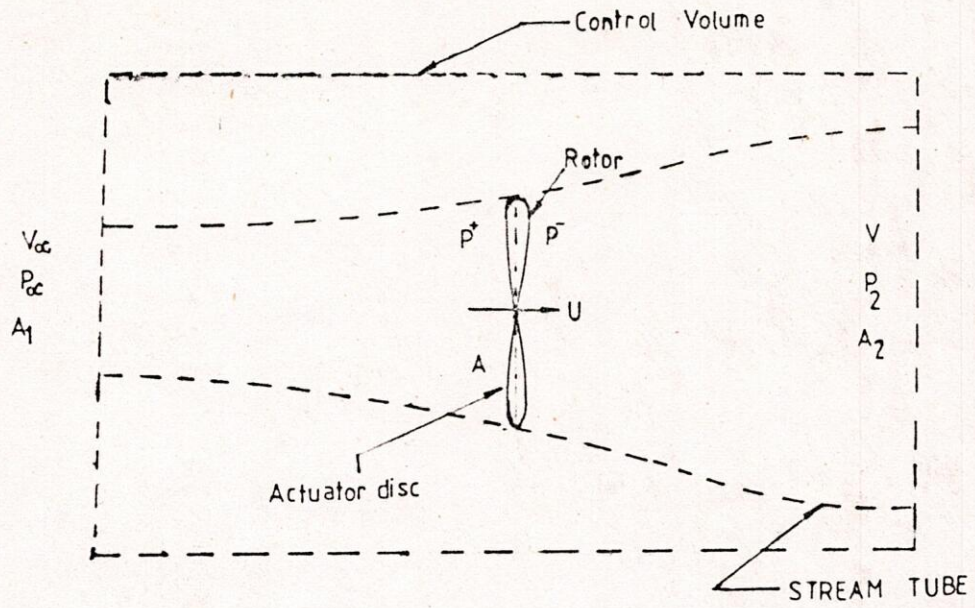


Fig3.1.1 : Wind Turbine Stream Tube.

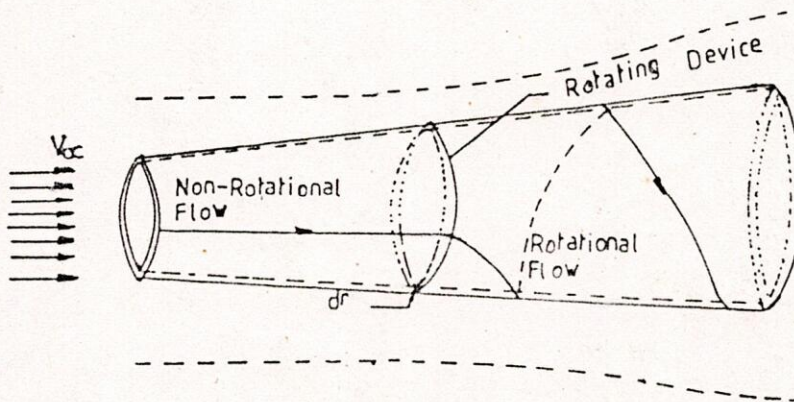


Fig.3.2.1 : Streamtube Showing Wake Rotation.

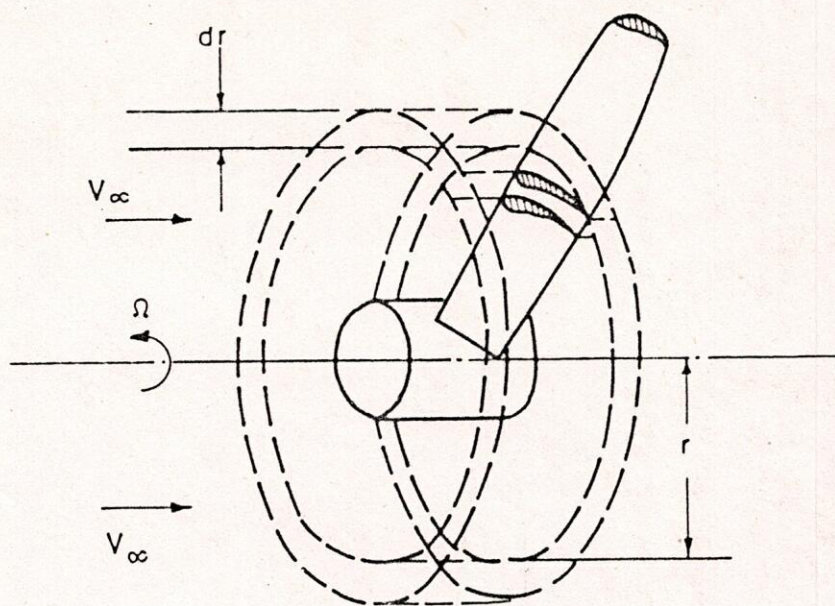


FIGURE 3.2.2: BLADE ELEMENT ANNULAR RING

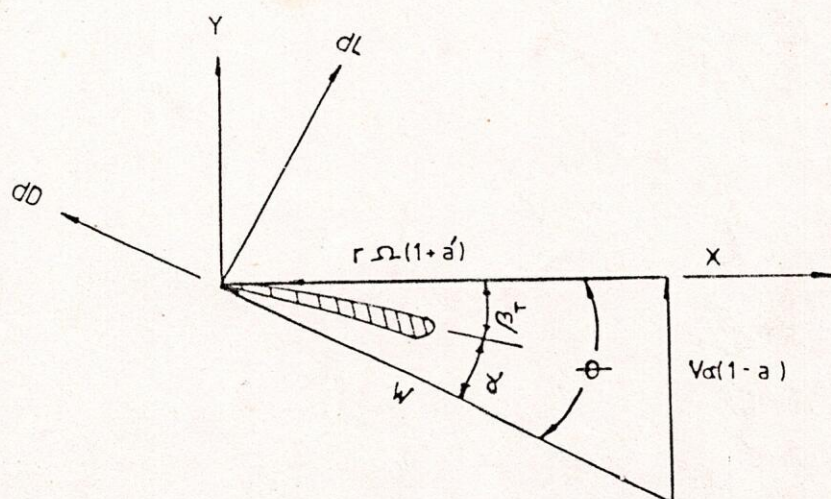


Fig3.3.1: Blade Element Velocity Diagram.

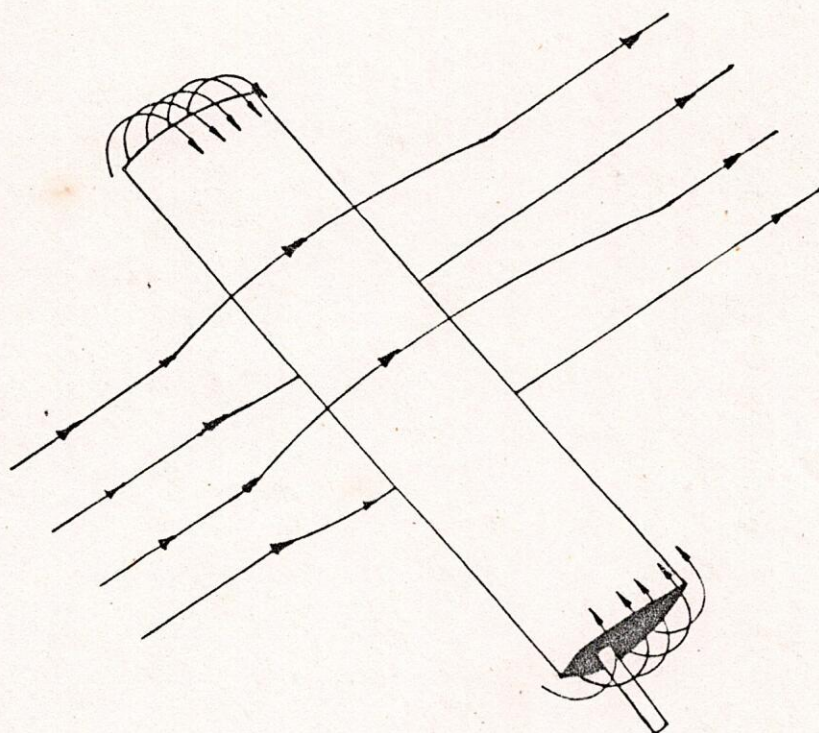


Fig. 3.5.1 : Tip and Hub Losses Flow Diagram [48].

CHAPTER IV

MODIFICATION OF EXISTING THEORIES

4.0 General

In the preceding chapter, the assumption is that the flow of stream is steady uniform. For performance analysis each individual streamtubes was taken as an annuli without interacting each other.

The velocity field of the wind may be non-uniform with time as well as spatial distribution. This means that effect of wind shear, wind shift, tower shadow, coning and tilting on performance must be considered. Angle of attack α and wind speed W are different from the previously used value for each blade segment and no longer axially symmetric. Which indicates that the wind velocity and the induction factors are not constant inside a annular streamtube, but they depend on the azimuthal position of the blade. The individual streamtubes can no longer be taken as annuli but must be of elemental area dA , perpendicular to the wind direction.

In the following chapter, the performance of a horizontal axis wind turbine is done in a quasi steady manner, it means lift, drag, axial and tangential induced velocities are calculated for several azimuthal position of the rotor. The procedure used is similar to the case a uniform wind velocity along the rotor axis and is used on a combination of moentum and blade element theory.

4.1: Velocity Components at the Blade at the Different Frame of Reference

For the aerodynamic and structural analysis the velocity components of the air flow relative to any point on the blade and the induced velocity components required to determine. Different frame of reference are considered to include the effects of wind shift, tilting, coning and azimuth. These frame of reference are shown in the Figures 4.1.1 to 4.1.4. A referance frame S_0 , is fixed at the top of the tower of a wind turbine with Z_0 is the vertical axis and (X_0, Y_0) forming horizontal plane. A second non-rotating frame S_1 is fixed at the tip of the nacelle is introduced by translation of the initial frame over a certain distance Y and a rotation of tilting angle α_r around the X_0 axis. A rotating frame S_2 is introduced by rotation of the reference frame S_1 over an azimuth angle θ_k . Finally, a local reference frame S_3 is attached to a particular point of the blade at a distance r from the hub and is rotated over a coning angle β . The relationships between the reference frames can be expressed as,

$$S_1 = [K_T] S_0$$

$$S_2 = [K_\theta] S_1$$

$$S_3 = [K_\beta] S_2$$

and inversely,

$$S_0 = [K_T]^T S_1$$

$$S_1 = [K_\theta]^T S_2$$

$$S_2 = [K_\beta]^T S_3$$

the superscript T indicates the transposed matrix. The transformation matrices are,

$$\text{for tilting, } K_T = \begin{vmatrix} 1 & 0 & 0 \\ 0 & \cos \alpha_T & -\sin \alpha_T \\ 0 & \sin \alpha_T & \cos \alpha_T \end{vmatrix}$$

$$\text{for azimuth, } K_\theta = \begin{vmatrix} \cos \theta_k & 0 & \sin \theta_k \\ 0 & 1 & 0 \\ -\sin \theta_k & 0 & \cos \theta_k \end{vmatrix}$$

$$\text{for coning, } K_\beta = \begin{vmatrix} 1 & 0 & 0 \\ 0 & \cos \beta & -\sin \beta \\ 0 & \sin \beta & \cos \beta \end{vmatrix}$$

In the fixed frame of reference S_0 , considering the wind shift the wind velocity can be expressed as,

$$\tilde{V}_{S_0} = V_\infty \begin{vmatrix} \cos \gamma \\ \sin \gamma \\ 0 \end{vmatrix} \quad \gamma = 90 - \gamma^* \quad (4.1.1)$$

Where, γ^* is the wind shift angle in relation to the nacelle axis. The wind velocity components in the S_3 frame of reference is,

$$\tilde{V}_{S_3} = [K_\beta]^T [K_\theta]^T [K_T]^T \tilde{V}_{S_0} \quad (4.1.2)$$

$$\text{or, } V_{S_3} = [K_\beta]^T [K_\theta]^T [K_T]^T \begin{vmatrix} \cos \gamma \\ \sin \gamma \\ 0 \end{vmatrix} V_\infty$$

Which can be expressed in the following form,

$$\vec{V}_{s3} = V_{\infty} \begin{vmatrix} \cos \gamma \cos \theta_k + \sin \gamma \sin \theta_k \sin \alpha \tau \\ \sin \gamma \cos \alpha \tau \cos \beta + \cos \gamma \sin \beta \sin \theta_k - \sin \gamma \sin \alpha \tau \cos \theta_k \sin \beta \\ -\sin \gamma \sin \beta \cos \alpha \tau + \cos \gamma \sin \theta_k \cos \beta - \sin \gamma \cos \theta_k \sin \alpha \tau \cos \beta \end{vmatrix} \quad (4.1.3)$$

4.2 Effect of Wind Shear

Wind flow is seriously affected by friction near the earth surface. Because of this friction, a boundary layer is developed and wind velocity gradient with altitude is created. The wind shear depends on the wind direction, the wind velocity and stability of the atmosphere. Surface roughness vary from coast (smooth) to city centre (rough). Velocity profile will depend upon the nature of the terrain.

Atmospheric boundary layer is considered two-dimensional for the present work, though it is three-dimensional and complicated. The velocity of the wind increases with the height up to a level where the friction is neglected. The level is called the gradient height Z_g and the velocity at gradient height is called the gradient velocity V_g . The distance between the surface of the earth and the gradient height is the thickness of the boundary layer.

The variation of the wind velocity with the height can be expressed analytically by a power law as,

$$\frac{V_{\infty 0}}{V_{Ref}} = \left(\frac{Z}{Z_{Ref}} \right)^n \quad 0.15 < n < 0.45 \quad (4.2.1)$$

Where,

$V_{\infty 0}$ = Wind velocity at the height, Z

V_{Ref} = Reference wind velocity.

Z_{Ref} = Reference height.

n = Power law exponent.

The main source of fluctuating aerodynamic load is the wind shear which is once per revolution for a wind turbine. The instantaneous wind velocity approaching an upwind or a downwind rotor corresponding to a particular point of the blade can be deduced as follows

Radial distance of a particular point on the blade can be expressed in S_0 co-ordinate system as,

$$\begin{vmatrix} X_0 \\ Y_0 \\ Z_0 \end{vmatrix} = [K_T][K_{\theta}][K_{\beta}] \begin{vmatrix} 0 \\ 0 \\ R_L \end{vmatrix} \quad (4.2.2)$$

Where, R_L is the radial distance of a point from the root of the blade. This leads to the following expression-

$$\begin{vmatrix} X_o \\ Y_o \\ Z_o \end{vmatrix} = \begin{vmatrix} R_L \cos \beta \sin \theta_k \\ -R_L \sin \beta \cos \alpha_T - R_L \cos \beta \cos \theta_k \sin \alpha_T \\ -R_L \sin \beta \sin \alpha_T + R_L \cos \beta \cos \theta_k \cos \alpha_T \end{vmatrix} \quad (4.2.3)$$

Now, the height of a particular point of the blade from the ground level is written as,

$$Z = Z_{Ref} + Z_o$$

$$\text{or, } Z = Z_{Ref} + R_L (-\sin \beta \sin \alpha_T + \cos \beta \cos \theta_k \cos \alpha_T) \quad (4.2.4)$$

Considering Z_{Ref} as the hub height of a wind turbine from the ground level and putting the value of Z in equation (4.2.1), one finds,

$$V_{\infty} = V_{Ref} \left[\frac{H + R_L (-\sin \beta \sin \alpha_T + \cos \beta \cos \theta_k \cos \alpha_T)}{H} \right]^n \quad (4.2.5)$$

Now the equation for wind velocity approaching at a particular point of the K th blade corresponding to an azimuthal angle θ and wind shift angle γ , can be expressed as

$$V_{\theta} = V_{Ref} \sin \gamma \left[1 - \frac{R_L}{H} (\sin \beta \sin \alpha_T - \cos \beta \cos \theta_k \cos \alpha_T) \right]^n \quad (4.2.6)$$

Where,

V_{Ref} = Reference wind velocity at the centre line of the rotor.
 H = Hub height from the ground level.

At hub height if the reference wind velocity is V_{∞} , above equation becomes

$$V_{\theta k} = V_{\infty} \sin \gamma \left[1 - \frac{R_L}{H} (\sin \beta \sin \alpha_T - \cos \beta \cos \theta_k \cos \alpha_T) \right]^n \quad (4.2.7)$$

This equation may be used for structural analysis.

The vertical wind gradient will induce forces and moments as shown in the Figure 4.2.1. The largest of these are torque variation and the pitching moment.

4.3 Momentum Theory

Radial elemental area dA subtended by a small angle $d\theta$ in the plane of the rotor is shown in the Figure 4.3.1. Introducing the angular interference factor \acute{a} from equation (3.2.2),

$$\acute{a} = \frac{\omega}{2\Omega} \quad (3.2.2)$$

and using the small segment in the above Figure the thrust can be written as,

$$dT = d\dot{m}(V_{\infty} - V)$$

$$\text{or, } dT = \rho U dA (V_{\infty} - V) \quad (4.3.1)$$

Equation (3.1.10) is expressed as,

$$U = V_{\infty} (1-a) \quad (3.1.10)$$

Considering the wind shear, wind shift and tilting, it may be rewritten as,

$$U = V_{\infty} \cos \alpha \tau \sin \gamma (1-a) \quad (4.3.2)$$

Equation (3.1.11) can be expressed as,

$$V_{\infty} - V = 2aV_{\infty} \quad (3.1.11)$$

With the addition of wind shear, yawing and tilting, this equation becomes,

$$V_{\infty} - V = 2aV_{\infty} \cos \alpha \tau \sin \gamma \quad (4.3.3)$$

Now for a coned blade the expression for differential area dA can be written as,

$$dA = r \cos^2 \beta dr d\theta \quad (4.3.4)$$

The expression for thrust becomes,

$$dT = 2 \rho r \cos^2 \beta \cos^2 \alpha \tau \sin^2 \gamma V_{\infty}^2 a (1-a) dr d\theta \quad (4.3.5)$$

Due to the change of momentum in the air in tangential direction tangential force acting upon the elemental area dA ,

$$\begin{aligned} dF_t &= \dot{m} \omega r \cos \beta \\ \text{or, } dF_t &= \rho U dA r \omega \cos \beta \end{aligned} \quad (4.3.6)$$

Taking the equations (3.2.2), (4.3.2) and (4.3.4) the tangential force is expressed as,

$$dF_t = 2 \rho a \Omega r^2 \cos^3 \beta (1-a) V_{\infty} \cos \alpha \tau \sin \gamma dr d\theta \quad (4.3.7)$$

The torque equation can be written as,

$$dQ = dF_t r \cos \beta$$

Putting the value of dF_t , from the equation (4.3.7) we have,

$$dQ = 2 \rho r^3 a (1-a) V_{\infty} \cos \alpha \tau \sin \gamma \cos^4 \beta \Omega dr d\theta \quad (4.3.8)$$

4.4 Blade Element Theory

The velocity components acting on a blade element rotating at a radius r are shown in the Figure 4.4.1. Now, introducing the induced velocity v in S_3 co-ordinate system as,

$$\vec{v}_{s3} = \begin{vmatrix} v_t \\ v_a \cos \beta \cos \alpha r \\ v_v \end{vmatrix} \quad (4.4.1)$$

Where,

v_t = Tangential component of induced velocity.

v_a = Axial component of induced velocity.

v_v = Vertical component of induced velocity.

Equation (4.4.1) may be written as,

$$\vec{v}_{s3} = \begin{vmatrix} \Omega r \cos \beta a \\ V_\infty a \cos \beta \cos \alpha r \sin \gamma \\ v_v \end{vmatrix} \quad (4.4.2)$$

The rotational motion of the blade will add a velocity component $\Omega r \cos \beta$ in the total velocity vector relative to blade and this component can be written in S_3 co-ordinate system as,

$$\vec{v}_{b1} = \begin{vmatrix} \Omega r \cos \beta \\ 0 \\ 0 \end{vmatrix} \quad (4.4.3)$$

With the effect of wind shear the components of the relative velocity W can be expressed from equation (4.1.3), (4.4.2) and (4.4.3) as,

$$W_x = V_\infty \cos \gamma \cos \theta_k + V_\infty \sin \gamma \sin \theta_k \sin \alpha r - \Omega r \cos \beta (1+a) \quad (4.4.4)$$

and

$$W_y = V_\infty [\sin \gamma \cos \alpha r \cos \beta (1-a) + \sin \beta \sin \theta_k \cos \gamma - \sin \gamma \sin \beta \sin \alpha r \cos \theta_k] \quad (4.4.5)$$

The local angle of attack α is defined as,

$$\alpha = \phi - \beta r = \tan^{-1} \frac{W_y}{W_x} - \beta r \quad (4.4.6)$$

and the relative velocity,

$$W = (W_x^2 + W_y^2)^{1/2} \quad (4.4.7)$$

The aerodynamic force components acting on the blade element are the lift force dL perpendicular to the resulting velocity vector and drag force dD acting along the direction of the resulting velocity vector. The following expressions are used for the sectional lift and drag forces.

$$dL = \frac{1}{2} C_L \rho W^2 dA \quad (4.4.8)$$

$$dD = \frac{1}{2} C_D \rho W^2 dA \quad (4.4.9)$$

Because we are assuming an infinite number of blades, the differential area dA is given as,

$$dA = \frac{BCd\theta dr}{2\pi} \cos\beta \quad (4.4.10)$$

So, the elemental lift and drag forces are,

$$dL = \frac{1}{2} C_L \rho W^2 \frac{BCd\theta dr}{2\pi} \cos\beta \quad (4.4.11)$$

$$dD = \frac{1}{2} C_D \rho W^2 \frac{BCd\theta dr}{2\pi} \cos\beta \quad (4.4.12)$$

The thrust and torque of the blade element are,

$$\text{or, } dT = dL \cos\theta + dD \sin\theta \quad (4.4.13)$$

$$\text{and, } dQ = (dL \sin\theta - dD \cos\theta) r$$

$$\text{or, } dQ = \sin\theta \left(dL - \frac{dD}{\tan\theta} \right) r \quad (4.4.14)$$

Considering the equations (4.4.11) and (4.4.12) the thrust and torque equations are,

$$dT = \frac{1}{2} \rho W^2 \cos\theta (C_L + C_D \tan\theta) \frac{BCd\theta dr}{2\pi} \cos\beta \quad (4.4.15)$$

$$\text{and, } dQ = \frac{1}{2} \rho W^2 \sin\theta \left(C_L - \frac{C_D}{\tan\theta} \right) \frac{BCr d\theta dr}{2\pi} \cos\beta \quad (4.4.16)$$

Equations for thrust and torque co-efficients are,

$$dC_T = \frac{dT}{\frac{1}{2} \rho A V_\infty^2} = \left(\frac{W}{V_\infty} \right)^2 \frac{\sigma r}{\pi R^2} \cos\theta (C_L + C_D \tan\theta) \cos\beta dr d\theta$$

$$\text{or, } dC_T = \left(\frac{W}{V_\infty} \right)^2 \frac{\sigma C_L \cos\theta}{\pi R^2} \left(1 + \frac{C_D}{C_L} \tan\theta \right) \cos\beta r dr d\theta \quad (4.4.17)$$

again,

$$dC_Q = \frac{dQ}{\frac{1}{2} \rho A V_\infty^2 R} = \left(\frac{W}{V_\infty} \right)^2 \frac{\sigma r^2}{\pi R^3} \sin\theta \left(C_L - \frac{C_D}{\tan\theta} \right) \cos\beta dr d\theta$$

$$\text{or, } dC_Q = \left(\frac{W}{V_\infty}\right)^2 \frac{\sigma C_L \sin\phi}{\pi R^3} \left(1 - \frac{C_D}{C_L \tan\phi}\right) \cos\beta r^2 dr d\theta \quad (4.4.18)$$

Therefore, elemental power coefficient is,

$$dC_P = \frac{dP}{\frac{1}{2}\rho AV_\infty^3} = \frac{\Omega dQ}{\frac{1}{2}\rho AV_\infty^3}$$

$$\text{or, } dC_P = \frac{\Omega R dQ}{\frac{1}{2}\rho AV_\infty^3 R} = dC_Q \cdot \lambda \quad (4.4.19)$$

4.5 Strip Theory

To calculate the interference factor a and a' equations for thrust and torque from the momentum theory and the blade element theory are to be equated.

$$dT_{\text{Blade Element}} = dT_{\text{Momentum}}$$

$$dQ_{\text{Blade Element}} = dQ_{\text{Momentum}}$$

Equating the equations (4.3.5) and (4.4.15) and introducing the tip loss factor F we have,

$$a(1-aF) = \frac{\sigma W^2 \cos\phi (C_L + C_D \tan\phi)}{8 \cos\beta \cos^2 \alpha_T \sin^2 \gamma V_\infty^2 F} \quad (4.5.1)$$

Again equating the equations (4.3.8) and (4.4.16) and considering tip loss factor F we have,

$$a'(1-aF) = \frac{\sigma W^2 \sin\phi (C_L - C_D / \tan\phi)}{8r \cos\beta^3 \cos \alpha_T \sin \gamma V_\infty F \Omega} \quad (4.5.2)$$

According to reference [47] the drag terms should be neglected in the calculations of a and a' , then the equations (4.5.1) and (4.5.2) become,

$$a(1-aF) = \frac{\sigma W^2 \cos\phi C_L}{8 \cos\beta \cos^2 \alpha_T \sin^2 \gamma V_\infty^2 F} \quad (4.5.3)$$

and,

$$a'(1-aF) = \frac{\sigma W^2 \sin\phi C_L}{8r \cos\beta^3 \cos \alpha_T \sin \gamma V_\infty F \Omega} \quad (4.5.4)$$

4.6 Equations for Thrust, Torque and Power Coefficient

From the equations (4.4.17) and (4.5.3) the elementary thrust coefficient can be written as,

$$dC_T = \frac{8}{\pi R^2} \left(\frac{V_{\infty o}}{V_{\infty}}\right)^2 aF(1-aF) \cos\beta^2 \cos^2\alpha_T \sin^2\gamma \left(1 + \frac{C_D}{C_L} \tan\phi\right) r dr d\theta \quad (4.6.1)$$

Therefore, the total thrust coefficient is,

$$C_T = \frac{8}{\pi R^2} \cos\beta^2 \cos^2\alpha_T \sin^2\gamma \int_0^{2\pi} \int_0^R \left(\frac{V_{\infty o}}{V_{\infty}}\right)^2 aF(1-aF) \left(1 + \frac{C_D}{C_L} \tan\phi\right) r dr d\theta \quad (4.6.2)$$

Considering equations (4.4.18) and (4.5.4) the elemental torque coefficient can be expressed as,

$$dC_Q = \frac{8}{\pi R^3} \frac{V_{\infty o} r^3}{V_{\infty}^2} aF(1-aF) \cos\beta^4 \cos\alpha_T \sin\gamma \left(1 - \frac{C_D}{C_L} \frac{1}{\tan\phi}\right) \Omega dr d\theta \quad (4.6.3)$$

So, the total torque coefficient is,

$$C_Q = \frac{8\Omega}{\pi R^3 V_{\infty}^2} \cos\beta^4 \cos\alpha_T \sin\gamma \int_0^{2\pi} \int_0^R V_{\infty o} r^3 aF(1-aF) \left(1 - \frac{C_D}{C_L} \frac{1}{\tan\phi}\right) dr d\theta \quad (4.6.4)$$

From the equation (4.4.19) elemental power coefficient will be,

$$dC_P = dC_Q \cdot \lambda \quad (4.4.19)$$

Hence the total power coefficient can be found as,

$$C_P = \frac{8\Omega^2}{\pi R^3 V_{\infty}^2} \cos\beta^4 \cos\alpha_T \sin\gamma \int_0^{2\pi} \int_0^R V_{\infty o} r^3 aF(1-aF) \left(1 - \frac{C_D}{C_L} \frac{1}{\tan\phi}\right) dr d\theta \quad (4.6.5)$$

4.7 Forces and Moments at the Different Frame of Reference

Four co-ordinate systems are required for forces and moments analysis. The forces are divided into two components. One acting in the plane of the rotor and another acting normal to the rotor plane. The co-ordinate systems are discussed and shown in Appendix A.

S₀= Initial system attached to tower top.

S₁= Inertial system attached to hub which is created by translation and a rotation over a tilting angle α_T .

S₂= Rotating frame at hub which is introduced by rotation of the reference frame S₁ over an azimuth angle θ .

S₃= Local reference frame S₃ is attached to a specific point of the blade at a distance r from the hub and is rotated over a coning angle β .

4.7.1 Forces

All the forces in the local S_3 co-ordinate system can be expressed as,

$$\underline{\hat{F}}_{S_3} = \begin{bmatrix} F_{x3} \\ F_{y3} \\ F_{z3} \end{bmatrix} \quad (4.7.1.1)$$

Considering the non-rotating system S_1 attached to the hub the equation of forces is

$$\underline{\hat{F}}_{S_1} = [K_\theta][K_\beta]F_{S_3} \quad (4.7.1.2)$$

The following equation is obtained above equations (4.7.1.1) and (4.7.1.2),

$$\underline{\hat{F}}_{S_1} = \begin{bmatrix} F_{x3}\cos\theta + F_{y3}\sin\theta\sin\beta + F_{z3}\sin\theta\cos\beta \\ F_{y3}\cos\beta - F_{z3}\sin\beta \\ -F_{x3}\sin\theta + F_{y3}\cos\theta\sin\beta + F_{z3}\cos\theta\cos\beta \end{bmatrix} \quad (4.7.1.3)$$

At the top of the tower, the forces become,

$$\underline{\hat{F}}_{S_0} = [K_T]F_{S_1} = [K_T][K_\theta][K_\beta]\underline{\hat{F}}_{S_3} \quad (4.7.1.4)$$

$$\underline{\hat{F}}_{S_0} = \begin{bmatrix} F_{x3}\cos\theta & +F_{y3}\sin\theta\sin\beta + F_{z3}\sin\theta\cos\beta \\ F_{x3}\sin\alpha_T\sin\theta + F_{y3}(\cos\beta\cos\alpha_T - \sin\alpha_T\sin\beta\cos\theta) & -F_{z3}(\sin\beta\cos\alpha_T + \sin\alpha_T\cos\beta\cos\theta) \\ -F_{x3}\cos\alpha_T\sin\theta + F_{y3}(\cos\beta\sin\alpha_T + \cos\alpha_T\sin\beta\cos\theta) & +F_{z3}(\cos\beta\cos\alpha_T\cos\theta - \sin\beta\sin\alpha_T) \end{bmatrix} \quad (4.7.1.5)$$

4.7.2 Moments

In large wind turbine, running with low shaft speeds, blade bending loads are much more complicated than other loads. These bending loads are divided into two components, one around the Z-axis known as flapwise and the other around the Y-axis known as edgewise bending moment, as shown in the Figure 4.7.2.1. The flapwise bending moment produces stresses on the pressure and suction surfaces of the blade. While the edgewise bending moment produces stresses at the leading and trailing edges. For a downwind rotor, the flapwise and chordwise moments are dominated by the impulse applied to the blade each time it passes through the tower wake. It is customary to take flapwise bending moments positive which produce compression in the blade high pressure side. It means negative bending moments when an uncoined rotor is extracting power from the wind. Edgewise bending moment is considered negative when tension is produced in the blade trailing edge, that is, when the rotor is extracting power from the wind.

At the blade attachment point, the expression for moment to a differential element can be written as,

$$\vec{dM}_{s3} = d\vec{F}_{s3} \times \vec{r}_{s3} \quad (4.7.2.1)$$

This can be expressed as,

$$\vec{dM}_{s3} = \begin{vmatrix} i_3 & j_3 & k_3 \\ dF_{x3} & dF_{y3} & dF_{z3} \\ 0 & 0 & r_3 \end{vmatrix} \quad (4.7.2.2)$$

Where r_3 is the distance from the blade root along Z_3 direction. Above equation can be reduced as,

$$\begin{vmatrix} dM_{x3} \\ dM_{y3} \\ dM_{z3} \end{vmatrix} = \begin{vmatrix} r_3 dF_{y3} \\ -r_3 dF_{x3} \\ 0 \end{vmatrix} \quad (4.7.2.3)$$

The equations for total moments in different directions for one blade are written as follows,

$$\text{Flapwise moment, } M_{x3} = \int_0^R r_3 dF_{y3} \quad (4.7.2.4)$$

and,

$$\text{Edgewise moment, } M_{y3} = -\int_0^R r_3 dF_{x3} \quad (4.7.2.5)$$

At the tower top corresponding to S_0 co-ordinate system the moment can be expressed as,

$$\vec{M}_{s0} = \vec{F}_{s0} \times \vec{r}_{s0} \quad (4.7.2.6)$$

The following equation may be obtained from the above equation,

$$\begin{vmatrix} M_{x0} \\ M_{y0} \\ M_{z0} \end{vmatrix} = \begin{vmatrix} i_0 & j_0 & k_0 \\ F_{x0} & F_{y0} & F_{z0} \\ X_0 & Y_0 & Z_0 \end{vmatrix} \quad (4.7.2.7)$$

Where, X_0 , Y_0 and Z_0 are the moments arm in the respective coordinate system. Equation (4.7.2.7) can be reduced as,

$$\begin{vmatrix} M_{x0} \\ M_{y0} \\ M_{z0} \end{vmatrix} = \begin{vmatrix} Z_0 F_{y0} - Y_0 F_{z0} \\ X_0 F_{z0} - Z_0 F_{x0} \\ Y_0 F_{x0} - X_0 F_{y0} \end{vmatrix} \quad (4.7.2.8)$$

Where,

M_{x0} is called the pitching moment = M_p .

M_{y0} is called the rolling moment.

M_{z0} is called the yawing moment = M_{yaw} .

Practically, the flow of wind neither uniform, steady and unidirectional. Due to wind gradient and wind shift periodic

variations in torque, yawing moment and pitching moments can occur. These forces and moments will affect the overall system dynamics. The analysis has been applied to a downwind horizontal axis wind turbine, but can equally be applied to an upwind machine with suitable changes of sign. The pitching moment coefficient is,

$$C_{mp} = \frac{M_p}{1/2 \rho A V_\infty^2 R} \quad (4.7.2.9)$$

And, the yawing moment coefficient is,

$$C_{mz} = \frac{M_{yaw}}{1/2 \rho A V_\infty^2 R} \quad (4.7.2.10)$$

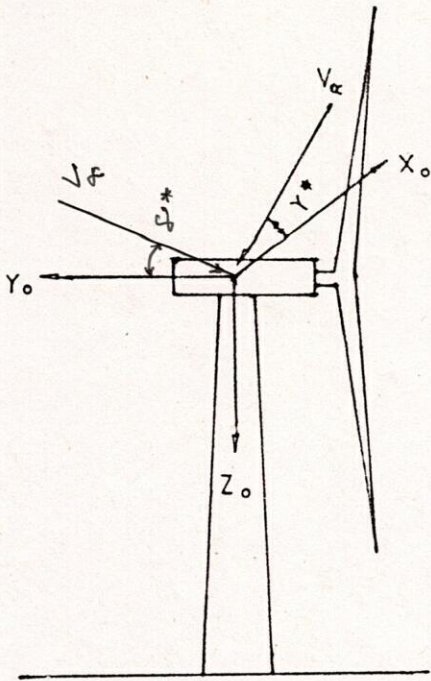


Fig. 4.1.1: Reference Frame S_0 .
(Coordinate System S_0)

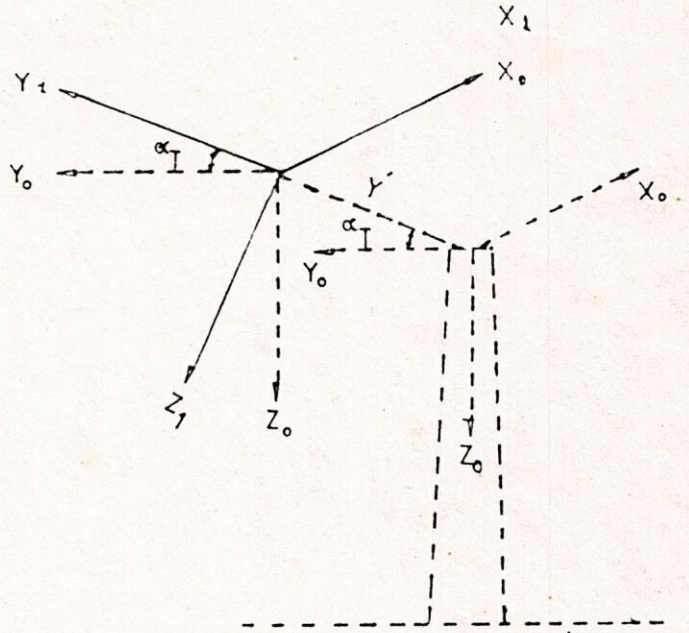


Fig. 4.1.2: Translation Over Y' and
Rotation About X_0 by Angle α_T .
(Coordinate System S_1)

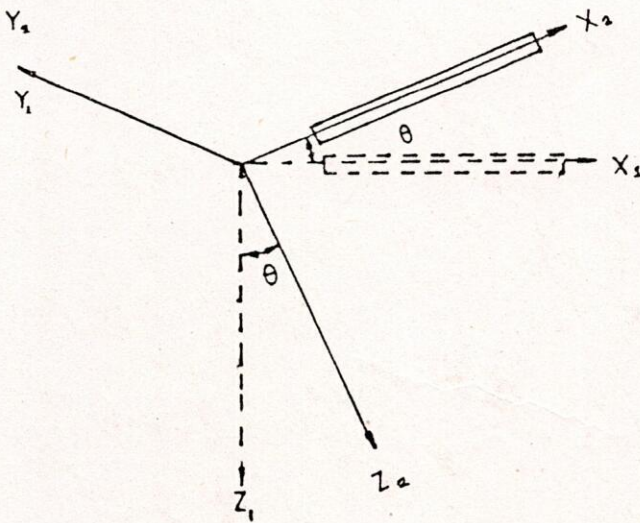


Fig. 4.1.3: Rotation About Y_1 by Angle θ .
(Coordinate System S_2)

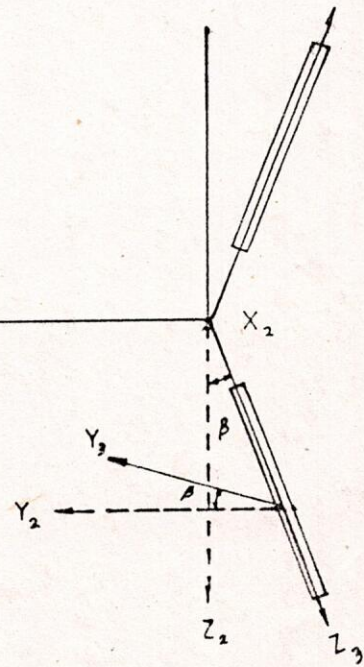


Fig. 4.1.4: Rotation About X_2 by Angle β .
(Coordinate System S_3)

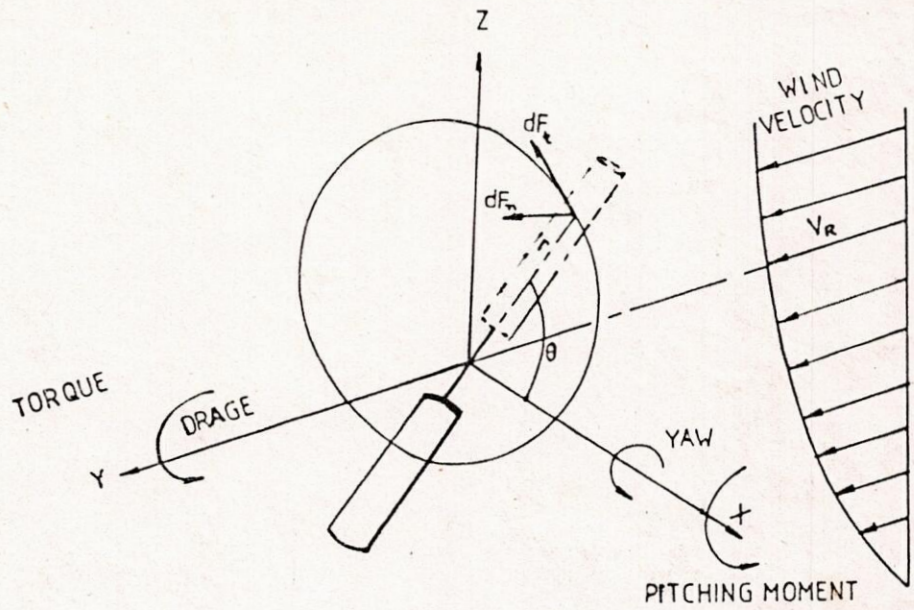


Fig.4.2.1: Effect of wind gradient on rotor.

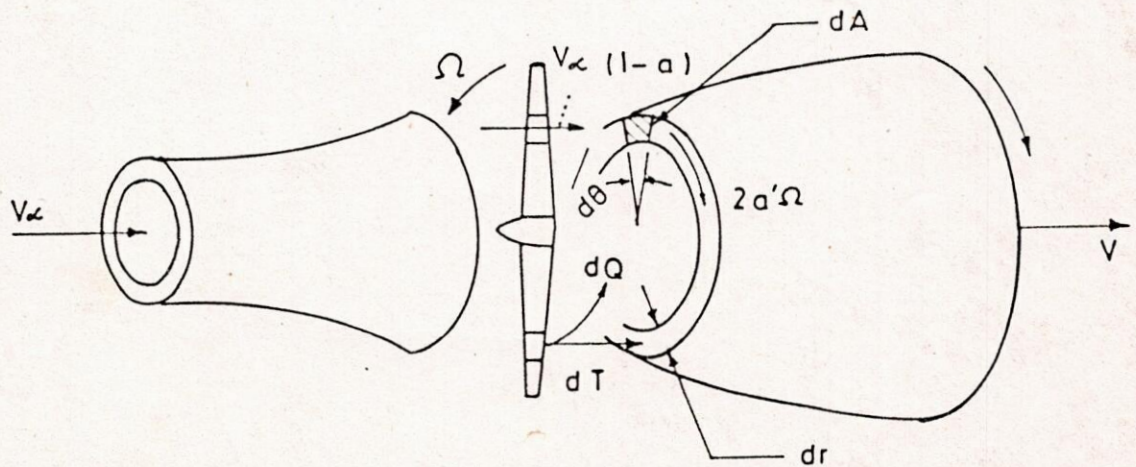


FIGURE 4.3.1.: ANALYTICAL MODEL FOR MOMENTUM THEORY.

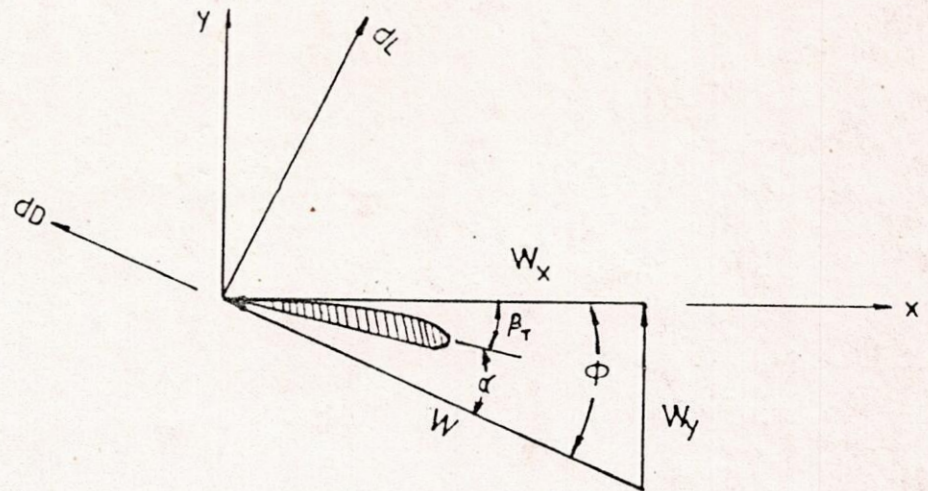


Fig.4.4.1 : Velocity Diagram for Rotor Blade Element.

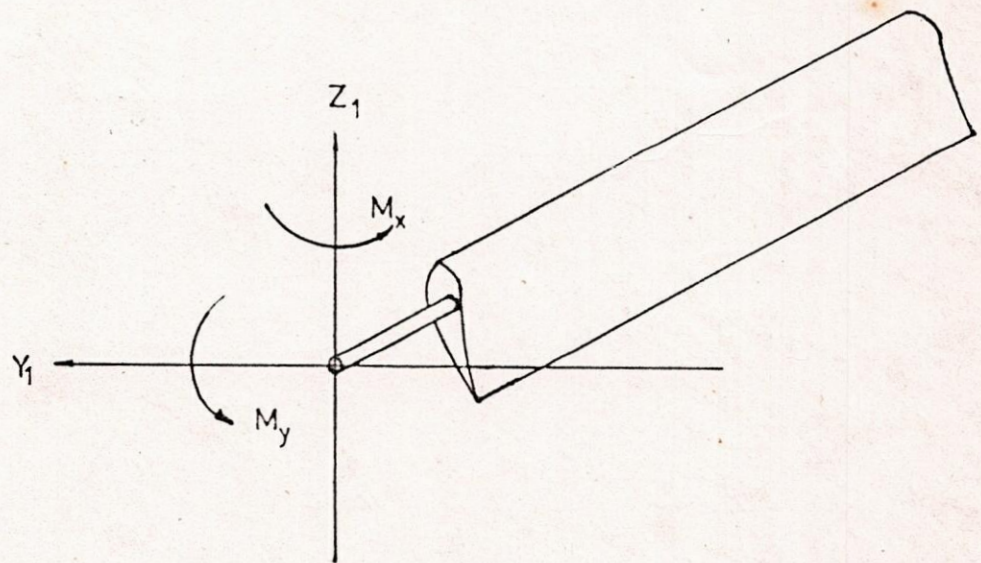


Fig.4.7.2.1: Flapwise and Edgewise Bending Moment.

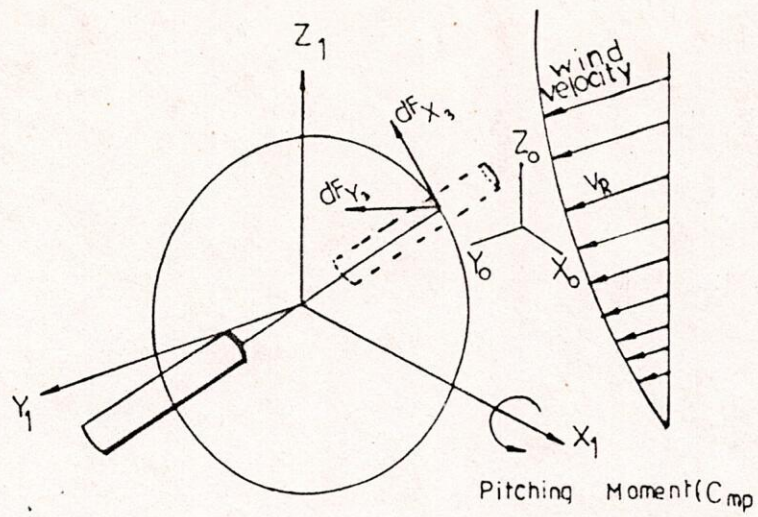


Fig.4.7.2.2 : Pitching Moment due to Wind Gradient.

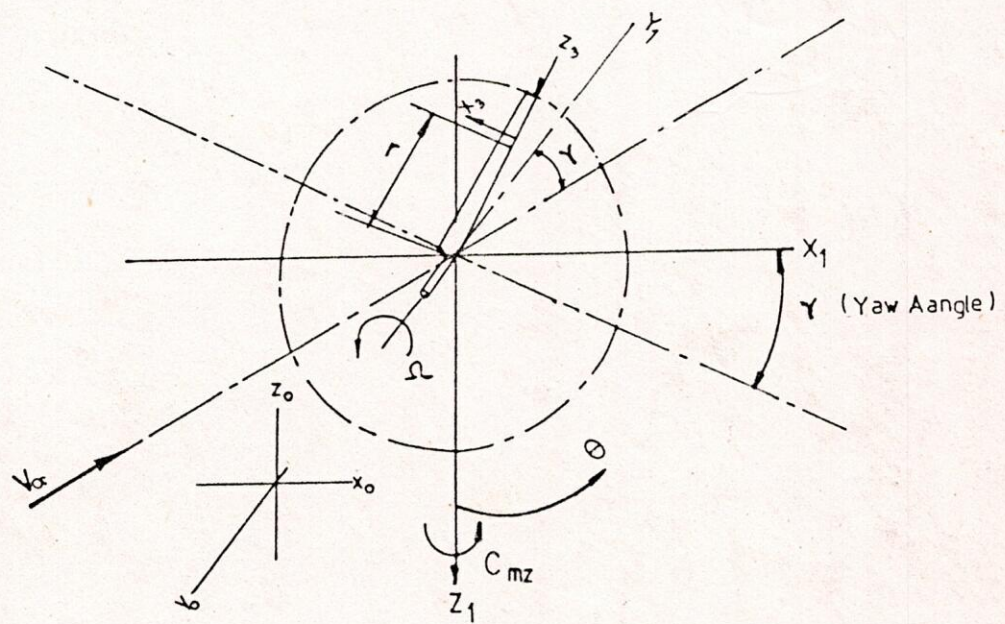


Fig.4.7.2.3 : Yawing Moment Due to Wind Shift.

CHAPTER V

DESIGN OF WIND TURBINE

5.0 General

In this chapter, the important parameters for the design of a horizontal axis wind turbine have been discussed. This includes the design tip speed ratio, the number of blades and airfoil data. Calculation scheme for blade configuration and performance analysis are also discussed. The design of a wind rotor consists of two steps:

1. The choice of basic parameters such as the design tip speed ratio, amount of power to be extracted, the radius of the rotor, the type of airfoil section and the numbers of blades.
2. The calculations of the blade twist angle βr and the chord C at a number of positions along the blade, in order to produce maximum power at a given tip speed ratio by every section of the blade.

The design procedure is discussed in the following sections,

5.1 Selection of Design Tip Speed Ratio and Number of Blades

In designing a wind turbine, the number of blades is an important parameter. If the number of blades increases, the cost of the wind turbine also increases, but we get improve performance and reduction of torque variations due to wind shear. Furthermore, power output increases with diminishing return [48]. The selection of λ_d and B is more or less related. The tip speed ratio is a dimensionless kinematic parameter and contains three most important variables of turbine design and analysis. These are, the wind speed, size of the rotor and the rotor rpm. Maximum power coefficient C_p versus λ for a rotor with a Rankine vortex wake [47] is shown in Figure 5.1.1, power coefficient approaches a larger value, for λ greater than 2. Also power output at larger values of λ depends upon the blades C_L/C_D ratio as shown in the Figure 5.1.2. Hence for maximum power output, the tip speed ratio which gives the maximum value of C_p in the C_L/C_D curve is to be selected. But this value of tip speed ratio must be greater than 2.

For the lower value of design tip speed ratios a higher number of blades is chosen. Because of the influence of B on C_p is larger at lower tip speed ratios. If the design tip speed ratio is higher, lower number of blades is selected. Because of the higher number of blades for high design tip speed ratio will lead to a vary thin and small blades which results in manufacturing problems. Type of load also influences upon the choice of the design tip speed ratio. If it is a slow running machine such as piston pump etc., will require a high starting torque, so the design speed of the rotor will usually be chosen low. Again, if it is a fast running machine such as generator or a centrifugal pump, it will require a low starting torque, so, a

high design speed of the rotor should be selected. The following table can be considered as the guidelines for the choice of the design tip speed ratio and the number of blades [21].

λ_d	B
1	6-20
2	4-12
3	3-6
4	2-4
5-8	2-3
8-15	1-2

To obtain the optimum configuration, the blade is divided into a number of radial stations. Four formulas [20] will be used to describe the information about β_T and C :

$$\text{Local tip speed ratio: } \lambda_r = \lambda_d \frac{r}{R} \quad (3.2.8)$$

$$\text{Relation for flow angle : } \lambda_r = \frac{\sin\phi(2\cos\phi-1)}{(1-\cos\phi)(2\cos\phi+1)} \quad (3.7.3)$$

$$\text{or, } \phi = \frac{2}{3} \tan^{-1} \frac{1}{\lambda_r} \quad (3.7.4)$$

$$\text{Twist angle : } \beta_T = \phi - \alpha \quad (3.7.4)$$

$$\text{Chord : } C = \frac{8\pi r(1-\cos\phi)}{BC_{Ld}} \quad (3.7.2)$$

The blade starting torque can be calculated by,

$$Q_{st} = \frac{1}{2} V_\infty^2 \rho B \int_r^R C(r) C_L [90 - \beta_T(r)] r dr \quad (5.1.1)$$

The rotor configuration is determined using the assumption of zero drag and without any tip loss. Each radial element is optimised independently by continuously varying the chord and twist angle to obtain a maximum energy extraction.

5.2 Selection of Airfoil Data

Power coefficient of the wind turbine is affected by C_D and C_L values of the airfoil sections. For a fast running device, a high design tip speed ratio will be chosen and airfoil section with a low C_D/C_L ratio will be preferred. On the other hand, for a high starting torque device with low design tip speed ratio, a airfoil section having higher C_D/C_L ratio is preferred. For the design and performance calculations of the wind turbines two-dimensional airfoil data are to be used in terms of lift and drag coefficients which can be found in references [3], [4] and [9]. The available data are normally limited to a range of angles of attack upto maximum lift and the behaviour above this is not well known.

Once the airfoil section is selected, the design lift coefficient and the design angle of attack correspond to the minimum value of C_D/C_L ratio is found from the $C_L-\alpha$ characteristic curve, Figure 5.2.1 and C_L-C_D characteristics curve Figure 5.2.2, for that particular airfoil section. In C_L-C_D characteristics curve a tangent is drawn through the origin. The point where the tangent touches the curve, indicates the minimum C_D/C_L ratio. This ratio determines the maximum power coefficients that can be reached particularly at high tip speed ratio. With this value of C_L (for minimum value of C_D/C_L ratio), the design angle of attack is found from $C_L-\alpha$ characteristic curve.

5.3 Calculation Scheme for Blade Configuration

To determine the blade geometry the following data must be required beforehand:

Design tip speed ratio, λ_d .

Amount of power to be extracted, P_e .

Design wind velocity, V_d .

Type of airfoil section.

The following steps are to be carried out for getting the blade configurations:

1. Assume a definite number of radial stations for which the chord and blade twist angle are to be calculated.
2. Draw a tangent from the origin to C_L-C_D graph of airfoil section to locate the maximum value of C_L/C_D . Corresponding to this value find the design angle of attack α_d and design lift coefficient C_{Ld} . This is explained in Appendix B.
3. Select the number of blades B corresponding to the design tip speed ratio λ_d .
4. Assume a reasonable value of C_p . Estimation of the value of

C_p has been explained in Appendix B.

5. Calculate the blade radius from the equation,

$$C_p = \frac{P_e}{1/2 \rho \pi R^2 V^3 \omega}$$

6. Select a fixed value of hub and tip radius ratio, $\frac{r_{hub}}{R}$

7. Calculate the value of λ_r for each radial station using the equation,
- $$\lambda_r = \frac{r}{R} \lambda_d$$

8. Determine the value of ϕ from the equation, $\phi = \frac{2}{3} \tan^{-1} \frac{1}{\lambda_r}$

9. Find the value of chord for each radial station from the equation,

$$C = \frac{8\pi r(1 - \cos\phi)}{BC_L \alpha}$$

10. Calculate the value of blade twist angle using the equation, $\beta_r = \phi - \alpha_d$.

11. Consider a fixed value of coning or tilt angle.

12. After finding the blade geometry, the following iteration procedures are adopted to calculate the value of actual C_p .

- a) Assume initial value of a and α .
- b) Considering the wind shear and no yawing angle, calculate the components of relative velocity W from the equations,

$$W_x = V_{\infty} \sin\theta_k \sin\alpha_r - \Omega r \cos\beta(1 + \alpha)$$

$$\text{and, } W_y = V_{\infty} [\cos\alpha_r \cos\beta(1 - a) - \sin\beta \sin\alpha_r \cos\theta_k]$$

- c) Determine ϕ from the equation, $\phi = \tan^{-1} \frac{W_y}{W_x}$
- d) Calculate the local angle of attack α by subtracting the local twist angle β_r from the relation $\alpha = \phi - \beta_r$.
- e) Find the values of lift and drag coefficients from a given table or polynomial.
- f) Determine the correction factor F for tip and hub losses.

- g) Calculate a with, $a(1-aF) = \frac{\sigma W^2 \cos \phi C_L}{8 \cos \beta \cos \alpha r^2 V^2 \omega_o F}$
- h) Calculate a' with, $a'(1-aF) = \frac{\sigma W^2 \sin \phi C_L}{8 r \cos \beta^3 \cos \alpha r \Omega V^2 \omega_o F}$
- i) Compare the values of a and a' with the original assumed values and continue the iteration procedures until the new values are within the desired limit.
- j) The values α , ϕ , C_L and C_D from the final iteration step are used to calculate local force components. The local power for the blade element is calculated from the equation,

$$dP = \frac{1}{2} \rho W^2 \sin \phi \left(C_L - \frac{C_D}{\tan \phi} \right) \sigma \cos \beta r^2 \Omega dr d\theta$$

and the elemental power coefficient is determined from the equation,

$$dC_P = \frac{dP}{1/2 \rho A V \omega^3} = \left(\frac{W}{V \omega} \right)^2 \frac{r^2}{R^3} \sin \phi \left(C_L - \frac{C_D}{\tan \phi} \right) \lambda \sigma \cos \beta dr d\theta$$

- h) Calculate the total power coefficient by integrating the elemental power coefficients using the Simpson's rule.
- 13) Compare the calculated power coefficient with the earlier assumed value. If it is not within certain desired accuracy, repeat all the procedures starting from step 4.
- 14) Find the starting torque from the equation,

$$Q_{st} = \frac{1}{2} \rho V \omega^2 B \int_r^R C(r) C_L [90 - \beta_T(r)] r dr$$

- 15) If the starting torque is less than the desired load torque, increase number of blades and repeat all the procedure from the step 4.

5.4. Deviation from the Ideal Form

In the preceding section it has been described how to calculate the ideal blade form. The chords as well as blade twist angle vary in a non-linear manner along the blade. Such blades are usually difficult to manufacture and may not have structural integrity. To minimize the above problems, the chords and the twist angles are linearized. Due to this linearization loss of

power is small. If the linearization is done in a sensible way the loss of power will be a few percent. Due to this linearization, about 75% of the power is extracted by the rotor from the wind by the outer half of the blades. This is because, the blade swept area varies with the square of the radius and the efficiency of the blades is less at smaller radii, where the tip speed ratio λ_r is small. On the other hand, at the tip of the blade the efficiency is low due to the tip losses.

Due to the reasons mentioned previously it is better to linearize the chord and the blade angles β_r between $r=0.5R$ and $r=0.9R$ [25]. The equations for linearized chord and twist can be written in the following way,

$$C = rC_1 + C_2$$

$$\beta_r = rC_3 + C_4$$

Where C_1 , C_2 , C_3 and C_4 are constants. With the values of C and β_r at $0.5R$ and $0.9R$ from the ideal blade form the values of C_1 , C_2 , C_3 and C_4 can be calculated. The ultimate expressions for chord and twist of linearized blade can be written,

$$C = 2.5(C_{90} - C_{50}) \frac{r}{R} + 2.25C_{50} - 1.25C_{90} \quad (5.4.1)$$

$$\beta_r = 2.5(\beta_{90} - \beta_{50}) \frac{r}{R} + 2.25\beta_{50} - 1.25\beta_{90} \quad (5.4.2)$$

Where,

- C_{50} = Chord of the ideal blade form at $0.5R$
- C_{90} = Chord of the ideal blade form at $0.9R$
- β_{50} = Twist angle of the ideal blade form at $0.5R$
- β_{90} = Twist angle of the ideal blade form at $0.9R$

Further simplification of the blade shape consists of omitting the twist angle altogether. Rotor blade without twist angle results in a loss of power about 6% to 10% [44], which is acceptable for a single production unit. Since the main purpose is the design of a cheap wind turbine, an untwisted blade with a constant chord seems to be a good choice with only limited power losses.

5.5 Calculation Scheme for Performance Analysis

After the design of the rotor configurations has been completed according to the formulas in the preceding sections, the characteristics of the rotor can now be determined.

The following data of the rotor are assumed to be available beforehand,

Rotor radius, R.
 Chord(C) and twist angle(βr) distribution along the radius.
 Tip speed ratio, λ .
 Number of blades, B.
 Lift and drag coefficient of the blade airfoil section.

Now for a number of radial positions the values of axial and angular induction factors will be found out. As there is no analytical expressions for the induction factors, the following iteration procedures are to be performed for each radial station.

- 1) Assume reasonable value of a and a' .
- 2) Find the values of W_x and W_y from the following equations,

$$W_x = V_{\infty} \cos \gamma \cos \theta_k + V_{\infty} \sin \gamma \sin \theta_k \sin \alpha r - \Omega r \cos \beta (1 + a')$$
 and,
$$W_y = V_{\infty} [\sin \gamma \cos \alpha r \cos \beta (1 - a) - \sin \beta \sin \alpha r \sin \gamma \cos \theta_k + \sin \beta \sin \theta_k \cos \gamma]$$
- 3) Calculate, ϕ by using the equation, $\tan \phi = \frac{W_y}{W_x}$
- 4) Determine angle of attack α , from the equation, $\alpha = \phi - \beta r$.
- 5) Calculate C_L with C_L - α graph or table.
- 6) Determine the total correction factor F for tip and hub losses.

$$7) \text{ Calculate } a \text{ with, } a(1 - aF) = \frac{\sigma W^2 \cos \phi C_L}{8 \cos \beta \cos^2 \alpha r \sin^2 \gamma V_{\infty}^2 F}$$

$$\text{and, } a' \text{ with, } a'(1 - aF) = \frac{\sigma W^2 \sin \phi C_L}{8 r \cos \beta^3 \cos \alpha r \sin \gamma \Omega V_{\infty} F}$$

- 8) The new values of a and a' are compared with those from step 1 and the iteration procedure is continued until the desired accuracy is reached.
- 9) The value of α , ϕ , C_L and C_D from the final iteration step are used to calculate local force components.
- 10) The local contributions to thrust, torque and power coefficients are calculated from the following equations,

$$dC_T = \frac{8}{\pi R^2} \left(\frac{V_{\infty}}{V_{\infty}} \right)^2 a F (1 - a F) \cos^2 \alpha r \sin^2 \gamma \cos^2 \beta \left(1 + \frac{C_D}{C_L} \tan \phi \right) r dr d\theta$$

$$dC_Q = \frac{8}{\pi R^3} \frac{V_{\infty o} r^2}{V_{\infty}^2} \Delta F (1-aF) \cos \alpha \tau \sin \gamma \cos^4 \beta \left(1 - \frac{C_D}{C_L \tan \phi}\right) \Omega dr d\theta$$

and,

$$dC_P = \frac{8\Omega^2}{\pi R^2} \frac{V_{\infty o}}{V_{\infty}^3} r^3 \Delta F (1-aF) \cos \alpha \tau \sin \gamma \cos^4 \beta \left(1 - \frac{C_D}{C_L \tan \phi}\right) dr d\theta$$

When the iteration procedure is completed for all blade elements, the local contributions to torque, thrust and power are integrated by using Simson's rule to determine the performance of the rotor.

5.6 Design of a 350 kW Wind Turbine

For the present work, a two-bladed horizontal axis downwind turbine is selected. The design tip speed ratio is 8 and adjustable pitch angle changing mechanism is selected. Power to be extracted is 350 kW. The value of $r_{hub}/R=0.1$ is chosen arbitrarily. Throughout the theoretical studies NACA 4418 airfoil section and Prandtl's tip loss correction method are used to develop the curves. Average wind velocity 9 m/sec and no coning or tilting angles are considered to find out the optimum blade configuration. The blade radius has been divided into 12 number of radial stations. Each station has a distance r from the rotor centre having a local tip speed ratio λ_r . The relative wind velocity angle ϕ was found out by the equation (3.7.4). The chord and twist angle for each station were found out by equations (3.7.2) and (3.3.9). To find out the blade geometry, each radial station is optimised independently by continuously varying the chord and twist angle to obtain a maximum energy extraction. This is done when every element of the blade is operating at the maximum lift and drag ratio of the profile. The dependance of the torque at $\Omega=0$, on pitch angle is shown in the Figure 5.6.1. The starting torque coefficient increases with the increase of pitch angle. Where there is large internal resistance, high overall pitch angle is preferable to start the rotor from rest. Figures 5.6.2 and 5.6.3 show the distribution of twist angle and chord of the optimum designed wind turbine for the given conditions. Velocity distribution with tip speed ratio is shown in the Figure 5.6.4. At low tip speed ratio the velocity is high. The velocity decreases with the increase of tip speed ratio. The above mentioned configuration is studied because of, various test results concerning performance analysis are readily available [21] for comparison.

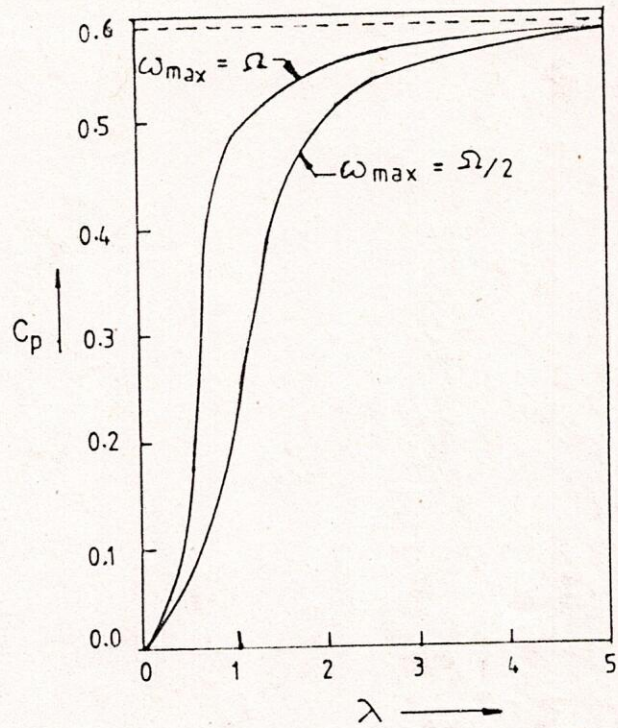


Fig.5.1.1 : Maximum Power Coefficient Versus λ for a Rotor with a Rankine Vortex wake

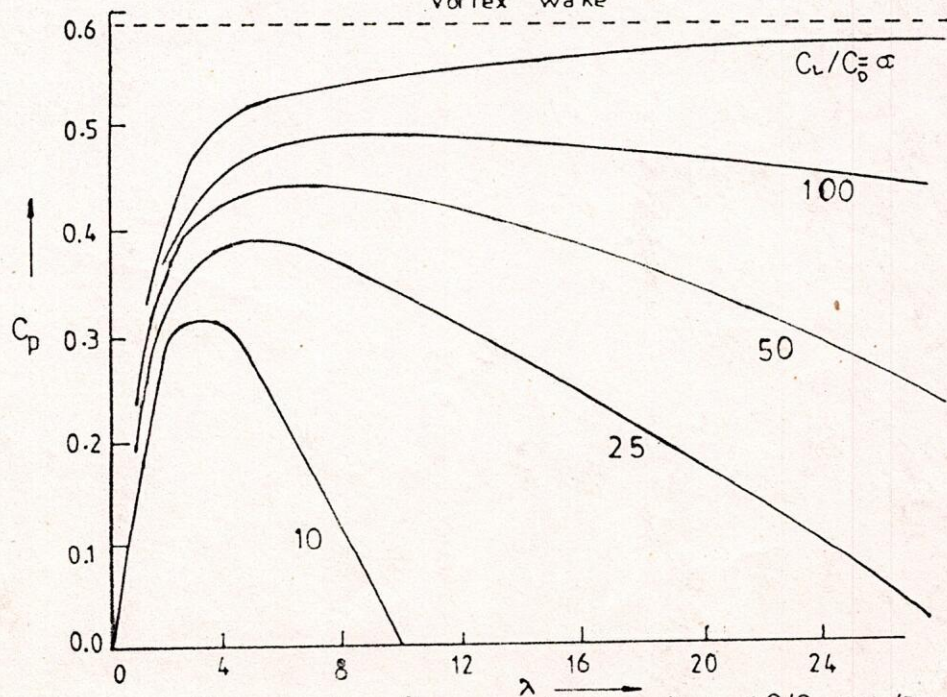


Fig.5.1.2 $C_p - \lambda$, Characteristics Curve showing the effect of C_l/C_0 ratio ($B = \alpha$).

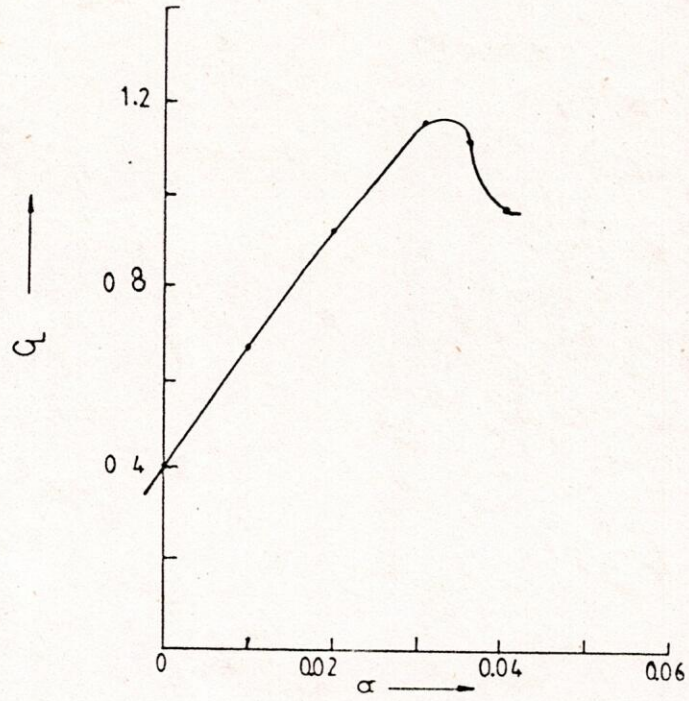


Fig. 5.2.1: C_L - α , Characteristics Curve for a given Airfoil Section [21].

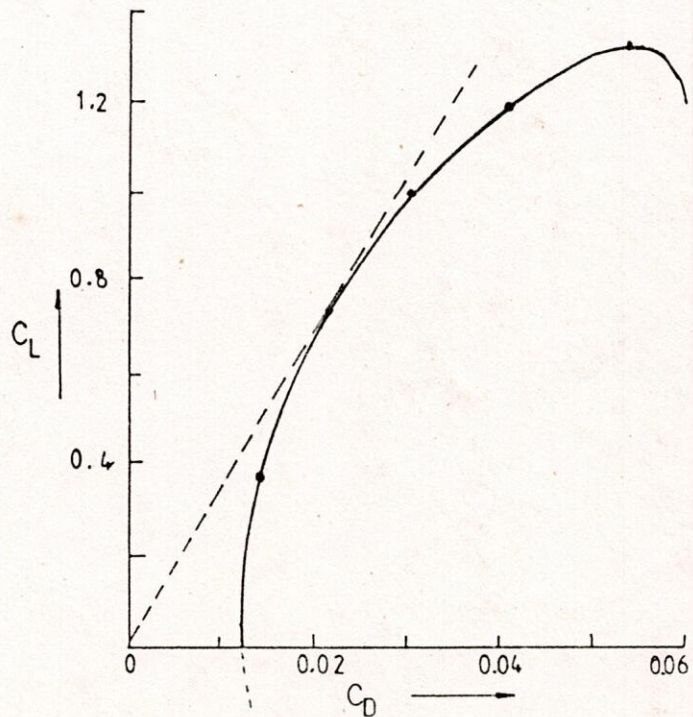


Fig. 5.2.2: C_L - C_D , Characteristics Curve for a given Airfoil Section [21].

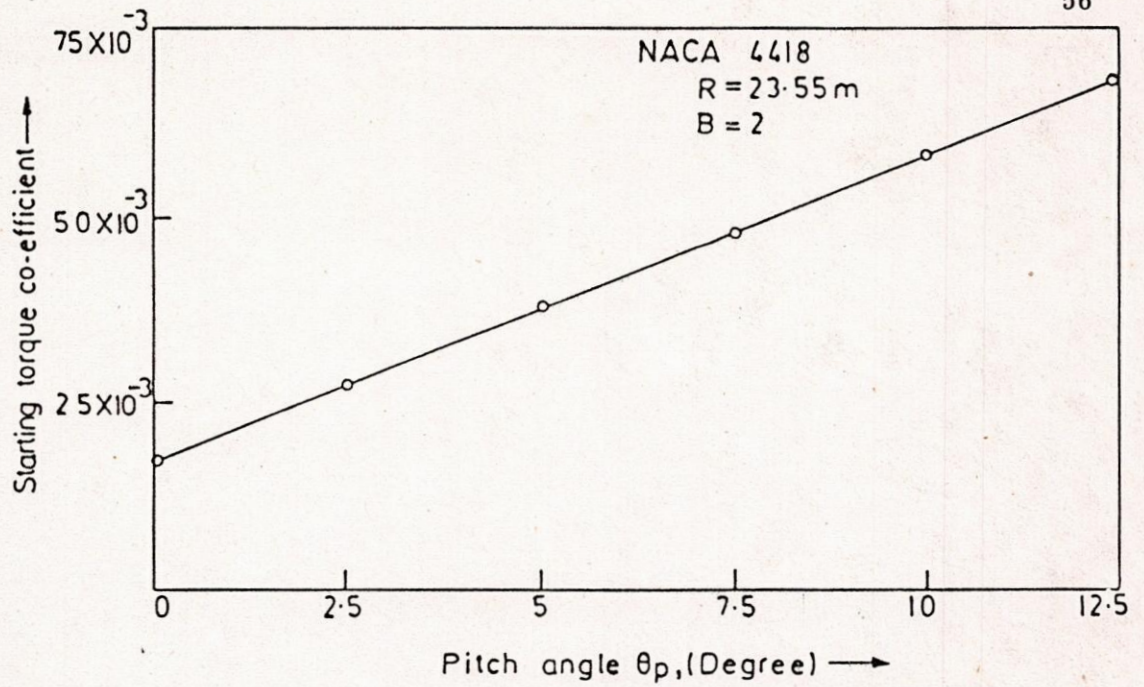


FIGURE 5.6.1: STARTING TORQUE CO-EFFICIENT AS A FUNCTION OF OVERALL PITCHING ANGLE.

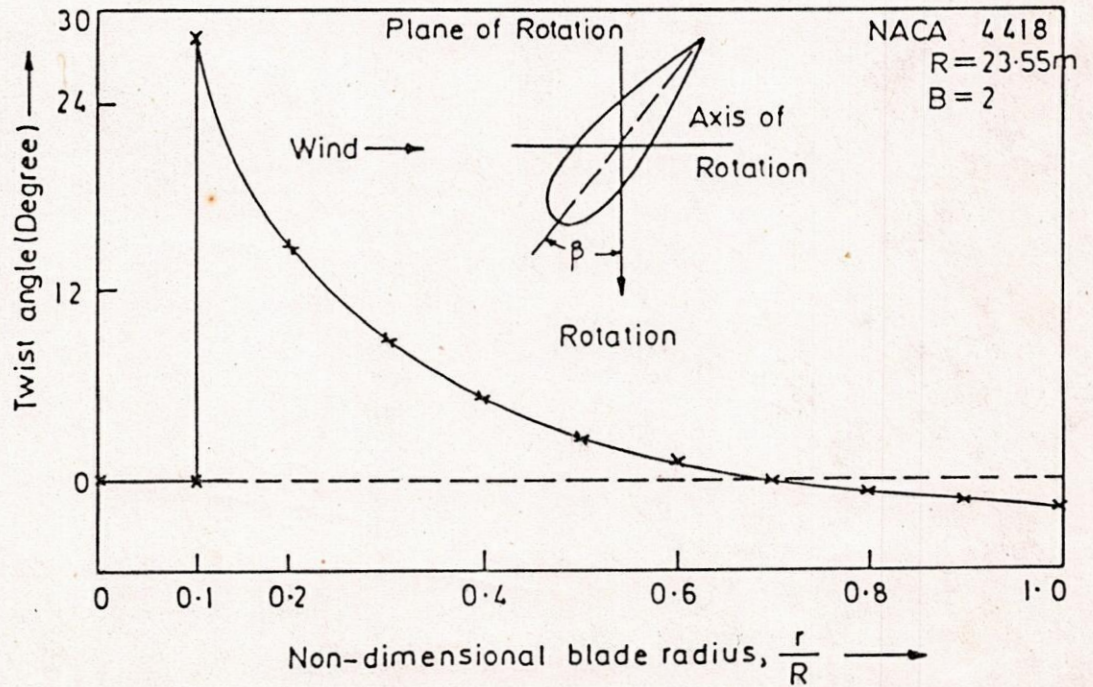


FIGURE 5.6.2: BLADE TWIST DISTRIBUTION FOR OPTIMUM DISTRIBUTION.

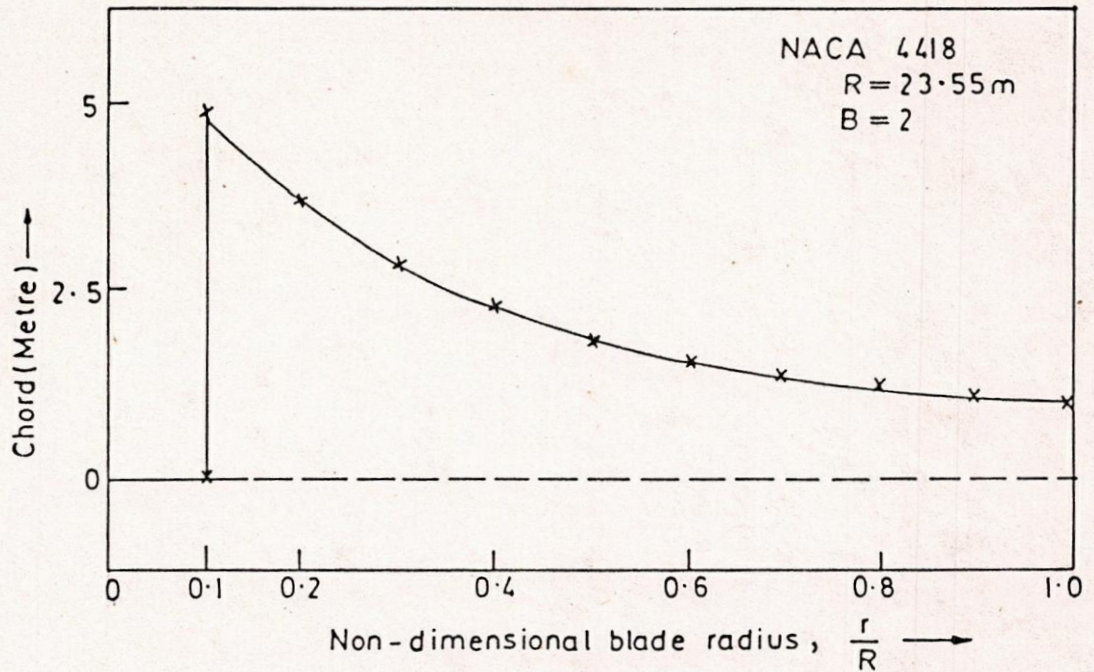


FIGURE 5.6.3: BLADE CHORD DISTRIBUTION FOR OPTIMUM PERFORMANCE .

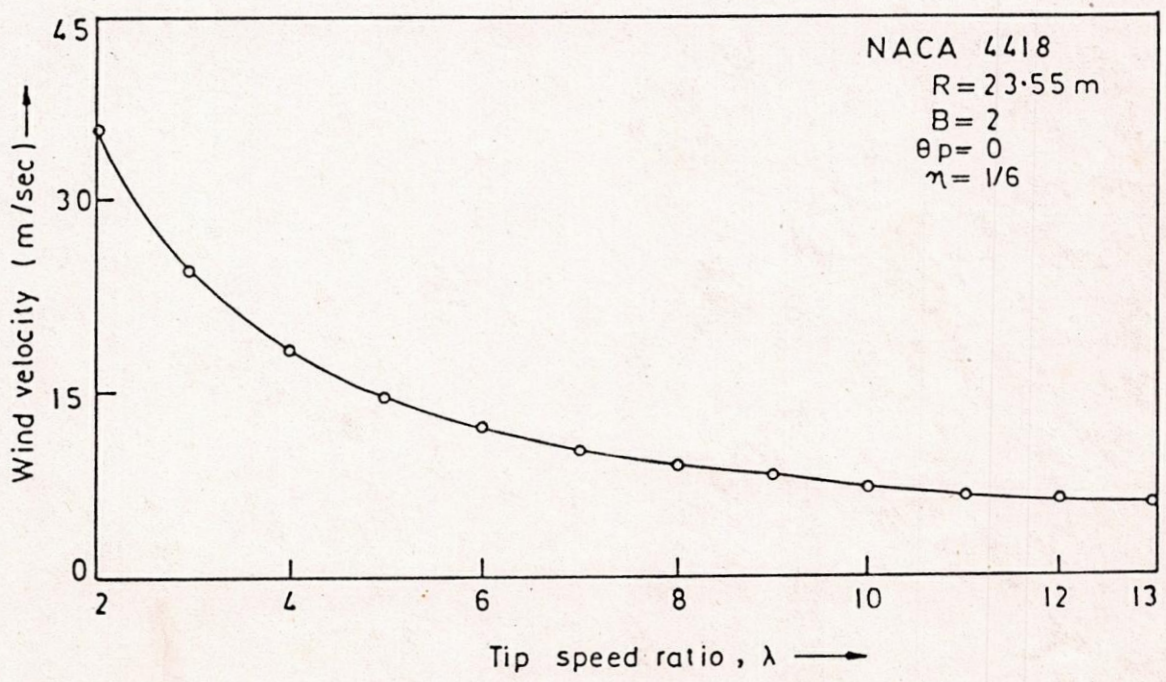


FIGURE 5.6.4: WIND VELOCITY VARIATION WITH TIP SPEED RATIO.

CHAPTER VI

YAW STABILITY ANALYSIS

6.0 General

In the present world of energy crisis, wind is an important source of energy. Which is one of the cheapest and renewable source of energy. In the region, where relatively strong wind exist, wind turbine may supply considerable energy for the generation of electrical power and for other use. Large horizontal axis wind turbine presently designed and studied for the generation of electrical power. The economic feasibility of this pollution free renewable source of energy must be effectively determined. An economically viable and proper designed wind turbine may be able to operate for long period without requiring excessive maintenance and replacement of parts. Therefore, for smooth running and to avoid fatigue problem of a wind turbine, it is necessary to minimize the vibratory loads and stresses in the rotor, tower and control system considerably.

A survey covering some aspects of the dynamic problems of large wind turbines is presented in reference [33], which contains a qualitative discussion of the effects of size, number of blades, hub configuration and type of control system on the turbine dynamic characteristics. Ormiston [34] considers the flapping response of a wind turbine blade using elementary analytic techniques for a simple rigid, centrally hinged and spring restrained blade model. Spera [39] has performed an approximate structural analysis for the NSF/NASA MOD-0 wind turbine rotors. Kaza and Hammond [27] have considered the flap-lag stability of wind turbine rotors in the presence of velocity gradients. Dugunji [10] has reviewed the whirl stability of a windmill on a flexible tower.

6.1 Present Approach

In the present work, the results obtained from a theoretical calculation model including the influence of yaw and tower shadow on the performance of horizontal axis wind turbines. Analytically a simple blade is chosen as the basic configuration for analysis to construct the rotor-tower model. A modified strip theory approach has been used to determine the effects of yaw and tower shadow. The tower shadow has a considerable effect on the flap response but leaves blade stability unchanged [28]. The model takes into account the drag of the blade and also the tip loss correction factor, modelled by Prandtl. Investigations are carried out for no coning and tilting angle. The analysis is applied to both downwind and upwind rotors.

6.2 Blade Forces Under the Influence of Yaw

If the rotor axis is not parallel to the direction of air flow, that is, where a yawing angle exists the aerodynamic forces

on the blades will vary during one revolution, although the windmill is situated in a steady flow of air. The reason behind this is, the change of both the magnitude and direction of the local resulting wind velocity, which varies with the cyclic movement of the blade and opposed to the direction of the wind alternately, which is shown in the Figure (6.2.1).

The effect of tower shadow on velocity at different azimuthal position greatly influence the forces and moments. Two blade configuration is chosen. when the blade is at 165° to 195° , there is a considerable decrease of velocity, which results decrease of tower top forces and moments and therefore vibratory load produce on the tower as a result, reduced the fatigue life of the wind turbine and also increase the noise of the turbine.

6.3 Stability Analysis

In this section, the analysis of yaw stability is explained for different types of horizontal axis wind turbines. Generally, horizontal axis wind turbines can be classified according to the following six factors [40];

- i) Rotor location with respect to the tower upwind or downwind.
- ii) Rotor axis inclination levelled or tilted.
- iii) Blade axis inclination radial or coned.
- iv) Number fo blades two, three or more.
- v) Blade root attachment cantelevered or hinged.
- vi) Blade pitch angle fixed or variable.

Fixing up the last three factors listed above as follows: two blades, cantelevered root attachments and fixed pitch angle, the following sub-sections evaluates the analysis of yaw stability. According to equations (4.7.1.5) and (4.7.2.8), the tower top forces and moments can be written as,

$$\vec{F}_{s0} = \begin{pmatrix} F_{x3}\cos\theta + F_{y3}\sin\theta\sin\beta + F_{z3}\sin\theta\cos\beta \\ F_{x3}\sin\alpha_T\sin\theta + F_{y3}(\cos\beta\cos\alpha_T - \sin\alpha_T\sin\beta\cos\theta) - F_{z3}(\sin\beta\cos\alpha_T + \sin\alpha_T\cos\beta\cos\theta) \\ -F_{x3}\cos\alpha_T\sin\theta + F_{y3}(\cos\beta\sin\alpha_T + \cos\alpha_T\sin\beta\cos\theta) + F_{z3}(\cos\beta\cos\alpha_T\cos\theta - \sin\beta\sin\alpha_T) \end{pmatrix} \quad (4.7.1.5)$$

and,

$$\begin{pmatrix} M_{x0} \\ M_{y0} \\ M_{z0} \end{pmatrix} = \begin{pmatrix} Z_0F_{y0} - Y_0F_{z0} \\ X_0F_{z0} - Z_0F_{x0} \\ Y_0F_{x0} - X_0F_{y0} \end{pmatrix} \quad (4.7.2.8)$$

A. Downwind Rotor Without Coning and Tilting Angle

A downwind rotor without coning and tilting angle is shown in the Figure (6.3.1). Now putting $\alpha_T=0$ and $\beta=0$ in the above two equations then, tower top forces are

$$\vec{F}_{s_o} = \begin{vmatrix} F_{x_3} \cos \theta & & +F_{z_3} \sin \theta \\ & F_{y_3} & \\ -F_{x_3} \sin \theta & & +F_{z_3} \cos \theta \end{vmatrix} \quad (6.3.1)$$

and the equation of yawing moment can be written as,

$$M_{z_o} = Y_o(F_{x_3} \cos \theta + F_{z_3} \sin \theta) - X_o F_{y_3} \quad (6.3.2)$$

B. Downwind Rotor With Coning Angle

For a downwind rotor with coned blade as shown in the Figure 6.3.2, putting $\alpha_T = 0$ in equation (4.7.1.5) gives, tower top forces,

$$\vec{F}_{s_o} = \begin{vmatrix} F_{x_3} \cos \theta & & +F_{y_3} \sin \theta \sin \beta + F_{z_3} \sin \theta \cos \beta \\ & F_{y_3} \cos \beta & -F_{z_3} \sin \beta \\ -F_{x_3} \sin \theta & & +F_{y_3} \sin \beta \cos \theta + F_{z_3} \cos \beta \cos \theta \end{vmatrix} \quad (6.3.3)$$

and the equation of yawing moment is,

$$M_{z_o} = Y_o(F_{x_3} \cos \theta + F_{y_3} \sin \theta \sin \beta + F_{z_3} \sin \theta \cos \beta) - X_o(F_{y_3} \cos \beta - F_{z_3} \sin \beta) \quad (6.3.4)$$

C. Upwind Rotor Without Coning or Tilting

For a upwind rotor without coning and tilting angle is shown in the Figure (6.3.3). The equation of tower top forces and moments are same as the equations (6.3.1) and (6.3.2), but the moment arms considered with appropriate sign.

D. Upwind Rotor With Coning and Tilting

For a upwind rotor with coning and tilting angle is shown in the Figure (6.3.4) and the equation of yawing moment can be expressed as,

$$\begin{aligned} M_{z_o} = & Y_o(F_{x_3} \cos \theta & & +F_{y_3} \sin \theta \sin \beta + F_{z_3} \sin \theta \cos \beta) \\ & -X_o[(F_{x_3} \sin \alpha_T \sin \theta & & +F_{y_3}(\cos \beta \cos \alpha_T - \sin \alpha_T \sin \beta \cos \theta) \\ & -F_{z_3}(\cos \alpha_T \sin \beta + \sin \alpha_T \cos \beta \cos \theta)] \end{aligned} \quad (6.3.5)$$

The stability of a downwind rotor depends on a large number of parameters such as coning, tilting, azimuthal angles, wind shift, wind shear, tower shadow factor, pitching angle and the tip speed ratio. A wide investigation of these parameters are necessary.

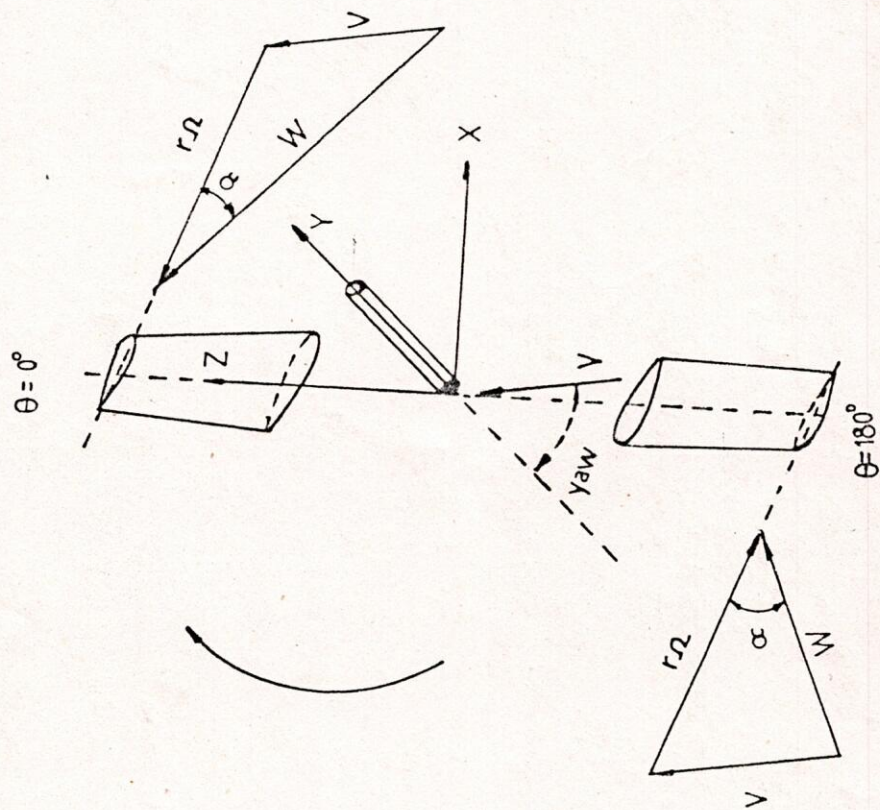


Fig.6-2-1: The Relative Wind Velocities at Upper and Lower Position of The Blade in yaw.

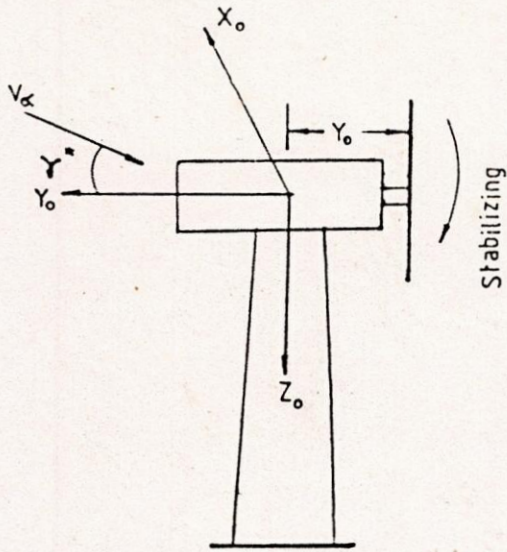


Fig. 6.3.1: Downwind Rotor Without Coning Angle.

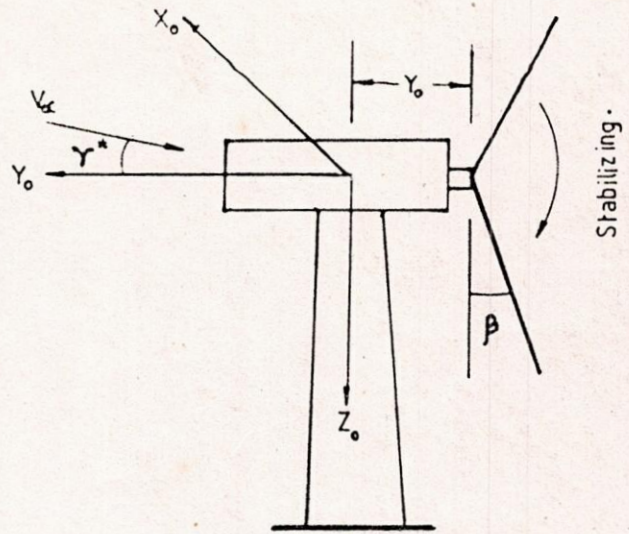


Fig. 6.3.2: Downwind Rotor With Coning Angle.

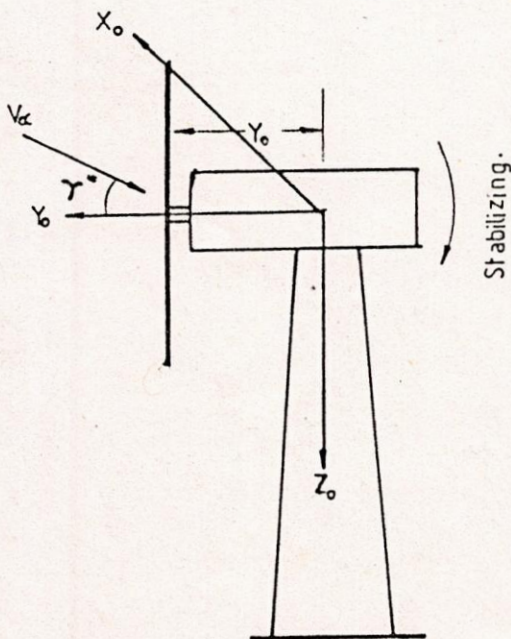


Fig. 6.3.3: Upwind Rotor Without Coning or Tilting Angle.

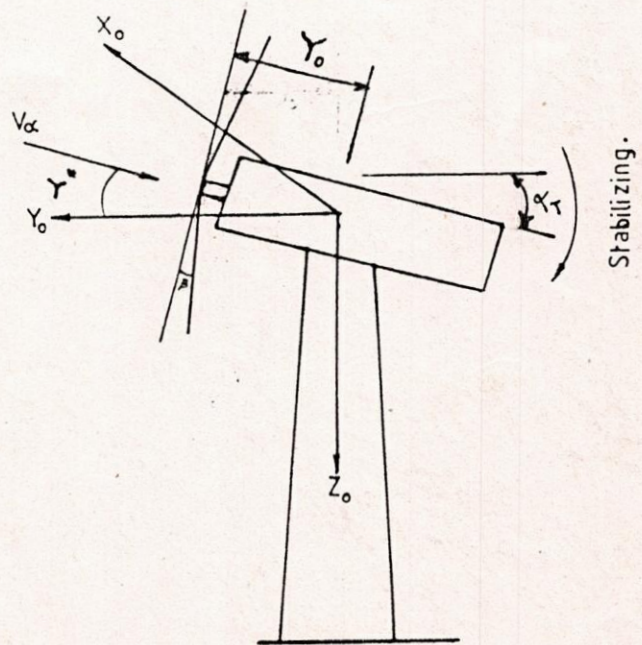


Fig. 6.3.4: Upwind Rotor With Coning and Tilting Angle.

I
E

CHAPTER VII

RESULTS AND DISCUSSION

7.0 General

In the following chapter, the results obtained are discussed. The effect of pitch angle variation, blade shapes, wind shift and tower blockage are discussed elaborately. Also a brief discussion about the effect of wind shear, number of blades, coning angle and tilting angle are presented in the following chapter for general information.

7.1 Results of a 350 KW Wind Turbine

The power, thrust and torque coefficients variation with respect to tip speed ratio for a 350 KW horizontal axis wind turbine are shown in Figures 7.1.1, 7.1.2 and 7.1.3, considering fixed pitch angle i.e. at zero pitch angle. The turbine is designed for a tip speed ratio 8 with a rated wind velocity 9 m/sec. The maximum power coefficient is attained at a tip speed ratio 8, as shown in the Figure 7.1.1. The thrust coefficient is found to increase continuously and the value greater than unity is reached, which is shown in the Figure 7.1.2. This is because at high tip speed ratios the velocities through the turbine actuator disc are less than half the free stream velocity. Which means that the velocity in the fully developed wake has reversed in direction and flows back towards the turbine actuator disc.

The flow reversal induces a vortex flow in the wake which violates a basic assumption for the blade element theory. The theoretical predictions in this condition by the present method are not accurate [21]. The variation of torque coefficient with respect to tip speed ratio is shown in the Figure 7.1.3. This Figure shows that the maximum torque coefficient moves towards a lower value of tip speed ratio than the value of the designed tip speed ratio.

7.2 Effect of Pitch Angle Variation

The calculated power, thrust and torque coefficient with respect to tip speed ratio at different pitch angle are shown in the Figures from 7.2.1 to 7.2.3. Increased pitch angle reduces the maximum power but increase the power available at low tip speed ratios. Figure 7.2.1 shows some general features of horizontal axis wind turbine. At low tip speed ratios, the power coefficient is strongly influenced by the maximum lift coefficient. The relative flow velocity angle ϕ is large at low tip speed ratios and much of the rotor, particularly the inboard stations, can be stalled when operating below the designed tip speed ratio. At tip speed ratios above the peak power coefficient, the effect of drag becomes dominant. Rapid power decrease will occur due to high drag coefficient and at some large tip speed ratio the net power output will become zero. The

power curve is sensitive mainly due to blade pitch angle in the stalling region.

To avoid too much drop off of the power after the stalling point a blade pitch angle of 2.5° and 5° are seen to be more convenient than the performance at 0° pitch angle. Increase of pitch angle shows the shifting of maximum power coefficients to the lower values of tip speed ratios. Figure 7.2.2, shows that the thrust coefficient is increasing continuously with tip speed ratio and value becomes more than unity. With the increase of blade pitch angle the values of induced velocity factor a , close to or lower than 0.5, which means a more relative solution. Therefore, the thrust coefficient more than unity is possible. But with the increase of pitch angle, peak value of thrust coefficients decreases and they occur at a particular tip speed ratio beyond which the coefficients gradually decrease. The variation of torque coefficient with tip speed ratio is shown in the Figure 7.2.3. With the increase of pitch angle the maximum value of torque coefficient moves towards the lower values of tip speed ratio. Change of the blade pitch angle means that the resulting angle of attack is reduced and the lift coefficient is shifted from the stalling region. Pitching of the blade provides higher torque coefficient at lower tip speed ratios. Therefore, a small change in pitch angle seems to give better results than other conditions.

When any part of the turbine blade operates with a resulting angle of attack that is higher than the value corresponding to maximum lift for the local blade section flow separation is encountered. This implies three dimensional effects which violate the basic assumption of the blade element theory and the solutions obtained are not fully reliable. Such conditions occur for high wind speeds. The flow angle ϕ will then increase with increasing wind speed keeping other parameters constant. Flow separation will first occur in the hub region, where ϕ has its largest values. Increasing the blade pitch angle means that the resulting angle of attack is lowered and more reliable solutions are obtained.

7.3 Effect of Blade Shapes

The normal procedure for determining the blade shape of a horizontal axis wind turbine is to optimize independently each radial element by continuously varying the chord and twist angle to obtain maximum energy extraction. This method results in complex blade shapes which is expensive to manufacture and may not have structural integrity. In order to reduce these problems it is possible to linearize the chord and twist angles. This results in a small loss of power. But, if the linearization is done in a sensible way the loss is only a few percent.

In the present analysis three types of blade shapes have been considered; optimum-chord optimum-twist, linear-chord linear-twist and linear-chord zero-twist. In the preceding section, the power, thrust and torque coefficient with respect to

tip speed ratio at different pitch angles for optimum-chord optimum-twist are discussed. Figures 7.3.1 to 7.3.3 show the power, torque and thrust coefficient with tip speed ratio at different pitch angle for linear-chord linear-twist blade. Figures 7.3.4 to 7.3.6 show the power, torque and thrust coefficient with tip speed ratio at different pitch angles for linear-chord zero-twist blade. Figures 7.3.7 to 7.3.9 show the comparison among the power, torque and thrust coefficient at zero pitch angle. Figure 7.3.7 shows that the power coefficient for other two blade shapes is less than the optimum-chord optimum-twist blade at lower value of tip speed ratio but approximately same at high tip speed ratio. The Figure 7.3.8 shows the torque coefficient for three blade shapes. Optimum-chord optimum-twist blade has the greater value of torque coefficient than the other two blade shapes at lower tip speed ratio but same at higher tip speed ratio. Figure 7.3.9 shows the thrust coefficient for three type of blade shapes. Which also gives the same result as for power and torque coefficient.

The linearization of the chords and twist angles have been done by taking the values from the optimum blade configuration at $r=0.5R$ and $r=0.9R$. Radial distribution of power coefficient, thrust coefficient and torque coefficient, power, thrust, torque, axial force and axial bending moment are shown in the Figures from 7.3.10 to 7.3.18. It is to be noted that about 75% of the power, thrust and torque are produced by the outer 50% radius. The reason behind this, is that, the blade swept area varies with the square of the radius and also the efficiency of the blades is less at small radii, where the local tip speed ratio r is small. On the other hand due to the tip losses there is a decrease of power, moments and forces near the tip of the blade.

Figures 7.3.19 to 7.3.20 show the distribution of chord and blade twist angles for three types of blades. From these Figures it is found that the changes in chords and twist angles are very small at the outer half of the blade. Large variations with the linear chord and twist distributions are found only at the lower part of the blade i.e. inner half of the blade. It is realized that about 75% of the power that is extracted by the rotor from the wind is extracted by the outer half of the rotor. So this will not lead to any significant loss of power but the starting torque will be less. In cases, where the starting torque is an important factor, this effect must be considered. Variation of starting torque for different blade configuration at various pitch angle is shown in the Figure 7.3.21, where approximately 30% differences may occur between the optimum blade and zero-twist blade.

7.4 Effect of Wind Shift

The aerodynamic forces on a blade will vary during a revolution in the case, where the rotor axis is not parallel to the wind direction, even though the wind speed is constant. This results from changes in both magnitude and direction of the resulting local wind speed for the profile, which alters with the

varying moment of the blade with and against the wind conditions.

The power, thrust and torque coefficients with tip speed ratio produced by the wind turbine at different yaw angles are presented in Figures 7.4.1 to 7.4.3. It can be concluded that the rotor can be yawed into and out of the wind either to maintain power level as wind speed varies or to unload the rotor for shutdown. The changes in both wind speed and direction give rise to change in blade performance with blade azimuth. Figures 7.4.4 to 7.4.7 show the variation of the power, thrust coefficients and edgewise and flapwise bending moments with azimuth for different yaw angle for single blade. At low wind speeds the effects of changes in the resulting wind speed and angle of attack almost cancel each other, so that the forces remain nearly constant. At high wind speeds under stalled conditions both the higher resulting wind speeds and the combined lower angle of attack will cause increasing lift on the blade when moving upwards relative to the wind. It appears that the variation achieves a maximum at 180° . At 0° and 180° a change of wind directions means a large change of angle of attack and hence of the blade force. Figures 7.4.8 to 7.4.11 show the distribution of yawing and pitching moment coefficient and tower top axial and tangential forces at different yawing angle. The variation achieves a maximum twice per revolution for each case. These Figures are plotted by considering a two blade configuration. So after passing 180° repetition of the same curve will take place. The two extremes will originate from structural coupling between the blades. The uniform sinusoidal wave shape indicates that it results primarily from wind shear, the wind velocity gradient with altitude. In non-axial flow, even at small angles of yaw, the cyclic variation in the aerodynamic forces at the blade root lead to resonance in either the blade, or the supporting structures and possibly reduce the lifetime of the turbine. The effects of non-axial flow, therefore, need to be considered in the design of horizontal axis wind turbine.

7.5 Effect of Tower Shadow

In case of horizontal axis wind turbine, the blades may be placed upwind or downwind of the tower support. Present analysis is for the downwind rotor arrangement. With a downwind rotor system, the blades can be mounted closer to the tower, because blade deflections will be away from the tower. Also the configuration tends to be self-orienting with changes in wind direction.

For a downwind rotor, the supporting tower of a wind turbine creates an aerodynamic shadow through which the rotor blades must pass. Tower shadow is typically a region of reduced wind speed and high turbulence. An important source of periodic wind load is the aerodynamic interference created by the tower, which is upwind of the rotor and known as the tower wake effect. The tower wake is a potential excitation source for variation at any integer multiple of the rotational speed. The flow disturbance

caused by the presence of the rotor will, in general, have an adverse effect on rotor fatigue life. It may also increase acoustic noise generation from the turbines. The tower wake has a fundamental frequency of once per revolution for each blade. The magnitude of the periodic load created by the tower shadow depends on the projected area of the tower structural elements, their average drag coefficients, and the sector of the rotor area affected by the wake.

For the present analysis, the blades are assumed to be in the tower wake at azimuths from 165° to 195° . When a blade is initially located vertically up behind the tower, $\theta=0^{\circ}$, and rotates to the vertically down at $\theta=180^{\circ}$, the tower blockage is modelled by [32],

$$V(\theta, \lambda) = (V_{\theta})_k [1 - B_f(1 + \cos n\theta)]$$

where,

λ = Tip speed ratio.

B_f = Tower blockage factor.

$$\leq 0.5 \text{ for } \pi \left(1 - \frac{\pi}{12}\right) \leq \theta \leq \pi \left(1 + \frac{\pi}{12}\right)$$

= 0, for other angles.

$(V_{\theta})_k$ = Instantaneous wind velocity corresponding to azimuthal point.

$n\theta$ = Angle of tower shadow area.

In the present work, an evaluation has been conducted for the effects of tower shadow on the forces, power, thrust and moments for a downwind mounted wind turbine blade. The large and abrupt changes that occur as the blade passes through the tower shadow will obviously cause significant changes in blade. The effect of tower shadow is to give a sharp kick to the blades in an upwind direction. The tower shadow for present analysis was selected to occupy a total arc of 30° . All the graphs have been plotted at design tip speed ratio 8 and the value of the wind power law exponent is taken as $\alpha=1/6$. The value of the tower shadow factor is chosen as $B_f=0.25$.

Figures 7.5.1 to 7.5.8, show the combined effect of wind shift and tower shadow on power and thrust coefficients, bending moments, yawing and pitching moment coefficients and on the tower top forces, with azimuthal angle. The maximum effect will occur when one blade will be at vertical position i.e. at 0° and the other blade is shielded from the wind by the tower i.e. at 180° . The blades of a downwind horizontal axis wind turbine passing through this shadow will be subjected to periodically varying large wind forces and bending moments, hence fatiguing stresses in the material of the blades. Since the tower wake has a fundamental frequency of once per revolution, it is a pulse load which can contain harmonics at many frequencies. In practice, once in the tower shadow the blade flapping motion results in increase in the blade angle of attack and thrust. When the blade

leaving the tower shadow, the abrupt increase in wind velocity combines with the already increasing angle of attack due to flapping, give a thrust that is briefly higher than the steady state value. One way to reduce the effect of the tower shadow is to make the tower aerodynamically smooth, thereby reducing the flow disturbance. However, because of changes in wind direction, it is necessary to have an aerodynamic tower fairing which is free to move in yaw with the turbine nacelle.

The wake behind the fairing is both narrower and much less deep. With the tower alone, there is an extensive turbulent region with no forward velocity at all, therefore the wind speed takes some distance to recover original speed. But the tower with fairing, there is no such turbulent region, and only much smaller velocity is reduced, which extends over a very narrow width. The addition of the fairing will greatly reduce the loss of the wind speed, so reducing the vibrations of the blade. In turbulent conditions, the recovery of velocity behind tower or fairing is expected to be quicker due to more rapid mixing at the boundary of the wake. The use of fairing also extends the fatigue life of the blade and reduces the noise levels to environmentally acceptable range [51].

7.6 Effect of Wind Shear

A wind shear arises from the fact that the wind near the surface of the earth is not entirely uniform. There exists a large scale boundary layer which may cause significant load variations on a blade as it passes from the bottom to the top of a rotation. The rotor of a wind turbine is placed at some distance above the ground level to avoid the extreme low velocity part of the atmospheric boundary layer. The influence of wind shear on the power output and the blade loading of a horizontal axis wind turbine is complicated, because each blade element is subjected to a varying wind velocity during one revolution of the rotor. There is some arbitrariness in the choice of the reference wind velocity to calculate C_p . Wind shear has been previously discussed in section 4.2.

7.7 Effect of Number of Blades

In designing a wind turbine, the question arises how many number of blades should be used. The increased number of blades increases the cost of blade manufacture. The advantages of increasing the number of blades are improved performance and lower torque variation due to wind shear. The maximum power coefficient is also affected by the number of blades, because of the tip losses that occur at the tips of the blades. These losses depend on the number of blades and tip speed ratios. For the lower design tip speed ratios, generally a high number of blades is chosen. This is done because the influence of number of blades on power coefficient is larger at lower tip speed ratios. For a high design tip speed ratio with a high number of blades will lead to very small and thin blades which results in manufacturing problems and a negative influence on the lift and drag properties

of blades. Increase of number of blades shows that the region of higher power coefficients move to the region of smaller values of tip speed ratios. Increase of pitch angle results in a decrease of angle of attack, therefore lift coefficient is shifted from the stall region and it moves towards the higher values at low tip speed ratios. Effect of number of blades has been previously discussed in section 5.1.

7.8 Effect of Blade Coning Angle

Since stresses induced by flapwise loads are greatest in magnitude, blades are frequently coned so that bending stresses are induced by centrifugal forces, cancelling those due to aerodynamic loads. Exact cancellation is only possible at one aerodynamic loading condition and equalisation of stresses along the entire blade requires a complex blade curvature. Blade coning introduces an additional cyclic gravitational bending moment in the flapwise direction. The amplitude of this load is normally small in comparison to other loads. The coning angle, as expected, is inversely proportional to the mass of the blade. Due to coning, there is change in both magnitude and direction of the resulting local wind speed for the profile which alters with azimuth.

For a downwind rotor coning angle tends to align the net drag force of the rotor with the wind direction and this cause a freely yawing wind turbine to track the wind. On the other hand, the effects of coning are statically destabilizing and the wind turbine must be mechanically aligned with the wind. Increase of the coning angle reduces the aerodynamic forces due to the reduction of the swept area of the rotor and a better balance between centrifugal forces and thrust, which reduces the flapping moment. At zero coning angle wind shear produces a periodic wind load with a frequency of twice per revolution for a two bladed wind turbine.

7.9 Effect of Rotor Tilt Angle

If rotor blades are coned it follows that the blade tip at its lowest point is moved nearer the supporting tower for an upwind rotor. To reduce the overhung required at the hub the axis of the drive shaft is frequently tilted. If the tilt angle equals the cone angle the blade becomes vertical when pointing downwards. Due to tilting of the rotor the blade angle is changed as it moves round the blade circle, the amplitude being equal to the tilt angle. Significant changes of the blade loads are induced by these changes which must be calculated with great accuracy by the simplified methods since the rotor tilt angle is not small relative to the design angle of attack. There will be change in both magnitude and direction of the local wind speed for the blade profile due to tilting of the rotor. This will also alter with the blade azimuth. For a blade in the lower half of the rotor disc the blade will move towards the wind and for the upper half of the disc it will be further away from the wind. Also due

to wind shear the blade will receive higher wind velocity when it will be at the upper half of the circle.

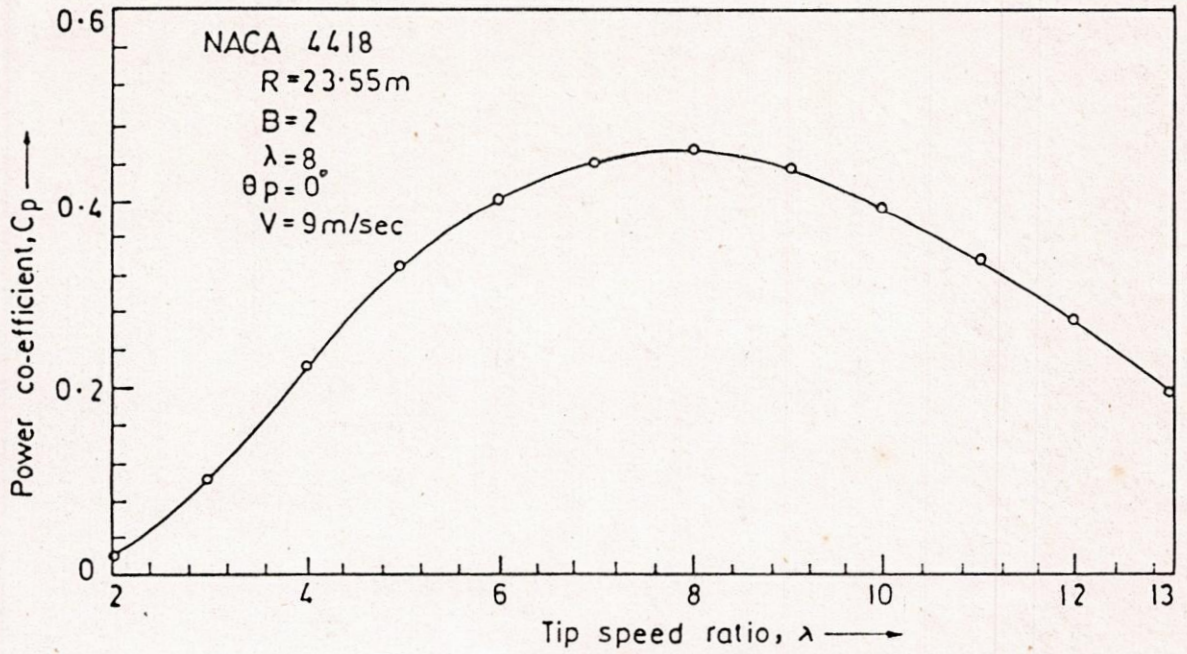


FIGURE 7.1.1: VARIATION OF POWER CO-EFFICIENT WITH TIP SPEED RATIO.

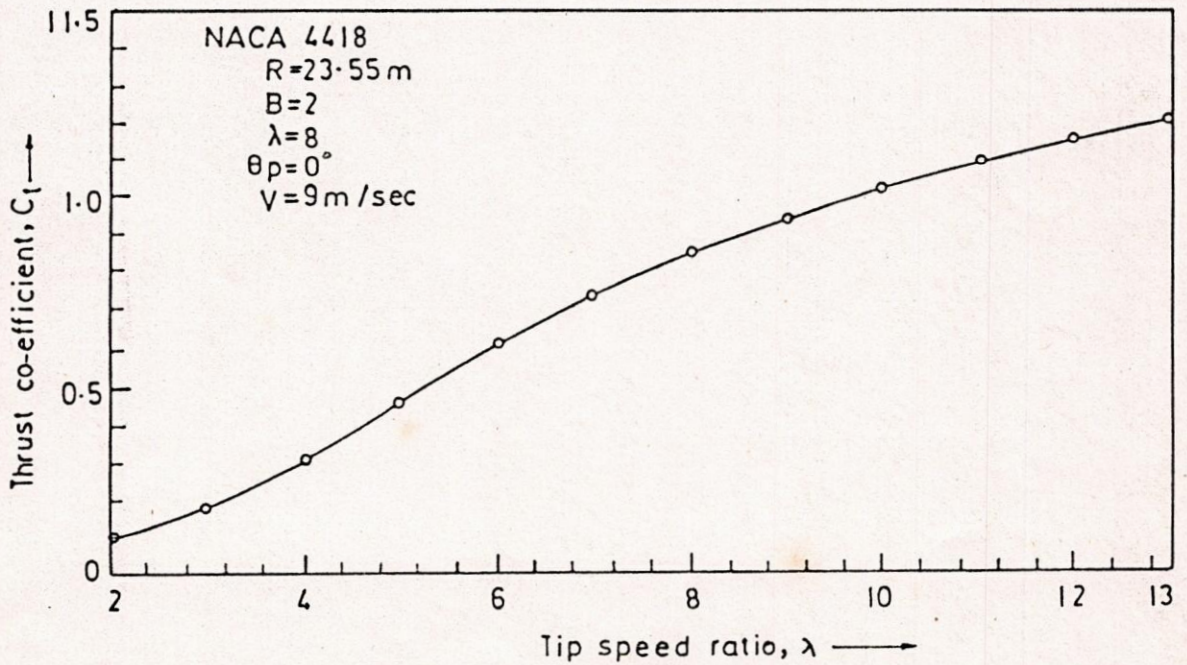


FIGURE 7.1.2: VARIATION OF THRUST CO-EFFICIENT WITH TIP SPEED RATIO.

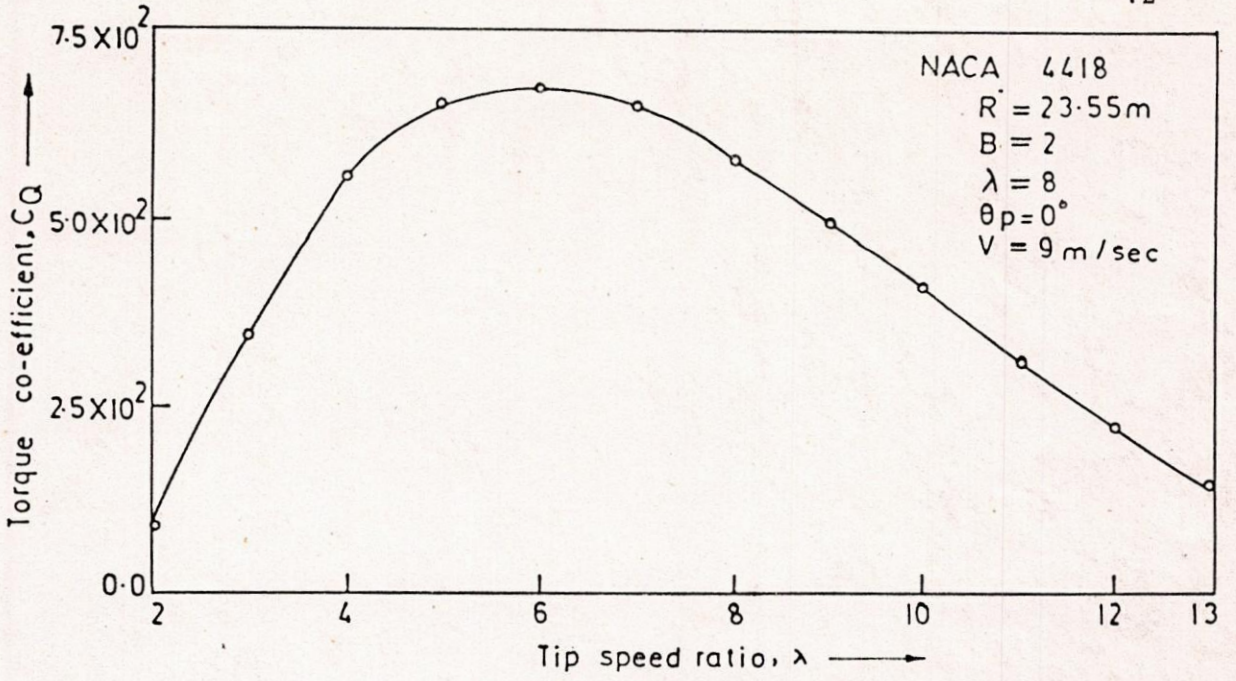


FIGURE 7.1.3-VARIATION OF TORQUE CO-EFFICIENT WITH TIP SPEED RATIO.

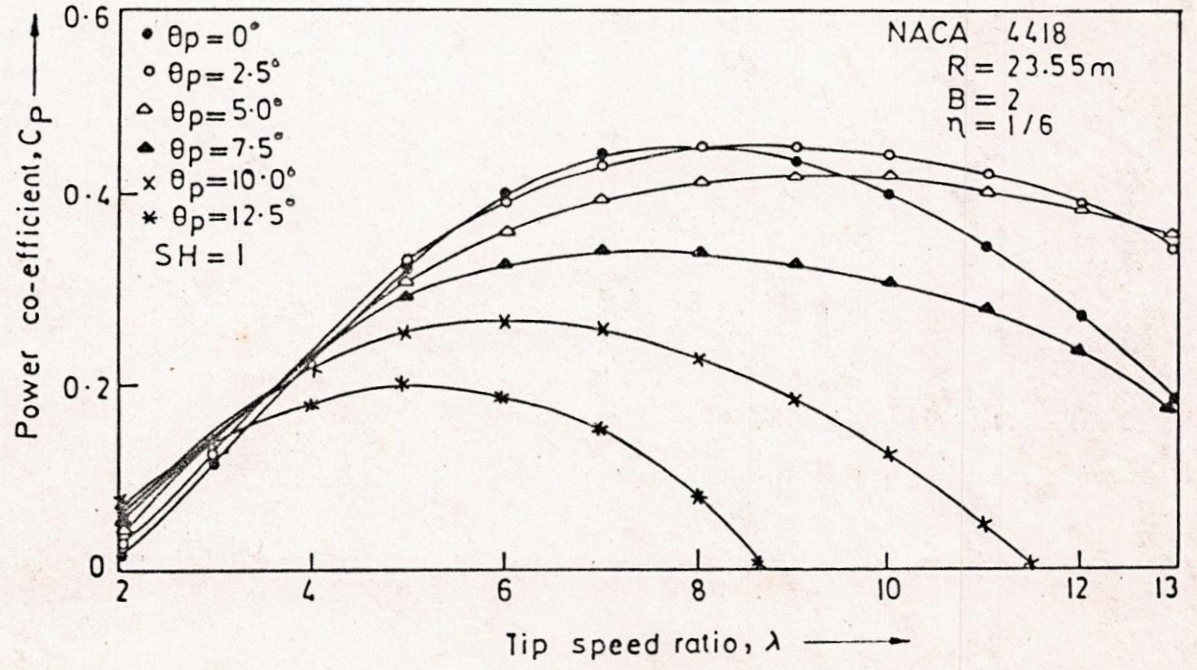


FIGURE 7.2.1: VARIATION OF POWER CO-EFFICIENT WITH TIP SPEED RATIO AT DIFFERENT PITCHING ANGLE.

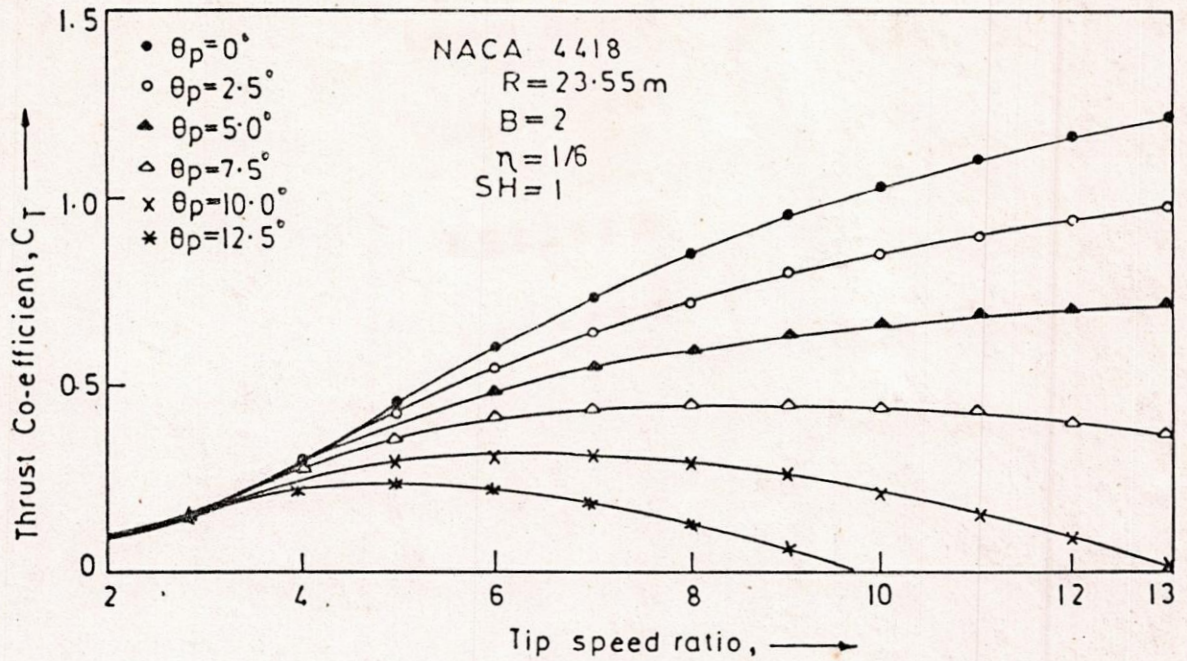


FIGURE 7.2.2: VARIATION OF THRUST CO-EFFICIENT WITH TIP SPEED RATIO AT DIFFERENT PITCHING ANGLES.

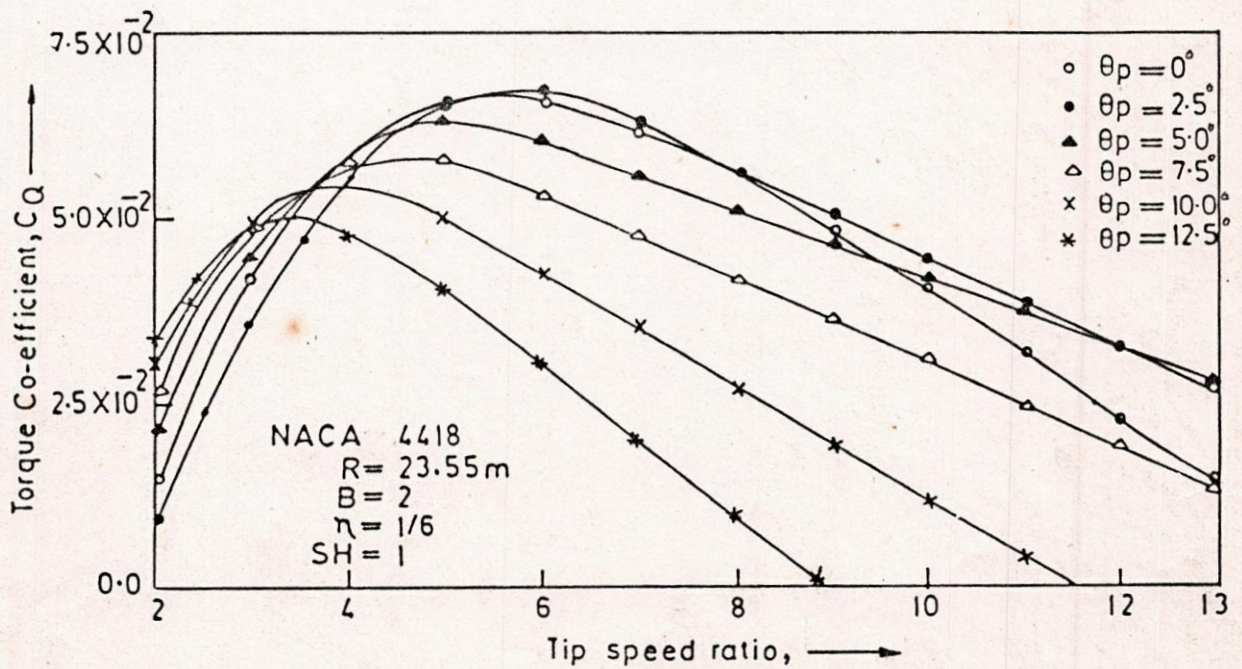


FIGURE 7.2.3: VARIATION OF TORQUE CO-EFFICIENT WITH TIP SPEED RATIO AT DIFFERENT PITCHING ANGLES.

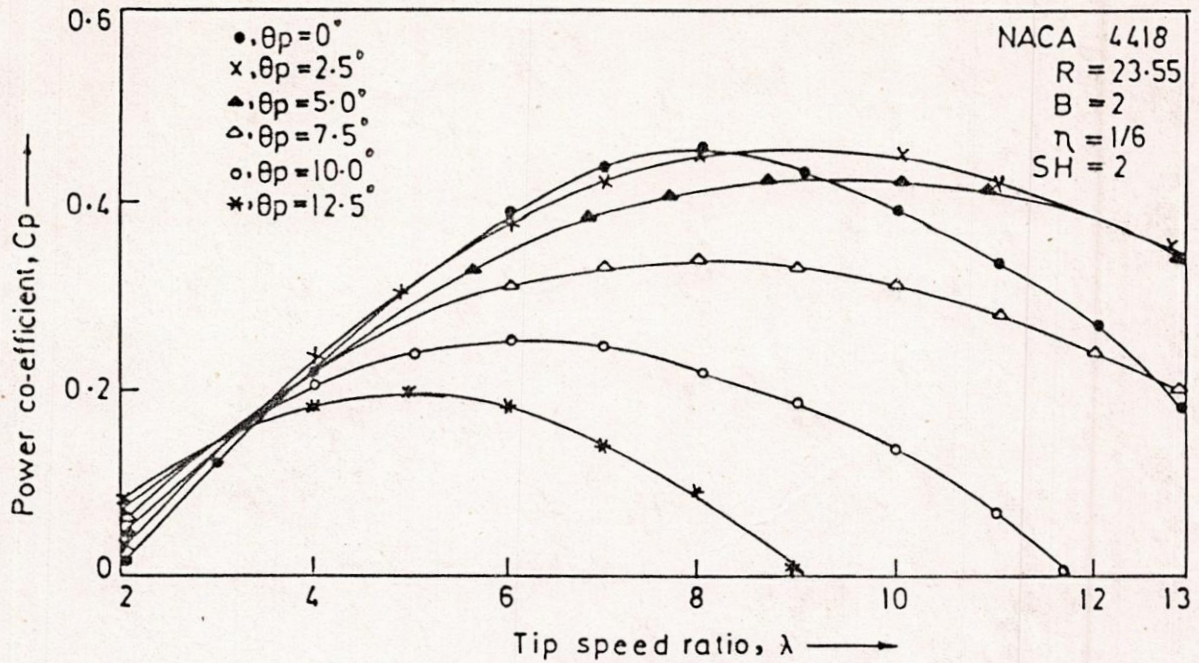


FIGURE 7.3.1: VARIATION OF POWER CO-EFFICIENT WITH TIP SPEED RATIO FOR LINEAR-CHORD-LINEAR-TWIST BLADE AT DIFFERENT PITCHING ANGLES.

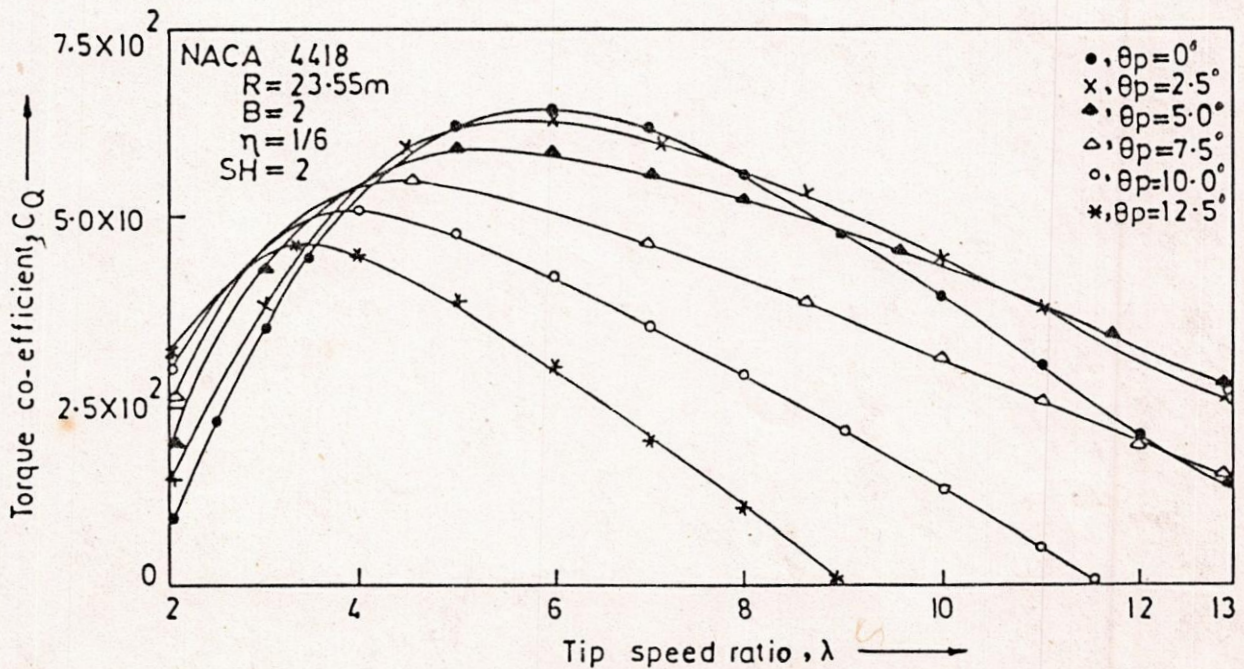


FIGURE 7.3.2: VARIATION OF TORQUE CO-EFFICIENT WITH TIP SPEED RATIO FOR LINEAR-CHORD-LINEAR-TWIST BLADE AT DIFFERENT PITCHING ANGLES.

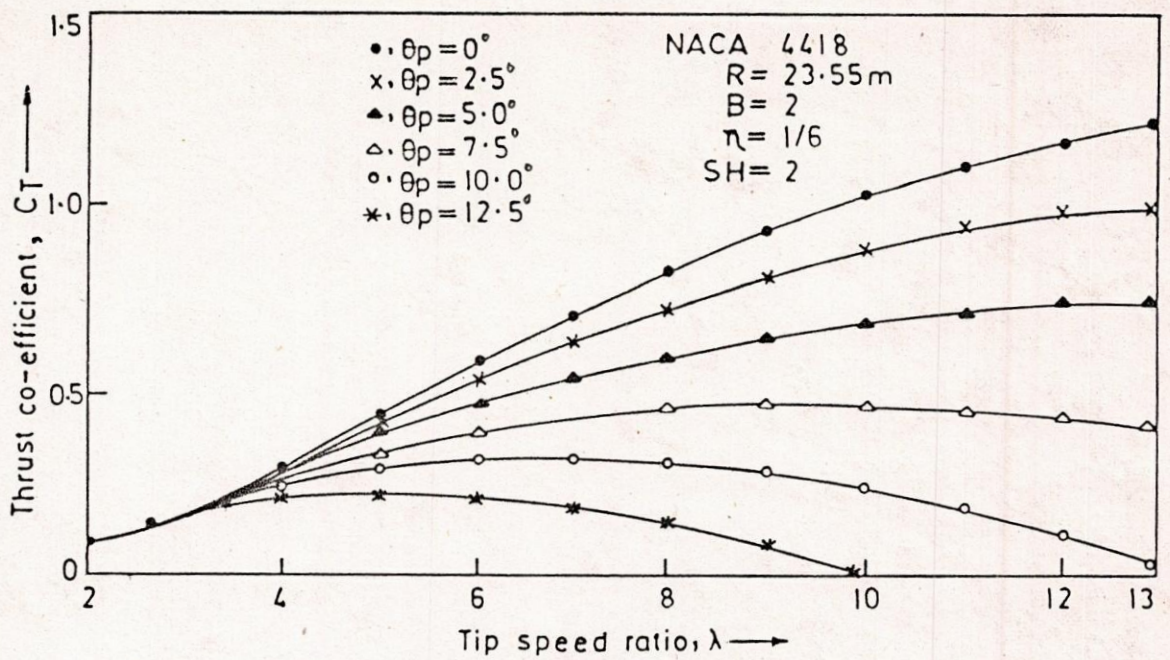


FIGURE 7.3.3: VARIATION OF THRUST CO-EFFICIENT WITH TIP SPEED RATIO FOR LINEAR-CHORD-LINEAR-TWIST BLADE AT DIFFERENT PITCHING ANGLES.

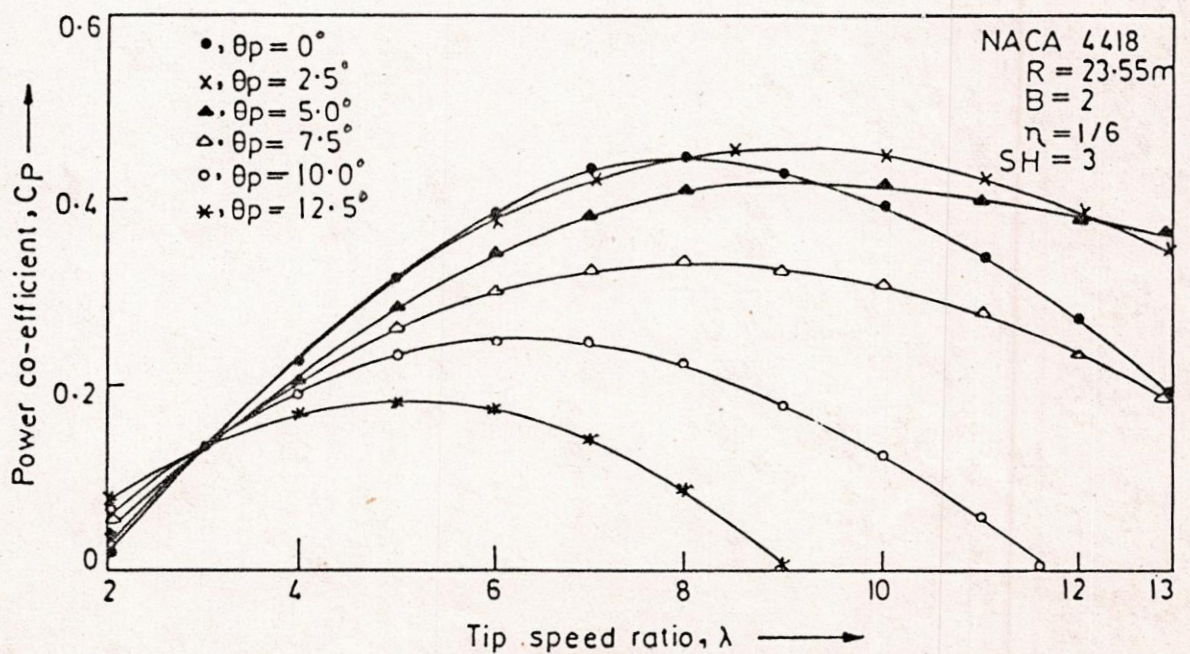


FIGURE 7.3.4: VARIATION OF POWER CO-EFFICIENT WITH TIP SPEED RATIO FOR LINEAR-CHORD-ZERO-TWIST BLADE AT DIFFERENT PITCHING ANGLES.

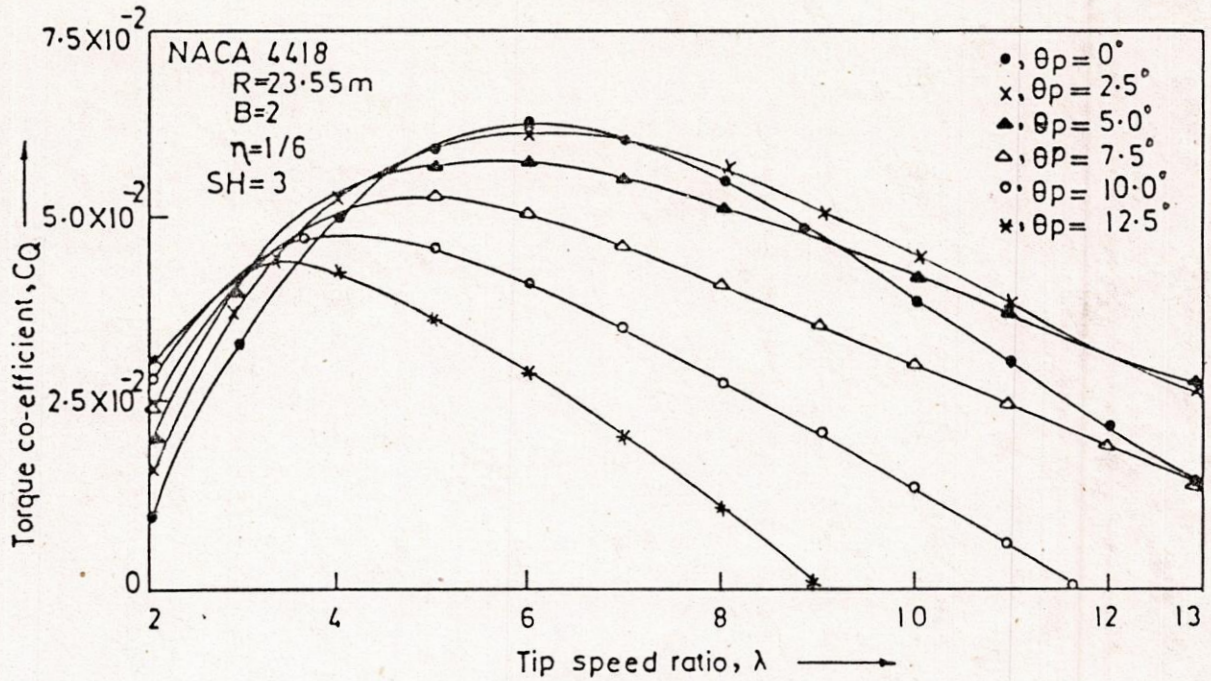


FIGURE 7.3.5: VARIATION OF TORQUE CO-EFFICIENT WITH TIP SPEED RATIO FOR LINEAR-CHORD-ZERO-TWIST BLADE AT DIFFERENT PITCHING ANGLES.

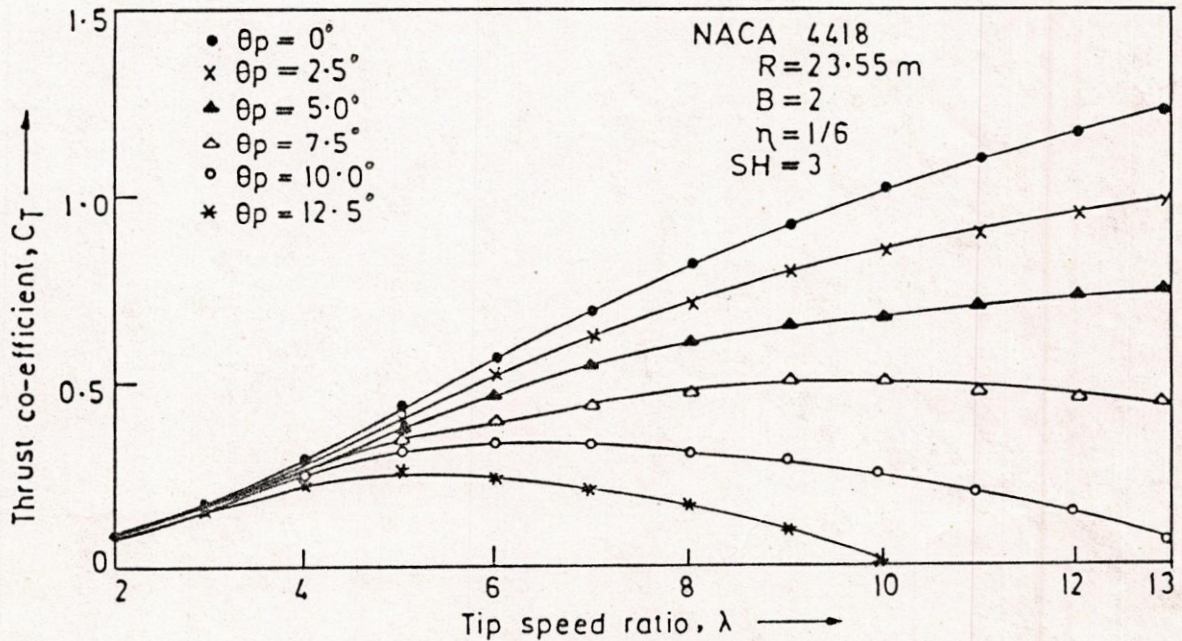


FIGURE 7.3.6: VARIATION OF THRUST CO-EFFICIENT WITH TIP SPEED RATIO FOR LINEAR-CHORD-ZERO-TWIST BLADE AT DIFFERENT PITCHING ANGLES.

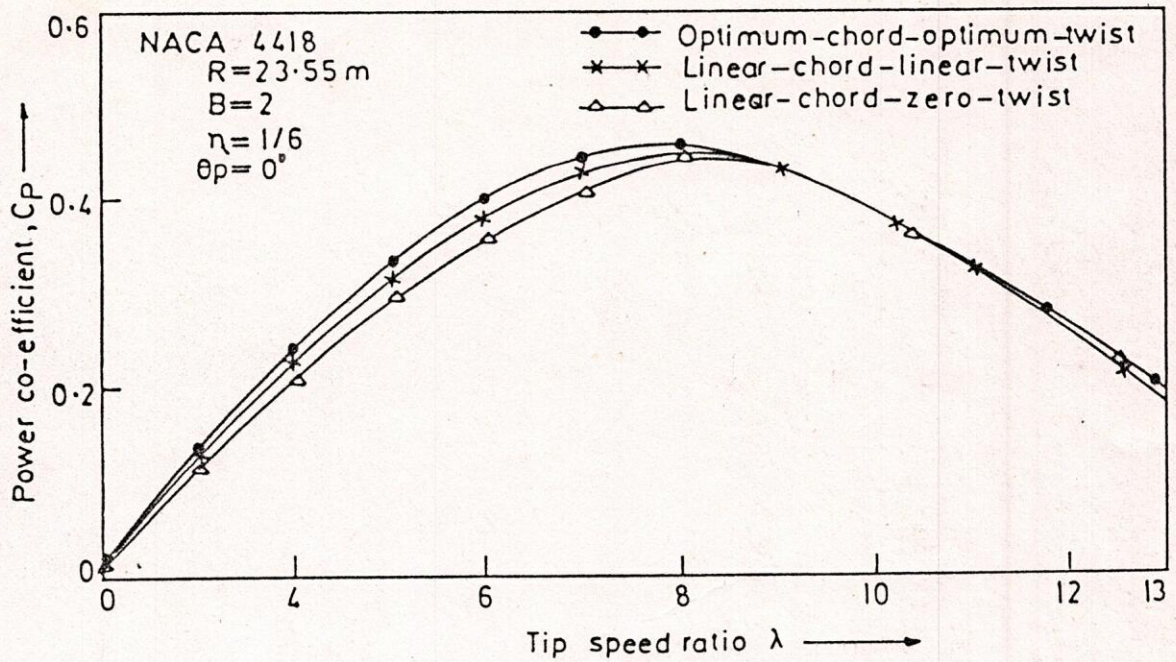


FIGURE 7.3.7: VARIATION OF POWER CO-EFFICIENT WITH TIP SPEED RATIO FOR DIFFERENT BLADE SHAPES.

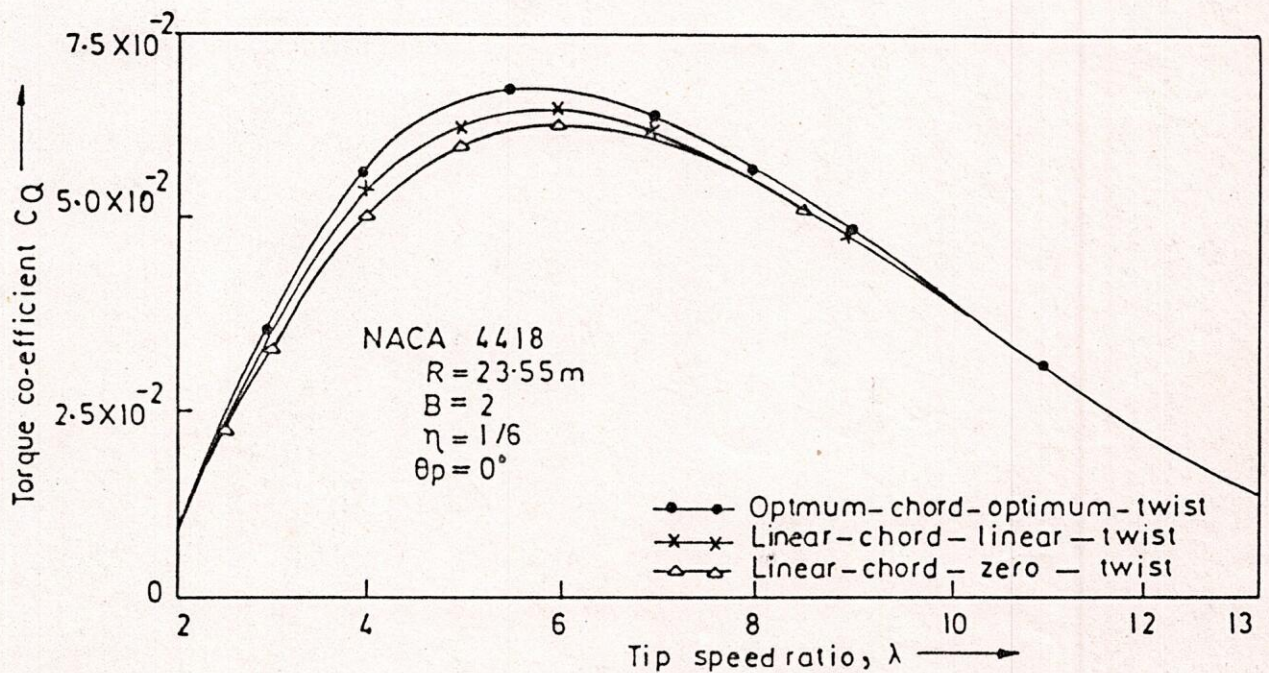


FIGURE 7.3.8: VARIATION OF TORQUE CO-EFFICIENT WITH TIP SPEED RATIO FOR DIFFERENT BLADE SHAPES.

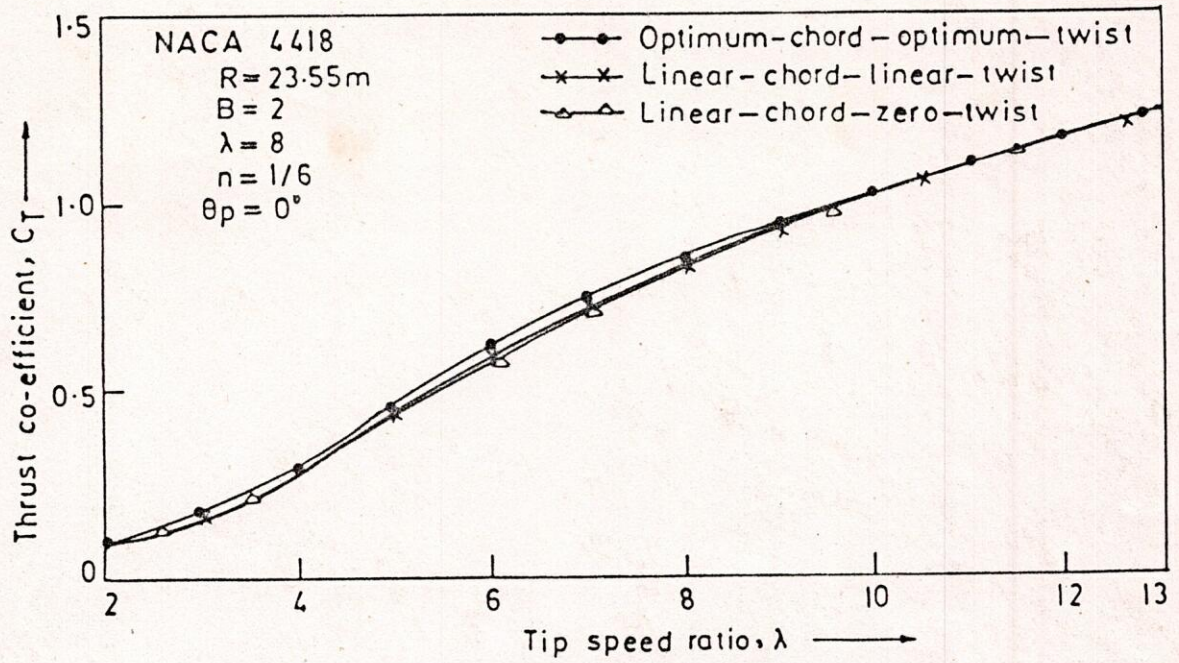


FIGURE 7.3.9: VARIATION OF THRUST CO-EFFICIENT WITH TIP SPEED RATIO FOR DIFFERENT BLADE SHAPES

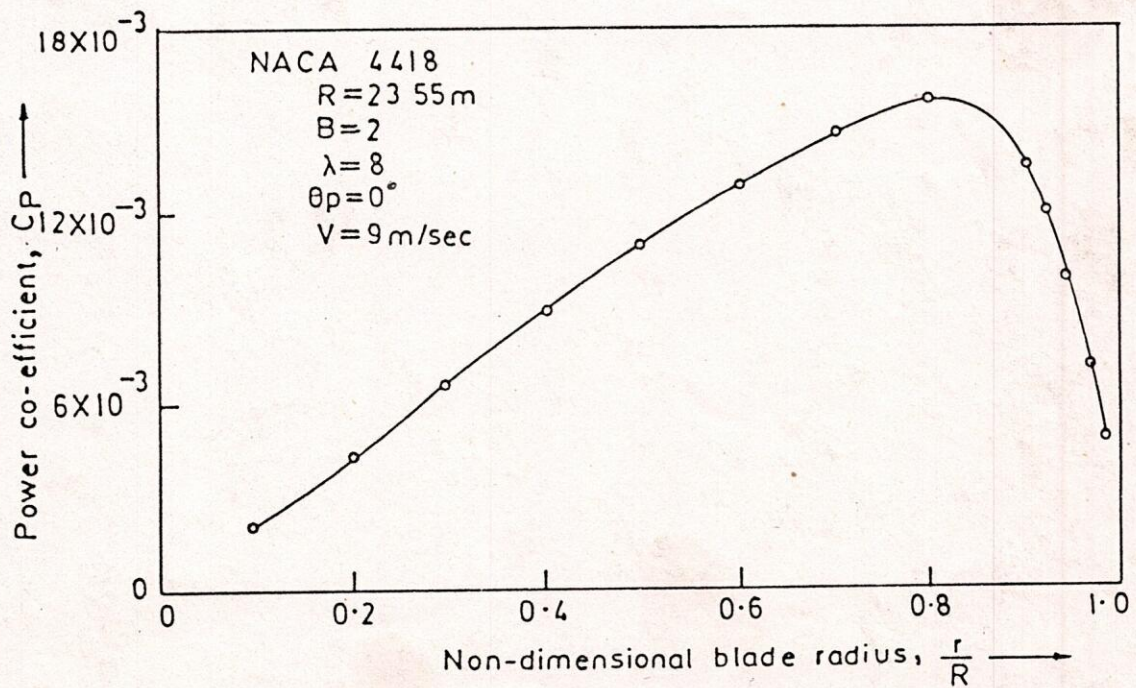


FIGURE 7.3.10: RADIAL VARIATION OF POWER CO-EFFICIENT

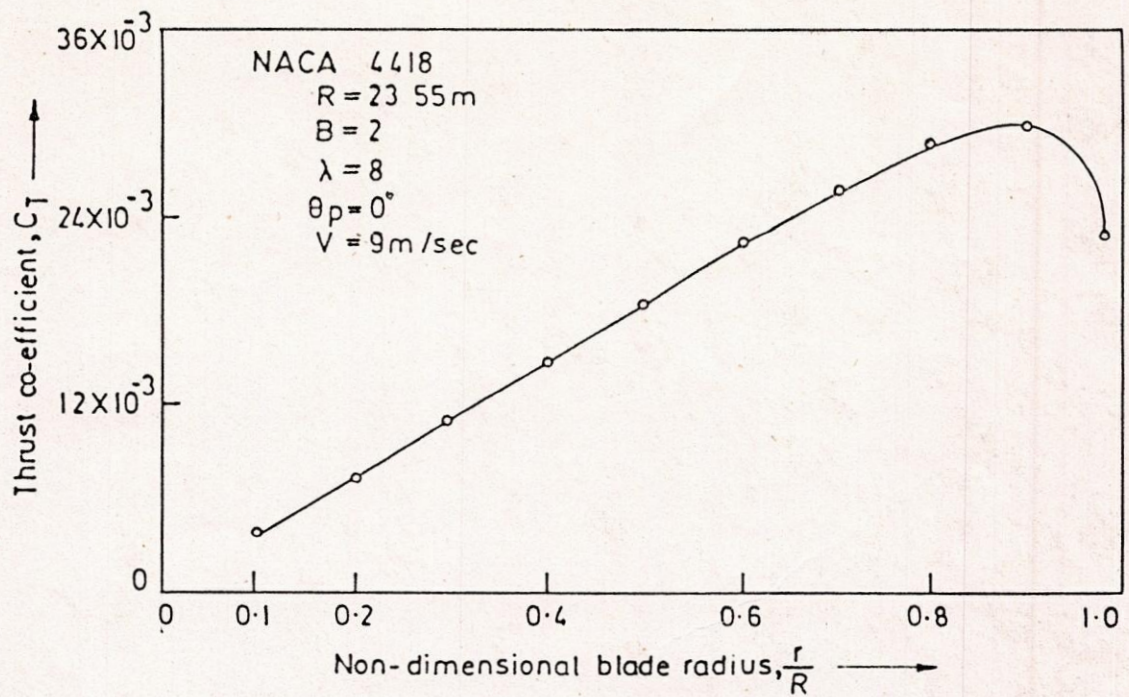


FIGURE 7.3.11: RADIAL VARIATION OF THRUST CO-EFFICIENT.

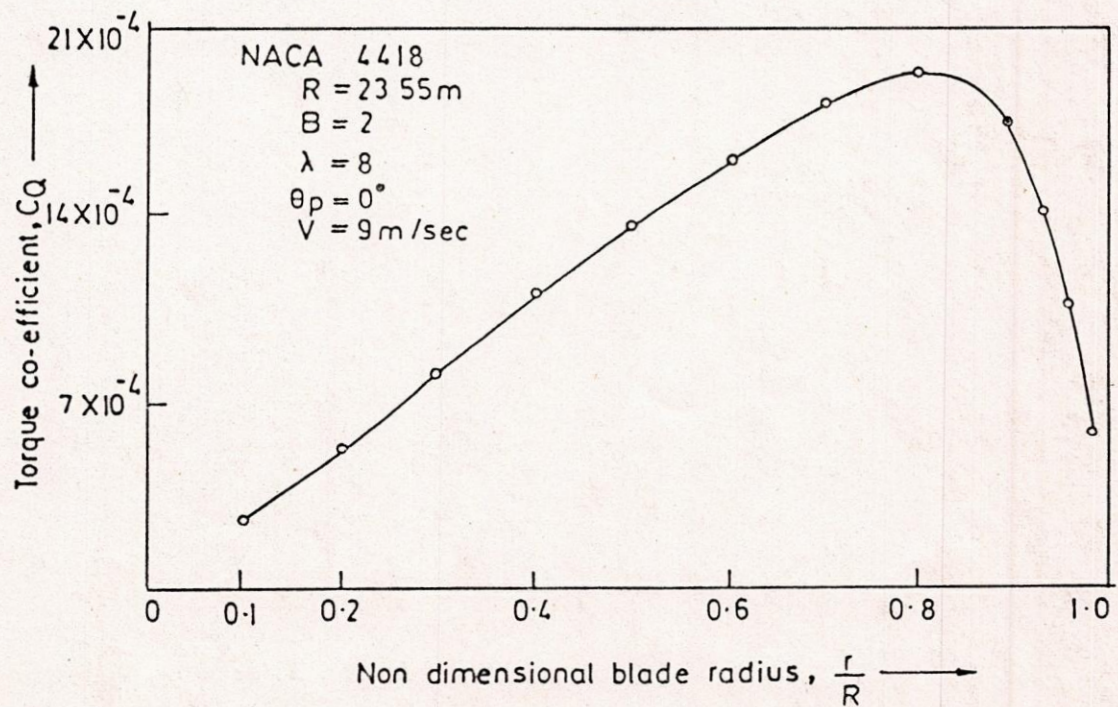


FIGURE 7.3.12: RADIAL VARIATION OF TORQUE CO-EFFICIENT.

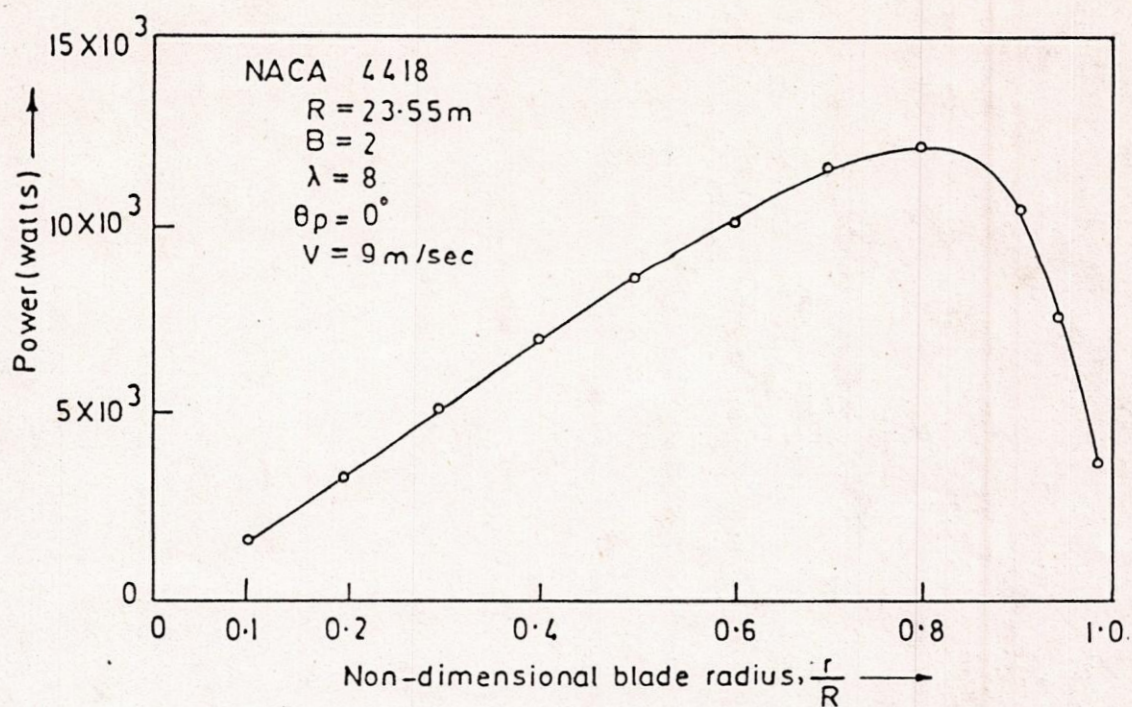


FIGURE 7-3-13: RADIAL VARIATION OF POWER.

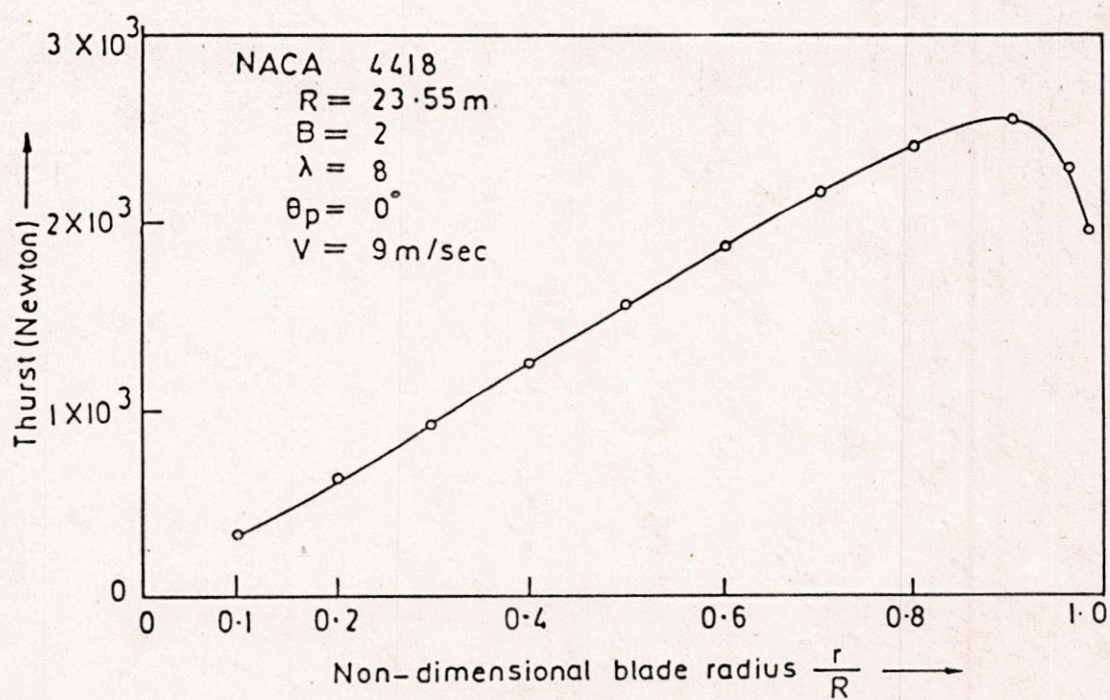


FIGURE 7-3-14: RADIAL VARIATION OF THRUST.

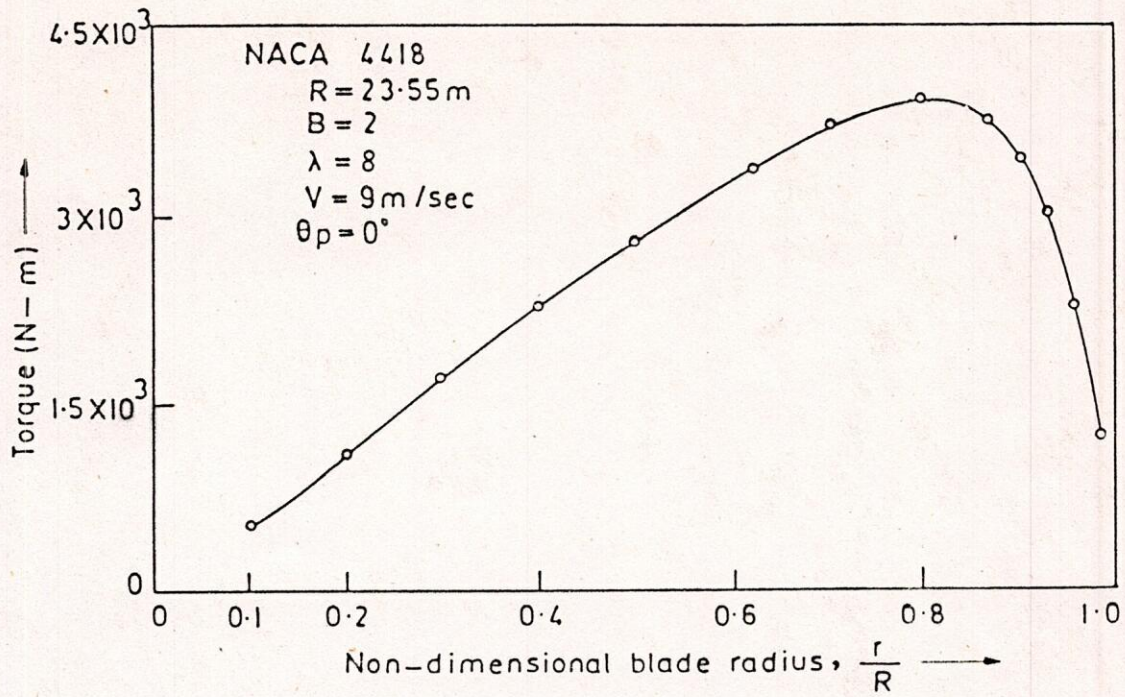


FIGURE 7.3-15: RADIAL VARIATION OF TORQUE.

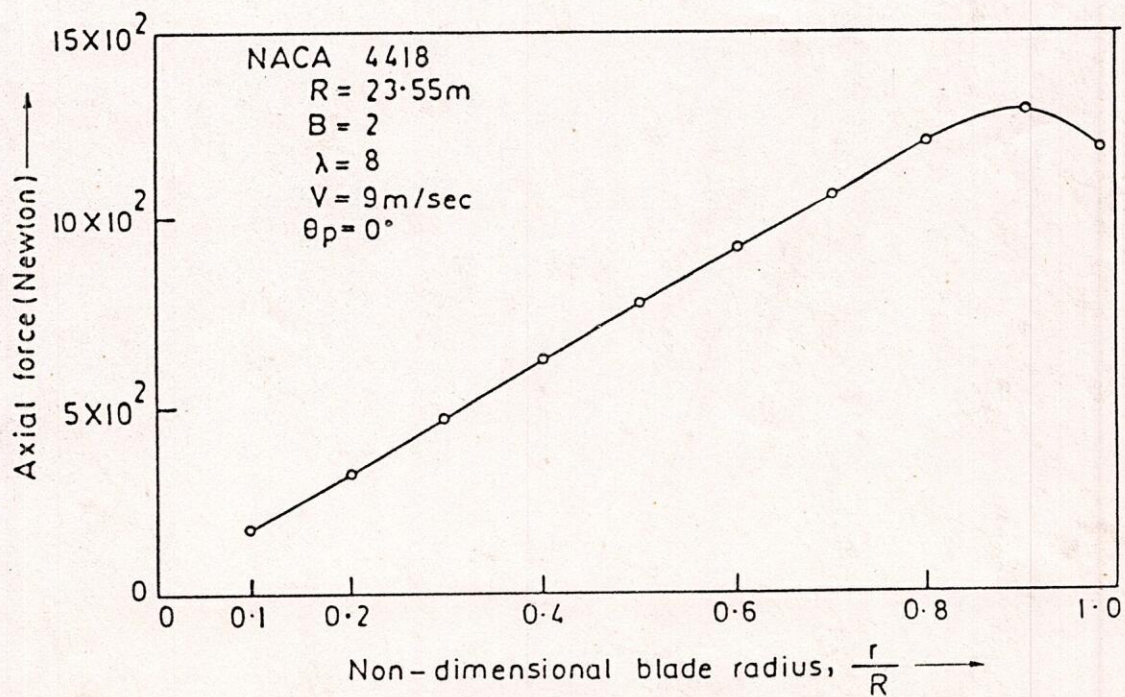


FIGURE 7.3-16: RADIAL VARIATION OF AXIAL FORCE.

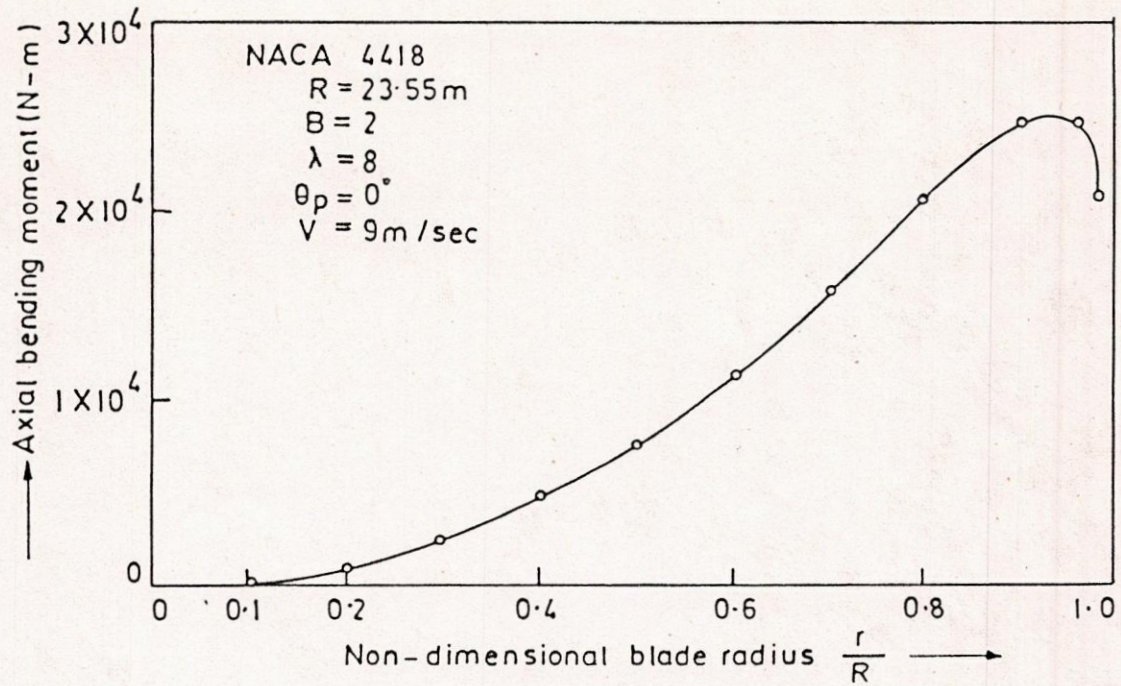


FIGURE 7.3.17: RADIAL VARIATION OF AXIAL BENDING MOMENT.

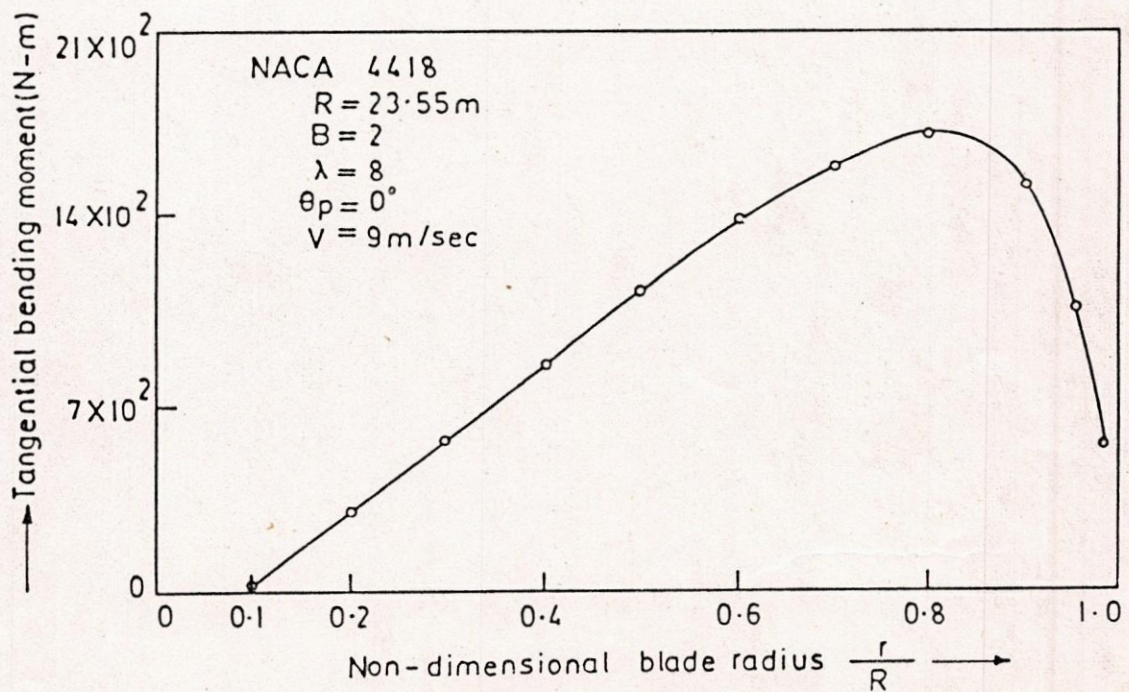


FIGURE 7.3.18: RADIAL VARIATION OF TANGENTIAL BENDING MOMENT.

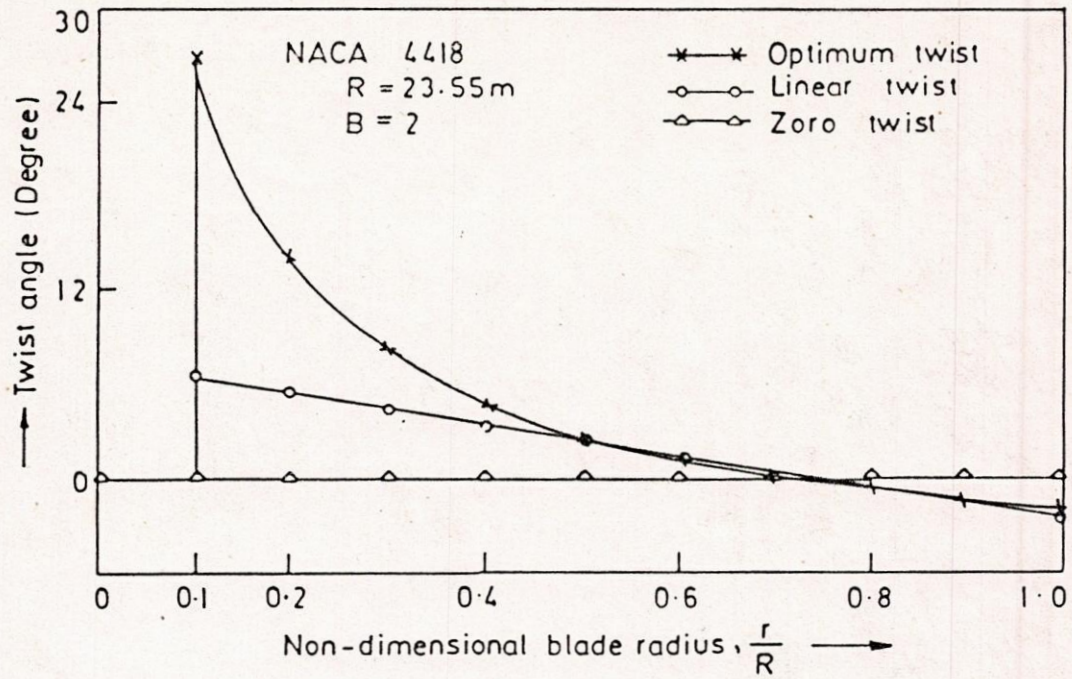


FIGURE 7-3-19: OPTIMUM AND LINEARIZED BLADE TWIST DISTRIBUTION.

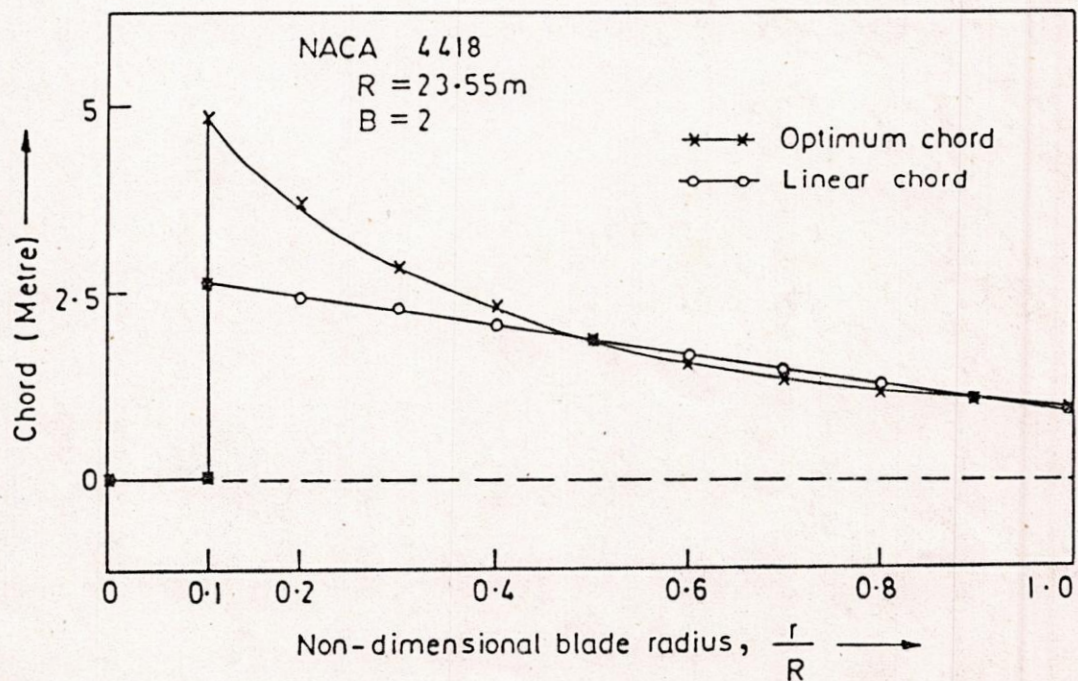


FIGURE 7-3-20: OPTIMUM AND LINEARIZED BLADE CHORD DISTRIBUTION.

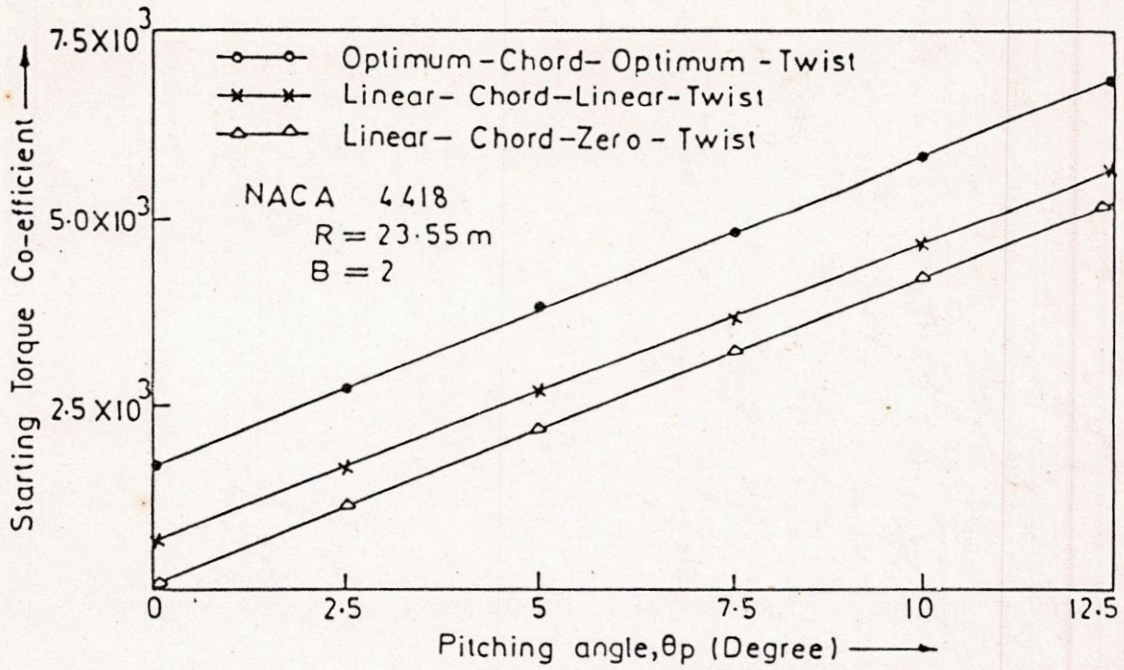


FIGURE 7.3.21: COMPARISON OF STARTING TORQUE CO-EFFICIENTS FOR DIFFERENT BLADE SHAPES WIND TURBINES.

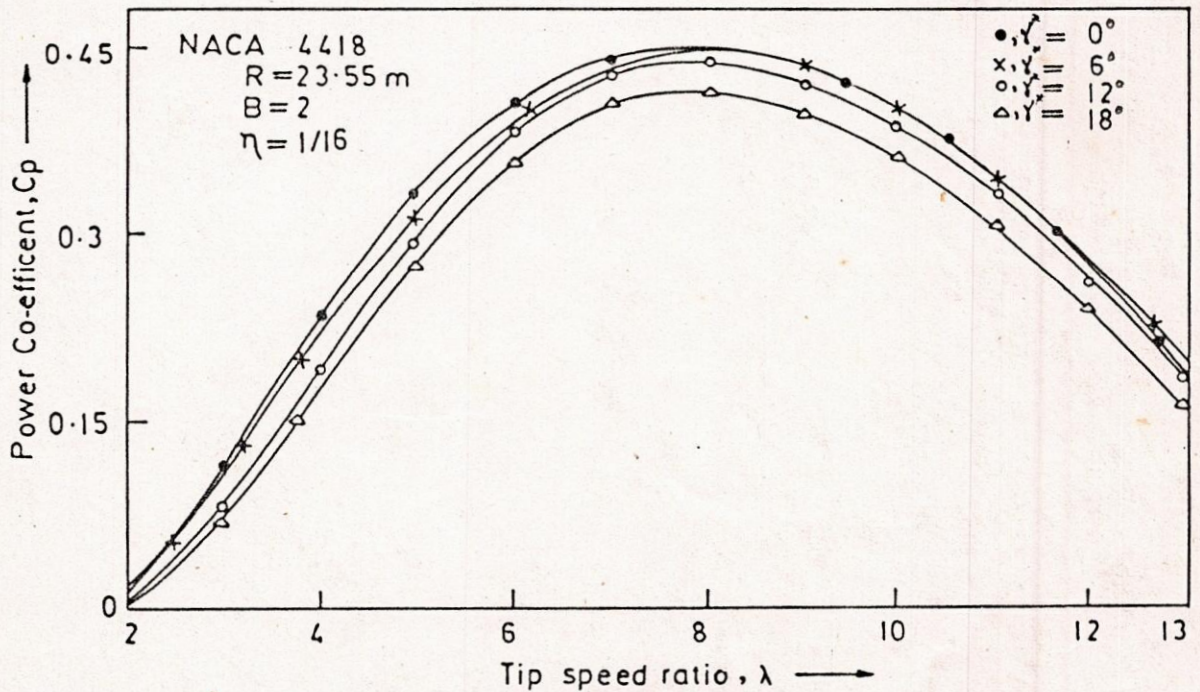


FIGURE 7.4.1: EFFECT OF YAW ANGLES ON POWER CO-EFFICIENT.

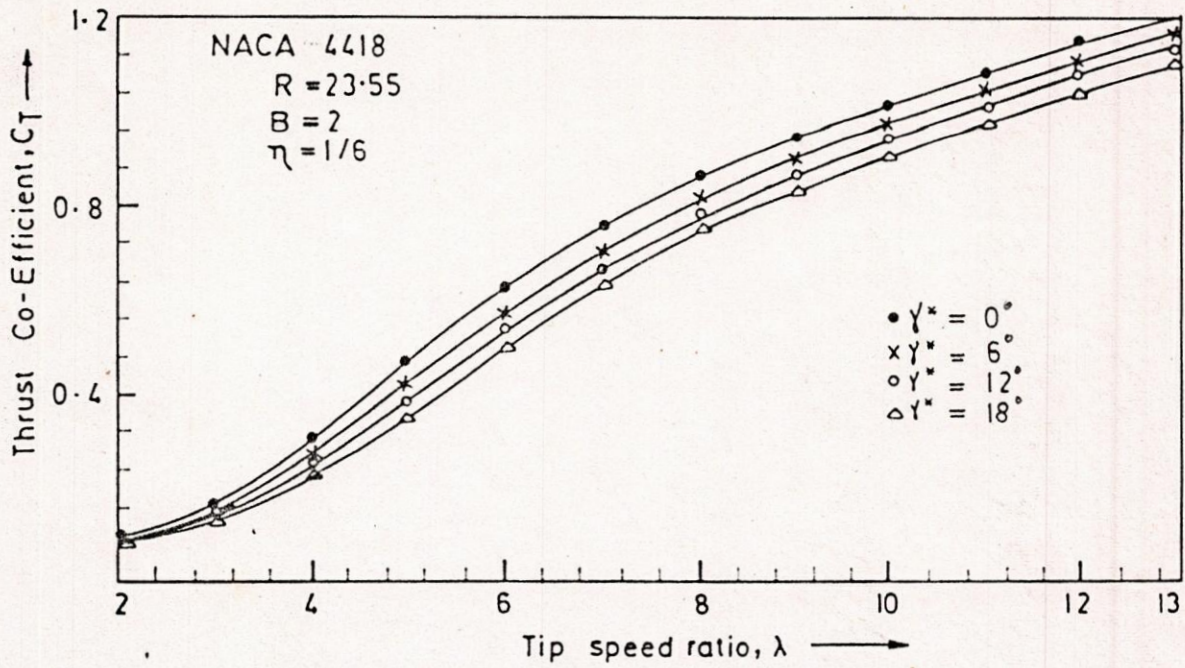


FIGURE 7.4.2: EFFECT OF YAW ANGLES ON THRUST CO-EFFICIENT.

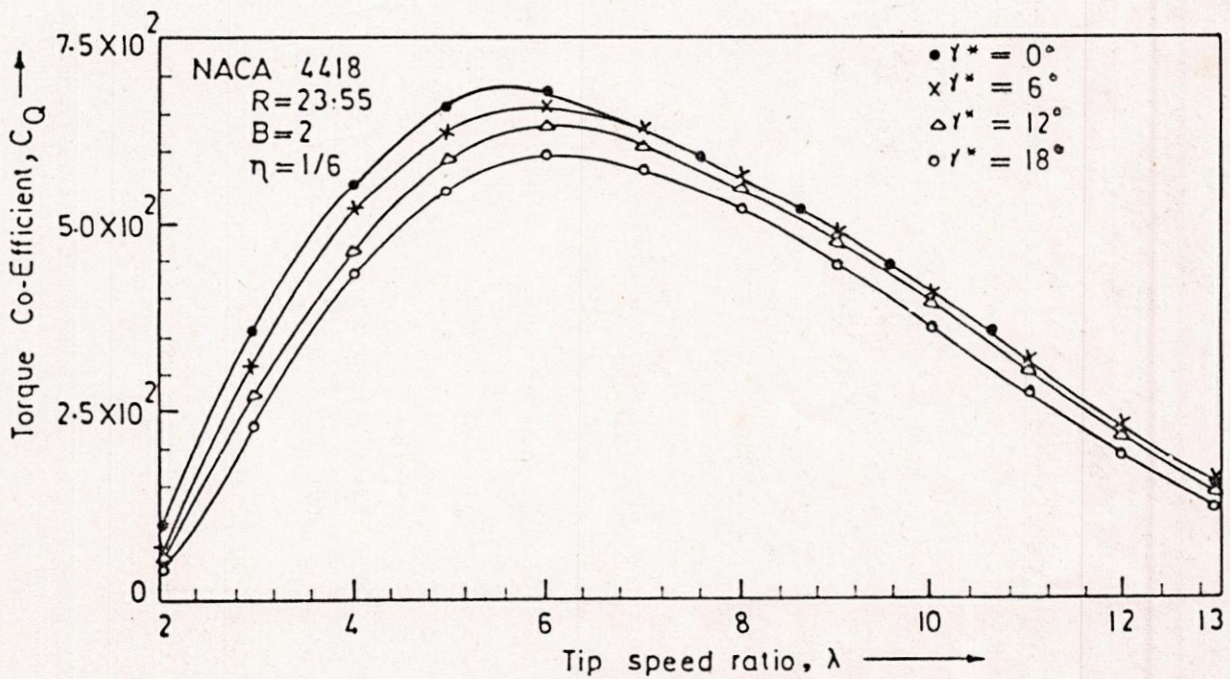


FIGURE 7.4.3: EFFECT OF YAW ANGLES ON TORQUE CO-EFFICIENT.

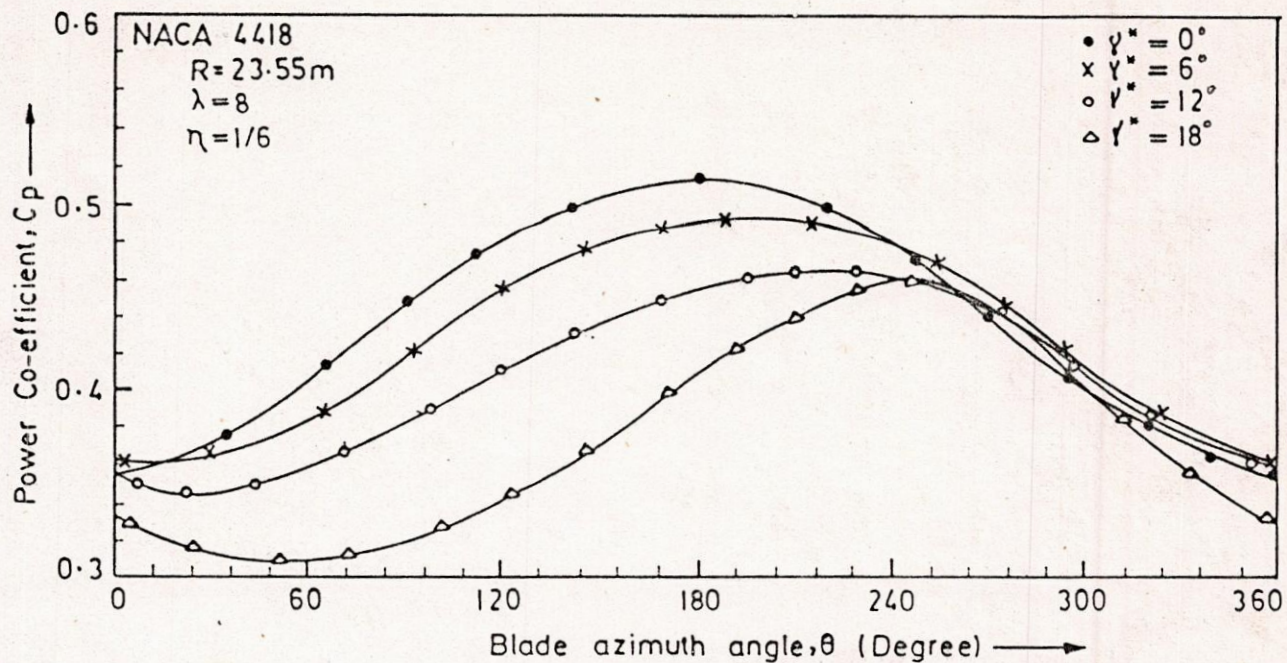


FIGURE 7.4.4: POWER CO-EFFICIENT AS A FUNCTION OF BLADE ANGULAR POSITION AT DIFFERENT YAWING ANGLES.

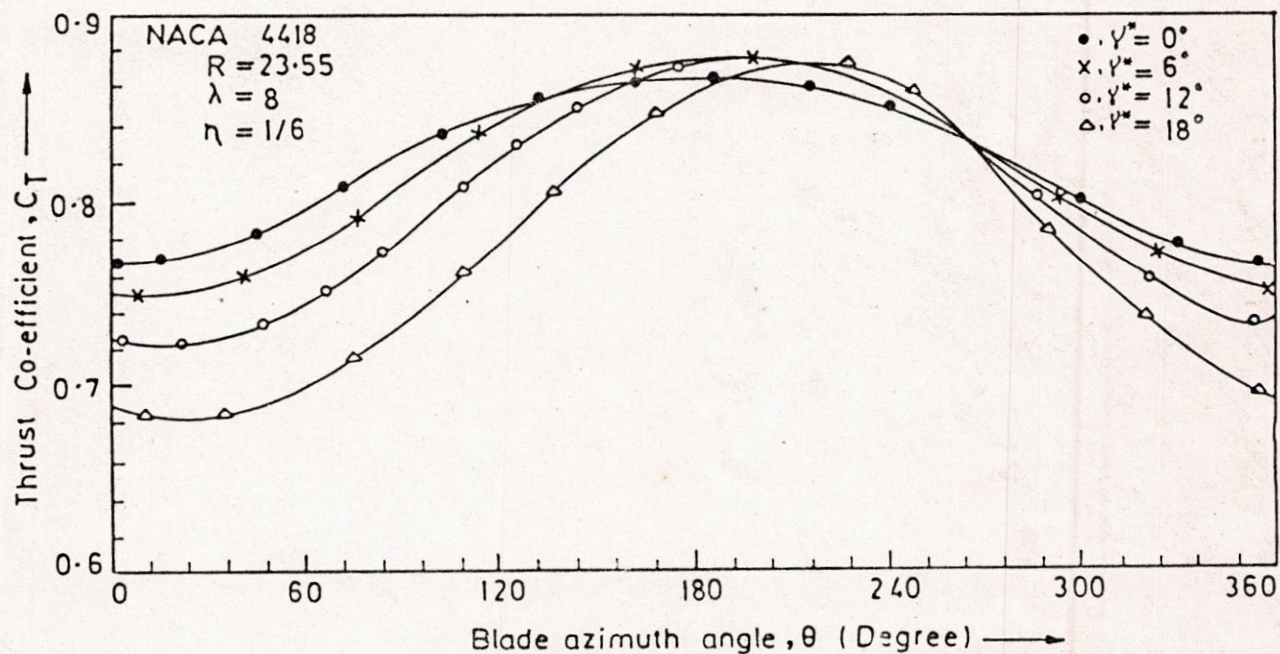


FIGURE 7.4.5: THRUST CO-EFFICIENT AS A FUNCTION OF BLADE ANGULAR POSITION AT DIFFERENT YAWING ANGLES.

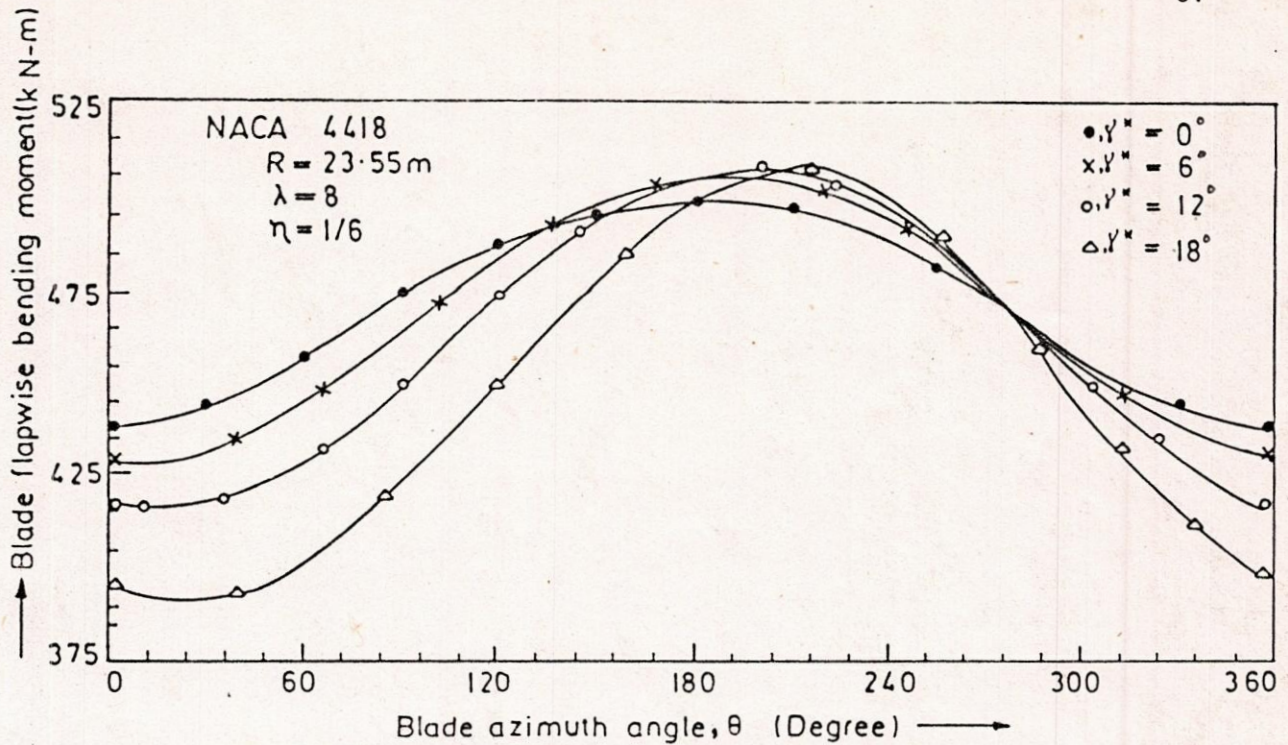


FIGURE 7.4.6: BLADE FLAPWISE BENDING MOMENT AS A FUNCTION OF BLADE ANGULAR POSITION AT DIFFERENT YAWING ANGLES.

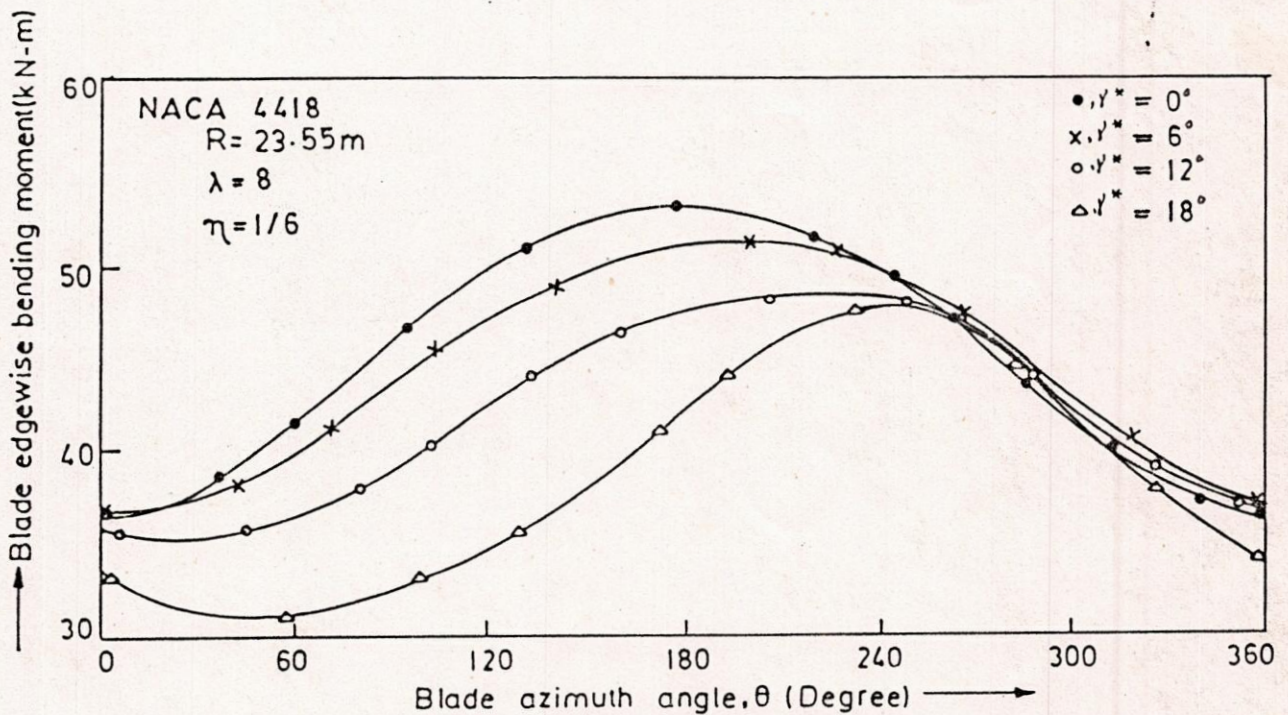


FIGURE 7.4.7: BLADE EDGEWISE BENDING MOMENT AS A FUNCTION OF BLADE ANGULAR POSITION AT DIFFERENT YAWING ANGLES.

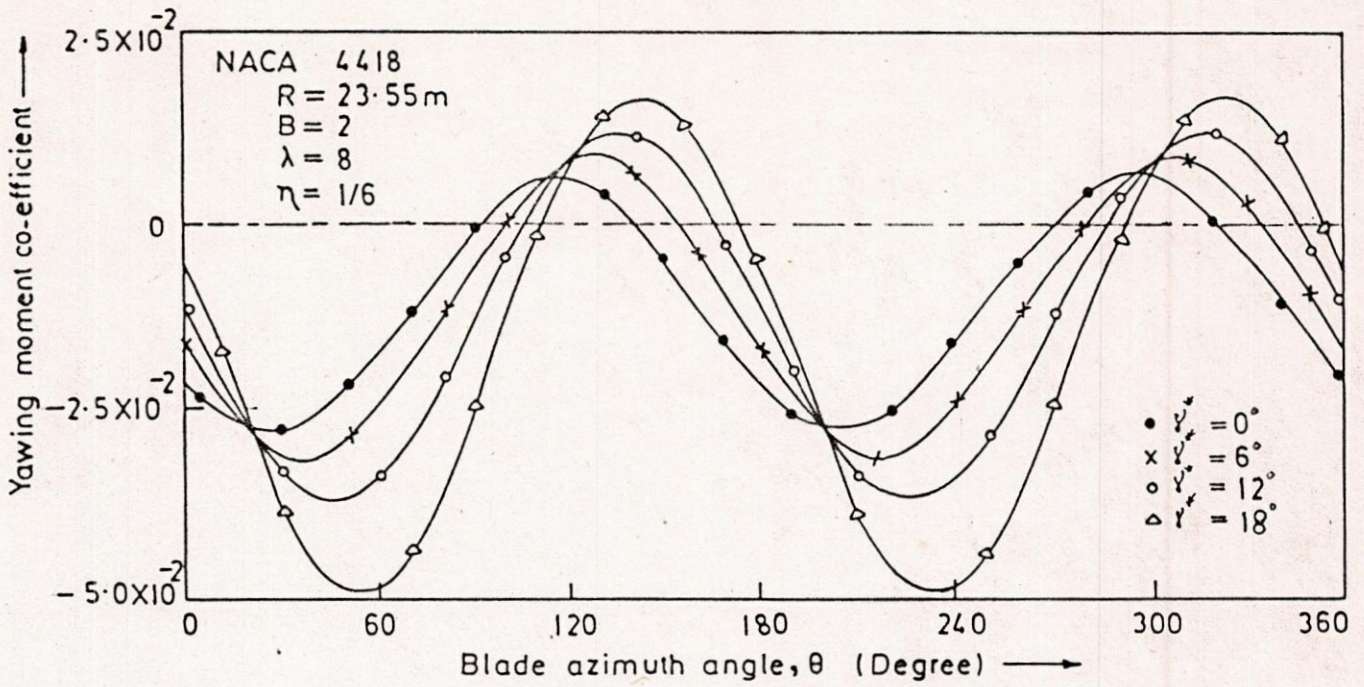


FIGURE 7.4.8: EFFECT OF YAWING ANGLES ON YAWING MOMENT CO-EFFICIENT DURING ONE REVOLUTION.

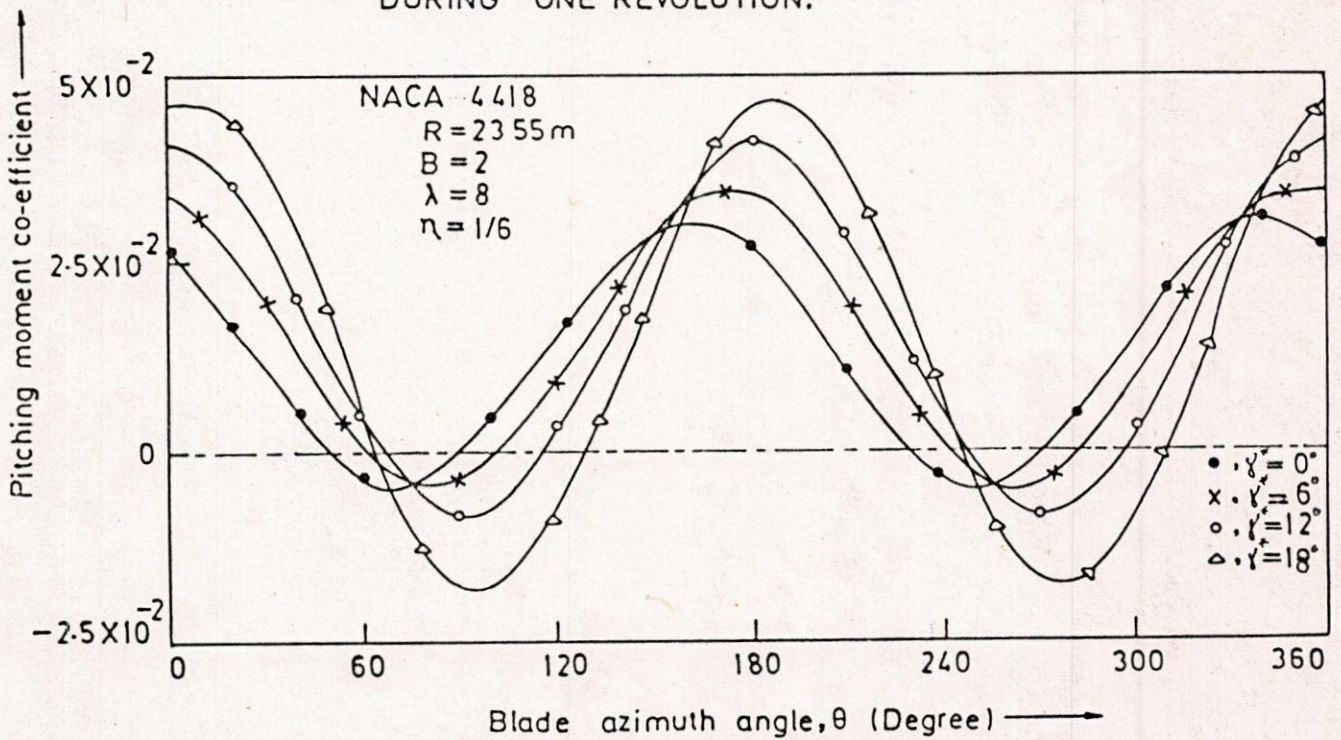


FIGURE 7.4.9: EFFECT OF YAWING ANGLES ON PITCHING MOMENT CO-EFFICIENT DURING ONE REVOLUTION.

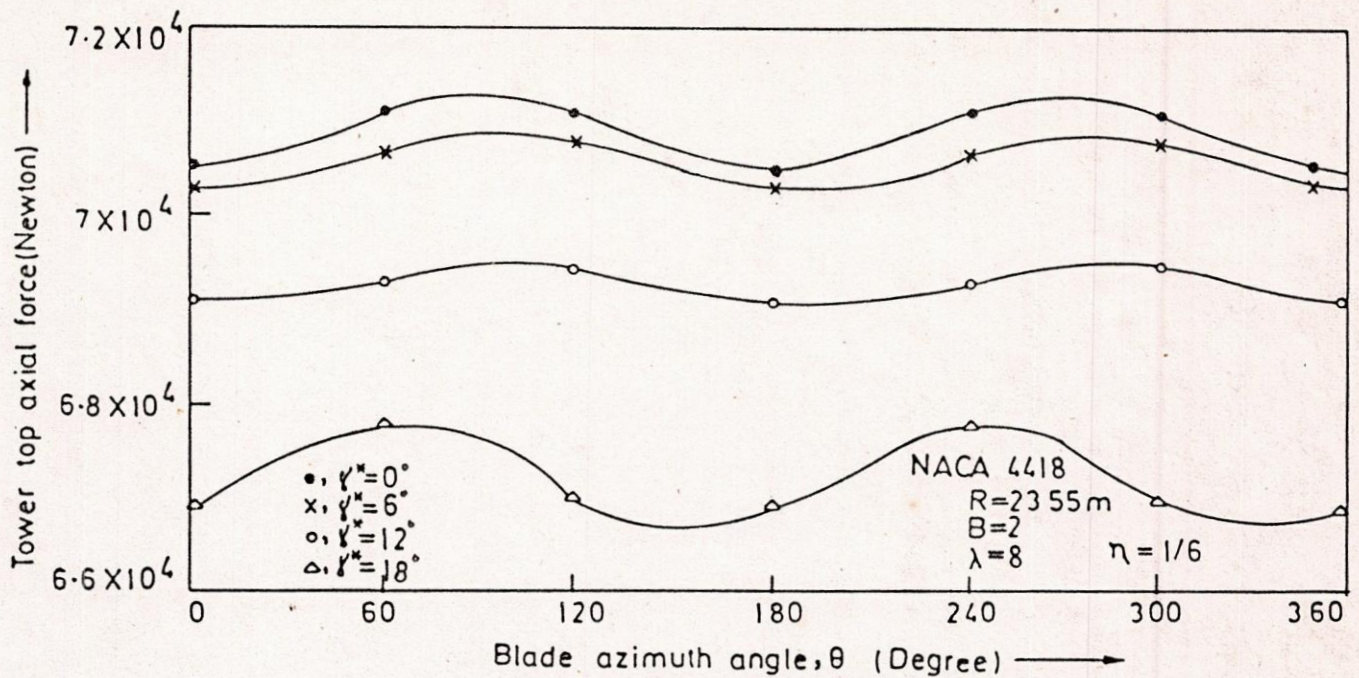


FIGURE 7.4.10: TOWER TOP AXIAL FORCE DURING ONE REVOLUTION AT DIFFERENT YAWING ANGLES.

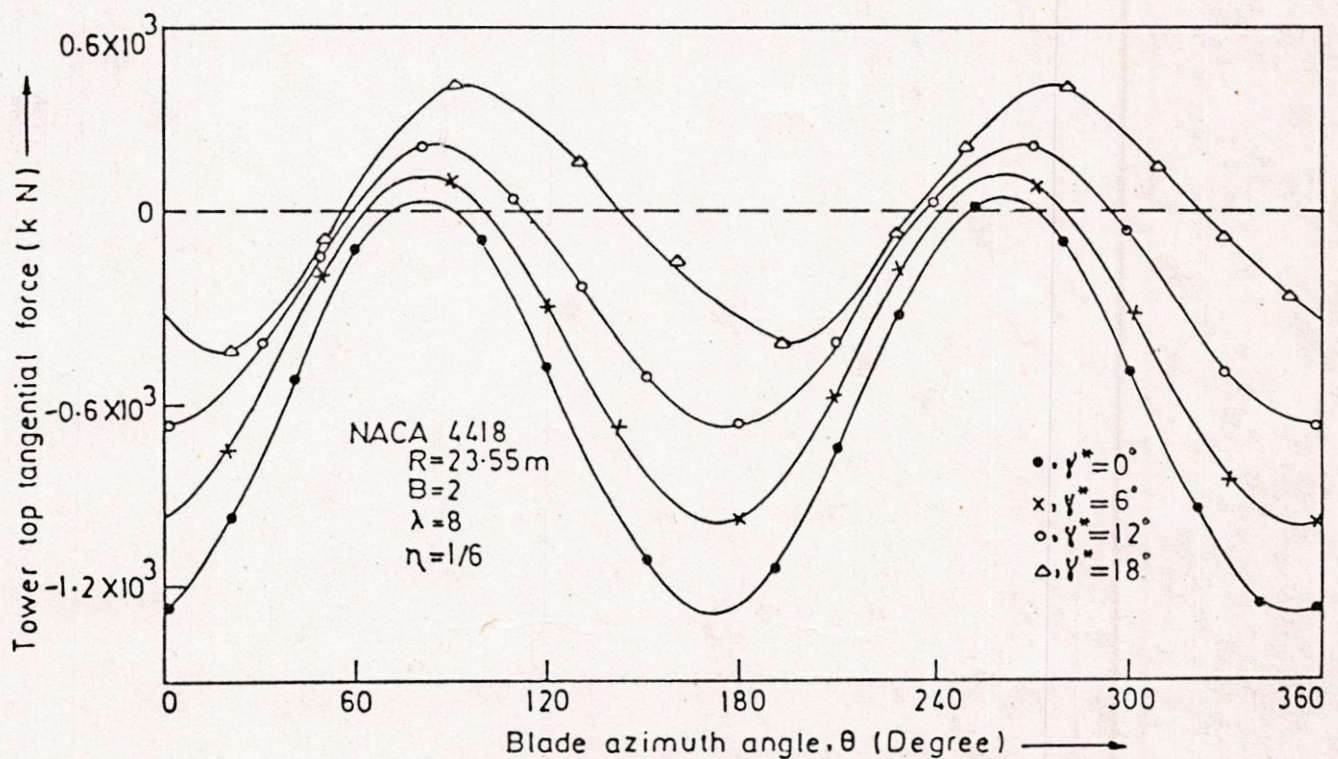


FIGURE 7.4.11: EFFECT OF YAWING ANGLE ON TOWER TOP TANGENTIAL FORCE DURING ONE REVOLUTION.

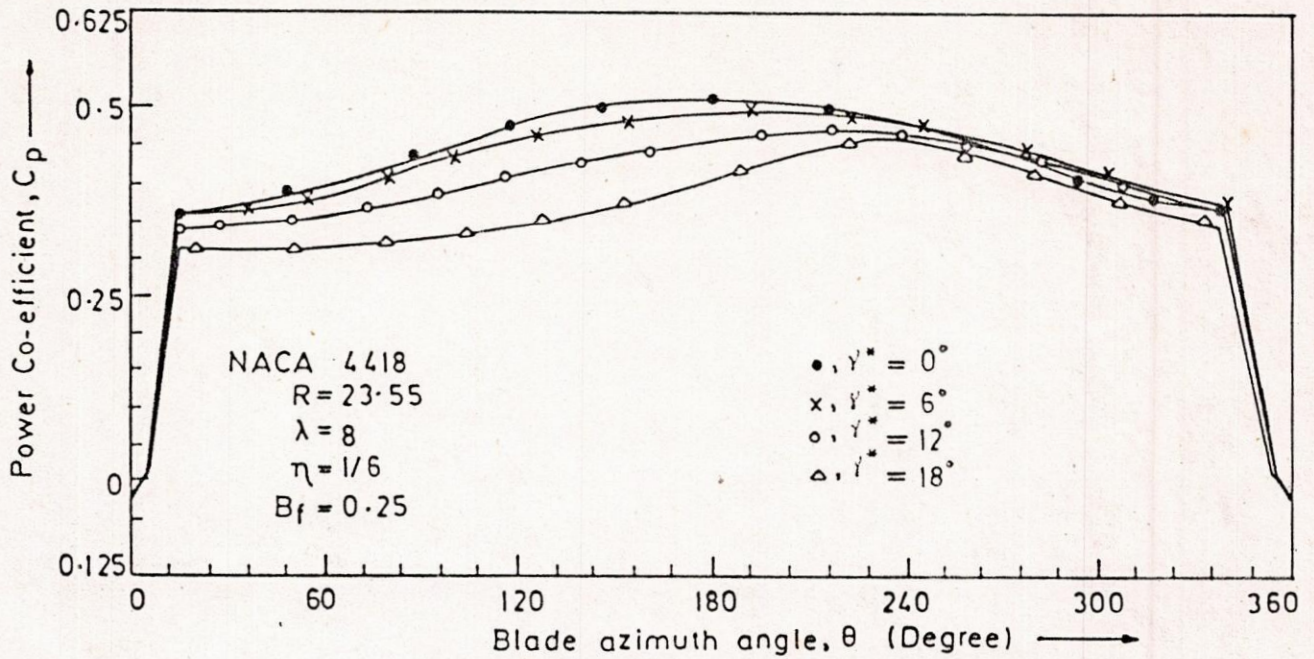


FIGURE 7.5.1: EFFECT OF TOWER SHADOW ON POWER CO-EFFICIENT AT DIFFERENT YAW ANGLES DURING ONE REVOLUTION.

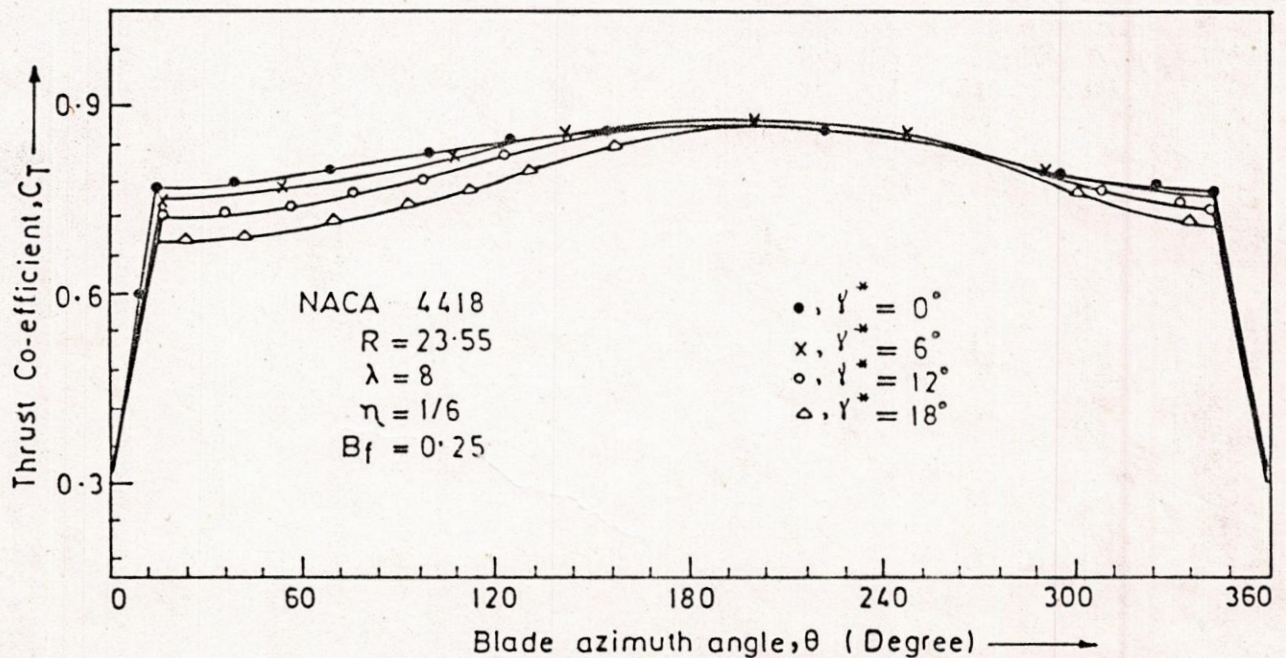


FIGURE 7.5.2: VARIATION OF THRUST CO-EFFICIENT DUE TO TOWER SHADOW AND YAWING ANGLES DURING ONE REVOLUTION.

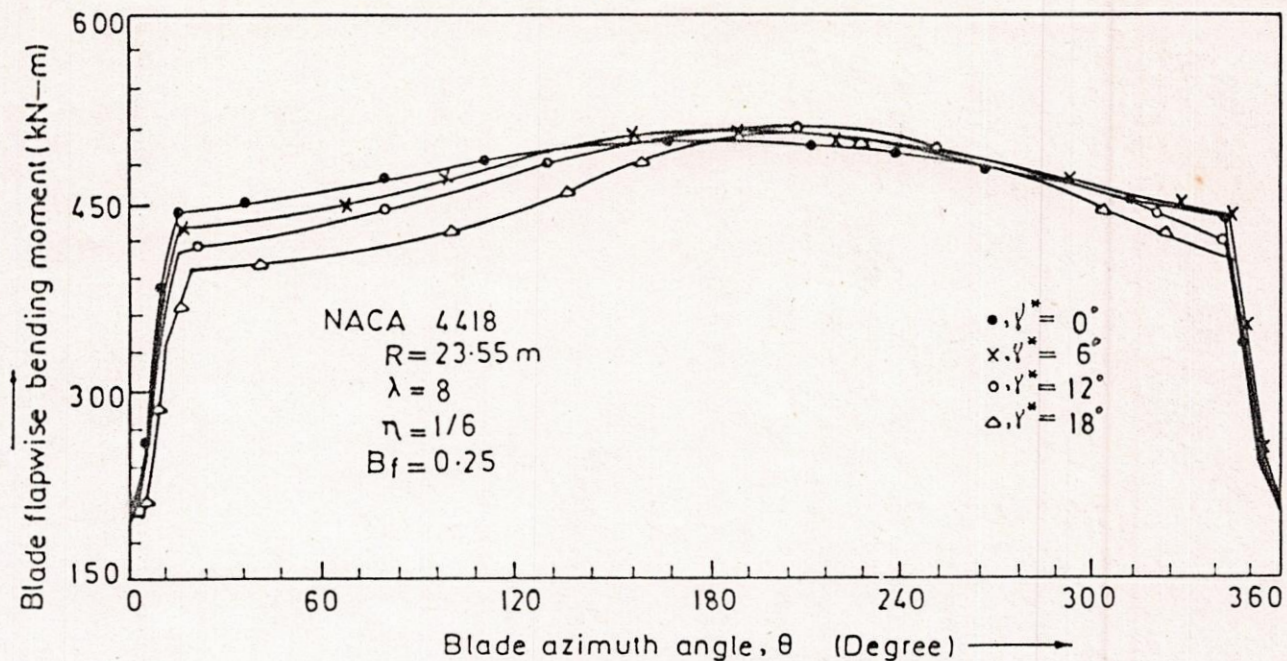


FIGURE 7.5.3: EFFECT OF TOWER SHADOW ON BLADE FLAPWISE ROOT BENDING MOMENT AT DIFFERENT YAW ANGLES DURING ONE REVOLUTION.

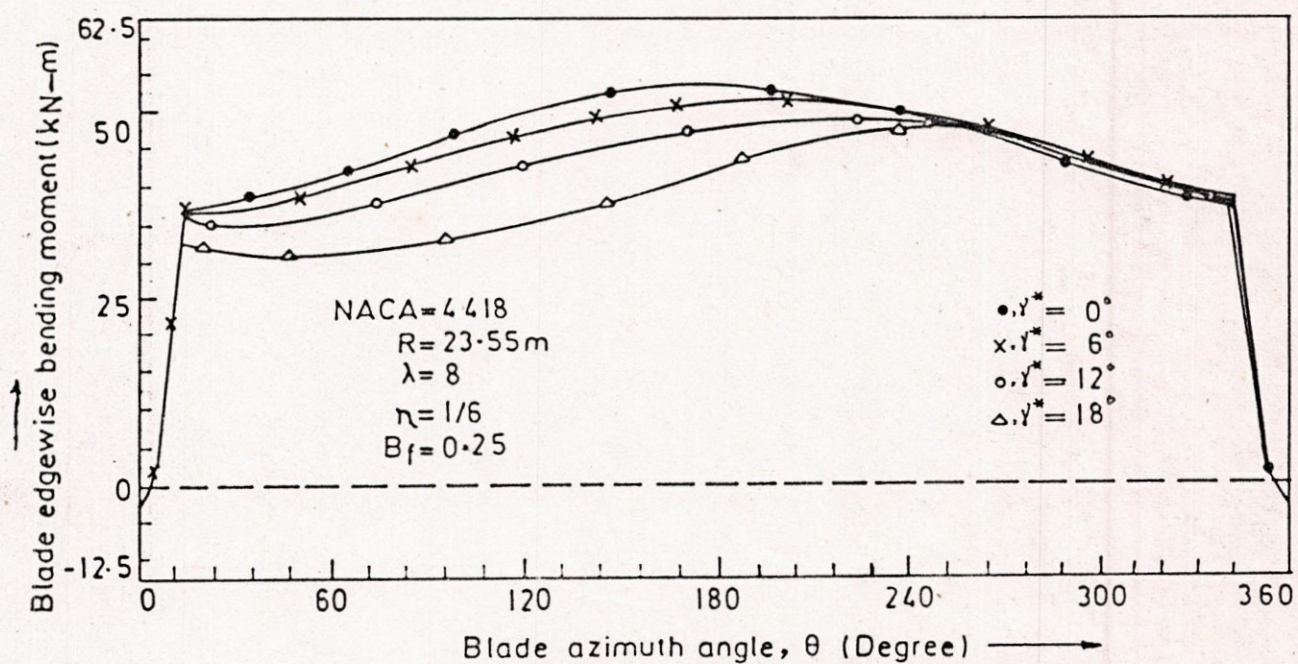


FIGURE 7.5.4: EFFECT OF TOWER SHADOW ON BLADE EDGEWISE BENDING MOMENT AT DIFFERENT YAW ANGLES DURING ONE REVOLUTION.

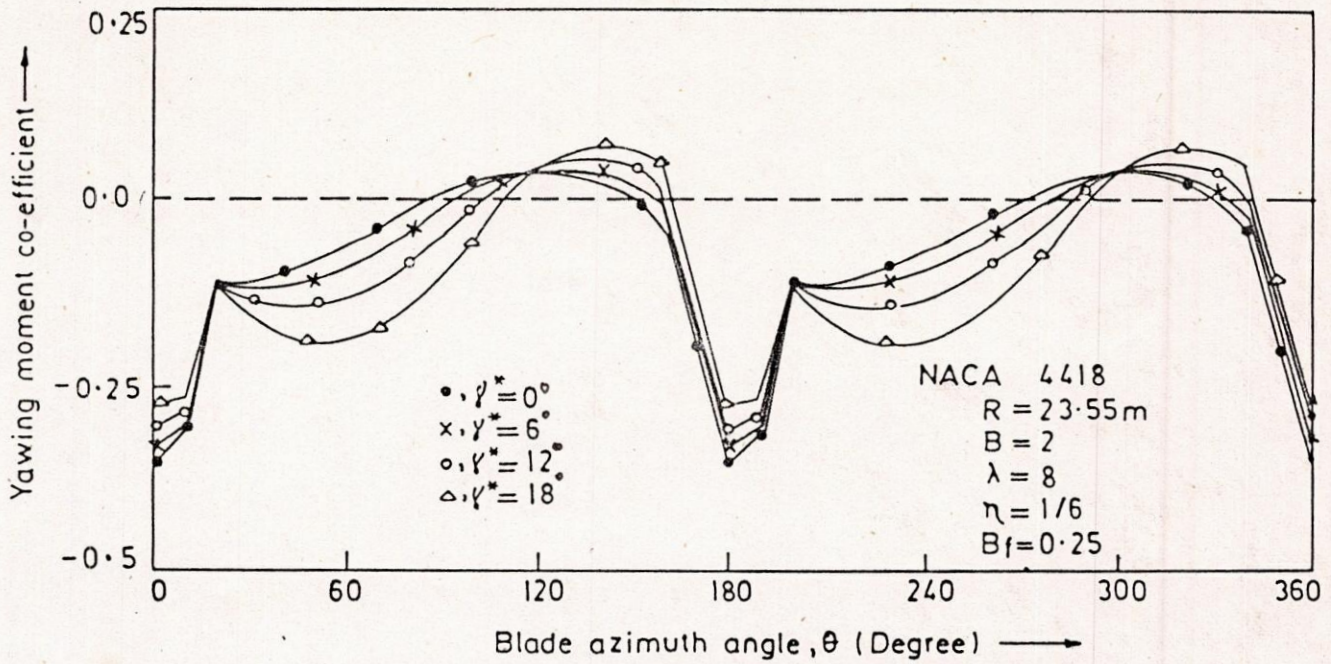


FIGURE 7.5.5: EFFECT OF TOWER SHADOW ON YAWING MOMENT CO-EFFICIENT AT DIFFERENT YAW ANGLES DURING ONE REVOLUTION.

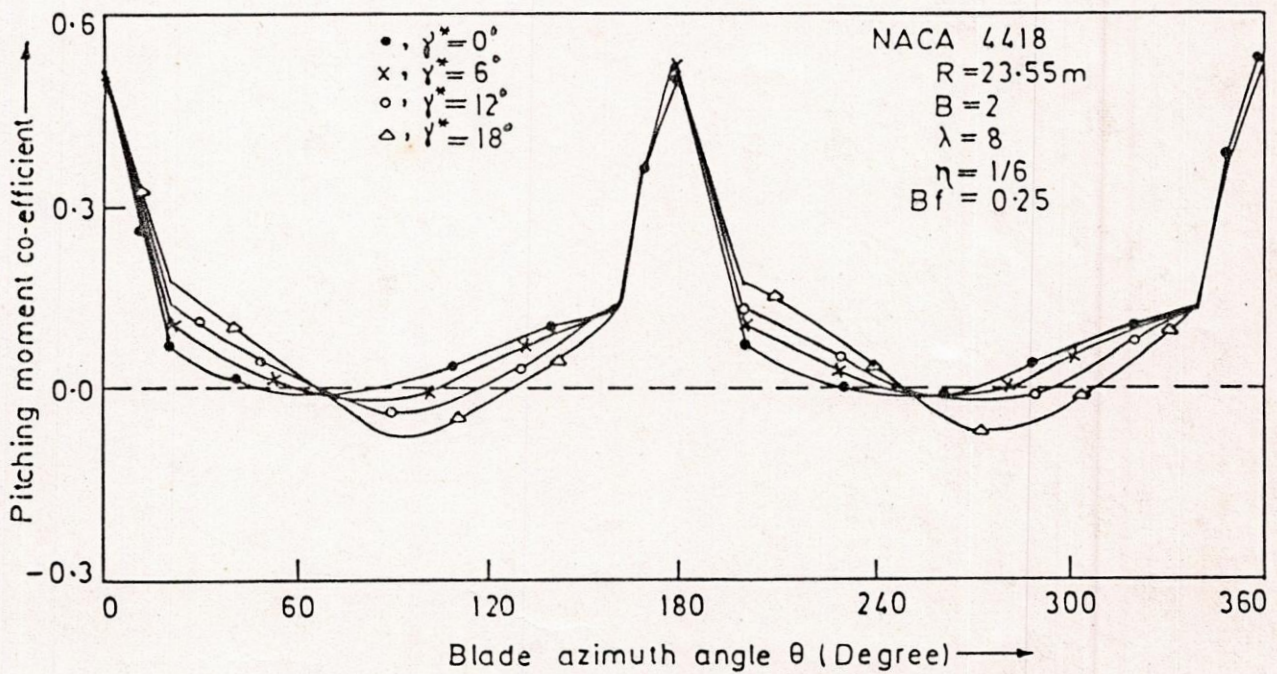


FIGURE 7.5.6: VARIATION OF PITCHING MOMENT CO-EFFICIENT DUE TO TOWER SHADOW AND YAW ANGLES DURING ONE REVOLUTION.

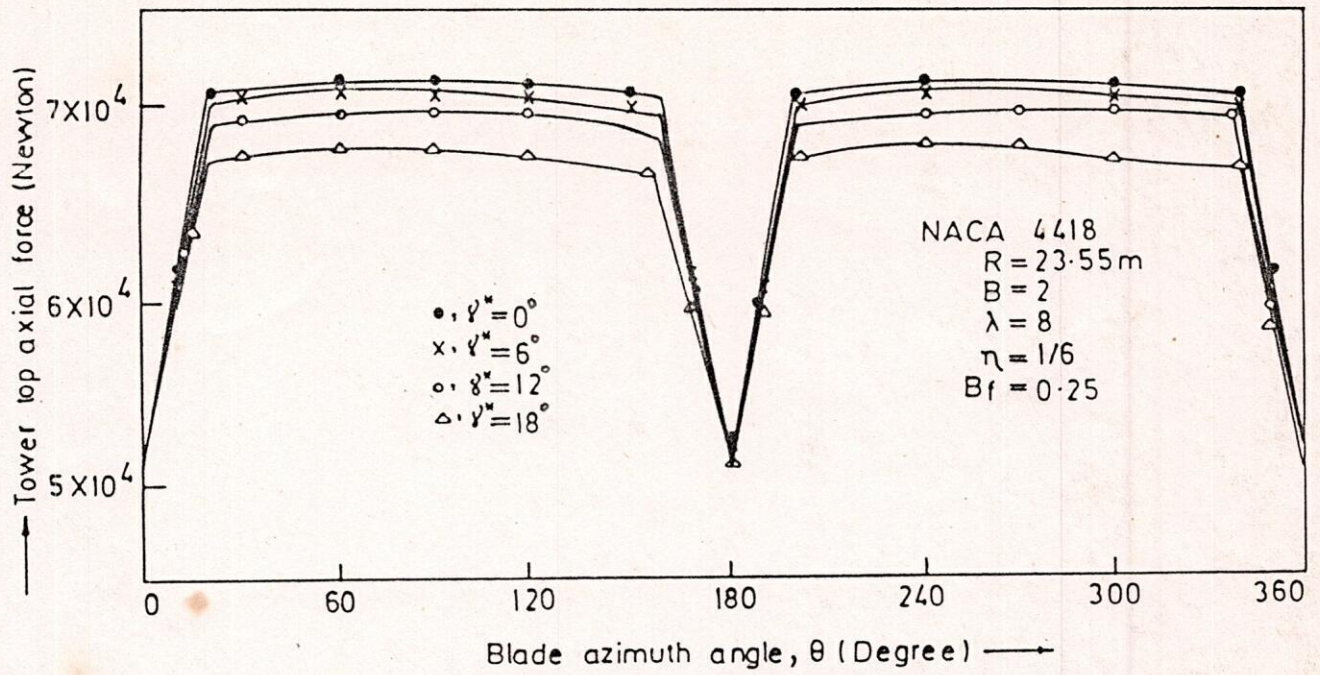


FIGURE 7.5.7: EFFECT OF TOWER SHADOW ON TOWER TOP AXIAL FORCE AT DIFFERENT YAW ANGLES DURING ONE REVOLUTION.

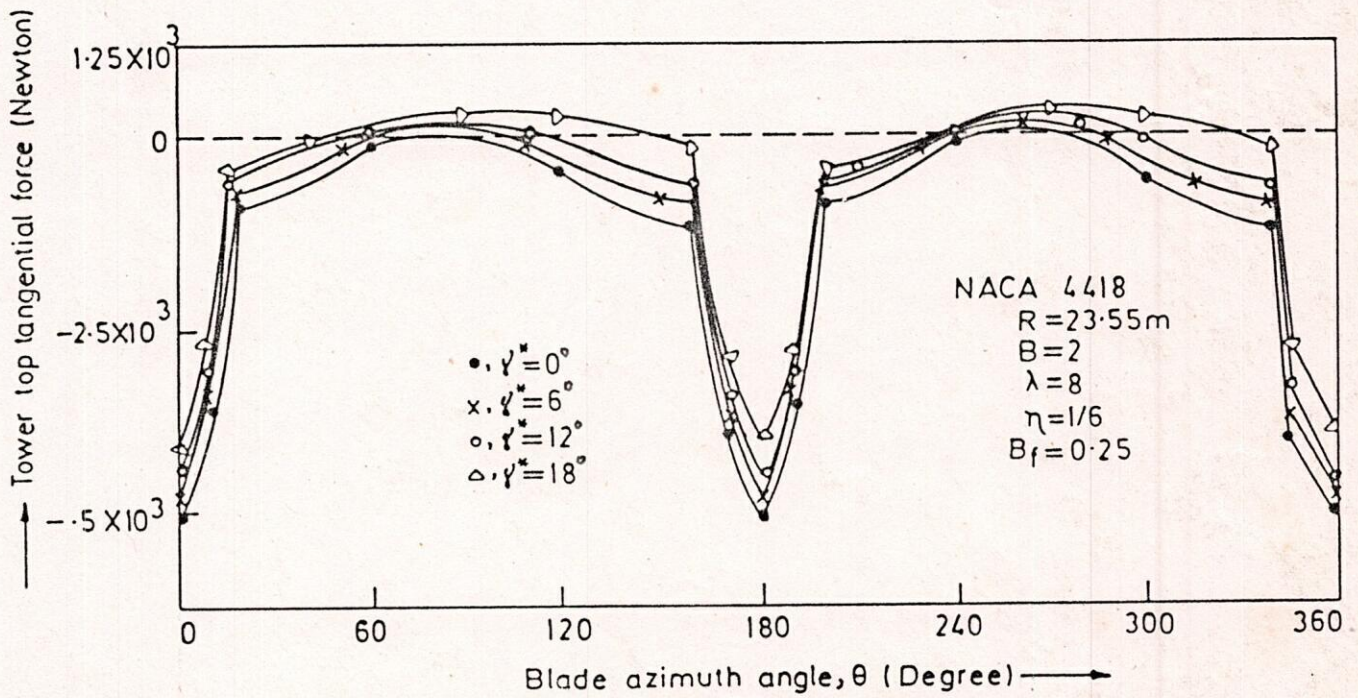


FIGURE 7.5.8: EFFECT OF TOWER SHADOW ON TOWER TOP TANGENTIAL FORCE AT DIFFERENT YAW ANGLES DURING ONE REVOLUTION.

CHAPTER VIII

CONCLUSIONS AND RECOMMENDATIONS

The purpose of this study is to find out a suitable method to calculate the overall design and performance analysis for a horizontal axis wind turbine utilizing a simplified method. Most of existing design programs are considered separately the important effects of wind shear, wind shift, coning angle, tilting angle, azimuth angle, and tower shadow. But the present analysis considers all the effects of these parameters combinedly. The theoretical results obtained by the present method are studied thoroughly. From the study the following conclusions may be drawn,

1. In the designing of a horizontal axis wind turbine the combined influence of coning, tilting, azimuthal, and wind shear, wind shift and tower shadow should be considered.
2. By the existing blade element theory, a rotor blade can be designed that produces an optimum C_p at a fixed value of the tip speed ratio. A first condition to get optimum C_p is to choose the maximum value of lift and drag ratio $(C_L/C_D)_{max}$ of the given profile and to keep it constant along the entire blade span. That is, the corresponding C_L and α , is to be taken constant along the entire span. A second condition is that, the continuously varying blade chord and twist angle along the entire length of the blade are accepted. This gives very complicated rotor blade that is expensive to manufacture and may not have structural integrity. It is possible to achieve very close value of the optimum C_p by considering linear-chord linear-twist blade. The power difference between a ideal blade and zero twist blade only about 6% to 10%. This might be acceptable for a single production unit, but loses its attraction in case of mass production. Choosing an untwisted blade design, the constant chord blade seems rather attractive, because the blade area in the hub region is reduced, where the blade stall starts at relatively high values of λ .
3. For two-bladed horizontal axis wind turbine operating with uniform velocity and without any disturbances the loads will be steady. The introduction of wind shear and a certain yawing angle will cause each blade to experience a periodic force and moment.
4. With the variation of blade pitch angle θ_p , the maximum power reduces but increases the power available at relatively low tip speed ratios. The power coefficient Versus tip speed ratio curves are sensitive to blade pitch angle in the stalling region. To avoid too much drop off, of power after stalling region, blade pitch angle between 2.5° to 5° are seem to be more convenient than the performance at

- 0° pitch angle.
5. The minimum clearance between blade and tower depends on the coning angle and the dynamic response of the blade on sudden gusts. This clearance creates a larger problem in case of upwind turbines and reduced by tilting the rotor. The downwind rotor has the disadvantages of the fatigue load due to tower blockage. Again, the tilted rotor shows the disadvantages of fluctuating loads due to misalignment with the wind direction.
 6. The present study shows that large thrust, power, torque, moments and tower top forces variation can occur as the blade passes through the tower shadow. The magnitude of this variations is a function of the amount of flow blockage occurring and duration of the turbine blade remains in the tower shadow. The results show that studies of future wind turbines should include a careful evaluation of the tower shadow effect to ensure that the rotor blades and support system can withstand the stresses set up as the blades transit through the varying wind environment of tower shadow. Works need to be done on wake modelling of specific tower designs.
 7. The effect of tower shadow on turbine noise is another area that needs additional study. The vibration of the tower must be considered in relation to blade vibrations because of the possibility of its natural period of oscillation coinciding with that of some of the alternating forces on the blades.
 8. In non-axial flow, even at small angles of yaw, the cyclic variation in the forces and moments at the blade root could lead to resonance in either the blade, or the supporting structure and possibly reduce the lifetime of the turbine. The effects of non-axial flow therefore need to be considered in the design of horizontal axis wind turbines.
 9. Power losses due to aerodynamic profile drag can be reduced by increasing the rotor solidity and reducing tip speed ratio, but at the expense of increased blade weight and cost. Improvements in airfoil lift and drag ratio will permit reduced solidity and higher tip speed ratios.
 10. To start a low speed rotor that has high internal resistance primarily requires a high pitch angle. Usually the internal resistance decreases as the device started and accelerated. So after attainment to a certain angular speed, the pitch angle is to be reduced to the required value.
 11. Location of rotor, whether, it will be upwind or downwind, has a significant effects on yaw stability of the horizontal axis wind turbines.
 12. Yaw has a significant effect upon the power developed by the

rotor. This effect can be approximated for yaw angles less than 30° by defining rotor power as a function of the wind velocity normal to the rotor plane cubed or equal to $f[\cos\psi]^3$.

Present world of energy crisis, demands large scale wind power generating systems with sufficient aerodynamic design, lightweight, mechanically simple design, requiring a minimum maintenance, low initial and operating costs but maximum power output per unit cost.

REFERENCES

1. Anderson M. B.,
"A Vortex Wake Analysis of a Horizontal Axis Wind Turbine and Comparison with a Modified Blade Element Theory."
Proc. of Third International Symposium of Wind Energy Systems, Copenhagen. August, 1980.
2. Anderson M. B.,
"Blade Shapes for Horizontal Axis Wind Turbines."
Proc. of Second BWEA Wind Energy Workshop, Cranfield, April, 1980.
3. Abbott I. H., Von Doenhoff A. E.,
"Theory of Wind Sections."
Dover Publications, New York, 1959.
4. Althous D.,
"Stuttgarter Profil katalog I."
Universitat Stuttgart, 1972.
5. Alam M. M.,
"Analysis of Yaw Stability of Horizontal Axis Wind Turbines"
M.Sc. Engg. Thesis,
B.U.E.T., DHAKA, July, 1987.
6. Betz, A.
"Gotinger Nochr.", 1919.
7. Crigler J. L.,
"Application of Theodorsen's Theory to Propeller Design."
NACA Report 924.
8. Drzewieck, S.,
"Bulletin Del' Association Technique."
Maritime, 1892.
9. Dommasch, D. O., Sherby, S.S., Connolly T. F.,
"Airplane Aerodynamics."
Pitman Publishing Corporation, New York, 1961
10. Dugunji , J.,
"Some Dynamic Problems of Rotating Windmill Systems."
Advances in Engineering Science,
Proc. 13th. Annual Meeting of the Society of Engineering Science,
NASA CP-2001, 1976.
11. Froude, W.,
"Transactions"
Institute of Naval Architects, Vol.-19, 1878.

12. Froude, R. E.,
"Transactions."
Institute of Naval Architects, Vol.-30, 1889.
13. Golding, E.W.,
"The Generation of Electricity by Wind Power."
Spon Ltd., London, 1955 & 1976.
14. Golding, S.,
"On the Vortex Theory of Screw Propellers."
Journal of Applied Energy, No.-4, 1978.
15. Glauert, H.,
"An Aerodynamic Theory of Air Screw."
Reports and Memoranda, A.E.43, No.-786, January, 1922.
16. Glauert, H.,
Br. Aeronautical Research Council Reports and Memoranda,
No.-869, 1922.
17. Glauert, H., Durand, W. F., (Ed.)
"Airplane Propellers."
Vol.-IV, Division-I, Chapter-VII, Section-4,
Julius Springer, Berlin, 1953.
18. Glauert, H.,
"The Analysis of Experimental Results in the Wind mill Brake
and Vortex Ring States of an Air Screw."
Aeronautical Research Council Reports and Memoranda,
No.-1026, February, 1926.
19. Glasgow, J.C., Miller, D, Sullivan, T.,
"Rotor Blade Bending Loads for Mod-0 Experimental Wind
Turbine."
NASA PIR 163, October, 1980.
20. Hirsch, ch., Derdelinckx, R., Islam, M.Q.,
"A Theoretical Investigation of the Design of a Horizontal
Axis Wind Turbines."
Proc. of the European Wind Energy Conferance,
Hamburg, 22-26, October, 1984.
21. Islam, M. Q.,
"A Theoretical Investigation of the Design of a Horizontal
Axis Wind Turbines."
Ph. D. Thesis, Verije Universiteit, Brussel, January, 1986.
22. Imtiaz, K.,
"Study of a Wind Powered Water Pumping Set for Bangladesh."
M.Sc. Engg. Thesis, B.U.E.T., DHAKA, January, 1988.
23. Johnson, W.,
"Helicopter Theory."
Princeton University Press., 1980.

24. Jansen, W. A. M.,
"Horizontal Axis Fast Running Wind Turbines for Developing Countries."
Steering Committee for Wind Energy in Developing Countries,
P.O. Box-85, Amersfoot, The Natherland, June, 1976.
25. Jansen, W. A. M., Smulders, P. T.,
"Rotor Design for Horizontal Axis Windmills."
Steering Committee for Wind Energy in Developing Countries,
P.O. Box-85, Amersfoot, The Natherland, May, 1977.
26. Kawda, S.,
"Tokyo Imperial University."
Aero. Res. Inst., No.-14, 1926.
27. Kaza, K. R. V., & Hammand, C. E.,
"Investigation of Flap-Lag Stability of Wind Turbine Rotors
in the Presence of Velocity Gradients and Helicopters in
Forward Flight."
Proc. 17th. Structures, Structural Dynamics and Materials
Coferece, Sponsored by AIAA, ASME and SAE,
King of Purssia, may, 1976.
28. Kottapalli, S. B. R., Friedman P. P.,
(University of California, U.S.A.)
Rosen, A.,
(Technion-Israel Institute of Technology, Israel.)
"Aeroelastic Stability and Response of Horizontal Axis Wind
Turbine Blades."
Second International Symposium on Wind Energy System.
October, 1978.
29. Lerbs, H. M.,
"Moderately Loaded Propellers with a Finite Number of Blades
and an Arbitrary Distribution of Circulation."
Trans. Soc. Naval Architects and Marine Engrs., 60, 1957.
30. Lock, C. N. H.
"Note on the Characteritic Curve for an Air Screw and
Helicopter."
Aeronautical Research Council Reports and Memoranda,
No.-2673, June, 1947.
31. Lock C. N. H., Bateman, H.
"Some Exreriments on Air Screws at Zero Torque, With
Application to a Helicopter Descending with the Engines off,
and to the Design of Windmills."
Aeronautical Research Council Reports and Memoranda,
No.-885, September 1923.
32. Linscott, B.S., Glasgow, J., Anderson, W.D., Donham, R.E.,
"Experimental Data and Theoritical Analysis of an Operating
100 KW Wind Turbine."
NASA TM-779273, 1980.

33. Ormiston, R. A.,
"Rotor Dynamic Consideration for Large Wind Power Generation System."
Wind Energy Conversion System Workshop Preceedings,
National Science Foundation,
NSF/FA/W-73-006, December, 1973.
34. Ormiston, R.A.,
"Dynamic Response Of Wind Turbine Rotor System."
31st. Annual National Forum of the American Helicopter Society."
Washington, D. C., May, 1975.
35. Pistolesti, E.,
"Vortrage Aus Dem Gebiete Der Hydro-Und Aerodynamik."
Inns Bruck, 1922.
36. Powels, S. R. J.
"The Effects of Tower Shadow on the Dynamics of a Horizontal Axis Wind Turbine."
Journal of Wind Engineering, Vol.-7, No.-1, 1983.
37. Rohrbachc, Worobel, R.,
"Performance Characteristics of Aeronautically Optimum Turbines for Wind Energy Generators."
American Helicopter Society, Reprint No.S-996, May, 1975.
38. Shephered, D. G.,
"Note on a Simplified Approach to Design Point Performance Analysis of HAWT Rotors."
Journal of Wind Engineering, Vol.-8, No.-2, 1984.
39. Spera, D. A.,
"Structural Analysis of Wind Power Rotors for NSF/NASA Mod-0 Wind Power System."
NASA-TMX-3198, March 1975.
40. Spera, D.A., and Janetzke, D. C.,
"Effects of Rotor Location, Coning and Tilting on Critical Loads in Large Wind Turbines."
NASA Lewis Research Centre, Cleveland, Ohio 44135, July, 1977.
41. Theodorson, T.,
"The Theory of Propellers, I-Determination of the Circulation Function and the Mass Coefficient for Dual-Rotating Propellers."
NACA Report 775, 1944.
42. Theodorson, T.,
"The Theory of Propellers, IV-Thrust, Energy and Efficiency Formulas for Single and Dual-Rotating Propellers with Ideal Ciculation Distribution."
NACA Report 778, 1944.

43. Theodorson, T.,
"The Theory of Propellers."
Mcgraw-Hill Book Co. Inc., New York, 1984.
44. Vries O. de,
"Fluid Dynamics Aspects of Wind Energy Conversion."
NATO Advisory Group of Aerospace Research and Development,
The Natherland, July, 1979.
45. Wilson R. E., Lisaman, P. B. S., Walker, S. N.,
"Aerodynamic Performance of Wind Turbines"
Oregon State University, March, 1981.
46. Wilson R. E.,
"Aerodynamic potpourri."
Proc. of the DOE/NASA Wind Turbine Dynamics Conference,
NASA CP-2185, DOE CONF-801226, February 1981.
47. Wilson R. E., Lisaman, P. B. S.,
"Applied Aerodynamics of Wind Power Machines."
Oregon State University, Corvallis,
Oregon 97331, U. S. A., July, 1974.
48. Wilson R. E., Walker, S. N.,
"Performance Analysis Program for Propeller Type Wind
Turbines."
Oregon State University, March, 1981.
49. Wilson R. E.,
"Wind Turbine Aerodynamics."
Oregon State University, Covallis, Oregon, U.S.A.
50. Walker S. N.,
"Performance and Optimum Design Analysis/Computation for
Propeller Type Wind Turbines."
Ph. D. Thesis,
Oregon State University, Oregon, May, 1976.
51. Wilmshurst, S. M., Powels, S. R.J., Wilson, D. M. A.
"The Problem of Tower Shadow."
Proc. of the 7th. BWEA Wind Energy Conference,
Oxford 27-29, March, 1985.
52. Yamane, T., Tsutsui, Y., Orita, T.,
"The Aerodynamic Performance of a Horizontal Axis Wind
Turbine in Large Velocity Induced States."
Proc. of the 4th. International Symposium on Wind Energy
Systems,
Stockhom, September, 1984.

APPENDICES

APPENDIX-A

Local Frame of Reference

To calculate aerodynamic forces acting on the rotor, several coordinate systems are introduced in the present analysis. These frames include a reference frame S_0 , fixed at the top of the tower of the wind turbine with Z_0 being the vertical axis and (X_0, Y_0) forming horizontal plane. A second non-rotating frame S_1 is fixed at the tip of the nacelle is introduced by translation of the initial frame over a certain distance Y and a rotation of tilting angle α_T around the X_0 axis. A rotating frame S_2 is introduced by rotation of the reference frame S_1 over an azimuth angle θ_k . Finally, a local reference frame S_3 is attached to a particular point of the blade at a distance r from the hub and is rotated over a coning angle β . These are shown in Figures (A.1) to (A.4). The relationships between the reference frames can be expressed as,

$$S_1 = [K_T] S_0$$

$$S_2 = [K_\theta] S_1$$

$$S_3 = [K_\beta] S_2$$

and inversely,

$$S_0 = [K_T]^T S_1$$

$$S_1 = [K_\theta]^T S_2$$

$$S_2 = [K_\beta]^T S_3$$

the superscript T indicates the transposed matrix. The transformation matrices are,

$$\text{for tilting, } K_T = \begin{vmatrix} 1 & 0 & 0 \\ 0 & \cos \alpha_T & -\sin \alpha_T \\ 0 & \sin \alpha_T & \cos \alpha_T \end{vmatrix} \quad (\text{A.1})$$

$$\text{for azimuth, } K_\theta = \begin{vmatrix} \cos \theta_k & 0 & \sin \theta_k \\ 0 & 1 & 0 \\ -\sin \theta_k & 0 & \cos \theta_k \end{vmatrix} \quad (\text{A.2})$$

$$\text{for coning, } K_{\beta} = \begin{vmatrix} 1 & 0 & 0 \\ 0 & \cos\beta & -\sin\beta \\ 0 & \sin\beta & \cos\beta \end{vmatrix} \quad (\text{A.3})$$

Thus a point on the blade can be expressed in the local S_3 coordinate system as,

$$\hat{r}_{s3} = \begin{vmatrix} X_3 \\ Y_3 \\ Z_3 \end{vmatrix} \quad (\text{A.4})$$

Considering the non-rotating system S_1 attached to the hub, above equation becomes,

$$\hat{r}_{s1} = [K_{\theta}][K_{\beta}]r_{s3} \quad (\text{A.5})$$

This can be written as,

$$\begin{vmatrix} X_1 \\ Y_1 \\ Z_1 \end{vmatrix} = \begin{vmatrix} r\cos\beta\sin\theta \\ -r\sin\beta \\ r\cos\beta\cos\theta \end{vmatrix} \quad (\text{A.6})$$

In S_0 coordinate system,

$$\hat{r}_{s0} = [K_T][K_{\theta}][K_{\beta}]\hat{r}_{s3} \quad (\text{A.7})$$

The following equation can be obtained from the above equation,

$$\begin{vmatrix} X_0 \\ Y_0 \\ Z_0 \end{vmatrix} = \begin{vmatrix} r\cos\theta\sin\beta \\ -r\sin\beta\cos\alpha_T - r\cos\theta\cos\beta\sin\alpha_T \\ -r\sin\beta\sin\alpha_T + r\cos\theta\cos\beta\cos\alpha_T \end{vmatrix} \quad (\text{A.8})$$

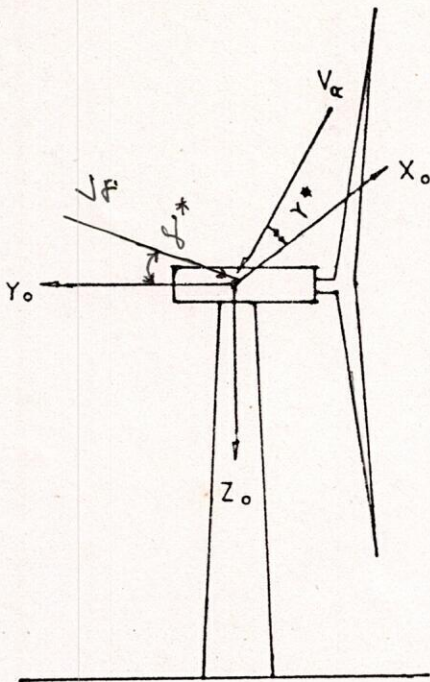


Fig. A.1: Reference Frame S_0 .
(Coordinate System S_0)

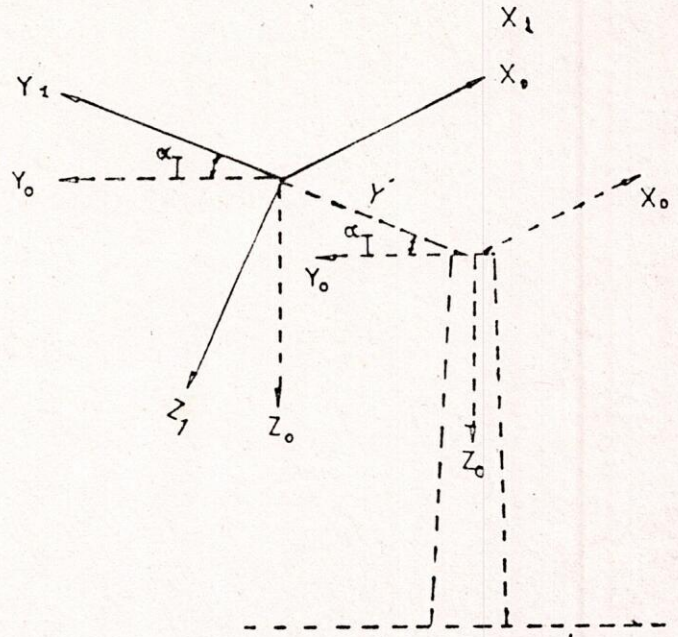


Fig. A.2: Translation Over Y' and
Rotation About X_0 by Angle α .
(Coordinate System S_1).

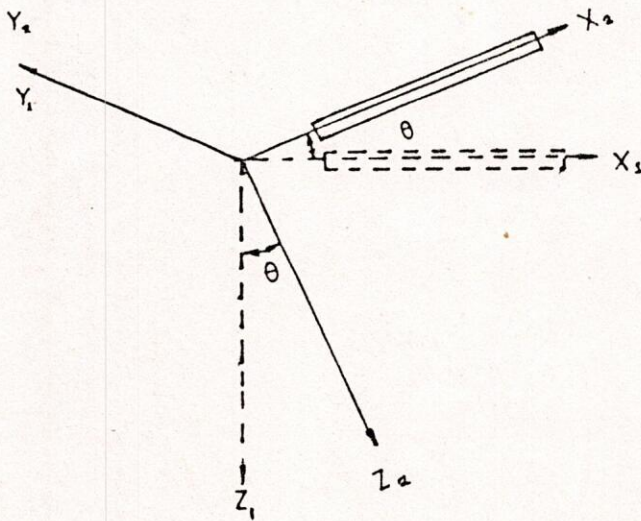


Fig. A.3: Rotation About Y_1 by Angle θ .
(Coordinate System S_2)

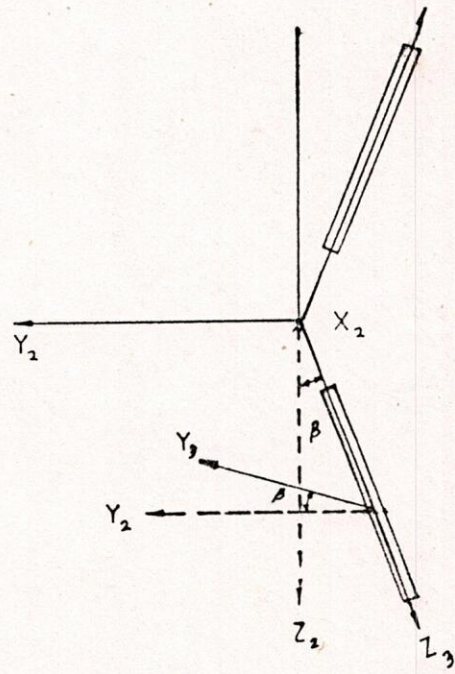


Fig. A.4: Rotation About X_2 by Angle β .
(Coordinate System S_3)

APPENDIX-B

Selection of Design Parameters

In the Designing of a horizontal axis wind turbine it is important to find the value of design lift coefficient and design angle of attack from graphs that correspond to a minimum value of C_D/C_L ratio. To carry out the iteration procedure for the blade configuration, estimation of design power coefficient is also important. Determination of these parameters are discussed in the following sections.

B.1 Determination of Minimum C_D/C_L Ratio

The lift and drag coefficients of a given airfoil for a given Reynolds number are shown in Figure B.1.1.

In the C_D/C_L graph a tangent is drawn through $C_D=C_L=0$. From the point where the tangent touches the curve indicates the minimum C_D/C_L ratio. This ratio determines the maximum power coefficients that can be reached, particularly at high tip speed ratios. From the $C_L-\alpha$ curve corresponding to minimum C_D/C_L ratio, the values of lift coefficient and angle of attack are found. The C_L and α values found in this way are known as design lift coefficient, C_{Ld} and design angle of attack, α_d and these are very important parameters in the design process.

B.2 Determination of the Design C_p

The power coefficient is affected by the profile drag via the C_D/C_L ratio. The reduction of the maximum power coefficient is proportional to the tip speed ratio and to C_D/C_L ratio. The result is shown in the Figure B.2.1. The curve shows for each the maximum attainable power coefficient with the number of blade and C_D/C_L ratio as a parameter. In this collection of maximum power coefficient it is seen that for a range of design tip speed ratio from 1 to 10 the maximum theoretically attainable power coefficients lie between 0.3 to 0.5.

Now we can design a windmill rotor for a given wind speed V_w and a power demand. First the minimum C_D/C_L ratio of an airfoil is to be determined. The procedure for selection of number of blades, B and the design tip speed ratio λ_d has been explained in chapter-5. From Figure B.2.1 the maximum expected power coefficient can be found out. For conservative design, the design C_p is calculated as [25]

$$C_p = 0.8 \times C_{p_{max}}$$

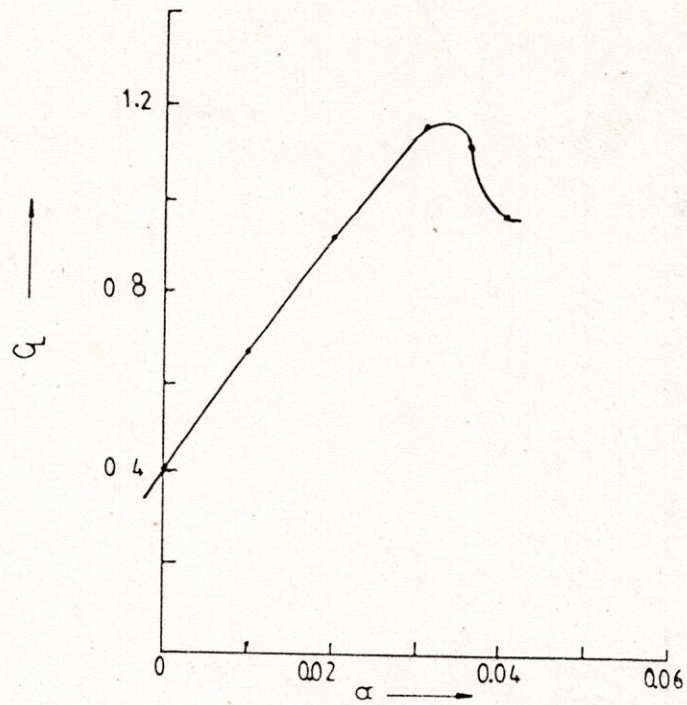


Fig. B.1.1: C_L - α , Characteristics Curve for a given Airfoil Section [21].

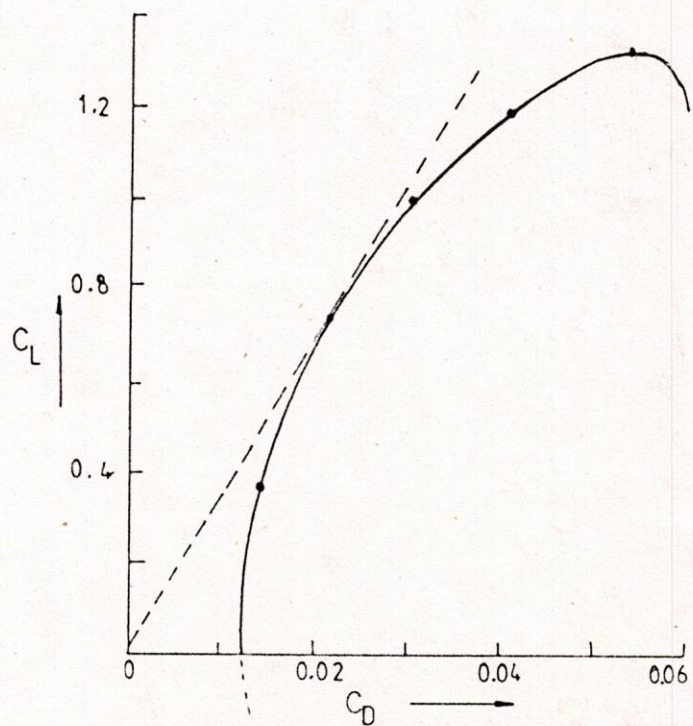


Fig. B.2.1: C_L - C_D , Characteristics Curve for a given Airfoil Section [21].

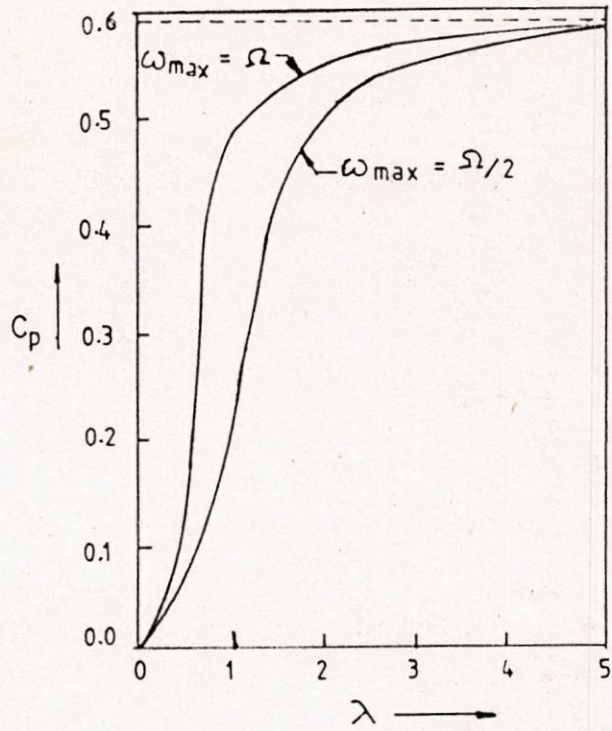


Fig. B.2.1 : Maximum Power Coefficient Versus λ for a Rotor with a Rankine Vortex wake

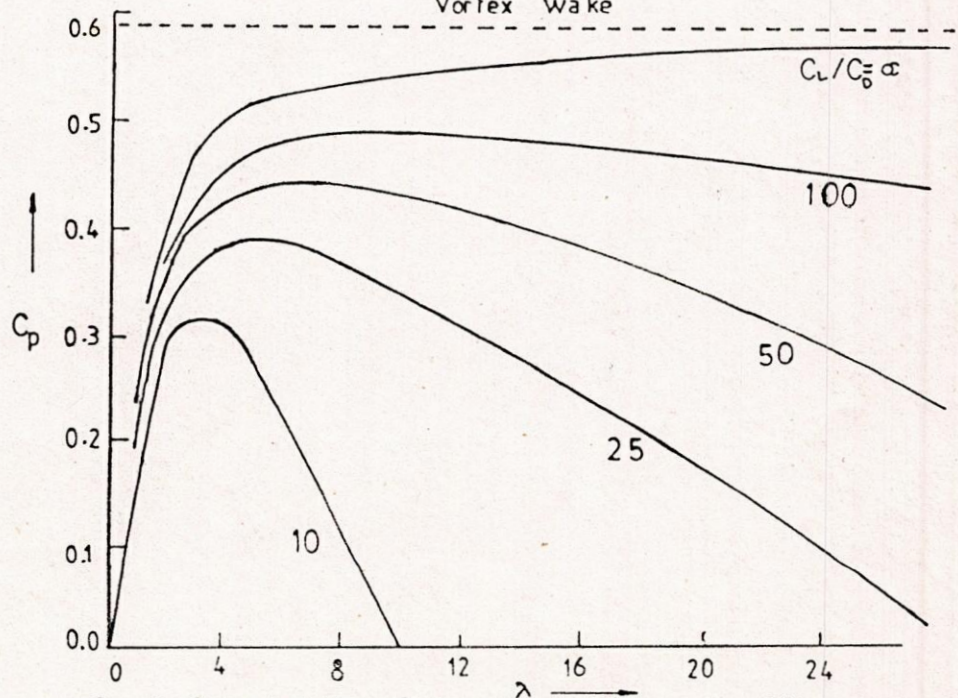


Fig. B.2.2 $C_p - \lambda$, Characteristics Curve showing the effect of C_l/C_0 ratio ($B = \alpha$).

APPENDIX-C

C.1 Maximum Power Coefficient

The plot C_p versus a , shows that the maximum value of C_p occurs when $a=1/3$ and the value is $16/27$ or 0.593 . Analytically, by equation (3.1.14):

$$C_p = 4a(1-a)^2 = 4(a-2a^2+a^3)$$

Now for maximum power coefficient,

$$\frac{dC_p}{da} = 0, \text{ gives } 4(1-4a+3a^2)$$

or, $a=1/3$, and $a=1$

For $a=1$, C_p has the minimum value zero.

For $a=1/3$, C_p has the maximum value of $16/27$.

C.2 Influence of Wake Axial Induction Factor.

The addition of a vortex component reduce the torque and power given to the actuator disk, because it produces rotational kinetic energy to the fluid passing through the disk. It is shown in reference [49] that, for constant angular momentum, in the wake flow (irrotational vortex, $r^2 = \text{constant}$).

$$a = -\frac{1}{2}b \left[1 - \left\{ \frac{b^2(1-a)}{4\lambda^2(b-a)} \right\} \right] \quad (\text{C.2.1})$$

108

Where, $b=1-(V/V_\infty)$, is called the wake axial induction factor.

Figure C.2.1 (reference [49]) shows a plot of the relationship of equation (C.2.1) and it is seen that for the ideal actuator disk, with $\lambda = \infty$, b is exactly equal to $2a$. For $\lambda \geq 2$, b is little different from $2a$, but rapidly differs from this value for $\lambda < 1$. The second terms within brackets in equation (C.2.1) is usually small and if b is replaced therein by its approximate value $2a$, the equation reduces to,

$$a \approx -\frac{1}{2}b \left[1 - \left\{ \frac{a(1-a)}{\lambda^2} \right\} \right] \quad (\text{C.2.2})$$

The power coefficient with a rotational component is then found to be,

$$C_p = \frac{b^2(1-a)^2}{(b-a)} \quad (\text{C.2.3})$$

with $b=2a$, this reduces to,

109

$C_p=4a(1-a)^2$,
the same as found from the axial momentum theory.

C.3 Relation between ω and U .

With respect to the disk, the relative angular velocity Ω changes to $(\Omega + \omega)$ and the other components of the velocity remain unchanged. Applying the Bernoulli's equation at upstream and downstream of the actuator disk,

$$P^+ + 1/2 \rho (U^2 + \omega^2 + \Omega^2 r^2) = P^- + 1/2 \rho [U^2 + \omega^2 + (\Omega + \omega)^2 r^2]$$

$$\text{or, } P^+ - P^- = 1/2 \rho (2 \Omega \omega + \omega^2) r^2 \quad (\text{C.3.1})$$

Thrust force on the annulus is given by,

$$dT = (P^+ - P^-) dA$$

Using the equation (C.3.1) which becomes,

$$dT = 1/2 \rho (2 \Omega \omega + \omega^2) r^2 dA \quad (\text{C.3.2})$$

But thrust force of the wind is,

$$dT = \rho U dA (V_\infty - U) = 2 \rho U dA (V_\infty - U) \quad (\text{C.3.3})$$

Equating equations (C.2.3) and (C.3.3) we have,

$$2 \rho U dA (V_\infty - U) = 1/2 \rho (2 \Omega \omega + \omega^2) r^2 dA$$

$$\text{or, } U(V_\infty - U) = 1/2 (\Omega \omega + \omega^2/2) r^2$$

$$\text{or, } U(V_\infty - U) = 1/2 \omega r (\Omega + \omega/2) r$$

Rearranging in the form,

$$\frac{U}{V_\infty} \frac{U}{V_\infty} = \frac{1}{2} \omega r (\Omega r + \frac{1}{2} \omega r) \quad (\text{C.3.5})$$

$$\text{Since } \acute{a} = \frac{\omega}{2\Omega} \quad \text{i.e.} \quad 1/2 \omega r = \acute{a} \Omega r$$

$$\text{and } \lambda_r = r\Omega/V_\infty \quad \text{i.e.} \quad \Omega r = \lambda_r V_\infty$$

$1 - U/V_\infty = a$, one may get from equation (C.3.5),

$$\begin{aligned} (1-a)aV_\infty^2 &= a \Omega r (\lambda_r V_\infty + \acute{a} \Omega r) \\ &= \acute{a} \lambda_r V_\infty (\lambda_r V_\infty + a \lambda_r V_\infty) \\ &= a \lambda_r^2 V_\infty^2 (1 + \acute{a}) \end{aligned}$$

$$\text{That is, } a(1-a) = \acute{a}(1+\acute{a}) \lambda_r \quad (\text{C.3.6})$$

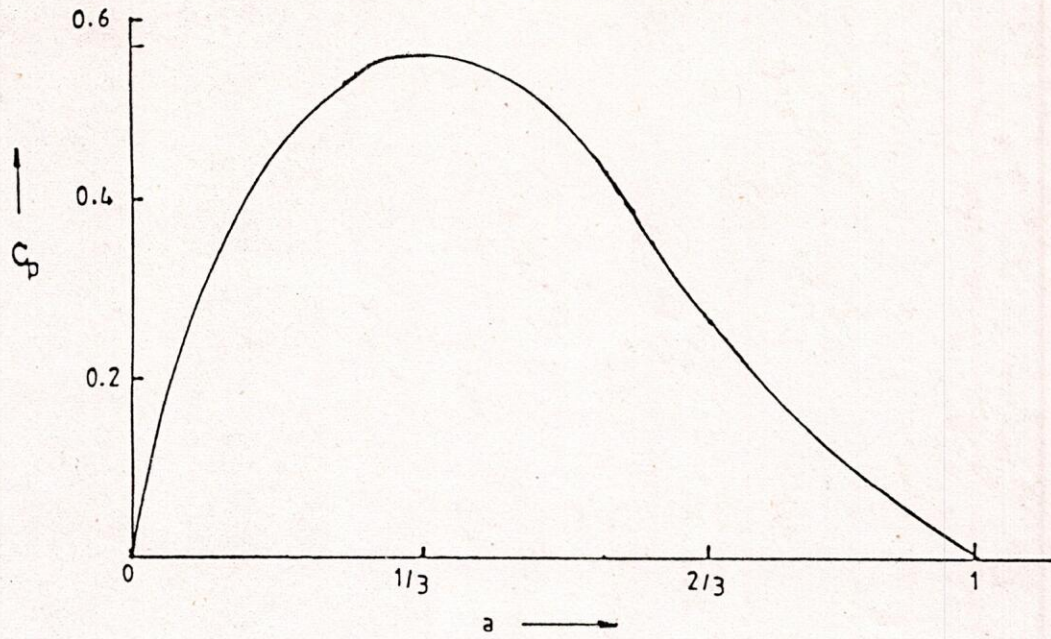


Fig. C.1.1: C_p Vs. a curve

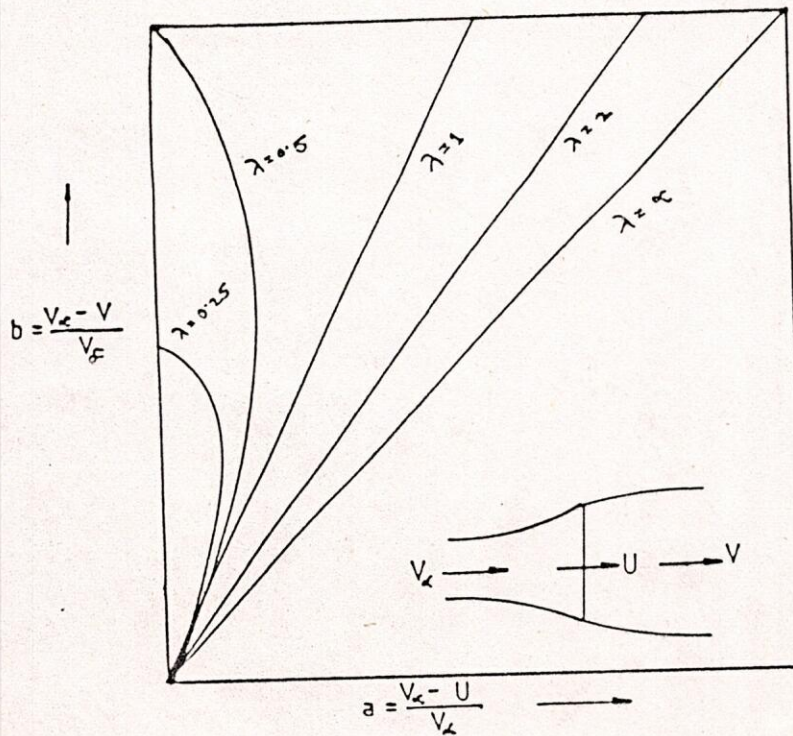


Fig. C.2.1: Effect of Tip Speed Ratio on Induction Factors.

APPENDIX-D

D.1 C_P in Terms of λ

$$\text{we have, } C_P = \frac{P}{1/2 \rho A V_\infty^3}$$

$$= \frac{P}{1/2 \rho \pi R^2 V_\infty^3}$$

Using the equation (3.2.9) & (3.2.10) this becomes,

$$C_P = \frac{2 \rho \pi \Omega \int_0^R \omega r^3 dr}{1/2 \rho \pi R^2 V_\infty^3}$$

Using the equation (3.1.10) this becomes,

$$C_P = \frac{4 \Omega \int_0^R (1-a) V_\infty r^3 dr \omega}{R^2 V_\infty^3} \quad (\text{D.1.1})$$

$$\text{Since, } \lambda_r = \Omega r / V_\infty \text{ i.e. } r = \lambda_r V_\infty / \Omega \quad (\text{D.1.2})$$

$$dr = (V_\infty / \Omega) d\lambda_r \text{ and when } r \rightarrow R, \lambda_r \rightarrow \lambda \quad (\text{D.1.3})$$

Substituting all these values into equation (D.1.1),

$$C_P = \frac{4 \Omega \int_0^\lambda (1-a) V_\infty (\lambda_r^3 V_\infty^3 / \Omega^3) (V_\infty / \Omega) d\lambda_r}{R^2 V_\infty^3}$$

$$= 4 \int_0^\lambda (1-a) \frac{V_\infty^2}{R^2 \Omega^2 \Omega} \lambda_r^3 d\lambda_r$$

$$= \frac{8}{\lambda^2} \int_0^\lambda (1-a) \lambda_r^3 d\lambda_r \quad (\text{D.1.4})$$

D.2 Relation Between a and á

Differentiating equation (D.1.4) with respect to a, and equating to zero (Since, at a particular radius $\lambda_r = \text{constant}$), one have,

$$\frac{dC_p}{da} = \dot{a}(1-a) = 0$$

$$\text{or, } (1-a) \frac{d\dot{a}}{da} + \dot{a} \frac{d}{da}(1-a) = 0$$

$$\text{or, } (1-a) \frac{d\dot{a}}{da} = \dot{a}$$

$$\text{or, } \frac{d\dot{a}}{da} = \frac{\dot{a}}{(1-a)} \quad (\text{D.2.1})$$

Now differentiating equation (C.3.6), with $\lambda_r = \text{constant}$ as before, with respect to a,

$$\frac{d}{da}[a(1-a)] = \frac{d}{da}[\dot{a}(1-a) \lambda_r^2]$$

$$1-2a = (1+2\dot{a}) \lambda_r^2 \frac{d\dot{a}}{da} \quad (\text{D.2.2})$$

Substituting the value of $\frac{d\dot{a}}{da}$ from (D.2.1) it becomes,

$$1-2a = (1+2\dot{a}) \lambda_r^2 \frac{\dot{a}}{(1-a)}$$

$$\text{or, } (1-a)(1-2a) = \dot{a}(1+2\dot{a}) \lambda_r^2$$

inserting the value of λ_r^2 from the equation (C.3.6) in it one may get,

$$(1-a)(1-2a) = \dot{a}(1+2\dot{a}) \left[\frac{(1-a)a}{\dot{a}(1+\dot{a})} \right]$$

$$\text{or, } \dot{a} = \frac{1-3a}{4a-1} \quad (\text{D.2.3})$$

D.3 Table for Average Wind Speed

Ten stations from all over the Bangladesh analysed the availability of wind velocity. The following stations are found to have good potential for the use of wind power [22].

Sl. No.	Stations	Potential month(s) for power generation by windmill.	Average wind speed(m/sec).
1.	Chittagong	March to September	4.0
2.	Dhaka	March to October	3.2
3.	Khepupara	February to September	3.5
4.	Comilla.	March to September	2.8
5.	Teknaf	June to September	2.3
6.	Jessore	April to September	2.1
7.	Cox's Bazer	May to August	2.0
8.	Hatiya	Ends of April to July	1.9
9.	Dinajpur	March to August	2.0
10.	Rangamati	April to May	1.9

* Source : Dhaka Meteorological Department.

COMPUTER PROGRAM

```

CM=1 -----
C]      MM      MM      AAAAAA      II NN      NN      ] ]      HAD00010
C]      MM MM MM MM AA      AA      II NN NN      NN      ] ]      HAD00020
C]      MM MMM MM AA      AA      II NN      NN      NN      ] ]      HAD00030
C]      MM M MM AAAAAAAAAA      II NN      NN NN      ] ]      HAD00040
C]      MM      MM AA      AA      II NN      NN      ] ]      HAD00050
C]      MM      MM AA      AA      II NN      NN      ] ]      HAD00060
CM -----
C      ] ] ] HAD00070
C      ] ] ] HAD00080
C KHANDKAR AFTAB HOSSAIN ] ROLL NO.-871402F ] REDG NO.85502 ] HAD00090
C      ] ] ] HAD00100
C      ] ] ] HAD00110
C      ] ] ] HAD00120
C      ] ] ] HAD00130
C THIS PROGRAM IS USED TO GET THE RESULTS OF YAW ANGLE VARIATIONS HAD00140
C      ] ] ] HAD00150
C      ] ] ] HAD00160
C      ] ] ] HAD00170
C      ] ] ] HAD00180
C      ] ] ] HAD00190
C      ] ] ] HAD00200
C      ] ] ] HAD00210
CM -----
C      ] ] ] HAD00220
C      ] ] ] HAD00230
C      ] ] ] HAD00240
C      ] ] ] HAD00250
C      ] ] ] HAD00260
C      ] ] ] HAD00270
C      ] ] ] HAD00280
C      ] ] ] HAD00290
C      ] ] ] HAD00300
C      ] ] ] HAD00310
C      ] ] ] HAD00320
C      ] ] ] HAD00330
C      ] ] ] HAD00340
C      ] ] ] HAD00350
C      ] ] ] HAD00360
C      ] ] ] HAD00370
C      ] ] ] HAD00380
C      ] ] ] HAD00390
C      ] ] ] HAD00400
C      ] ] ] HAD00410
C      ] ] ] HAD00420
C      ] ] ] HAD00430
C      ] ] ] HAD00440
C      ] ] ] HAD00450
C      ] ] ] HAD00460
C      ] ] ] HAD00470
C      ] ] ] HAD00480

```

THIS PROGRAM IS USED TO GET THE RESULTS OF YAW ANGLE VARIATIONS

MAIN PROGRAM

IT IS USED TO DESIGN A NEW HORIZONTAL AXIS WIND TURBINE (H.A.W.T) & CALCULATION OF ITS PERFORMANCE OR TO CALCULATE THE PERFORMANCE OF AN EXISTING H.A.W.T. IT UTILIZES A SIMPSON'S-RULE METHOD / THREE PASS TECHNIQUE OF NUMERICAL INTEGRATION.

```

INTEGER T,PRINT,SH,PITCH,GO,APP,VAL,Z1,CAT,CNTROL
DIMENSION RR(45),CI(45),THETI(45),AAT(45),CLT(45),CDT(45),
&CPCONT(45),PCCCR(45),CP(23,7),XX(23),CT(23,7),RR1(45),PY4(45),
&TY4(45),QY2(45),CQY(23,7),TP1(23,7),V1(23),TP2(23,7),V2(23),
&XMY2(23,7),RA(23,7),XMY3(45),V33(21,4),THETP1(22),V3(14),
&T1P(13,21),WWR(4),DXMAS(45),SM(45),N1(22),XX1(23),XMYAW(37,4),
&ANGL(8),FY8(45),POYA(12,4),TOYA(12,4),CQC(45),CTCONT(45),
&SQC(8),RR8(45),SIA3(37),QOYA(12,4),PIM(37,4),TOFX(37,4),Y9(45,5),
&C11(45),SIA2(29),FLAP1(29,3),EDGE1(29,3),SUP(12,2),T3P(29),
&CPYS1(29,3),CTYS1(29,3),FX8(45),C12(45),XMYAH(37,4),PIM1(37,4),
&TOFY(37,4),TOFZ(37,4),TOFX1(37,4),TOFY1(37,4),TOFZ1(37,4)
EQUIVALENCE (Y9(1,1),PY4),(Y9(1,2),TY4),
&(Y9(1,3),QY2),(Y9(1,4),XMY3)
COMMON/C1/R,DR,HB,B,V,X,THETP,H,SI,GO,OMEGA,RHO,VIS,HL,PI,RX,W,
&NPROF,APP,T1,T2,T3,T4,T5,T6,T7,T8,TEST,XETA,HH,ALO,AC,TH
COMMON/C2/DTSR,PRINT,T
COMMON/C3/Z1,SH,CONST,ZOAN1
COMMON/C4/QU,RR8,NFIT,RHOM,GAL
COMMON/C5/OME,EIGV,EIGL,EXCI,GAM
COMMON/C6/SIA,BF,COAN1,YA
COMMON/C7/GG
COMMON/C9/TILT
COMMON/AA1/WWR,XXP

```

```

C..... HAD00450
C      OPEN(UNIT=60,FILE='INPUT',STATUS='OLD') HAD00460
C      OPEN(UNIT=61,FILE='OUTPUT',STATUS='NEW') HAD00470
C..... HAD00480

```


C		HAD00490
C	----- PROGRAM OPERATION CONTROLLER -----	HAD00500
C		HAD00510
C		HAD00520
CT-TYPE	HAD00530
C1-NEW	HAD00540
C2-EXISTING	HAD00550
C		HAD00560
CPITCH-CONTROL	HAD00570
C1-FIXED	HAD00580
C2-VARIABLE	HAD00590
C		HAD00600
CR=RADIUS OF BLADE(METER)	HAD00610
CP=POWER TO BE EXTRACTED(KW)	HAD00620
C		HAD00630
CSH=SHAPE OF BLADE	HAD00640
C1-IDEAL	HAD00650
C2-LINEARIZING CHORD AND TWIST ANGLES BETEWEEN	HAD00660
C	0.5R & 0.9R.	HAD00670
C3-LINEARIZING CHORD BETEWEEN 0.5R & 0.9R BUT	HAD00680
C	TWIST ANGLE IS ZERO.	HAD00690
C		HAD00700
CPRINT-CODE	HAD00710
C1-RESULTS & GRAPHS	HAD00720
C2-GRAPHS ONLY	HAD00730
C3-RESULTS IN DETAILS	HAD00740
C4-RESULTS IN SHORT	HAD00750
CHB =HUB RADIUS (NEW-10% OF RADIUS)	HAD00760
CDTSR =DESIGN TIP SPEED RATIO	HAD00770
CDR =INCREMENTAL % (0.02 OR HIGHER)	HAD00780
CTHETP=PITCH ANGLE (DEGREE)	HAD00790
CB =NO. OF BLADE	HAD00800
CV =WIND VELOCITY (M/SEC)	HAD00810
CVM =WIND VELOCITY (M/SEC)	HAD00820
CXETA =VELOCITY POWER LAW EXPONENT (1/6 FOR NEW D/N)	HAD00830
CRPM =ANGULAR VELOCITY OF THE TURBINE (RPM)	HAD00840
CXMIN =STARTING TIP SPEED RATIO FOR EVALUATION	HAD00850
CDX =TIP SPEED RATIO INTERVAL FOR EVALUATION	HAD00860
CXMAX =MAXIMUM TIP SPEED RATIO FOR EVALUATION	HAD00870
CH =HUB ABOVE SEA LEVEL (METER ; FOR NEW D/N=2*R)	HAD00880
CHH =HUB ABOVE GROUND LEVEL (METER ; FOR NEW D/N=2*R)	HAD00890
CSI =CONING ANGLE (DEGREE)	HAD00900
CNF =NO. OF INPUTED STATIONS FOR BLADE GEOMETRY	HAD00910
CNPROF=NACA PROFILE (SUBROUTINE)	HAD00920
C4418	HAD00930
C0012	HAD00940
C0015	HAD00950
C23024	HAD00960
C8888 DATA IN TABULER FORM	HAD00970
C9999 PROFILE CURVE FIT IN NACAXX	HAD00980
C		HAD00990
CGO=TIP LOSS MODEL CONTROLLER	HAD01000
C0-PRANDTL	HAD01010
C1-GOLDSTEIN	HAD01020
C2-NO MODEL	HAD01030

C.....HL=HUB LOSS MODEL CONTROLLER	HAD01040
C.....0-NONE	HAD01050
C.....1-PRANDTL	HAD01060
C	HAD01070
C.....APP=ANGULAR INTERFERENCE LOCKOUT	HAD01080
C.....0-FACTOR CALCULATED	HAD01090
C.....1-FACTOR=0.	HAD01100
C	HAD01110
C.....RR(I) =% RADIUS FOR STATIONS	HAD01120
C.....CI(I) =CHORD FOR STATIONS (METER)	HAD01130
C.....THETI(I)=TWIST ANGLE FOR STATIONS (DEGREE)	HAD01140
C.....TH =MAXIMUM THICKNESS / CHORD RATIO	HAD01150
C.....ALO =ANGLE OF ATTACK FOR ZERO LIFT (DEGREE)	HAD01160
C.....CLT(I) =CO-EFFICIENT OF LIFT DATA	HAD01170
C.....CDT(I) =CO-EFFICIENT OF DRAG DATA	HAD01180
C.....AAT(I) =ANGLE OF ATTACK (DEGREE)	HAD01190
C	HAD01200
C.....VAL=VALUES OF H,HH,XETA,HB.	HAD01210
C.....1-SPECIFIED	HAD01220
C.....2-NOT SPECIFIED	HAD01230
C	HAD01240
READ(60,7001)T,PRINT	HAD01250
WRITE(61,8000)	HAD01260
WRITE(61,8001)T,PRINT	HAD01270
READ(60,7003)VM,P,DTSR,SH,PITCH	HAD01280
WRITE(61,8003)VM,P,DTSR,SH,PITCH	HAD01290
READ(60,7004)HH,XETA,HB,H,VAL	HAD01300
WRITE(61,8004)HH,XETA,HB,H,VAL	HAD01310
GO TO 15	HAD01320
15 CONTINUE	HAD01330
YA=0.	HAD01340
TILT=0.	HAD01350
Z1=0	HAD01360
Z2=0.	HAD01370
IF(T.EQ.2)GO TO 1	HAD01380
IF(T.EQ.1)COAN=9.	HAD01390
I11=1	HAD01400
HI1=0.	HAD01410
101 THETP=HI1	HAD01420
IF(PITCH.EQ.1)THETP=0.	HAD01430
IF(DTSR.LE.3.)B=3.	HAD01440
IF(DTSR.GE.4.)B=2.	HAD01450
XMIN=2.	HAD01460
XMAX=13.	HAD01470
DX=0.5	HAD01480
APP=0	HAD01490
X=DTSR	HAD01500
GO=0	HAD01510
HL=1	HAD01520
PI=3.1415926536	HAD01530
DR=0.02	HAD01540
RHOS=1.225	HAD01550
SI=0.	HAD01560
CP1=0.45	HAD01570
NF=12	HAD01580


```

R=SQRT((2.*P*1000.)/(PI*RHOS*VM**3*CP1))
RPM=(X*60.*VM)/(R*2.*PI)
IF(VAL.EQ.1)GO TO 666
HH=2.*R
H=2.*R
XETA=1./6.
HB=0.10*R
666 CONTINUE
RL=R
IF(DTSR.GE.4.)NPROF=4418
IF(NPROF.EQ.4418)TH=0.18
ALO=0.
288 CONTINUE
IF(I11.GT.1)GO TO 1
IF(NPROF.EQ.4418)GO TO 93
93 ALPH=7.
CL=1.07
DO 11 I=1,NF
I3=NF
I2=NF-1
IF(I.GE.I2)GO TO 13
RR(I)=110.-I*10.
IF(SH.GE.2)GO TO 16
XL=RL/R*X
ZHI=2./3.*ATAN(1./XL)
CI(I)=((8.*PI*RL)/(B*CL))*(1.-COS(ZHI))
ZHI=ZHI*180./PI
THETI(I)=ZHI-ALPH
GO TO 17
16 XL=0.5*X
XHI5=2./3.*ATAN(1./XL)
C5=((8.*PI*0.5*R)/(B*CL))*(1.-COS(XHI5))
B5=XHI5*180./PI-ALPH
XL=0.9*X
XHI9=2./3.*ATAN(1./XL)
C9=((8.*PI*0.9*R)/(B*CL))*(1.-COS(XHI9))
B9=XHI9*180./PI-ALPH
CI(I)=(((C9-C5)/(0.4*R))*RL+2.25*C5-1.25*C9)
THETI(I)=((B9-B5)/(0.4*R))*RL+2.25*B5-1.25*B9
IF(SH.EQ.3)THETI(I)=0.
17 RL=R-I/10.*R
11 CONTINUE
13 RR(I2)=(HB-0.0001*R)/R*100.
CI(I2)=0.
THETI(I2)=0.
RR(I3)=0.
CI(I3)=0.
THETI(I3)=0.
R5=R
1 PI=3.1415926536
IF(T.NE.2)GO TO 63
R6=R
THETP=0.
106 CONTINUE
DR=0.02

```

HAD01590
HAD01600
HAD01610
HAD01620
HAD01630
HAD01640
HAD01650
HAD01660
HAD01670
HAD01680
HAD01690
HAD01700
HAD01710
HAD01720
HAD01730
HAD01740
HAD01750
HAD01760
HAD01770
HAD01780
HAD01790
HAD01800
HAD01810
HAD01820
HAD01830
HAD01840
HAD01850
HAD01860
HAD01870
HAD01880
HAD01890
HAD01900
HAD01910
HAD01920
HAD01930
HAD01940
HAD01950
HAD01960
HAD01970
HAD01980
HAD01990
HAD02000
HAD02010
HAD02020
HAD02030
HAD02040
HAD02050
HAD02060
HAD02070
HAD02080
HAD02090
HAD02100
HAD02110
HAD02120
HAD02130

HB=0.1*R	HAD02140
H=2.*R	HAD02150
HH=H	HAD02160
XMIN=2.	HAD02170
XMAX=13.	HAD02180
DX=0.5	HAD02190
HL=1	HAD02200
SI=0.	HAD02210
GO=0	HAD02220
APP=0	HAD02230
TH=0.18	HAD02240
ALO=0.	HAD02250
NFS=NF	HAD02260
NPROF=4418	HAD02270
63 IF(T.EQ.1)X=DTSR	HAD02280
IF(T.EQ.2)X=XMIN	HAD02290
OMEGA=RPM*PI/30.	HAD02300
V=R*OMEGA/X	HAD02310
H1=H	HAD02320
HH1=HH	HAD02330
R1=R	HAD02340
HB1=HB	HAD02350
DR1=DR	HAD02360
Z1=0	HAD02370
IF(Z1.EQ.0)COAN=9.	HAD02380
IF(Z1.EQ.1)GO TO 62	HAD02390
C-----]	HAD02400
CPRINT INPUT AND TITLES FOR OUTPUT.....]	HAD02410
C-----]	HAD02420
622 CALL TITLES(RR,CI,THETI,NF,SOLD,RPM)	HAD02430
62 CONTINUE	HAD02440
RHO=1.225	HAD02450
C-----]	HAD02460
CSTARTING TORQUE COEFFICIENT.....]	HAD02470
C-----]	HAD02480
IF(PITCH.EQ.1)GO TO 255	HAD02490
NS=20	HAD02500
NS1=NS+1	HAD02510
DRST=(R-HB)/FLOAT(NS)	HAD02520
DRST2=DRST/2.	HAD02530
SFX=0.	HAD02540
SQX=0.	HAD02550
DO 250 K=1,NS1	HAD02560
QU=1.	HAD02570
RL=HB+FLOAT(K-1)*DRST	HAD02580
CALL SEARCH(RL,RR,CI,THETI,NS,C,THET)	HAD02590
ALF=PI/2.-(THET+THETP*PI/180.)	HAD02600
CALL CLCD(ALF,ALFD,CL,CLD,CLT,CD,CDD,CDT,RL,AAT,NFS,SOLD)	HAD02610
SFX=SFX+(2-(1/K+K/NS1))*CL*C*DRST2/(PI*R**2)	HAD02620
SQX=SQX+(2-(1/K+K/NS1))*CL*C*RL*DRST2/(PI*R**3)	HAD02630
250 CONTINUE	HAD02640
SQC(I11)=SQX*B	HAD02650
ANGL(I11)=THETP	HAD02660
QU=2.	HAD02670
255 CONTINUE	HAD02680

C		HAD02690
CINITIALIZATION AND CONST. PARAMETER CALCULATIONS.....]	HAD02700
C]	HAD02710
	X=XMIN	HAD02720
	M=1	HAD02730
	MM=1	HAD02740
	BF=0.	HAD02750
	STRESM=0.	HAD02760
	FX8(1)=0.	HAD02770
	FY8(1)=0.	HAD02780
	TILT=0.	HAD02790
100	CONTINUE	HAD02800
	C11(1)=0.	HAD02810
	C12(1)=0.	HAD02820
	JMAX=1	HAD02830
	IF(Z1.EQ.1)JMAX=21	HAD02840
	DO 166 J=1,JMAX	HAD02850
	IF(Z1.EQ.1)THETP=0.+FLOAT(J-1)	HAD02860
	IF(Z1.EQ.1)THETP1(J)=THETP	HAD02870
	IMAX=1	HAD02880
	IF(Z1.EQ.1)IMAX=13	HAD02890
	DO 167 I=1,IMAX	HAD02900
	IF(Z1.EQ.1)V3(I)=8.+FLOAT(I-1)	HAD02910
	ITOT=-1	HAD02920
	DR=0.02	HAD02930
	R=R1	HAD02940
	IF(T.EQ.1.AND.PITCH.EQ.2)R=R5	HAD02950
	IF(T.EQ.2.AND.PITCH.EQ.2)R=R6	HAD02960
	IF(Z1.EQ.3.OR.Z1.EQ.4)X=DTSR	HAD02970
	IF(Z1.EQ.3.OR.Z1.EQ.4)THETP=0.	HAD02980
	IF(Z1.EQ.3.OR.Z1.EQ.4)VXV=R*OMEGA/DTSR	HAD02990
	IF(Z1.EQ.5)X=XV	HAD03000
	IF(Z1.EQ.5)THETP=0.	HAD03010
	IF(Z1.NE.1)V=R*OMEGA/X	HAD03020
	IF(Z1.EQ.1)V=V3(I)	HAD03030
	J1=1	HAD03040
	IK=1	HAD03050
	IF(Z1.GE.3)GO TO 302	HAD03060
	IF(VAL.EQ.1.AND.ABS(Z2-1.).LT.1.E-25)GO TO 302	HAD03070
	H=H1	HAD03080
	HB=HB1	HAD03090
	HH=HH1	HAD03100
302	KL=1	HAD03110
	T7=0.	HAD03120
	T8=0.	HAD03130
	XMXX=0.	HAD03140
	XMYX=0.	HAD03150
	XMYA=0.	HAD03160
	XMPI=0.	HAD03170
	QX=0.	HAD03180
	AC=0.38	HAD03190
	AK=0.	HAD03200
	SFAC=1.25	HAD03210
	TX=0.	HAD03220
	FXXP1=0.	HAD03230

FYXP1=0.	HAD03240
QY=0.	HAD03250
TY=0.	HAD03260
PY=0.	HAD03270
FX=0.	HAD03280
FY=0.	HAD03290
XXY=0.	HAD03300
XMY=0.	HAD03310
XMYAW1=0.	HAD03320
XMPIT1=0.	HAD03330
TFXT=0.	HAD03340
TFYT=0.	HAD03350
TFZT=0.	HAD03360
ASTOP=0.	HAD03370
A=0.	HAD03380
NFIT=4	HAD03390
AP=0.	HAD03400
COAN1=COAN*PI/180.	HAD03410
CNTROL=3	HAD03420
SI=SI*PI/180.	HAD03430
REF=R*COS(SI)	HAD03440
THETP=THETP*PI/180.	HAD03450
ALO=ALO*PI/180.	HAD03460
RHO=1.225	HAD03470
VIS=(0.0000003719-0.00000000204*H/3280.)*32.174*4.88243	HAD03480
AN=(R-HB)/(R*DR)+1.	HAD03490
NN=IFIX(AN)	HAD03500
NN1=NN-1	HAD03510
XMS=0.	HAD03520
IF(Z1.NE.1.OR.Z1.NE.3)GO TO 743	HAD03530
IF(X.NE.DTSR .AND. THETP.NE.0.0)GO TO 743	HAD03540
DIMAS=0.	HAD03550
DIMS=0.	HAD03560
DIM2=0.	HAD03570
DIM=0.	HAD03580
743 CONTINUE	HAD03590
AIYY=0.	HAD03600
AIXX=0.	HAD03610
EAL=7.33944954E09*9.81	HAD03620
RHAL=2700.	HAD03630
GAL=2.6759E10	HAD03640
RHOM=RHAL	HAD03650
FR=0.98	HAD03660
N9=1	HAD03670
RX=R	HAD03680
RLB=(1.-DR)*RX	HAD03690
DR=(RX-RLB)*COS(SI)	HAD03700
DRO=DR	HAD03710
R=R*COS(SI)	HAD03720
HB=HB*COS(SI)	HAD03730
RL=R	HAD03740
C	HAD03750
CTHREE PASS-NUMERICAL INT -TIP TO HUB.....]	HAD03760
C	HAD03770
CAT=1	HAD03780

	IF(GO.EQ.2)CAT=2	HAD03790
	CLFA=1.	HAD03800
	IF(GO.EQ.3)CLFA=0.	HAD03810
	IF(GO.LT.2)GO TO 2	HAD03820
	CALL SEARCH(RL,RR,CI,THETI,NF,C,THET)	HAD03830
	CALL CALC(RL,C,THET,FXXP1,FYXP1,XMXX,XMYX,QX,TX,RE,PHIR,CL,CD,CX,	HAD03840
	&CY,A,AP,XL,AK,ALPHA,F,CLFA,CAT,AAT,CLT,CDT,NFS,SOLD,XMYA,XMPI,	HAD03850
	&TFX1,TFY1,TFZ1)	HAD03860
2	A=0.	HAD03870
	CAT=0	HAD03880
	DO 8 L=1,NN	HAD03890
	TIP=0.	HAD03900
	IF((RL-HB) .GE. DR)GO TO 3	HAD03910
	ASTOP=ASTOP+1.	HAD03920
	IF(ASTOP.GE.2.)GO TO 9	HAD03930
	DR=(RL-HB)	HAD03940
3	IF(GO.LT.3)GO TO 5	HAD03950
	IF(CNTROL .EQ. 0)GO TO 5	HAD03960
	TIP=RL-DR	HAD03970
	IF(TIP .GT.REF)GO TO 4	HAD03980
	IF(CNTROL .EQ. 2)GO TO 5	HAD03990
	DR=(RL-REF)	HAD04000
	CLFO=(REF-TIP)/(RL-TIP)	HAD04010
	CLF=0.5*CLFO	HAD04020
	CNTROL=1	HAD04030
	GO TO 5	HAD04040
4	CLF=0.	HAD04050
5	DR2=DR/2.	HAD04060
	DT6=DR/6.	HAD04070
	RL=RL-DR2	HAD04080
	IF(CNTROL .EQ. 0)CLF=1.	HAD04090
	IF(CNTROL .EQ. 2)CLF=(CLFO+1.)/2.	HAD04100
	AK=1.	HAD04110
	CALL SEARCH(RL,RR,CI,THETI,NF,C,THET)	HAD04120
	CALL CALC(RL,C,THET,FXXP1,FYXP1,XMXXP1,XMYXP1,QXP1,TXP1,RE,	HAD04130
	&PHIR,CL,CD,CX,CY,A,AP,XL,AK,ALPHA,F,CLF,CAT,AAT,CLT,CDT,NFS,	HAD04140
	&SOLD,XMYA1,XMPI1,TFX2,TFY2,TFZ2)	HAD04150
	IF(Z1.EQ.1.OR.Z1.GE.3)GO TO 185	HAD04160
	IF(T.EQ.2)GO TO 185	HAD04170
	IF(THETP.NE.0.)GO TO 185	HAD04180
	IF(X.NE.DTSR)GO TO 185	HAD04190
	XMS1=CL*CONST/((OMEGA**2*RL*COS(COAN1))*SIN(COAN1)))*SFAC	HAD04200
	AXMS1=XMS1/(RHAL)	HAD04210
	ATH1=AXMS1/(2.6206*C)	HAD04220
	AIYY1=0.05172*ATH1**3+0.19175*C**3*ATH1	HAD04230
	AIXX1=0.66666*C*ATH1**3+0.0104389*C**3*ATH1-0.12434*C**2*ATH1**2	HAD04240
185	RL=RL-DR2	HAD04250
	IF(CNTROL.EQ.0)CLF=1.	HAD04260
	IF(CNTROL.EQ.1)CLF=CLFO	HAD04270
	IF(CNTROL.EQ.2)CLF=1.	HAD04280
	AK=0.	HAD04290
	CALL SEARCH(RL,RR,CI,THETI,NF,C,THET)	HAD04300
	CALL CALC(RL,C,THET,FX,Y,FYY,XMXXP,XMYXP,QXP,TXP,RE,PHIR,CL,CD,	HAD04310
	&CX,CY,A,AP,XL,AK,ALPHA,F,CLF,CAT,AAT,CLT,CDT,NFS,SOLD,	HAD04320
	&XMYA2,XMPI2,TFX3,TFY3,TFZ3)	HAD04330

	QYX=DT6*(QX+4.*QXP1+QXP)	HAD04340
	QY=QY+QYX	HAD04350
	IF(Z1.EQ.1.OR.Z1.GE.3)GO TO 111	HAD04360
	IF(T.EQ.2)GO TO 240	HAD04370
	IF(THETP.NE.0.)GO TO 240	HAD04380
	IF(X.NE.DTSR)GO TO 240	HAD04390
	IF(N9.GT.NN)GO TO 240	HAD04400
	XMS2=CL*CONST/((OMEGA**2*RL*COS(COAN1)*SIN(COAN1)))*SFAC	HAD04410
	AXMS2=XMS2/RHAL	HAD04420
	ATH2=AXMS2/(2.6206*C)	HAD04430
	IF(N9.EQ.1)GO TO 241	HAD04440
241	CONTINUE	HAD04450
	XMS=XMS2	HAD04460
	AIYY=AIYY2	HAD04470
	AIXX=AIXX2	HAD04480
	N9=N9+1	HAD04490
240	CONTINUE	HAD04500
	TYX=DT6*(TX+4.*TXP1+TXP)	HAD04510
	TY=TY+TYX	HAD04520
	IF(THETP.NE.0.)GO TO 111	HAD04530
	IF(X.NE.DTSR)GO TO 111	HAD04540
	TY4(KL)=TYX	HAD04550
	PY4(KL)=OMEGA*QYX	HAD04560
	QY2(KL)=QYX	HAD04570
	FY8(KL)=DT6*(FYXP1+4.*FYXP1+FYY)	HAD04580
	C11(KL)=TH/2.*C	HAD04590
	FX8(KL)=DT6*(FXXP1+4.*FXXP1+FXY)	HAD04600
	C12(KL)=0.75*C	HAD04610
111	PY=PY+OMEGA*QYX	HAD04620
	IF(Z1.EQ.6) TY=TY+DT6*(TX+4.*TXP1+TXP)	HAD04630
	IF(Z1.NE.3)GO TO 8691	HAD04640
	TY=TY+DT6*(TX+4.*TXP1+TXP)	HAD04650
8691	IF(Z1.GE.3)GO TO 869	HAD04660
	IF(Z1.EQ.1)GO TO 161	HAD04670
C	HAD04680
C	FOLLOWING 10 LINES GIVES DEL-POWER,-TORQUE,-THRUST,-AXIAL]	HAD04690
C	BENDING MOMENT,TANGENTIAL BENDING MOMENT, & -AXIAL FORCE WITH]	HAD04700
C	RADIAL VARIATION.]	HAD04710
C	HAD04720
	TY4(KL)=TYX	HAD04730
	PY4(KL)=OMEGA*QYX	HAD04740
	QY2(KL)=QYX	HAD04750
	FY8(KL)=DT6*(FYXP1+4.*FYXP1+FYY)	HAD04760
	FX8(KL)=DT6*(FXXP1+4.*FXXP1+FXY)	HAD04770
	CPCONT(KL)=(OMEGA*QYX)/(0.5*RHO*V**3*PI*RX**2)	HAD04780
	CQCONT(KL)=CPCONT(KL)/X	HAD04790
	CTCONT(KL)=TY4(KL)/(.5*RHO*V**2*PI*RX**2)	HAD04800
	FX=FX+DT6*(FXXP1+4.*FXXP1+FXY)	HAD04810
	FY=FY+DT6*(FYXP1+4.*FYXP1+FYY)	HAD04820
869	XMY=XY+DT6*(XMYX+4.*XMYXP1+XMYXP)	HAD04830
	XMY=XY+DT6*(XMYX+4.*XMYXP1+XMYXP)	HAD04840
	IF(Z1.NE.4)GO TO 161	HAD04850
C	-----	HAD04860
C	FOLLOWING 5 LINES GIVES THE TOWER TOP AXIAL,VERTICAL, AND]	HAD04870
C	TANGENTIAL FORCE. ALSO GIVES YAWING & PITCHING MOMENT CO-EFFICIENTS]	HAD04880

C	WITH YAW ANGLE VARIATIONS AT DIFFERENT BLADE POSITIONS(Z1=4)]HAD04890
C	-----	HAD04900
	XMYAW1=XMYAW1+DT6*(XMYA+4.*XMYA1+XMYA2)	HAD04910
	XMPIT1=XMPIT1+DT6*(XMPI+4.*XMPI1+XMPI2)	HAD04920
	TFXT=TFXT+DT6*(TFX1+4.*TFX2+TFX3)	HAD04930
	TFYT=TFYT+DT6*(TFY1+4.*TFY2+TFY3)	HAD04940
	TFZT=TFZT+DT6*(TFZ1+4.*TFZ2+TFZ3)	HAD04950
161	IF(CNTROL.EQ.2) CNTROL=0	HAD04960
	IF(CNTROL.EQ.0)GO TO 6	HAD04970
	IF(ABS(RL-TIP).LT.1.E-25)GO TO 6	HAD04980
	IF(CNTROL.EQ.1) DR=REF-TIP	HAD04990
	IF(CNTROL.EQ.1) CNTROL=2	HAD05000
	GO TO 7	HAD05010
6	DR=DRO	HAD05020
7	CONTINUE	HAD05030
	QX=QXP	HAD05040
	IF(Z1.GE.3)GO TO 778	HAD05050
	IF(Z1.EQ.1)GO TO 777	HAD05060
778	TX=TXP	HAD05070
	XMXX=XMXXP	HAD05080
	XMYX=XMYXP	HAD05090
	XMYA=XMYA2	HAD05100
	XMPI=XMPI2	HAD05110
	TFX1=TFX3	HAD05120
	TFY1=TFY3	HAD05130
	TFZ1=TFZ3	HAD05140
	FXY=FXXP1	HAD05150
	FYY=FYXP1	HAD05160
	IF(Z1.EQ.3)GO TO 777	HAD05170
	CTY=TY/(0.5*RHO*V**2*PI*RX**2)	HAD05180
	CPY=PY/(0.5*RHO*V**3*PI*RX**2)	HAD05190
	RAT=CTY/CPY	HAD05200
777	TP=PY/1000.	HAD05210
	PHIO=PHIR*180./PI	HAD05220
	ALPHA=ALPHA*180./PI	HAD05230
	PR=RL/(RX*COS(SI))	HAD05240
	IF(Z1.EQ.1.OR.Z1.GE.3)GO TO 8	HAD05250
	QY1=QY	HAD05260
	CQ=CPY/X	HAD05270
	TY1=TY	HAD05280
	FX1=FX	HAD05290
	FY1=FY	HAD05300
	XMX1=XMX	HAD05310
	XMY1=XMY	HAD05320
C	-----	HAD05330
CPRINT OUTPUT.....]HAD05340
C	-----	HAD05350
	VOUT=V	HAD05360
	PCCR=RL/(RX*COS(SI))	HAD05370
	IF(X.EQ.DTSR.AND.THETP.EQ.0.) RR1(KL)=RL	HAD05380
	PCCCR(KL)=PCCR	HAD05390
	KL=KL+1	HAD05400
	RCD=CD/CL	HAD05410
	IF(PRINT.NE.3)GO TO 8	HAD05420
C	-----]HAD05430

C	WRITES DIFFERENT AERODYNAMIC PARAMETERS WITH RADIAL VARIATIONS.]	HAD05440
C	-----]	HAD05450
	WRITE(61,14)PCCR,A,AP,CL,CD,PHIO,ALPHA,F,RE,CTY,CPY,RCD	HAD05460
8	CONTINUE	HAD05470
	IF(Z1.LT.4)GO TO 77	HAD05480
C	-----]	HAD05490
C	FOLLOWING 4 LINES GIVES POWER,TORQUE & THRUST CO-EFFICIENTS]	HAD05500
C	WITH YAW ANGLE VARIATIONS (Z1=6).]	HAD05510
C	-----]	HAD05520
	IF(Z1.EQ.6) POYA(IA,IB)=CPY	HAD05530
	IF(Z1.EQ.6) TOYA(IA,IB)=CTY	HAD05540
	IF(Z1.EQ.6) QOYA(IA,IB)=CPY/X	HAD05550
	CQ1=CPY/X	HAD05560
	IF(Z1.EQ.5) T3P(IA)=PY/1000.	HAD05570
	IF(Z1.EQ.5.OR.Z1.EQ.6)GO TO 55	HAD05580
	IF(Z1.NE.4)GO TO 77	HAD05590
C	-----]	HAD05600
C	NEXT 5 LINES ARE FOR TOWER TOP AXIAL,TANGENTIAL&]	HAD05610
C	VERTICAL FORCE AND YAWING & PITCHING MOMENT CO-EFFICIENT]	HAD05620
C	CALCULATION WITH YAW ANGLE &TOWER SHADOW FACTOR VARITIONS(Z1=4).]	HAD05630
C	-----]	HAD05640
	TOFX(IA,IB)=TFXT	HAD05650
	TOFY(IA,IB)=TFYT	HAD05660
	TOFZ(IA,IB)=TFZT	HAD05670
	XMYAW(IA,IB)=XMYAW1	HAD05680
	PIM(IA,IB)=XMPIT1	HAD05690
	GO TO 55	HAD05700
77	IF(T.EQ.2)GO TO 637	HAD05710
	IF(Z1.NE.3)GO TO 244	HAD05720
C	-----]	HAD05730
C	FOLLWING 7 LINES GIVES FLAPWISE & EDGEWISE BENDING MOMENT,]	HAD05740
C	POWER & TORQUE CO-EFFICIENT WITH YAW ANGLE AND TOWER SHADOW FACTOR]	HAD05750
C	VARIATIONS AT DIFFERENT BLADE POSITIONS.]	HAD05760
C	-----]	HAD05770
	FLAP1(IA,IB)=XMY/1000.	HAD05780
	EDGE1(IA,IB)=XMX/1000.	HAD05790
	CPYS1(IA,IB)=PY/(0.5*RHO*PI*R**2*VXV**3)	HAD05800
	CTYS1(IA,IB)=TY/(0.5*RHO*PI*R**2*VXV**2)	HAD05810
	WRITE(61,213)SIA,FLAP1(IA,IB),EDGE1(IA,IB),CPYS1(IA,IB),CTYS1(IA,	HAD05820
	&IB)	HAD05830
	IF(X.NE.DTSR)GO TO 55	HAD05840
	IF(IA.GT.1)GO TO 55	HAD05850
	DO 741 L1=10,370,10	HAD05860
	SPA=FLOAT(L1-10)	HAD05870
	SIA3(L1/10)=SPA	HAD05880
741	CONTINUE	HAD05890
	GO TO 55	HAD05900
244	IF(Z1.EQ.1)GO TO 637	HAD05910
	IF(Z1.GE.3)GO TO 55	HAD05920
	IF(THETP.NE.0.)GO TO 637	HAD05930
	IF(X.NE.DTSR)GO TO 637	HAD05940
	STRESM=0.	HAD05950
	DO 639 IM=1,44	HAD05960
639	CONTINUE	HAD05970
	GO TO 637	HAD05980

640	COAN=COAN-1.	HAD05990
	X=DTSR	HAD06000
	ZOAN1=COAN	HAD06010
	GO TO 55	HAD06020
637	IF(Z1.NE.1)GO TO 9	HAD06030
	T1P(I,J)=TP	HAD06040
	GO TO 55	HAD06050
9	HP=TP*1.3410	HAD06060
	IF(PRINT.NE.3)GO TO 53	HAD06070
	WRITE(61,33)X	HAD06080
	WRITE(61,99)VOUT	HAD06090
	WRITE(61,36)CPY	HAD06100
53	XX(M)=X	HAD06110
	IF(VOUT.LE.20.) V2(MM)=VOUT	HAD06120
	V1(M)=VOUT	HAD06130
	PISTEL=T7/(PI*RX**5)	HAD06140
	PI2TEL=T8*X/(PI*RX**6)	HAD06150
	CPAV=CPY	HAD06160
	IF(PRINT.NE.3)GO TO 54	HAD06170
	WRITE(61,37)CPAV	HAD06180
	WRITE(61,38)CTY	HAD06190
	WRITE(61,51)PISTEL	HAD06200
	WRITE(61,52)PI2TEL	HAD06210
54	II=I11	HAD06220
	TP2(MM,II)=0.	HAD06230
	CQY(M,II)=CQ	HAD06240
	CP(M,II)=CPAV	HAD06250
	TP1(M,II)=TP	HAD06260
	IF(VOUT.LE.20.) TP2(MM,II)=TP	HAD06270
	IF(TP2(MM,II).GE.P) TP2(MM,II)=P	HAD06280
	IF(TP2(MM,II).LE.0.) TP2(MM,II)=0.	HAD06290
	CT(M,II)=CTY	HAD06300
	RA(M,II)=RAT	HAD06310
	XMY2(M,II)=XMY1/1000.	HAD06320
	M=M+1	HAD06330
	IF(VOUT.GT.20.)GO TO 862	HAD06340
	MM=MM+1	HAD06350
862	IF(PRINT.EQ.2.OR.PRINT.EQ.3)GO TO 86	HAD06360
	IF(X.GT.XMIN)GO TO 861	HAD06370
	WRITE(61,118)HP	HAD06380
	WRITE(61,120)SQC(I11)	HAD06390
	WRITE(61,81)	HAD06400
	WRITE(61,82)	HAD06410
	WRITE(61,83)	HAD06420
861	IF(PRINT.EQ.2.OR.PRINT.EQ.3)GO TO 86	HAD06430
C	-----	HAD06440
C	WRITES DIFFERENT AERODYNAMIC PARAMETERS WITH TIP SPEED RATIO.]	HAD06450
C	-----	HAD06460
	WRITE(61,84)X,VOUT,TP,CPAV,QY1,CQ,TY1,CTY,XMY1,XMY1,FX1,FY1	HAD06470
86	X=X+DX	HAD06480
	IF(PRINT.NE.3)GO TO 55	HAD06490
C	-----	HAD06500
C	FOLLOWING 11 LINES WRITES DEL-POWER,TORQUE,THRUST,AXIAL & TANGE]	HAD06510
C	-NTIAL FORCE,AXIAL & TANGENTIAL MOMENT,DEL-POWER,TORQUE & THRUST]	HAD06520
C	CO-EFFICIENTS WITH RADIAL VARIATIONS.]	HAD06530

C-----	HAD06540
WRITE(61,224)	HAD06550
KKL=KL-1	HAD06560
DO 222 JJ=1,KKL	HAD06570
WRITE(61,223)PCCCR(JJ),CPCONT(JJ),PY4(JJ),QY2(JJ),TY4(JJ),FX8(JJ)	HAD06580
&,FY8(JJ)	HAD06590
222 CONTINUE	HAD06600
WRITE(61,204)	HAD06610
DO 206 MK=1,KKL	HAD06620
WRITE(61,205)PCCCR(MK),CPCONT(MK),CQCONT(MK),CTCONT(MK)	HAD06630
206 CONTINUE	HAD06640
55 SI=SI*180./PI	HAD06650
THETP=THETP*180./PI	HAD06660
ALO=ALO*180./PI	HAD06670
167 CONTINUE	HAD06680
166 CONTINUE	HAD06690
IF(Z1.EQ.6)GO TO 988	HAD06700
IF(Z1.LT.3)GO TO 986	HAD06710
IF(Z1.NE.4)GO TO 990	HAD06720
SIA=SIA+10.	HAD06730
GO TO 988	HAD06740
990 IF(SIA.LE.15..OR.SIA.GE.345.) GO TO 987	HAD06750
SIA=SIA+15.	HAD06760
GO TO 988	HAD06770
987 SIA=SIA+5.	HAD06780
988 IF(Z1.GE.3) IA=IA+1	HAD06790
IF(Z1.EQ.6)GO TO 993	HAD06800
IF(SIA.LE.360.)GO TO 587	HAD06810
IF(Z1.EQ.4)GO TO 605	HAD06820
IF(Z1.EQ.3)GO TO 603	HAD06830
587 IF(Z1.GE.3)GO TO 100	HAD06840
986 IF(ABS(X-DTSR).LT.1.E-25 .AND. STRESM.GE. 98.)GO TO 100	HAD06850
IF(Z1.EQ.1)GO TO 159	HAD06860
IF(X.GT.XMAX)GO TO 102	HAD06870
IF(PRINT.NE.3)GO TO 56	HAD06880
WRITE(61,47)	HAD06890
WRITE(61,57)	HAD06900
56 GO TO 100	HAD06910
102 CONTINUE	HAD06920
IF(T.EQ.2)GO TO 103	HAD06930
IF(PITCH.EQ.1)GO TO 103	HAD06940
I11=I11+1	HAD06950
HI1=HI1+2.5	HAD06960
IF(HI1.LT.14.)GO TO 101	HAD06970
103 CONTINUE	HAD06980
IF(T.NE.2)GO TO 588	HAD06990
IF(PITCH.EQ.1)GO TO 58	HAD07000
IF(PITCH.EQ.2)THETP=THETP+2.	HAD07010
IF(THETP.LE.12.)GO TO 106.	HAD07020
GO TO 58	HAD07030
588 IF(PRINT.GE.3)GO TO 160	HAD07040
IF(PITCH.EQ.1)GO TO 160	HAD07050
Z1=1	HAD07060
Z2=1.	HAD07070
GO TO 100	HAD07080

159 CONTINUE	HAD07090
C	HAD07100
C NEXT 19 LINES ARE FOR CONST.POWER CALCULATIONS.....]	HAD07110
C	HAD07120
P9=P	HAD07130
P10=P9+0.4*P9	HAD07140
1591 DO 168 J=1,21	HAD07150
IF(T1P(1,J).GT.P)GO TO 168	HAD07160
DO 169 I=1,13	HAD07170
IF(T1P(I,J).LT.P)GO TO 169	HAD07180
V33(J1,IK)=(V3(I)-V3(I-1))/(T1P(I,J)-T1P((I-1),J))*(P-T1P((I-1),J	HAD07190
&))+V3(I-1)	HAD07200
J1=J1+1	HAD07210
GO TO 168	HAD07220
169 CONTINUE	HAD07230
168 CONTINUE	HAD07240
N1(IK)=J1-1	HAD07250
P=P+35.	HAD07260
IF(P.GT.P10)GO TO 160	HAD07270
J1=1	HAD07280
IK=IK+1	HAD07290
GO TO 1591	HAD07300
160 CONTINUE	HAD07310
C-----	HAD07320
C * PUT CCCC BEFORE GO TO 58 * IF YAW REQD.(THIS LINE NO.IS 819)]	HAD07330
C	HAD07340
**** GO TO 58	HAD07350
C-----	HAD07360
C NEXT 20 LINES ARE FOR FLAPWISE,EDGEWISE BENDING MOMENT,]	HAD07370
C POWER & THRUST CO-EFFICIENT CALCULATIONS WITH YAW ANGLE &]	HAD07380
C TOWER SHADOW VARIATIONS.]	HAD07390
CZ3-----	HAD07400
888 Z1=3	HAD07410
IA=1	HAD07420
IB=1	HAD07430
BF=0.6	HAD07440
YA=89.99	HAD07450
SIA=0.	HAD07460
WRITE(61,211)	HAD07470
WRITE(61,214)DTSR,BF	HAD07480
WRITE(61,210)YA	HAD07490
WRITE(61,212)	HAD07500
GO TO 100	HAD07510
603 IA=1	HAD07520
IB=IB+1	HAD07530
BF=0.6	HAD07540
SIA=0.	HAD07550
YA=YA-6.	HAD07560
IF(YA.LE.69.)GO TO 604	HAD07570
WRITE(61,214)DTSR,BF	HAD07580
WRITE(61,210)YA	HAD07590
WRITE(61,212)	HAD07600
PRINT*,YA,Z1	HAD07610
GO TO 100	HAD07620
C-----	HAD07630


```

C          NEXT 47 LINES ARE FOR TOWER TOP AXIAL,TANGENTIAL& ] HAD07640
C VERTICAL FORCE AND YAWING & PITCHING MOMENT CO-EFFICIENT ] HAD07650
C CALCULATION WITH YAW ANGLE &TOWER SHADOW VARITIONS. ] HAD07660
CZ4-----] HAD07670
604 Z1=4 ] HAD07680
    SIA=0. ] HAD07690
    BF=0.6 ] HAD07700
    IA=1 ] HAD07710
    IB=1 ] HAD07720
    YA=89.99 ] HAD07730
    GO TO 100 ] HAD07740
605 IA=1 ] HAD07750
    Z1=4 ] HAD07760
    IB=IB+1 ] HAD07770
    YA=YA-6. ] HAD07780
    BF=0.6 ] HAD07790
    SIA=0. ] HAD07800
    IF(YA.LE.69.)GO TO 606 ] HAD07810
    PRINT*,YA,Z1 ] HAD07820
    GO TO 100 ] HAD07830
606 CONTINUE ] HAD07840
] HAD07850
C-----]
C .....NEXT 3 LINES ARE FOR CENTRIFUGAL STRESS..... ] HAD07860
C ] HAD07870
C.....REJECTED..... ] HAD07880
C CENTS(1)=0. ] HAD07890
C DO 78 I=2,45 ] HAD07900
C 78 CENTS(I)=GG(46-I)/CROS(I) ] HAD07910
C-----] HAD07920
ARR=0.5*RHO*PI*R**3*V**2 ] HAD07930
DO 88 J=1,4 ] HAD07940
DO 88 I=1,37 ] HAD07950
IF(I.GT.18)GO TO 909 ] HAD07960
XMYAH(I,J)=(XMYAW(18+I,J)+XMYAW(I,J))/ARR ] HAD07970
PIM1(I,J)=(PIM(18+I,J)+PIM(I,J))/ARR ] HAD07980
TOFX1(I,J)=TOFX(18+I,J)+TOFX(I,J) ] HAD07990
TOFY1(I,J)=TOFY(18+I,J)+TOFY(I,J) ] HAD08000
TOFZ1(I,J)=TOFZ(18+I,J)+TOFZ(I,J) ] HAD08010
GO TO 88 ] HAD08020
909 XMYAH(I,J)=(XMYAW(I,J)+XMYAW(I-18,J))/ARR ] HAD08030
PIM1(I,J)=(PIM(I,J)+PIM(I-18,J))/ARR ] HAD08040
TOFX1(I,J)=TOFX(I,J)+TOFX(I-18,J) ] HAD08050
TOFY1(I,J)=TOFY(I,J)+TOFY(I-18,J) ] HAD08060
TOFZ1(I,J)=TOFZ(I,J)+TOFZ(I-18,J) ] HAD08070
88 CONTINUE ] HAD08080
DO 129 KKK=1,37 ] HAD08090
XMYAH(KKK,1)=XMYAH(KKK,1)*100. ] HAD08100
129 CONTINUE ] HAD08110
C-----] HAD08120
C NEXT 16 LINES WRITES TOWER TOP AXIAL,TANGENTIAL& ] HAD08130
C VERTICAL FORCE AND YAWING & PITCHING MOMENT CO-EFFICIENT ] HAD08140
C FOR DIFFERENT YAW ANGLE &TOWER SHADOW FACTORS. ] HAD08150
C-----] HAD08160
WRITE(61,211) ] HAD08170
WRITE(61,214)DTSR,BF ] HAD08180

```


WRITE(61,215)	HAD08190
WRITE(61,1000)	HAD08200
WRITE(61,1001)	HAD08210
DO 216 J=1,4	HAD08220
WRITE(61,1008)J	HAD08230
DO 216 I=1,37	HAD08240
WRITE(61,1009)I,XMYAH(I,J),PIM1(I,J),TOFY1(I,J),TOFX1(I,J),	HAD08250
+TOFZ1(I,J)	HAD08260
216 CONTINUE	HAD08270
C-----	HAD08280
C NEXT 29 LINES ARE FOR POWER,TORQUE,&THRUST CO-EFFICIENT]	HAD08290
C CALCULATION WITH YAW ANGLE VARITIONS.]	HAD08300
CZ6-----	HAD08310
984 CONTINUE	HAD08320
Z1=6	HAD08330
IA=1	HAD08340
IB=1	HAD08350
SIA=0.	HAD08360
X=XMIN	HAD08370
BF=0.	HAD08380
THETP=0.	HAD08390
YA=84.	HAD08400
XETA=0.167	HAD08410
WRITE(61,209)	HAD08420
WRITE(61,217)YA	HAD08430
WRITE(61,208)	HAD08440
GO TO 100	HAD08450
993 CONTINUE	HAD08460
WRITE(61,207)X,CPY,CTY,CQ1	HAD08470
X=X+1.	HAD08480
IF(X.GT.XMAX)GO TO 992	HAD08490
GO TO 100	HAD08500
992 IA=1	HAD08510
IB=IB+1	HAD08520
X=XMIN	HAD08530
YA=YA-6.	HAD08540
IF(YA.LT.69.)GO TO 994	HAD08550
WRITE(61,217)YA	HAD08560
WRITE(61,208)	HAD08570
PRINT*,YA,Z1	HAD08580
GO TO 100	HAD08590
994 CONTINUE	HAD08600
PRINT*, '***** END OF EXECUTION ***** '	HAD08610
58 CONTINUE	HAD08620
C-----	HAD08630
CFORMAT FOR INPUT/OUTPUT.....	HAD08640
CM-----	HAD08650
10 FORMAT(3F10.4)	HAD08660
14 FORMAT(F5.3,1X,F7.4,3X,F6.4,1X,F5.2,3X,F5.3,2X,F6.2,2X,	HAD08670
&F6.2,2X,F6.4,2X,E10.3,1X,F7.4,2X,F8.4,2X,F8.5)	HAD08680
33 FORMAT(///,' PERFORMANCE SUMMARY= ',30X,'TIP SPEED RATIO=',F8.3)	HAD08690
36 FORMAT(/,15X,27H TOTAL POWER COEFFICIENT = ,F7.5)	HAD08700
37 FORMAT(/,15X,43H AVERAGE POWER COEFFICIENT WITH GRADIENT = ,F10.5)	HAD08710
38 FORMAT(/,15X,28H TOTAL THRUST COEFFICIENT = ,F7.4)	HAD08720
39 FORMAT(7F10.4)	HAD08730


```

CM ----- HAD08740
8000 FORMAT(22X, ' INPUTED VALUES ',/22X,28('_')//) HAD08750
7001 FORMAT(2I2) HAD08760
8001 FORMAT(5X, 'T=', I2, ' PRINT=', I2) HAD08770
7002 FORMAT(I2) HAD08780
8002 FORMAT(25X, 'NFIT=', I2) HAD08790
7003 FORMAT(3F10.5, 2I2) HAD08800
8003 FORMAT(5X, 'VM=', F5.2, ' P=', F6.2, ' DTSR=', F4.2, ' SH=', I2, ' HAD08810
& PITCH=', I2) HAD08820
7004 FORMAT(4F10.5, I2) HAD08830
8004 FORMAT(5X, 'HH=', F4.2, ' XETA=', F6.4, ' HB=', F4.2, ' H=', F4.2, ' HAD08840
& VAL=', I2) HAD08850
CM ----- HAD08860
7005 FORMAT(4F10.5, I2) HAD08870
8005 FORMAT(9X, 'R=', F7.3, ' B=', F3.1, ' RPM=', F5.2, ' XETA=', F6.4, ' HAD08880
& PITCH=', I2) HAD08890
7006 FORMAT(I2) HAD08900
8006 FORMAT(25X, 'NF=', I2) HAD08910
7007 FORMAT(3F10.5) HAD08920
9001 FORMAT(/, 10X, 'RR(I) CI(I) THETI(I)') HAD08930
8007 FORMAT(10X, 3(F10.5, 5X)) HAD08940
7008 FORMAT(3F10.5) HAD08950
9002 FORMAT(/, 20X, 'AAT(I) CLT(I) CDT(I)') HAD08960
8008 FORMAT(20X, 3(F10.5, 5X)) HAD08970
C----- HAD08980
40 FORMAT(3F10.4) HAD08990
41 FORMAT(2I2, I4) HAD09000
47 FORMAT(/, 5X, 22H PERFORMANCE ANALYSIS:) HAD09010
51 FORMAT(/, ' TORQUE VARIATION DUE TO AERODYNAMIC SECOND DERIVATIVE HAD09020
&=', F15.4) HAD09030
52 FORMAT(/, ' TORQUE VARIATION DUE TO SHEAR SECOND DERIVATIVE =', HAD09040
&F15.4) HAD09050
57 FORMAT(////, 1X, 'PCCR', 5X, 'A', 6X, 'AP', 5X, 'CL', 6X, 'CD', 5X, 'PHI', HAD09060
&4X, 'ALPHA', 5X, 'F', 8X, ' RE-NO.', 6X, 'CT', 6X, 'CP', 5X, 'CD/CL', /) HAD09070
99 FORMAT(/, 15X, 'WIND VELOCITY (METER/SEC) =', F8.2) HAD09080
224 FORMAT(/, 3X, 'STATION', 5X, 'DEL-CP', 7X, 'POWER', 8X, 'TORQUE', 8X, HAD09090
&'THRUST', 8X, 'X-FORCE', 5X, 'Y-FORCE', 6X, 'X-MOMENT', 4X, 'Y-MOMENT' /) HAD09100
223 FORMAT(F8.2, 5X, F10.5, 7(3X, F10.3), /) HAD09110
81 FORMAT(///, 3X, 'TIP SPEED WIND POWER POWER TORQUE TORQUE THAD09120
&HRUST THRUST MOMENT/BLADE MOMENT/BLADE FORCE/BLADE FORCE/BLAHAD09130
&DE') HAD09140
82 FORMAT(3X, ' RATIO VEL. COFF. COFF. HAD09150
& COFF. X-DIRECTION Y-DIRECTION X-DIRECTION Y-DIRECTION HAD09160
& ') HAD09170
HAD09180
83 FORMAT(3X, ' (M/SEC) (KW) (CP) (N-M) (CQ) (N)HAD09190
& (CT) (N-M) (N-M) (N) (N)') HAD09200
84 FORMAT(5X, F5.2, 2X, F5.2, 2X, G8.2, 2X, G8.2, 1X, G9.3, 2X, G10.3, HAD09210
&1X, G9.3, 2X, G9.3, 1X, G10.4, 3X, G10.4, 2X, G11.5, 3X, G11.5) HAD09220
118 FORMAT(/, 15X, 'HORSE POWER , H.P. = ', F10.2//) HAD09230
120 FORMAT(15X, 'STARTING TORQUE CO-EFFICIENT= ', G10.3//) HAD09240
204 FORMAT(/, 3X, 'STATION', 5X, 'DEL-CP', 7X, 'DEL-CQ', 5X, 'DEL-CT') HAD09250
205 FORMAT(F8.2, 7X, F8.6, 5X, F8.6, 3X, F8.6//) HAD09260
CFYAW----- HAD09270
1000 FORMAT(///, 10X, 'ADDED VALUES OBTAINED FROM THE LOOP Z1 = 4 ', / HAD09280

```



```

& 10X,'YAWING MOMENT CO-EFF.,PITCHING MOMENT CO-EFF.,')/
1001 FORMAT(10X,'TOWER TOP AXIL,VERTICAL & TANGENTIAL FORCE.'////) HAD09290
1007 FORMAT(3X,I3,6X,F10.6,/) HAD09300
1008 FORMAT(//,I2,8X,'YAW MOMENT CO-EFF.',2X,'PITCH MOMENT CO-EFF.',3X HAD09310
+, 'AXIL FORCE',3X,'TANGENTIAL FORCE',3X,'VERTICAL FORCE'//) HAD09320
1009 FORMAT(I3,5X,5(E16.8,3X)) HAD09330
C----- FORMAT FORMAT FORMAT FORMAT----- HAD09340
207 FORMAT(4X,F5.2,5X,F8.5,4X,F8.5,3X,F8.5/) HAD09350
208 FORMAT(/5X,'T.S.R.',7X,'CP',10X,'CT',8X,'CQ'/) HAD09360
209 FORMAT(//10X,'EFFECT OF YAWING ANGLE ON POWER,TORQUE & THRUST CO-EHAD09380
&FF.:-' ,/10X,53('-')//) HAD09390
210 FORMAT(/30X,' YAW ANGLE = ',F5.2//) HAD09400
211 FORMAT(//10X,'EFFECT OF YAWING ANGLE & TOWER SHADOW:-',/10X,37( HAD09410
&'-'//) HAD09420
212 FORMAT(/3X,'THETA',6X,'FLAP',9X,'EDGE',13X,'CP',12X,'CT'/) HAD09430
213 FORMAT(1X,F5.1,5X,G11.5,4X,G11.5,3X,G11.5,5X,G11.5/) HAD09440
214 FORMAT(//10X,'DESIGN TIP SPEED RATIO=',F5.2,17X,'TOWER SHADOW FACTHAD09450
&OR=',F5.3,//) HAD09460
215 FORMAT(///,25X,'YAW ANGLE INTERVAL = 6.0'////) HAD09470
217 FORMAT(/15X,' YAW ANGLE = ',F5.2//) HAD09480
STOP HAD09490
END HAD09500
CS=1 ----- HAD09510
C SUBROUTINE SEARCH ] HAD09520
C ] HAD09530
C ] HAD09540
C -----] HAD09550
SUBROUTINE SEARCH(RL,RR,CI,THETI,NF,C,THET) HAD09560
C HAD09570
C ....SEARCH DETERMINES CHORD AND TWIST ANGLE AT A GIVEN RADIUS ] HAD09580
C ALONG THE SPAN BY LINEAR INTERPOLATION.... ] HAD09590
C HAD09600
DIMENSION RR(25),CI(25),THETI(25) HAD09610
COMMON/C1/R,DR,HB,B,V,X,THETP,H,SI,GO,OMEGA,RHO,VIS,HL,PI,RX,W HAD09620
&,NPROF,APP,T1,T2,T3,T4,T5,T6,T7,T8,TEST,XETA,HH,ALO,AC,TH HAD09630
DO 1 I=1,NF HAD09640
RRV=RL/(RX*COS(SI))*100. HAD09650
CEQ IF(RRV.EQ.RR(I))GO TO 4 HAD09660
IF(ABS(RRV-RR(I)).LT.1.E-25)GO TO 4 HAD09670
IF(RRV.GE.RR(I))GO TO 2 HAD09680
IF(I.EQ.NF)GO TO 3 HAD09690
1 CONTINUE HAD09700
2 J=I+1 HAD09710
PER=(RRV-RR(J-1))/(RR(J-2)-RR(J-1)) HAD09720
C=PER*(CI(J-2)-CI(J-1))+CI(J-1) HAD09730
THET=PER*(THETI(J-2)-THETI(J-1))+THETI(J-1) HAD09740
GO TO 5 HAD09750
3 C=CI(NF) HAD09760
THET=THETI(NF) HAD09770
GO TO 5 HAD09780
4 C=CI(1) HAD09790
THET=THETI(1) HAD09800
5 THET=THET*PI/180. HAD09810
RETURN HAD09820
END HAD09830

```


CS=2	-----	HAD09840
C	SUBROUTINE TITLES]	HAD09850
C	_____]	HAD09860
C	_____]	HAD09870
C	-----]	HAD09880
	SUBROUTINE TITLES (RR, CI, THETI, NF, SOLD, RPM)	HAD09890
C	-----	HAD09900
CTITLES PRINTS OUT INPUT DATA, SYMBOLS/TITLES FOR OUTPUT]	HAD09910
C	-----	HAD09920
	INTEGER PRINT, GO, HL, APP	HAD09930
	DIMENSION RR(25), CI(25), THETI(25)	HAD09940
	COMMON/C1/R, DR, HB, B, V, X, THETP, H, SI, GO, OMEGA, RHO, VIS, HL, PI, RX, W,	HAD09950
	&NPROF, APP, T1, T2, T3, T4, T5, T6, T7, T8, TEST, XETA, HH, ALO, AC, TH	HAD09960
	COMMON/C2/DTSR, PRINT, T	HAD09970
	IF(PRINT.EQ.2)GO TO 61	HAD09980
	WRITE(61,12)	HAD09990
	WRITE(61,13)	HAD10000
	WRITE(61,15)	HAD10010
	WRITE(61,14)	HAD10020
	WRITE(61,16)XETA	HAD10030
	WRITE(61,17)HH	HAD10040
	WRITE(61,18)H	HAD10050
	WRITE(61,117)TH	HAD10060
	WRITE(61,119)RPM	HAD10070
	WRITE(61,19)OMEGA	HAD10080
	IF(T.EQ.1)GO TO 49	HAD10090
	WRITE(61,20)X	HAD10100
	GO TO 51	HAD10110
49	DTSR=X	HAD10120
	WRITE(61,50)DTSR	HAD10130
51	WRITE(61,21)THETP	HAD10140
61	RX=R	HAD10150
	CSI=SI	HAD10160
	SI=SI*PI/180.	HAD10170
	CRL=0.75*R	HAD10180
	CALL SEARCH(CRL, RR, CI, THETI, NF, C, THET)	HAD10190
	SI=CSI	HAD10200
	BANG=THET*180./PI+THETP	HAD10210
	IF(PRINT.EQ.2)GO TO 62	HAD10220
	WRITE(61,22)BANG	HAD10230
	WRITE(61,23)SI	HAD10240
	WRITE(61,24)	HAD10250
	WRITE(61,25)B	HAD10260
	WRITE(61,26)R	HAD10270
	WRITE(61,27)HB	HAD10280
62	CALL SOLIDT(RR, CI, NF, B, R, PI, SOLD)	HAD10290
	IF(PRINT.EQ.2)GO TO 63	HAD10300
	WRITE(61,28)SOLD	HAD10310
63	CALL ACTIVI(RR, CI, NF, B, R, PI, ACF)	HAD10320
	IF(PRINT.EQ.2)GO TO 60	HAD10330
	WRITE(61,29)ACF	HAD10340
	WRITE(61,30)NPROF	HAD10350
	GO TO 55	HAD10360
55	WRITE(61,31)NF	HAD10370
	WRITE(61,32)	HAD10380

WRITE(61,33)	HAD10390
WRITE(61,34)(RR(I),CI(I),THETI(I),I=1,NF)	HAD10400
WRITE(61,35)	HAD10410
WRITE(61,36)DR	HAD10420
IF(APP.EQ.0)GO TO 1	HAD10430
WRITE(61,37)	HAD10440
1 CONTINUE	HAD10450
2 WRITE(61,39)	HAD10460
3 IF(B.GT.2.)GO TO 4	HAD10470
IF(GO.EQ.0)GO TO 8	HAD10480
IF(GO.EQ.1)GO TO 5	HAD10490
IF(GO.EQ.2)GO TO 6	HAD10500
IF(GO.EQ.3)GO TO 7	HAD10510
GO TO 9	HAD10520
4 IF(GO.EQ.2)GO TO 6	HAD10530
IF(GO.EQ.3)GO TO 7	HAD10540
GO TO 8	HAD10550
5 WRITE(61,41)	HAD10560
GO TO 9	HAD10570
6 WRITE(61,42)	HAD10580
GO TO 9	HAD10590
7 WRITE(61,43)	HAD10600
GO TO 9	HAD10610
8 WRITE(61,40)	HAD10620
9 IF(HL.EQ.0)GO TO 10	HAD10630
WRITE(61,45)	HAD10640
GO TO 11	HAD10650
10 WRITE(61,44)	HAD10660
11 CONTINUE	HAD10670
WRITE(61,46)	HAD10680
WRITE(61,47)	HAD10690
IF(PRINT.NE.3)GO TO 60	HAD10700
WRITE(61,48)	HAD10710
60 RETURN	HAD10720
<hr/>	
C	
12 FORMAT(1H1)	HAD10740
13 FORMAT(12X,46H PERFORMANCE OF A HORIZONTAL AXIS WIND TURBINE)	HAD10750
15 FORMAT(18X,29H CALCULATED BY HAWTDP PROGRAM)	HAD10760
14 FORMAT(//,5X,22H OPERATING CONDITIONS:)	HAD10770
16 FORMAT(/,15X,'WIND VELOCITY GRADIENT EXPONENT=',F7.4)	HAD10780
17 FORMAT(/,15X,'HUB HEIGHT ABOVE GROUND LEVEL(METER)=',F12.4)	HAD10790
18 FORMAT(/,15X,'ALTITUDE OF HUB ABOVE SEA LEVEL(METER)=',F15.4)	HAD10800
117 FORMAT(/,15X,'MAXIMUM THICKNESS/ CHORD RATIO, = ',F6.2)	HAD10810
119 FORMAT(/,15X,'REVOLUTIONS PER MINUTE,R.P.M. = ',F7.2)	HAD10820
19 FORMAT(/,15X,'ANGULAR VELOCITY(RADIAN PER SECOND)=',F10.4)	HAD10830
20 FORMAT(/,15X,'TIP SPEED RATIO=',F7.4)	HAD10840
50 FORMAT(/,15X,'DESIGN TIP SPEED RATIO=',F7.4)	HAD10850
21 FORMAT(/,15X,'PITCH ANGLE FROM NOMINAL TWIST(DEGREES)=',F10.4)	HAD10860
22 FORMAT(/,15X,'PITCH ANGLE AT 0.75 RADIOUS(DEGREES)=',G14.8)	HAD10870
23 FORMAT(/,15X,'CONING ANGLE(DEGREES)=',F10.4)	HAD10880
24 FORMAT(/,10X,'BLADE DESIGN:')	HAD10890
25 FORMAT(/,15X,'NUMBER OF BLADES=',F3.0)	HAD10900
26 FORMAT(/,15X,'TIP RADIUS(METER)=',F7.4)	HAD10910
27 FORMAT(/,15X,'HUB RADIUS(METER)=',F7.4)	HAD10920
28 FORMAT(/,15X,'SOLIDITY=',F12.8)	HAD10930


```

29 FORMAT(/,15X,'ACTIVITY FACTOR=',G14.8) HAD10940
30 FORMAT(/,15X,'NACA PROFILE=',I5) HAD10950
52 FORMAT(/,15X,' NACA PROFILE=0012 ') HAD10960
53 FORMAT(/,15X,' NACA PROFILE=0015 ') HAD10970
31 FORMAT(/,15X,'NUMBER OF STATIONS ALONG SPAN=',I4) HAD10980
32 FORMAT(/,10X,'CHORD AND TWIST DISTRIBUTION') HAD10990
33 FORMAT(/,15X,'PERCENT RADIUS',5X,'CHORD(METER)',10X,'TWIST(DEG)') HAD11000
34 FORMAT(/,20X,F6.2,8X,F10.5,10X,F10.5) HAD11010
35 FORMAT(/,5X,'PROGRAM OPERATING CONDITIONS:') HAD11020
36 FORMAT(/,15X,'INCREMENTAL PERCENTAGE=',F7.4) HAD11030
37 FORMAT(/,15X,'ANGULAR INTERFERENCE FACTOR,AP=0.0') HAD11040
39 FORMAT(/,15X,'STANDARD AXIAL INTERFERENCE METHOD USED') HAD11050
40 FORMAT(/,15X,'TIP LOSSES MODELED BY PRANDTLES FORMULA') HAD11060
41 FORMAT(/,15X,'TIP LOSSES MODELED BY GOLDSTEINS FORMULA') HAD11070
42 FORMAT(/,15X,'NO TIP LOSS MODEL') HAD11080
43 FORMAT(/,15X,'TIP LOSS MODEL --> N A S A VERSION') HAD11090
44 FORMAT(/,15X,'NO HUB LOSS MODEL USED') HAD11100
45 FORMAT(/,15X,'HUB LOSSES MODELED BY PRANDTLE') HAD11110
46 FORMAT(1H1) HAD11120
47 FORMAT(/,3X,'PERFORMANCE ANALYSIS:-') HAD11130
48 FORMAT(/,1X,'PCCR',5X,'A',6X,'AP',5X,'CL',6X,'CD',5X,'PHI',
&4X,'ALPHA',5X,'F',8X,' RE-NO.',6X,'CT',6X,'CP',5X,'CD/CL'/) HAD11140
END HAD11150
CS=3 ----- HAD11160
C SUBROUTINE CALC ] HAD11170
C ] HAD11180
C ] HAD11190
C ] HAD11200
C ] HAD11210
SUBROUTINE CALC(RL,C,THET,FXF,FYF,XMFXF,XMFYF,QF,TF,RE,PHIR,CL,CD HAD11220
&,CX,CY,A,AP,XL,AK,ALPHA,F,CLF,CAT,AAT,CLT,CDT,NFS,SOLD,XM1Y,XM1P, HAD11230
&TFX,TFY,TFZ) HAD11240
C HAD11250
C ....CALC DETERMINES THE AXIAL AND ANGULAR INTERFERENCE FACTOR AT ] HAD11260
C A GIVEN RADIUS AND FUNCTIONS DEPENDENT UPON THESE PARAMETERS.].. HAD11270
C HAD11280
INTEGER T,GO,APP,Z1,CAT HAD11290
DIMENSION AAT(45),RR8(45),CLT(45),CDT(45) HAD11300
COMMON/C1/R,DR,HB,B,V,X,THETP,H,SI,GO,OMEGA,RHO,VIS,HL,PI,RX,W HAD11310
&,NPROF,APP,T1,T2,T3,T4,T5,T6,T7,T8,TEST,XETA,HH,ALO,AC,TH HAD11320
COMMON/C2/DTSR,PRINT,T HAD11330
COMMON/C3/Z1,SH,CONST,ZOAN1 HAD11340
COMMON/C6/SIA,BF,COAN1,YA HAD11350
COMMON/C4/QU,RR8,NFIT,RHOM,GAL HAD11360
COMMON/C9/TILT HAD11370
C ----- HAD11380
XREF=PI/12. HAD11390
HREF=1.5*R HAD11400
DDD=1.5*R HAD11410
ATILT=PI/180.*TILT HAD11420
IF(Z1.GE.3) ZOAN=PI/180.*ZOAN1 HAD11430
IF(T.EQ.2) ZOAN=PI/180.*0. HAD11440
VX=V HAD11450
IF(Z1.LT.3.OR.Z1.EQ.6) SIA1=0. HAD11460
YA1=YA*PI/180. HAD11470
IF(Z1.EQ.6)GO TO 242 HAD11480

```



```

IF(Z1.NE.4)YA1=PI/180.*90. HAD11490
IF(Z1.EQ.3)YA1=YA*PI/180. HAD11500
IF(Z1.LT.3)GO TO 242 HAD11510
VA=R*OMEGA/DTSR HAD11520
IF(Z1.EQ.5)VA=R*OMEGA/X HAD11530
SIA1=SIA*PI/180. HAD11540
XX=COS(ZOAN)*SIN(SIA1) HAD11550
YY=SIN(-ZOAN)*COS(ATILT)+COS(ZOAN)*COS(SIA1)*SIN(ATILT) HAD11560
YY2=-YY HAD11570
YY=YY2*RL-DDD*COS(ATILT) HAD11580
ZZ=-SIN(-ZOAN)*SIN(ATILT)+COS(ZOAN)*COS(SIA1)*COS(ATILT) HAD11590
ZZ2=ZZ HAD11600
ZZ=ZZ*RL HAD11610
ZZ=ZZ-DDD*SIN(ATILT) HAD11620
ZZZ=HH-(ZZ2*RL) HAD11630
VREF=VA/(HH/HREF)**XETA HAD11640
V=(ZZZ/HREF)**XETA*VREF HAD11650
XV=ABS(XX) HAD11660
IF(Z1.EQ.4)GO TO 243 HAD11670
IF(SIA.LE.15. .OR. SIA.GE.345.) V=V*(1.-BF*(1.+COS(12.*SIA1))) HAD11680
GO TO 242 HAD11690
243 IF(SIA.LT.20. .OR. SIA.GT.340.) V=V*(1.-BF*(1.+COS(9.*SIA1))) HAD11700
242 CONTINUE HAD11710
IF(ABS(V).LT.1.E-25) V=1.E-5 HAD11720
IF(Z1.LT.3) ZOAN=0. HAD11730
XL=RL*COS(ZOAN)*OMEGA/V HAD11740
RH=HB HAD11750
DO 15 J=1,40 HAD11760
JA=0 HAD11770
88 CONTINUE HAD11780
BETA=A HAD11790
DELTA=AP HAD11800
CSI=COS(SI) HAD11810
IF(ABS(A-1.).LT.1.E-25) A=0.999999 HAD11820
IF(ABS(AP+1.).LT.1.E-25) AP=-0.999999 HAD11830
CC1=COS(ZOAN)*SIN(YA1)*COS(ATILT)+SIN(SIA1)*COS(YA1)*SIN(-ZOAN) HAD11840
&-A*SIN(YA1)*COS(ZOAN)*COS(ATILT)-SIN(YA1)*SIN(-ZOAN)*SIN(ATILT) HAD11850
&*COS(SIA1) HAD11860
CC1=CC1*V HAD11870
CC2=-((1.+AP)*RL*COS(ZOAN)*OMEGA)+COS(YA1)*COS(SIA1)*V HAD11880
&+V*SIN(YA1)*SIN(SIA1)*SIN(ATILT) HAD11890
FC1=-(CC1/CC2) HAD11900
PHI=ATAN(FC1) HAD11910
IF(PHI.LT.0. .AND. CC1.GT.0.) PHI=PHI+PI HAD11920
SPHI=SIN(PHI) HAD11930
CPHI=COS(PHI) HAD11940
PHIAA=ABS(PHI) HAD11950
XXL=COS(PHIAA)/SIN(PHIAA) HAD11960
XXLO=XXL*R/RL HAD11970
PHIR=PHI HAD11980
ALPHA=PHI-THET-THETP HAD11990
IF(ABS(XL).LT.1.E-25) XL=1.E-9 HAD12000
DDTC=ATAN((1.-A)/(XL*(1.+2.*AP)))-ATAN((1.-A)/XL) HAD12010
DA1=DDTC/4. HAD12020
DA2=((4./15.)*(SOLD*TH)/X)/((1./X)**2+(RL/RX)**2) HAD12030

```


DALPHA=DA1+DA2	HAD12040
ALPHA=ALPHA-DALPHA	HAD12050
ALPHAD=ALPHA+0.001	HAD12060
C	HAD12070
C.....CAL OF SECTIONAL LIFT AND DRAG CO-EFF	HAD12080
C	HAD12090
IF(NPROF.EQ.4418)GO TO 1	HAD12100
1 CALL NACA44(ALPHA,CL,CD,ALO)	HAD12110
CALL NACA44(ALPHAD,CLD,CDD,ALO)	HAD12120
IF(GO.LT.3)GO TO 6	HAD12130
CL=CLF*CL	HAD12140
CLD=CLF*CLD	HAD12150
F=1.	HAD12160
GO TO 7	HAD12170
C	HAD12180
C.....CAL TIP & HUB LOSSES	HAD12190
C	HAD12200
6 IF(CAT.EQ.1) F=0.	HAD12210
IF(CAT.EQ.1)GO TO 7	HAD12220
CALL TIPLOS(XXL,XXLD,F,B,GO,HL,PI,R,RL,PHI,RH)	HAD12230
7 CONTINUE	HAD12240
70 CONTINUE	HAD12250
71 CXX=CL*SPHI	HAD12260
CYY=CL*CPHI	HAD12270
CX=CXX	HAD12280
CY=CYY	HAD12290
IF(PHI.GE.1.5272)GO TO 322	HAD12300
GO TO 323	HAD12310
322 CONTINUE	HAD12320
A=0.	HAD12330
AP=0.	HAD12340
CC1=COS(ZOAN)*COS(ATILT)*SIN(YA1)+SIN(SIA1)*COS(YA1)*SIN(-ZOAN)	HAD12350
&-A*SIN(YA1)*COS(ZOAN)*COS(ATILT)-SIN(YA1)*SIN(-ZOAN)*	HAD12360
&SIN(ATILT)*COS(SIA1)	HAD12370
CC1=CC1*V	HAD12380
CC2=-((1.+AP)*RL*COS(ZOAN)*OMEGA)+COS(YA1)*COS(SIA1)*V	HAD12390
&+V*SIN(YA1)*SIN(SIA1)*SIN(ATILT)	HAD12400
GO TO 325	HAD12410
323 CONTINUE	HAD12420
SIG=(B*C)/(PI*RL)	HAD12430
IF(SIG.GE.1.)GO TO 61	HAD12440
GO TO 8	HAD12450
61 CONTINUE	HAD12460
IF(XL.GE.35.)GO TO 8	HAD12470
Z=SIG*CL/8.	HAD12480
CSI4=CSI**4	HAD12490
Z2=Z*Z	HAD12500
BOB=Z2*CSI4*(1.-A)*(1.-A)/(XL*XL)	HAD12510
IF(ABS(CL).LT.1.E-25)GO TO 62	HAD12520
Z3=ABS(CL)	HAD12530
SIGN1=CL/Z3	HAD12540
GO TO 63	HAD12550
62 SIGN1=1.	HAD12560
63 ZZ=Z2+(1.-Z2)*BOB	HAD12570
IF(ZZ.LT.0.) ZZ=ABS(ZZ)	HAD12580


```

Z4=SQRT(ZZ)
AP=SIGN1*(Z2+Z4)/(1.-Z2)
RW=Z*(CSI**2)*CPHI*(CC1**2+CC2**2)/(COS(ZOAN)**2*COS(ATILT)**2
&*SIN(YA1)**2*V**2)
BIP=1.-4.*RW
IF(BIP.LT.0.) BIP=0.
A=0.5*(1.-SQRT(BIP))
GO TO 9
8 VBR=0.125*SIG*CYC*COS(ZOAN)
VAR=0.125*SIG*CXX/COS(ZOAN)
IF(ABS(VBR).LT.1.E-25) VBR=0.000001
IF(ABS(F).LT.1.E-25) F=0.000001
TBR=SIG/8.*CYC*(CC1**2+CC2**2)
TBR1=F*(V*COS(ATILT)*SIN(YA1))**2*COS(ZOAN)
IF(ABS(A-1.).LT.1.E-25) A=0.9999999
IF(ABS(TBR1).LT.1.E-25) TBR1=0.00000001
A=TBR/TBR1/(1.-A)
IF(A.LE.AC)GO TO 32
VBR=VBR/(SPHI**2)
B1=((1.-2.*AC)*F+2.*VBR)/VBR
C1=(VBR-AC*AC*F)/VBR
CANN=B1*B1-4.*C1
IF(CANN.LT.0.) CANN=0.
A=0.5*(B1-SQRT(CANN))
32 CONTINUE
IF(ABS(A-1.).LT.1.E-25) A=0.9999999
TAR=SIG/8.*CX*(CC1**2+CC2**2)
TAR1=F*V*COS(ATILT)*COS(ZOAN)*SIN(YA1)*OMEGA*RL
TAR1=TAR1*COS(ZOAN)**2
AP=TAR/TAR1/(1.-A)
IF(APP.EQ.1) AP=0.
9 PCCR=RL/(RX*CSI)
C .....DAMPING OF AXIAL & ANGULAR INTERFERENCEFACTOR ITERATIONS....
IF(J.EQ.1 .OR.J.EQ.40)GO TO 133
12 A=(A+BETA)*0.5
AP=(AP+DELTA)*0.5
13 CONTINUE
IF(APP.EQ.1)GO TO 14
IF(ABS(AP-DELTA).LE.0.001)GO TO 16
GO TO 15
14 IF(ABS(A-BETA).LE.0.001)GO TO 16
133 CONTINUE
IF(J.EQ.1)GO TO 15
JA=JA+1
IF(JA.EQ.2)GO TO 325
A=0.
AP=0.
GO TO 88
15 CONTINUE
16 IF(AK.GE.1.)GO TO 18
PCCR=RL/RX*CSI
C
C .....CAL OF FUNCTIONS DEPENDENT UPON AXIAL & ANG.INTERF. FACTOR....
C
18 CONTINUE

```

HAD12590
HAD12600
HAD12610
HAD12620
HAD12630
HAD12640
HAD12650
HAD12660
HAD12670
HAD12680
HAD12690
HAD12700
HAD12710
HAD12720
HAD12730
HAD12740
HAD12750
HAD12760
HAD12770
HAD12780
HAD12790
HAD12800
HAD12810
HAD12820
HAD12830
HAD12840
HAD12850
HAD12860
HAD12870
HAD12880
HAD12890
HAD12900
HAD12910
HAD12920
HAD12930
HAD12940
HAD12950
HAD12960
HAD12970
HAD12980
HAD12990
HAD13000
HAD13010
HAD13020
HAD13030
HAD13040
HAD13050
HAD13060
HAD13070
HAD13080
HAD13090
HAD13100
HAD13110
HAD13120
HAD13130


```

325 CONTINUE
W=SQRT(CC1**2+CC2**2)
CX=CL*SPHI-CD*CPHI
CY=CL*CPHI+CD*SPHI
IF(Z1.EQ.1)GO TO 50
RE=RHO*W*C/VIS
CONST=(0.5*RHO*(W**2)*C)
FXF=CONST*CX
FYF=CONST*CY
IF(Z1.NE.4)GO TO 97
TFX=FXF*COS(SIA1)+FYF*SIN(-ZOAN)*SIN(SIA1)
TFY=FYF*COS(ZOAN)*COS(ATILT)-(FYF*SIN(-ZOAN)*COS(SIA1)-FXF
&*SIN(SIA1))*SIN(ATILT)
TFZ=(FYF*SIN(-ZOAN)*COS(SIA1)-FXF*SIN(SIA1))*COS(ATILT)+
&FYF*COS(ZOAN)*SIN(ATILT)
XM1Y=TFY*XX*RL-TFX*YY
XM1P=-TFY*ZZ+TFZ*YY
GO TO 50
97 XMXF=FXF*(RL-HB)/CSI
XMFY=FYF*(RL-HB)/CSI
50 CT1=(0.5*RHO*B*C)*(W*W)
QF=CT1*RL*CX*COS(ZOAN)
IF(Z1.EQ.1)GO TO 51
TF=CT1*CY*CSI*COS(ZOAN)
CLA=(CLD-CL)/0.001
CDA=(CDD-CD)/0.001
19 CONTINUE
IF(A.LE.0.0001 .OR. AP.LE.0.0001)GO TO 51
T7=T7+(((2.+CPHI**2)*CL*SPHI-CPHI**3*CD+2.*CPHI*
&CLA)*(1.-A)**2*RL**3*C)*DR/2.
T8=T8+(((1.+SPHI**2)/CPHI*CL-CD*SPHI+CLA*SPHI)*
&(1.+AP)*(1.-A)*RL**4*C)*DR/2.
51 RETURN
END
CS=4 -----
C SUBROUTINE TIPLOS ]
C ]
C ]
C -----]
SUBROUTINE TIPLOS(U,UO,F,Q,GO,HL,PI,R,RL,PHI,RH)
C
C .....GIVES TIP & HUB LOSSES BASED ON 'GOLDSTEIN' OR 'PRANDTLE' OR ]
C FOR NO LOSS .....]
C
C
C INTEGER GO,HL
SUM2=0.
SUM=0.
AK=1.
AMM=1.
AM=0.
IF(Q.GT.2.)GO TO 1
IF(GO.EQ.0)GO TO 2
IF(GO.EQ.1)GO TO 4
IF(GO.EQ.2)GO TO 3
1 IF(GO.EQ.2)GO TO 3

```

HAD13140
HAD13150
HAD13160
HAD13170
HAD13180
HAD13190
HAD13200
HAD13210
HAD13220
HAD13230
HAD13240
HAD13250
HAD13260
HAD13270
HAD13280
HAD13290
HAD13300
HAD13310
HAD13320
HAD13330
HAD13340
HAD13350
HAD13360
HAD13370
HAD13380
HAD13390
HAD13400
HAD13410
HAD13420
HAD13430
HAD13440
HAD13450
HAD13460
HAD13470
HAD13480
HAD13490
HAD13500
HAD13510
HAD13520
HAD13530
HAD13540
HAD13550
HAD13560
HAD13570
HAD13580
HAD13590
HAD13600
HAD13610
HAD13620
HAD13630
HAD13640
HAD13650
HAD13660
HAD13670
HAD13680

2	CONTINUE	HAD13690
	P1=SIN(PHI)	HAD13700
	P1=P1*P1+0.0001	HAD13710
	SOMSAK=(Q*(R-RL))/(2.*R*SQRT(P1))	HAD13720
	IF(ABS(SOMSAK).LT.1.E-25) SOMSAK=1.E-10	HAD13730
	IF(SOMSAK.GE.10.)GO TO 3	HAD13740
	F=(2./PI)*ACOS(EXP(-SOMSAK))	HAD13750
	GO TO 5	HAD13760
3	F=1.	HAD13770
	GO TO 5	HAD13780
4	IF((ABS(SIN(PHI))).LT.0.0001) GO TO 2	HAD13790
C	-----	HAD13800
CGOLDSTEIN'S METHOD.....	HAD13810
C	-----	HAD13820
	DO 45 M=1,3	HAD13830
	V=(2.*AM+1.)	HAD13840
	ZO=UO*V	HAD13850
	V2=V*V	HAD13860
	Z=U*V	HAD13870
	Z2=Z*Z	HAD13880
C	-----	HAD13890
	CALL BESSEL(Z,V,AI)	HAD13900
	CALL BESSEL(ZO,V,AIO)	HAD13910
C	-----	HAD13920
	IF(Z.GE.3.5)GO TO 25	HAD13930
	A=2.*2.	HAD13940
	B=4.*4.	HAD13950
	C=6.*6.	HAD13960
	D=8.*8.	HAD13970
	T1VZ=Z2/(A-V2)+(Z2*Z2)/((A-V2)*(B-V2))+(Z2**3)/((A-V2)*(B-V2)*	HAD13980
	&(C-V2))+(Z2**4)/((A-V2)*(B-V2)*(C-V2)*(D-V2))	HAD13990
	CT1VZ=(V*PI*AI)/(2.*SIN(0.5*V*PI))-T1VZ	HAD14000
	GO TO 30	HAD14010
25	TO=(U*U)/(1.+U*U)	HAD14020
	T2=4.*U*U*(1.-U*U)/((1.+U*U)**4)	HAD14030
	T4=16.*U*U*(1.-14.*U*U+21.*U**4-4.*U**6)/((1.+U*U)**7)	HAD14040
	T6=64.*U*U*(1.-75.*U*U+603.*U**4-1065.*U**6+460.*U**8-36.*U**10)	HAD14050
	&/((1.+U*U)**10)	HAD14060
	CY1VZ=TO+T2/V2+T4/(V2**2)+T6/(V2**3)	HAD14070
30	FVU=(U*U)/(1.+U*U)-CT1VZ	HAD14080
	SUM=SUM+FVU/V2	HAD14090
	IF(AM.NE.0.)GO TO 35	HAD14100
	E=-0.098/(UO**0.668)	HAD14110
35	IF(AM.NE.1.)GO TO 40	HAD14120
	E=0.031/(UO**1.285)	HAD14130
40	IF(AM.GT.1.) E=0.	HAD14140
	SUM2=SUM2+((UO*UO*AMM)/(1.+UO*UO)-E)*(AI/AIO)	HAD14150
	AM=AM+1.	HAD14160
	AK=((2.*AM-1.)*AK)/(2.*AM)	HAD14170
45	AMM=AK/(2.*AM+1.)	HAD14180
	G=(U*U)/(1.+U*U)-(8./(PI*PI))*SUM	HAD14190
	CIRC=G-(2./PI)*SUM2	HAD14200
	F=((1.+U*U))*CIRC	HAD14210
C	-----	HAD14220
HUB LOSS CALCULATION.....	HAD14220
5	IF(HL.EQ.1)GO TO 6	HAD14230

	FI=1.	HAD14240
	GO TO 7	HAD14250
6	CONTINUE	HAD14260
	P1=SIN(PHI)	HAD14270
	P1=P1*P1+0.0001	HAD14280
	IF(RL.LE.RH) RL=0.00001+RH	HAD14290
	SOMSAK=(G*(RL-RH))/(2.*RH*SQRT(P1))	HAD14300
	IF(ABS(SOMSAK).LT.1.E-25) SOMSAK=1.E-10	HAD14310
	IF(SOMSAK.GE.10)GO TO 71	HAD14320
	FI=(2./PI)*ACOS(EXP(-SOMSAK))	HAD14330
	GO TO 7	HAD14340
71	FI=1.	HAD14350
7	F=F*FI	HAD14360
	RETURN	HAD14370
	END	HAD14380
CS=5	-----	HAD14390
C	SUBROUTINE BESSEL]	HAD14400
C	_____]	HAD14410
C	_____]	HAD14420
C	-----]	HAD14430
	SUBROUTINE BESSEL(Z,V,AI)	HAD14440
C	-----	HAD14450
C	...CALCULATES BESSEL FUNCTIONS FOR THE GOLDSTEIN TIP LOSS MODEL]...	HAD14460
C	-----	HAD14470
	S=0.	HAD14480
	AK=0.	HAD14490
	C=1.	HAD14500
	DO 3 K=1,10	HAD14510
	B=(0.25*Z*Z)**AK	HAD14520
	D=V+AK	HAD14530
	P=1.	HAD14540
1	TK=D-1.	HAD14550
	IF(TK.LE.0.)GO TO 2	HAD14560
	P=D*TK*P	HAD14570
	D=D-2	HAD14580
	GO TO 1	HAD14590
2	E=P	HAD14600
	S=B/(C*E)+S	HAD14610
	AK=AK+1.	HAD14620
	C=AK*C	HAD14630
3	CONTINUE	HAD14640
	AI=((0.5*Z)**V)*S	HAD14650
	RETURN	HAD14660
	END	HAD14670
CS=6	-----	HAD14680
C	SUBROUTINE NACA44]	HAD14690
C	_____]	HAD14700
C	_____]	HAD14710
C	-----]	HAD14720
	SUBROUTINE NACA44(ALPHA,CL,CD,ALO)	HAD14730
C	-----	HAD14740
C	...NACA DETERMINES THE -- CO-EFF OF LIFT & DRAG]	HAD14750
C	AT A GIVEN ANGLE OF ATTACK;ALPHA]	HAD14760
C	FOR A NACA 4418 AIRFOIL.]	HAD14770
C	-----]	HAD14780


```

C THE EQUATIONS WERE OBTAINED BY A ORTHOGONAL POLYNOMIAL ] HAD14790
C CURVE FIT OF NACA DATA PUBLISHED IN ] HAD14800
C NACA REPORT NO.824, PAGE 401. ] HAD14810
C ----- ] HAD14820
C DIMENSION AAD(5,4),AADG(4,3),AAL(9,3),AALG(3,3) ] HAD14830
C ----- ] HAD14840
C ] HAD14850
C DATA ] HAD14860
C ] HAD14870
C ] HAD14880
C DATA AAD/0.074402988,2.1595697,4.8372211,-13.874289,6.8311195 ] HAD14890
&, 0.31059104,-0.72021174,2.6283879,-5.1881313,3.7312441 ] HAD14900
&, 325.97302,-1448.9419,2417.5137,-1791.7397,497.47345 ] HAD14910
&, -1.2031252,11.246515,-14.671162,1.5634329,3.1053634/ ] HAD14920
DATA AADG/180.,14.,14.,0. ] HAD14930
&, 167.472,27.91252,37.9335,180.0792 ] HAD14940
&, 1.,0.04,0.04,1./ ] HAD14950
DATA AAL/0.230799449,8.1520996,-90.209305,483.0567,-1452.5042 ] HAD14960
&, 2499.7095,-2470.749,1316.7717,-294.75653 ] HAD14970
&, -0.84696233,1.3011253,11.170555,-26.763992,48.592003 ] HAD14980
&, -56.189163,23.942741,0.,0. ] HAD14990
&, 1.2345905,13.929703,-217.36517,1162.4739,-3131.7378 ] HAD15000
&, 4476.8242,-3240.5244,935.38135,0./ ] HAD15010
DATA AALG/180.,14.,0.,159.30945,38.,179.8416,1.,1.,1./ ] HAD15020
C ----- ] HAD15030
ALP=ALPHA*180./3.141593 ] HAD15040
IF((ALP.GE.-180.) .AND. (ALP.LT.-14.)) J=1 ] HAD15050
IF(ALP.GE.14. .AND. ALP.LT.-14.) J=2 ] HAD15060
IF(ALP.GE.14. .AND. ALP.LT.24.) J=3 ] HAD15070
IF(ALP.GE.24. .AND. ALP.LE.180.) J=4 ] HAD15080
ALFA=(ALP+AADG(J,1))/AADG(J,2) ] HAD15090
CD=AADG(J,3)*AAD(1,J) ] HAD15100
DO 100 JJ=2,5 ] HAD15110
CD=CD+AADG(J,3)*AAD(JJ,J)*ALFA**(JJ-1) ] HAD15120
100 CONTINUE ] HAD15130
IF(J.EQ.3) J=2 ] HAD15140
IF(J.EQ.4) J=3 ] HAD15150
ALFA=(ALP+AALG(J,1))/AALG(J,2) ] HAD15160
CL=AALG(J,3)*AAL(1,J) ] HAD15170
DO 200 JJ=2,9 ] HAD15180
CL=CL+AALG(J,3)*AAL(JJ,J)*ALFA**(JJ-1) ] HAD15190
200 CONTINUE ] HAD15200
IF((J.EQ.1) .AND. (ALP.GT.-20.69055)) ] HAD15210
& CL=-0.29817-0.0804763*(20.69055+ALP) ] HAD15220
RETURN ] HAD15230
END ] HAD15240
CS=7 ----- ] HAD15250
C SUBROUTINE CLCD ] HAD15260
C ] HAD15270
C ] HAD15280
C ] HAD15290
C ----- ] HAD15300
SUBROUTINE CLCD(ALPHA,ALPHAD,CL,CLD,CLT,CD,CDD,CDT,RL,AAT,NFS ] HAD15300
&,SOLD) ] HAD15310
DIMENSION AAT(45),RR8(45),CLT(45),CDT(45) ] HAD15320
COMMON/C1/R,DR,HB,B,V,X,THETP,H,SI,GO,OMEGA,RHO,VIS,HL,PI,RX,W ] HAD15330

```



```

&,NPROF,APP,T1,T2,T3,T4,T5,T6,T7,T8,TEST,XETA,HH,ALO,AC,TH      HAD15340
COMMON/C4/QU,RR8,NFIT,RHOM,GAL      HAD15350
IF(NPROF.EQ.4418)GO TO 1      HAD15360
1 CALL NACA44(ALPHA,CL,CD,ALO)      HAD15370
CALL NACA44(ALPHAD,CLD,CDD,ALO)      HAD15380
RETURN      HAD15390
END      HAD15400
CS=8 -----      HAD15410
C SUBROUTINE SOLIDT ]      HAD15420
C _____ ]      HAD15430
C ]      HAD15440
C -----]      HAD15450
SUBROUTINE SOLIDT (RR,CI,NF,B,R,PI,SOLD)      HAD15460
C      HAD15470
C .....SOLIDT DETERMINES THE TOTAL SOLIDITY OF THE ]      HAD15480
C WIND TURBINE DESIGN .....]...      HAD15490
C      HAD15500
DIMENSION RR(25),CI(25)      HAD15510
NFX=NF-1      HAD15520
S1=0.      HAD15530
DO 1 I=1,NFX      HAD15540
SOL=((CI(I+1)+CI(I))/2.)*(RR(I)-RR(I+1))*R/100.      HAD15550
S1=S1+SOL      HAD15560
1 CONTINUE      HAD15570
SOLD=B*S1/(PI*R**2)      HAD15580
RETURN      HAD15590
END      HAD15600
CS=9 -----      HAD15610
C SUBROUTINE ACTIVI ]      HAD15620
C _____ ]      HAD15630
C ]      HAD15640
C -----]      HAD15650
SUBROUTINE ACTIVI(RR,CI,NF,B,R,PI,ACF)      HAD15660
C      HAD15670
C .....ACTIVI DETERMINES THE ACTIVITY FACTOR OF THE      HAD15680
C WIND TURBINE DESIGN .....      HAD15690
C      HAD15700
DIMENSION RR(25),CI(25)      HAD15710
NFX=NF-1      HAD15720
S1=0.      HAD15730
DO 1 I=1,NFX      HAD15740
C1=(CI(I+1)+CI(I))/2.      HAD15750
ROR=((RR(I)-RR(I+1))/2.+RR(I+1))/100.      HAD15760
DROR=(RR(I)-RR(I+1))/100.      HAD15770
FAC=(C1/(2.*R))*ROR**3*DROR      HAD15780
S1=S1+FAC      HAD15790
1 CONTINUE      HAD15800
ACF=S1*100000./16.      HAD15810
RETURN      HAD15820
END      HAD15830

```